Radon in Natural Environment and its Impact on Human Health

Arindam Kumar Naskar

Thesis submitted for the award of

Degree of Doctor of Philosophy (Science)

Jadavpur University, 2024

JADAVPUR UNIVERSITY
KOLKATA - 700032

CERTIFICATE FROM THE SUPERVISOR(S)

This is to certify that the thesis entitled "**Radon in Natural Environment and its Impact on Human Health**" submitted by Sri **Arindam Kumar Naskar** who got his name registered on 04th July, 2016 (**04/07/2016**), for the award of Ph. D. (Science) degree of Jadavpur University, is absolutely based upon his own work under the supervision of **Prof. Mitali Mondal**, Professor, Department of Physics, Jadavpur University and Co-Supervisor **Prof. Argha Deb**, Professor, Department of Physics, Jadavpur University and that neither this thesis nor any part of it has been submitted for either any degree/diploma or any other academic award anywhere before.

30.01.2024
(Prof. Mitali Mondal)

30.01.24
(Prof. Argha Deb)

(Signature of the Supervisors date with official seal)

PROFESSOR MITALI MONDAL
Department of Physics
Jadavpur University
Kolkata – 700 032

Prof. Argha Deb
Department of Physics
Jadavpur University
Kolkata – 700 032

“Confidence and Hard-work is the only medicine to kill a disease called failure.” —

A.P.J. Abdul Kalam

Acknowledgements

I am deeply appreciates the guidance and supervision extended by the individuals mentioned below. Without their support, the completion of this work would not have been achievable.

Foremost, heartiest respect and deep gratitude to my Supervisor Prof. Mitali Mondal, Professor, Department of Physics, Jadavpur University and Co-Supervisor Prof. Argha Deb, Professor, Department of Physics, Jadavpur University. They have consistently supported me through difficult situations. In moments of challenge, their words of encouragement have acted as a revitalizing force, allowing me to embark on a new beginning. Their ongoing care and guidance in correcting my mistakes provide me with the opportunity to excel in my endeavors. I am eternally grateful to them for their generosity.

Special thanks to Mr. Mahasin Gazi who served as a senior co-worker; his continuous support played an important role in the successful completion of the research work. I would like to express my gratitude to Dr. Javed Akhter for his invaluable assistance throughout the entire duration of my PhD work. I am also thankful for the support and help provided by my fellow lab-mates.

I am also deeply grateful to Dr. Sunando Kumar Patra for his valuable advices in my research endeavors. Also his constant encouragement to approach the work with passion has been truly inspiring.

It would be grossly amiss if I failed to acknowledge the invaluable support of Dr. Banamali Roy. His persistent positivity has been a constant presence in every endeavor of mine. He stands by me as a steadfast friend, philosopher, and guide.

I would like to express gratitude to the residents of the study areas of the present thesis work, for their invaluable assistance in conducting our fieldwork, including sample collection and measurements.

Finally, deepest gratitude to my parents, my wife, my son and all my dearest friends for their unwavering support throughout the research journey. Without their support I am not

able to finish this work. I am also expressing my gratitude to seniors, juniors, friends, colleagues, and students, inviting them to fill in the provided space if inadvertently omitted.

Arindam Kumar Naskar
30/01/2024

January, 2024

Arindam Kumar Naskar

List of Publications

Publications in Journal

1. Deb, A., Gazi, M., Bhoumik, G., **Naskar, A.**, & Barman, C. (2017). Exposure to underground radon in and around Kolkata Municipal Corporation area: an exhaustive study. Journal of Radioanalytical and Nuclear Chemistry, 311, 375-384.
2. **Naskar, A. K.**, Gazi, M., Barman, C., Chowdhury, S., Mondal, M., Ghosh, D., ... & Deb, A. (2018). Estimation of underground water radon danger in Bakreswar and Tantloi Geothermal Region, India. Journal of Radioanalytical and Nuclear Chemistry, 315, 273-283.
3. **Naskar, A. K.**, Gazi, M., Mondal, M., & Deb, A. (2022). Water radon risk in Susunia hill area: an assessment in terms of radiation dose. Environmental Science and Pollution Research, 29(8), 11160-11171.
4. *Gazi, M., **Naskar, A. K.**, Mondal, M., & Deb, A. (2022). Radiological safety assessment of drinking water in Darjeeling hill and foothill areas: An experimental finding. Water Supply, 22(8), 6504-6515.
5. *Gazi, M., Chowdhury, S., **Naskar, A. K.**, Deb, A., & Ghosh, D. (2022). Alpha radioactivity in human blood and its possible correlation to ailment pattern. Journal of Radioanalytical and Nuclear Chemistry, 331(3), 1225-1236.
6. **Naskar, A. K.**, Akhter, J., Gazi, M., Mondal, M., & Deb, A. (2023). Impact of meteorological parameters on soil radon at Kolkata, India: investigation using machine learning techniques. Environmental Science and Pollution Research, 1-13.
7. Naskar, A. K., Gazi, M., Mondal, M., & Deb, A. (2023). Elevated radon level in drinking water of Ajodhya Hill Area of West Bengal, India: probable health impact on lung and stomach. Environmental Geochemistry and Health, 45(11), 8153-8168.
8. **Naskar, A. K.**, Gazi, M., Mondal, M., & Deb, A. (2023). Seasonal variation of ^{222}Rn concentration in tube-well water and dose assessment of water dissolved ^{222}Rn to the local people of Bankura District of West Bengal, India. Journal of Radioanalytical and Nuclear Chemistry, 1-12.

*Publications those are not included in this thesis

Presentations in Seminar/Conference/Symposiums

1. **Naskar, A. K.**, Mondal, M., & Deb, A. Distribution of Radon Concentration in Ground Water in and Around Susunia Hill, India. 2nd Regional Science and Technology Congress (Southern Region), University of Kalyani, West Bengal, December, 14 -15, 2017.
2. **Naskar, A. K.**, Akhter, J., Chowdhury, S., Mondal, A., Mondal, M., & Deb, A. Radon Risk Assessment of Radon in Drinking Water in and around Susunia Hill area, West Bengal. International Conference of Ecotoxicology and Environmental Sciences (ICEES), Institute of Ecotoxicology and Environmental Sciences and Netaji Subhas Institute of Technology, Delhi, February 19-21, 2018.
3. **Naskar, A. K.**, Gazi, M., Akhter, J., Mondal, M., & Deb, A. A study on seasonal variation of radon levels in tube-well water of Susunia hill region, West Bengal. International Conference on Nuclear, Particle and Accelerator Physics (ICNPAP), Central University of Jharkhand, October, 23-26, 2018.
4. **Naskar, A. K.**, Gazi, M., Akhter, J., Mondal, J., Mondal, A., Maity, S., Mondal, M., & Deb, A. Radon Danger in Ground Water: An Experimental Study in Ajodhya Hill and Nearby Areas of West Bengal. Environmental Radiation: Impact on Society and its Implications (ERISI), Jadavpur University, November, 15-16, 2019.
5. **Naskar, A. K.**, Gazi, M., Mondal, M., & Deb, A. Study of Water-borne Radon Levels in Some Selected Nursery and Primery Schools Located at High Radon Prone Zones in Susunia Hill Region of West Bengal, India. New Directions in Physical Sciences (NDPS), Jadavpur University, February, 25, 2020.

Table of Contents

List of Tables

List of Figures

Chapter – 1

Introduction

1.1 Motivation

We are all afraid of radioactivity because of our horrible memories of nuclear bomb explosions and nuclear reactor disasters, but these occur seldom. On the contrary, human civilization has developed in the background of environmental radioactivity. Environmental radioactivity is a phenomenon that has garnered significant attention in recent times due to its potential impact on human health and its uses in different field for the sake of mankind. It refers to the presence of radioactive materials in the environment, such as air, water, soil, commonly used materials and living organisms. The sources of environmental radioactivity can be both natural and human-made. Natural sources include cosmic radiation, naturally occurring radioactive elements such as uranium, thorium, and radium, and their decay products, specially radon gas. Human-made sources of environmental radioactivity include nuclear power plants, nuclear weapons testing, medical and industrial products, and radioactive waste. Nuclear power plants produce large amounts of radioactive waste that must be stored safely to prevent harm to the environment and human health. Weapon testing, such as the testing of atomic bombs, releases radioactive materials into the atmosphere, soil, and water. Medical applications such as ordinary X-rays and CT scans can expose patients to ionizing radiation, which can potentially cause harm.

Radioactive substances emit ionizing radiation which can be harmful to living organisms including humans and the environment. The potential health effects of exposure to environmental radioactivity depend on several factors: the type and amount of radioactive substance present, the duration of exposure, and the radio sensitivity of the individuals. Exposure to ionizing radiation can damage DNA and other cellular structures, leading to cancer, genetic mutations, and other health effects. Sudden high level exposure above a certain value cause deterministic health effect which includes nausea, weakness, hair loss, diminishing organ failure, it can even cause immediate death. However, generally low levels of radiation are present in the environment at all times, and most people receive a small amount of radiation exposure from natural sources such as cosmic radiation and radon gas. Long term low level exposure to radiation can cause stochastic health effects like cancer, gene mutation etc. Environmental radioactivity can also have effects on ecosystems, such as changes in the growth and reproductive rates of plants and animals. Radioactive materials can accumulate in the food chain, potentially causing harm to higher-level predators that consume contaminated prey. This process is known as bio-magnification.

Monitoring of environmental radioactivity is important to ensure public safety and assess the impact of human activities on the environment. Monitoring and testing for environmental radioactivity are essential to identify sources of contamination and ensure that levels of exposure are within permissible limits. This monitoring can include the measurement of radiation levels in the air, water, soil, food and other used materials. Healthcare providers also monitor patients who are exposed to radioactive

materials during medical procedures to ensure that they are not exposed to unsafe levels of radiation. Workers in industries that handle radioactive materials are also monitored to ensure that their exposure is within reference limits.

Radon and its decay products are the most important contributors to human exposure from natural sources. Radon is a colorless, odorless, and tasteless radioactive gas that is naturally produced through the successive radioactive decay of uranium-238, which is present in varying concentrations in soil, rock, and groundwater. Radon levels can vary significantly depending on geological and environmental factors. Certain regions, particularly those with granite or uranium-rich soils, may have higher radon concentrations. Uranium undergoes a series of decay steps, eventually leading to the formation of radon from its parent radium. The radon decay chain typically involves several radioactive isotopes, including radon-222 (Rn-222), polonium-218 (Po-218), lead-214 (Pb-214), bismuth – 214 (Bi- 214), polonium – 210 (Po-210) and others. Among the other radon isotopes radon-222 is the most common isotope with 3.8 day half-life and is responsible for the majority of radon-related health concerns. During its decay process radon emits energetic (4.55 MeV) alpha particles. The alpha particles can damage lung tissue if inhaled, increasing the risk of lung cancer. Radon-222 is a noble gas and belongs to the group of inert gases. Radon is chemically inert, but its radioactive decay products are solid particles that can be inhaled into the lungs, posing potential health risks. Radon exposure is a leading cause of lung cancer, especially in non-smokers. Radon-induced lung cancer is attributed to the inhalation of radon decay products, particularly polonium-210. Exposure to radon gas over a long period can increase the risk of developing lung cancer. Radon is the second leading cause of lung cancer after smoking and is responsible for about 21,000 lung cancer deaths each year in the United States alone (***Hogle 2005***). Radon can enter buildings through the ground and accumulate to elevate concentrations in the indoors. Entry points include cracks in foundations, gaps around pipes, and other openings in the building structure. Building materials used for construction can add to the concentration of indoor radon.

Water may be radiologically contaminated in different ways. Uranium containing soil and rocks and their successive decay product radon can contaminate the water aquifers, water flowing over rocks can also accumulate radio isotopes. If such water is used for drinking or other purposes, people can be exposed to radio isotopes, especially radon through ingestion as well as inhalation. Thus water-borne radon can enhance the risks of occurrence of lung as well as stomach cancer.

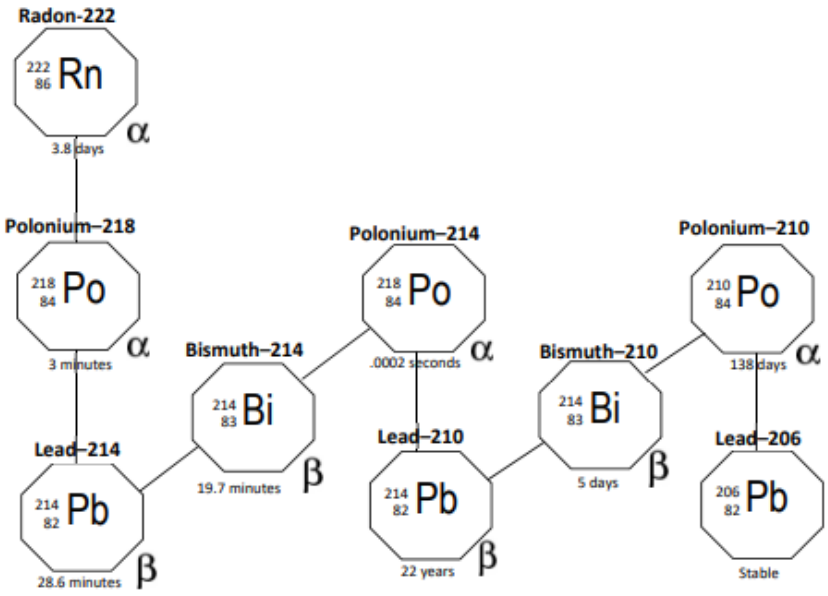

Fig. 1.1 Radon decay chain

Based on the findings of the risk of radon, international agencies like World Health Organization (WHO), United States Environmental Protection Agency (USEPA), United Nations Scientific Committee on the Effect of Atomic Radiation (UNSCEAR), International Atomic Energy Agency (IAEA) etc. have recommended reference limits and suggested for taking remedial action to reduce the environmental radon levels for public health if greater than the permissible limits. Governments of many countries around the world have taken action to reduce the radon levels in the highly exposed areas. For example, some first world countries like Denmark, Finland, Germany, Greece, Ireland, Sweden and the Czech Republic (***Synnott and Fenton 2005***) have implemented stricter regulations and recommended to test homes and buildings for radon and take steps to reduce radon levels if they are found to be high. In their radon reduction methods, they included sealing cracks and gaps in the foundation and installing a radon mitigation system. Other developed countries have invested in research and development of new technologies that can help reduce the risk of radon exposure.

Radon can not only cause harms to human society but also can serve positive purposes. Environmental radon can play important role in other fields for the benefit of mankind like (a) identifying resources like uranium, oil, and geothermal energy reservoirs (***Matos et al. 2019***) (b) study of active geological faults (***Khattak et al. 2011***) (c) forecasting earthquakes (***Woith 2015***) and (d) conducting research on volcanic activities (***Neri et al. 2016***). Considering its multifaceted importance, environmental radon is a subject of global interest. Many researches about radon are carried out world-wide (***Thomas 1972; Miles 2001; George 2008; Al-Zoughool and Krewski 2009; Yoon et al. 2016; Jobbágy et al. 2017; Degu Belete and Alemu Anteneh 2021; Sukanya et al. 2022***)

However, there is still lack of investigations regarding monitoring of radon levels in soil, air and water in a developing country like India. Especially, in the state of West Bengal

very few studies have been conducted to measure the radon levels in air, water or soil. In this perspective the author has chosen the topic "**Radon in natural environment and its impact on Human Health**" for his PhD thesis work.

1.2 Major Objectives

The present thesis work has been carried out with the following major objectives:

a. To measure water radon concentration in three areas of West Bengal namely Bakreswar and Tantloi geothermal region, Susunia hill area and Ajodhya hill area and to find possible reason for its variation. This is a part of our venture to develop water radon map of Chotanagpur Plateau region.
b. To estimate the radon dose to the local people of the study areas due to water borne radon for assessing the possible health risks.
c. To study the seasonal variation of water radon.
d. To measure radon level in indoor air specially in basements within Kolkata Municipal Corporation area where basements of building are used for different purposes.
e. To study soil radon emission and to assess the impact of other factors on its emission. Such study will help the workers who are trying to find proper soil radon fluctuation signal for predicting earthquakes.

Hope our studies will provide baseline data of radon contamination in different matrices of West Bengal state in India. Such data will help the local authorities to take necessary steps whenever necessary. As in India there is still no recommendation level for radon, we hope that our findings will be helpful to the regulatory bodies of India in setting a reference level for radon in different media.

1.3 Organization of the thesis as follows

The thesis has been organized in the following way.

In **Chapter 1** motivation behind the present thesis work and major objectives of thesis are discussed. This Chapter also contains organization of the thesis.

In **Chapter 2** basic ideas about environmental radioactivity is given, like: discovery of radioactivity, types of radiations, harmful effects of radiation on human health, types of radionuclides and their positive and negative effects, presence of radioactive substances in different media and materials etc.. Discussion on different types of radiation dose and their description is also given in this chapter.

Literature survey of experimental environmental radioactivity studies on various materials and mediums is the subject of **Chapter 3**. Worldwide studies as well as study performed within India have been discussed. Among the other natural radionuclides radon has greater importance for its immense potential for causing fatal disease like cancer and is the subject matter of this thesis. So, special emphasis has been given on radon studies.

For this present thesis work we have used Alpha Guard radon monitor for measurement of radon concentration in water and air underground spaces (in basements and subways). For soil radon concentration measurement Barasol probe is used. **Chapter 4** contains description about the experimental set-ups and working process of these two instruments.

In **Chapter 5** studies about underground air radon exposure in and around Kolkata municipal corporation area at West Bengal, India has been discussed. In this work air radon concentration in basements and subways is measured. The total annual effective dose due to radon in basement air is also calculated.

Chapter 6 presents radon concentration measurement study of underground water in Bakreswar and Tantloi Geothermal Region, India. Statistical analyses of the data have been performed. To highlight the radon prone zones, 3D scatter plot and 2D surface plot have been presented. For, estimation of probable health risk annual effective dose due to ingestion and inhalation of water borne radon has been calculated. Possible origins of high radon concentrations have been indicated. Radon mitigation procedures have been discussed.

Chapter 7 deals with the groundwater radon measurement study conducted in Susunia hill area at Bankura, India. Like the previous study, also in this work we have measured the water radon concentration of large numbers of tube-wells of the study area. Correlations of radon concentration with tube-well depth and also with pH level of the tube-well water have been investigated in this chapter. Annual effective dose estimation has also been done.

In view of the findings about radon concentration in drinking water of Bankura District of West Bengal, India (discussed in **Chapter 7**) its seasonal variation is studied in selected tube-wells with concentration level low, medium and high and are discussed in **Chapter 8**. Possible reasons behind such seasonal variation have been discussed here. Seasonal water radon dose is also estimated for knowing the season in which the local people are in more danger.

In **Chapter 9** water radon concentration study in Ajodhya hill area at Purulia, West Bengal, India is given. We have chosen this area because this area has also same geological formations like Susunia hill area. Here also we have performed correlation and other studies that were done in **Chapter 7**. Excess Life time Cancer Risk (ELCR) has also been calculated in this research work.

In **Chapter 10** impacts of meteorological parameters on soil radon studied at Kolkata, India is discussed. In this work we have measured soil radon concentration, soil temperature, soil pressure, humidity, air temperature and rainfall. Correlation studies have been performed to find out the possible effects of these parameters on the fluctuations of radon concentrations. To assess simultaneous effects of all the parameters, multiparameter correlations on radon concentration have been investigated using machine learning (ML) techniques like Principal Component Regression (PCR), Support Vector Regression (SVR), Random Forest (RF) and Gradient Boosting Machine (GBM). Results indicating their relative performance have been discussed in this chapter.

The thesis ends with the concluding remarks and future directions of the present study in **Chapter 11**.

References

Al-Zoughool, M., & Krewski, D. (2009). Health effects of radon: a review of the literature. International journal of radiation biology, 85(1), 57-69.

Becker, K. (2004). One century of radon therapy. International journal of low radiation, 1(3), 333-357.

Degu Belete, G., & Alemu Anteneh, Y. (2021). General overview of radon studies in health hazard perspectives. Journal of Oncology, 2021.

George, A. C. (2008). World history of radon research and measurement from the early 1900's to today. In AIP Conference Proceedings (Vol. 1034, No. 1, pp. 20-33). American Institute of Physics.

Hogle, W. P. (2005). Surgeon General Releases National Health Advisory on Radon. Clinical Journal of Oncology Nursing, 9(2), 146.

Jobbágy, V., Altzitzoglou, T., Malo, P., Tanner, V., & Hult, M. (2017). A brief overview on radon measurements in drinking water. Journal of environmental radioactivity, 173, 18-24.

Khan, H. A. (1993). Usefulness of radon measurements in earth sciences. Nuclear Tracks and Radiation Measurements, 22(1-4), 355-364.

Khattak, N. U., Khan, M. A., Ali, N., & Abbas, S. M. (2011). Radon Monitoring for geological exploration: A review. Journal of Himalayan Earth Sciences, 44(2), 91-102.

Matos, C. R., Carneiro, J. F., & Silva, P. P. (2019). Overview of large-scale underground energy storage technologies for integration of renewable energies and criteria for reservoir identification. Journal of Energy Storage, 21, 241-258.

Miles, J. (2001). Temporal variation of radon levels in houses and implications for radon measurement strategies. Radiation Protection Dosimetry, 93(4), 369-375.

Neri, M., Ferrera, E., Giammanco, S., Currenti, G., Cirrincione, R., Patanè, G., & Zanon, V. (2016). Soil radon measurements as a potential tracer of tectonic and volcanic activity. Scientific Reports, 6(1), 24581.

Sukanya, S., Noble, J., & Joseph, S. (2022). Application of radon (222Rn) as an environmental tracer in hydrogeological and geological investigations: An overview. Chemosphere, 303, 135141.

Synnott, H., & Fenton, D. (2005). An evaluation of radon reference levels and radon measurement techniques and protocols in European countries. European Radon

Research and Industry Collaborative Concerted Action (ERRICCA2), European Commission Contract (FIRI-CT-2001-20142).

Thomas, J. W. (1972). Measurement of radon daughters in air. Health Physics, 23(6), 783-789.

Woith, H. (2015). Radon earthquake precursor: A short review. The European Physical Journal Special Topics, 224(4), 611-627.

Yoon, J. Y., Lee, J. D., Joo, S. W., & Kang, D. R. (2016). Indoor radon exposure and lung cancer: a review of ecological studies. Annals of occupational and environmental medicine, 28(1), 1-9.

Chapter – 2

Environmental Radioactivity Basics And Its Impact

Radioactivity

Radioactivity is a fascinating and complex phenomenon that has captivated scientists and the public alike for over a century. It refers to the spontaneous emission of energy and particles from the nucleus of an atom, a process that can lead to the formation of new elements and the release of energy. The discovery of radioactivity revolutionized our understanding of the nature of matter and energy, and has had profound implications for many areas of science, technology, and medicine.

2.1 Discovery of radioactivity and further researches

The discovery of radioactivity can be traced back to the late 19th century, when scientists were exploring the properties of atoms and their constituents. In 1896, French physicist **Henri Becquerel** discovered that certain uranium compounds emitted invisible, penetrating rays that could expose photographic film. This was the first indication of a new type of radiation, which was later named "radioactivity" by **Marie Curie**.

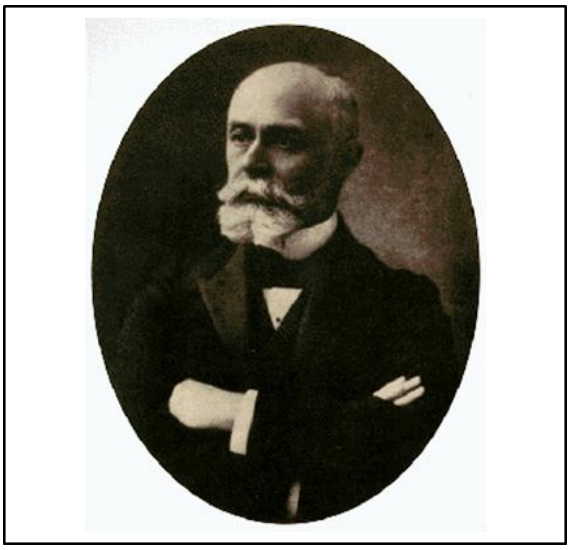

Fig. 2.1 Henri Becquerel

Becquerel's discovery was quickly followed up by the Polish-born French physicist **Marie Curie** and her husband **Pierre Curie**. Together, they discovered two new radioactive elements, polonium and radium. They isolated the new elements from uranium ore, and were able to show that they were highly radioactive. They along with Rutherford also that radioactivity was accompanied by the emission of three types of radiation: alpha particles, beta particles, and gamma rays.

Marie Curie developed a method for measuring the amount of radiation emitted by a substance using a device called electrometer. She also discovered that the radiation emitted by radium was able to kill cancer cells, and went on to develop the use of radiation therapy as a cancer treatment.

The **Curies** were awarded the Nobel Prize in Physics in 1903, along with **Becquerel**, for their work on radioactivity. **Marie Curie** went on to become the first person to be awarded two Nobel Prizes, receiving the Nobel Prize in Chemistry in 1911 for her work on the isolation and analysis of radium and polonium.

British physicist **Ernest Rutherford** discovered that radioactive decay involved the emission of alpha and beta particles from the nucleus of an atom. **Rutherford's** work led to the development of the concept of nuclear structure, and he was awarded the Nobel Prize in Chemistry in 1908 for his work on the disintegration of elements and the chemistry of radioactive substances.

The German physicist **Wilhelm Conrad Roentgen** also made important contributions to the study of radioactivity. In 1895, **Roentgen** discovered X-rays, a form of radiation that could penetrate solid objects and produce images of internal structures. **Roentgen's** discovery had a major impact on medicine and led to the development of X-ray machines for medical diagnosis.

In summary, the pioneers of radioactivity, including **Henri Becquerel, Marie Curie, Pierre Curie, Ernest Rutherford,** and **Wilhelm Conrad Roentgen**, made significant contributions to the understanding of this phenomenon and its applications in medicine and science. Their work laid the foundation for the development of nuclear physics and radiation therapy, which continue to be important areas of research today.

2.2 Radioactive decay

The radioactive decay process can be described by the following equation:

$$\frac{\boldsymbol{dN(t)}}{\boldsymbol{dt}} = -\boldsymbol{\lambda N(t)}$$

Alternatively, it can be expressed as:

$$\boldsymbol{N(t) = N_0 e^{-\lambda t}} \tag{2.1}$$

In this context:

N_0 represents the initial quantity of radioactive atoms in the sample

N(t) corresponds to the number of radioactive atoms at a specific time

λ is the decay constant of the radioactive element, indicating the probability per unit time that a given radioactive nucleus will undergo decay

This exponential equation illustrates that radioactive decay is inherently exponential in nature.

The concept of **half-life** ($t_{1/2}$) pertains to the time required for half of the initial quantity to decay. By substituting N ($t_{1/2}$) = $N_0/2$ into equation (1.1), we can derive the half-life as follows:

$$\boldsymbol{t_{1/2}} = \frac{\boldsymbol{ln2}}{\boldsymbol{\lambda}} \tag{2.2}$$

To visualize this decay process, a typical graph displaying the amount of radioactive particles in a sample over time is presented below.

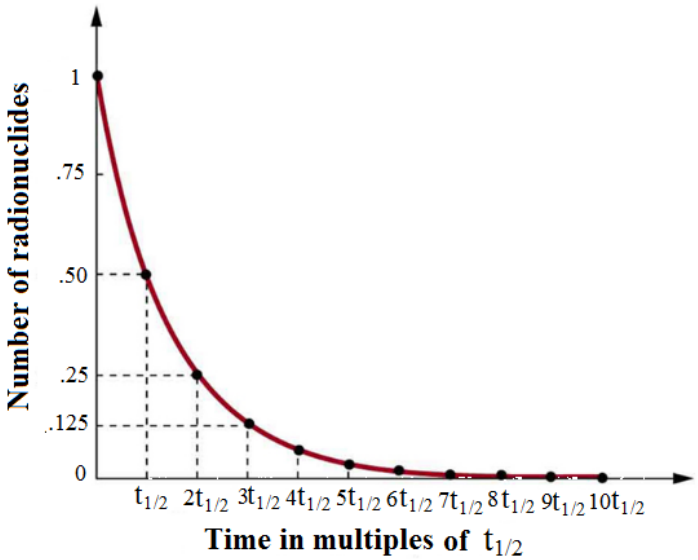

Fig. 2.2 Graphical representation radioactive decay process

Activity or Concentration

The activity in a radioactive decay process refers to the rate of disintegrations per unit time, or the frequency at which unstable atomic nuclei decay within a specific sample.

$$\boldsymbol{A(t)} = \frac{\boldsymbol{dN(t)}}{\boldsymbol{dt}} = \boldsymbol{\lambda\, N(t)} \tag{2.3}$$

This has the same exponential fall off with time as N(t).

2.3 Types of radiation

There are three main types of radiation: alpha, beta, and gamma radiation. Each type of radiation has different properties, and they interact with matter in different ways.

2.3.1 Alpha radiation

Alpha radiation is a type of ionizing radiation that consists of helium nucleus. Alpha particles are composed of two protons and two neutrons, making them relatively large and heavy compared to other forms of radiation, such as beta and gamma radiation. Due to their size, they carry significant kinetic energy (4-10 MeV). Because of their size and

charge alpha particles are relatively low in penetration and high in ionization, which can have both beneficial and harmful effects on biological organisms.

The primary concern with alpha radiation exposure is its potential for harm when it enters the human body. Inhaling or ingesting alpha-emitting materials can lead to the internal deposition of radioactive particles, which can irradiate surrounding tissues and organs, increasing the risk of cancer and other health problems.

To protect against alpha radiation, proper safety measures, such as containment, shielding, and personal protective equipment, should be used when handling alpha-emitting materials. When it comes to external exposure, alpha radiation is not a significant concern due to its limited penetration capability.

2.3.2 Beta radiation

Beta particles are high-energy electrons that are emitted by certain radioactive isotopes. They have a longer range than alpha particles and can penetrate through materials such as plastic, wood, and aluminum. However, they can be stopped by a few millimeters of lead or other heavy materials. Beta radiation can cause skin burns and other tissue damage if it contacts the skin, and can also be harmful if ingested or inhaled.

2.3.3 Gamma radiation

Gamma rays are high-energy photons that are emitted by the nucleus of an atom during radioactive decay. They have a very long range and can penetrate through most materials, including the layers of concrete and lead. Gamma rays are highly ionizing and can cause significant damage to living tissue, including DNA damage and radiation sickness. Shielding with thick layers of lead or concrete is required to protect against gamma radiation.

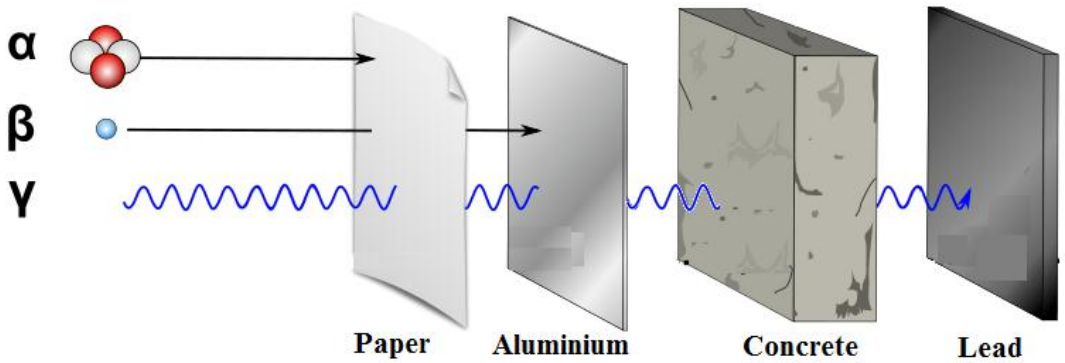

Fig. 2.3 Various decay products exhibit distinct levels of penetration

In addition to these three types of radiation, there are also other types such as neutron radiation, which is emitted during nuclear reactions, and cosmic radiation, which comes from space and can include high-energy protons and other particles.

2.4 Units of radioactivity

There are several units of measurement used to quantify the amount of radioactivity, including:

Becquerel (Bq): This is the SI unit of radioactivity and measures the number of radioactive decays per second.

1 Bq= 1 disintegrations per second

Curie (Ci): The curie (Ci) is a measure of radioactivity, equivalent to 3.7×10^{10} nuclear disintegrations or transformations per second. This quantity is roughly equivalent to the radioactivity emitted by one gram (1 g) of radium-226. The curie is named in honor of the pioneering scientists, Marie and Pierre Curie. This is a commonly used non-SI unit of radioactivity.

1 Ci = 3.7×10^{10} Bq

Rutherford (Rd): The rutherford (Rd) is a non-SI unit used to quantify radioactive decay. It is defined as the activity of a radioactive substance in which one million atomic nuclei undergo decay every second. As a result, it is equivalent to one mega-becquerel, and conversely, one becquerel is equal to one microrutherford. To put it in perspective, 1 Rd = 1×10^{6} Bq

2.5 Radioactive series

A radioactive series, also known as a radioactive decay chain or decay series, refers to a sequence of radioactive decays that occur in a particular order. It involves the transformation of one radioactive element into another through a series of nuclear decays. These series are often associated with heavy, unstable elements, typically found in the actinide and lanthanide series of the periodic table. This process can continue in a chain until a stable, non-radioactive element is reached. Radioactive decay series play a significant role in nuclear physics, geology, and radiometric dating.

There are three natural radioactive decay series:

1) **Uranium series** ($_{92}U^{238} \rightarrow {}_{82}Pb^{206}$)

2) **Actinium series** ($_{92}U^{235} \rightarrow {}_{82}Pb^{207}$)

3) **Thorium series** ($_{90}Th^{232} \rightarrow {}_{82}Pb^{208}$)

There is also an artificial radioactive series, called **Neptunium series** ($_{94}Np^{238} \rightarrow {}_{83}Bi^{209}$).

One of the most famous radioactive decay series is the uranium decay series, which starts with uranium-238 (U-238) and eventually ends with lead-206 (Pb-206). This series includes several intermediate steps, each involving the emission of alpha or beta particles. The full uranium decay series looks like this:

U-238 → Th-234, Th-234 → Pa-234m, Pa-234m → U-234, U-234 → Th-230, Th-230 → Ra-226, Ra-226 → Rn-222, Rn-222 → Po-218, Po-218 → Pb-214, Pb-214 → Bi-214, Bi-214 → Po-214, Po-214 → Pb-210, Pb-210 → Bi-210, Bi-210 → Po-210, Po-210 → Pb-206 (stable)

Each step in the series represents a specific nuclear decay, and the elements produced at each stage may have varying half-lives. The entire decay series can take a very long time to reach stability, with some isotopes having extremely long half-lives, spanning millions of years.

2.6 Radionuclide

A radionuclide, also known as a radioactive nuclide, radioisotope, or radioactive isotope, is a nuclide characterized by instability leading to its disintegration. Radionuclides can occur naturally or be artificially produced in various settings such as nuclear reactors, particle accelerators, or radionuclide generation. There are approximately 730 radionuclides with half-lives longer than 60 minutes, including 32 primordial radionuclides formed before the Earth's formation. Another 60 radionuclides are detectable in nature, either as descendants of primordial radionuclides or as products of natural production on Earth due to cosmic radiation. Additionally, over 2400 radionuclides have half-lives less than 60 minutes, mostly produced artificially with very short half-lives. In comparison, there are around 251 stable nuclides, with only 146 theoretically stable, while the other 105 are believed to undergo various decay processes (***Atwood 2013***).

Radionuclides exist for all chemical elements, with even the lightest element, hydrogen, having a well-known radionuclide, tritium. Elements heavier than lead, as well as technetium and promethium, exclusively exist as radionuclides. While some elements heavier than dysprosium theoretically exist solely as radionuclides, certain elements like gold and platinum are observationally stable.

Unintended exposure to radionuclides typically has harmful effects on living organisms, including humans, although natural low-level exposures occur without harm. The extent of harm depends on factors such as the nature and intensity of radiation, the amount and type of exposure (close contact, inhalation, or ingestion), and the biochemical properties of the element, with an increased risk of cancer being a common consequence. Despite these risks, radionuclides with suitable properties are deliberately used in nuclear medicine for both diagnostic and therapeutic purposes. An

imaging tracer incorporating radionuclides is termed a radioactive tracer, while a pharmaceutical drug utilizing radionuclides is referred to as a radiopharmaceutical.

2.6.1 Natural Radionuclides

Our natural environment is radioactive containing many radionuclides. Naturally occurring radionuclides on Earth fall into three distinct categories: primordial radionuclides, secondary radionuclides, and cosmogenic radionuclides.

Primordial radionuclides - Primordial radionuclides like uranium and thorium, originate from stellar nucleosynthesis and supernova explosions. While most radionuclides decay relatively quickly, some, such as uranium and thorium, have half-lives exceeding 100 million years, allowing them to persist in the present. Notably, bismuth-209, previously considered stable, was found to decay recently, prompting a reevaluation of its stability. Other nuclides may also exhibit delayed decay, expanding the roster of primordial radionuclides.

Secondary radionuclides - Secondary radionuclides emerge from the decay of primordial radionuclides like thorium-232, uranium-238, and uranium-235. Characterized by shorter half-lives, examples include natural isotopes of polonium and radium.

Cosmogenic isotopes - Cosmogenic isotopes exemplified by carbon-14, are continually formed in the atmosphere due to cosmic rays.

Many of these radionuclides, especially cosmogenic nuclides, exist in trace amounts in nature. The occurrence of secondary radionuclides is directly proportional to their half-lives, resulting in the rarity of short-lived ones. For instance, polonium is found in uranium ores at a mere 0.1 mg per metric ton (1 part in 10^{10}). Additional radionuclides may exist in nature in nearly undetectable amounts, stemming from rare events like spontaneous fission or uncommon cosmic ray interactions.

2.6.2 Application of radionuclides

Radionuclides find application in two primary ways: either for their radiation alone, or for the combination of their chemical properties and radiation, as observed in applications such as tracers and biopharmaceuticals (***Irvine 1949; Naftz et al. 2002, Qaim 2017***). In the realm of biology, carbon radionuclides act as radioactive tracers due to their close chemical resemblance to nonradioactive nuclides (***Kamen 2013***). This similarity allows for the examination of chemical, biological, and ecological processes, with a radiation detector like a Geiger counter revealing the incorporation sites of provided radioactive atoms. For instance, cultivating plants in an environment containing radioactive carbon dioxide enables the detection of radioactivity in plant parts that absorbed atmospheric carbon, aiding in monitoring processes like DNA replication and amino acid transport.

In physics and biology, radionuclide X-ray fluorescence spectrometry serves to determine the chemical composition of compounds. The radiation from a radionuclide source interacts with the sample, exciting characteristic X-rays that, when analyzed, reveal the chemical composition. This method is particularly useful in understanding proton numbers and concentrations of chemical elements.

Nuclear medicine employs radioisotopes for diagnostic, therapeutic, and research purposes. Radioactive tracers emitting gamma rays or positrons offer diagnostic insights into internal anatomy and organ function, utilized in imaging techniques like single-photon emission computed tomography (SPECT), positron emission tomography (PET) scanning, and Cherenkov luminescence imaging. Additionally, radioisotopes play a role in treating certain tumors and sterilizing medical equipments (***Qaim 2017***).

In various fields, radionuclides serve diverse purposes, including food preservation (***Akinloye 2015***), industrial applications (***Dash et al. 2013***), spacecraft energy generations (***Sanchez-Torres 2011***) and ecological studies (***Beaugelin-Seiller et al. 2019***). They also contribute to understanding stellar and planetary processes in astronomy, discovering new physics in particle physics, and dating rocks, minerals, and fossils in geology, archaeology, and paleontology. Radon is used for exploration of uranium mines, geothermal energy sources and other purposes.

2.7 Radioactive sources

Radioactive sources are materials that emit ionizing radiation due to the spontaneous decay of unstable atomic nuclei. These sources can be found in various natural and artificial forms and they play essential roles in medical, industrial, scientific, and energy applications. Here are some common types of radioactive sources:

2.7.1 Natural Radioactive Sources

Uranium and Thorium: Naturally occurring radioactive elements are found in soil, rocks, and minerals. They are the primary contributors to natural background radiation.

Radon Gas: A radioactive gas which is produced by the successive decay of uranium in soil and rocks. Radon can accumulate in buildings and contribute to indoor radiation exposure.

K-40: K-40 is a naturally occurring radioactive isotope of potassium, a common element found in the Earth's crust. It exists in trace amounts within the human body as potassium is an essential element for biological functions. The potassium content in food, including fruits and vegetables, contributes to the internal radiation dose received by individuals.

C-14: Carbon-14, commonly denoted as C-14, is a radioactive isotope of carbon. It is formed in the Earth's atmosphere. All organic matter (both plant and animal) contains radioactive carbon (^{14}C).

2.7.2 Manmade Radioactive Sources

Radioisotopes: Man-made radioactive isotopes are produced in nuclear reactors or particle accelerators. These isotopes are often used in medical, industrial, and research applications.

Nuclear Waste: Radioactive materials are generated as byproducts of nuclear power generation, industrial processes, and medical treatments. Proper management and disposal of nuclear waste are critical to prevent environmental contamination.

2.7.3 Industrial and Scientific Radioactive Sources

Radiography Sources: In non-destructive testing (NDT) applications, radioactive sources, often utilizing gamma rays, are used to inspect the internal structure of materials such as welds, pipelines, and industrial components.

Level Gauges: Radioactive sources, typically containing sealed radioactive materials, are used in industrial level gauges to measure the level of liquids in tanks. These are commonly used in the petrochemical industry.

Diagnostics in Oil Wells: Radioactive tracers can be introduced into oil wells to help monitor fluid flow and identify the presence of oil or gas. This aids in reservoir management and enhances oil recovery.

Smoke Detectors: Some smoke detectors use small amounts of americium-241, a radioactive isotope, to ionize the air in a chamber. This ionization is disrupted by smoke particles, triggering the alarm.

Nuclear Medicine: Radioactive isotopes are widely used in medicine for diagnostic imaging and treatment. Examples include technetium-99m for imaging and iodine-131 for thyroid treatment.

Research and Development: Radioactive sources are used in scientific research for various purposes, including studying the properties of materials, tracing biological processes, and conducting experiments in nuclear physics.

Radiation Therapy: In oncology, radioactive sources, such as cobalt-60 or linear accelerators, are used for external beam radiation therapy to treat cancer.

Neutron Sources: Some scientific applications, like neutron radiography or neutron activation analysis, use radioactive sources that emit neutrons for specific experiments.

2.7.4 Consumer Products

Tritium: A radioactive isotope of hydrogen used in self-luminous exit signs, watch dials, and certain novelty items.

2.7.5 Radiation Generators

X-ray Tubes: Devices used in medical diagnostics, industry, and research to generate X-rays for imaging purposes.

2.7.6 Power Sources for Space Exploration

Radioisotope Thermoelectric Generators (RTGs): Use the heat generated by the radioactive decay of isotopes, such as plutonium-238, to produce electrical power for spacecraft and deep-space probes.

It's crucial to manage and handle radioactive sources with care to prevent unnecessary exposure and contamination. Regulations and safety protocols are in place to ensure the safe use, transportation, and disposal of radioactive materials, minimizing the risks to human health and the environment.

2.8 Radioactive sources in different natural media

2.8.1 Natural radioactivity in air

Natural radioactivity in the air is primarily attributed to the presence of radioactive elements in air and their decay products (***Blifford et al. 1952; Rama and Honda 1961; Mathew et al. 2012***). These elements can emit ionizing radiation, contributing to the background radiation levels in the Earth's atmosphere. Key sources of natural radioactivity in the air include:

Radon Gas: Radon is a colorless, odorless, and tasteless radioactive gas that arises from the successive decay of uranium in the Earth's crust. It is a significant contributor to natural background radiation and is found in various concentrations in indoor and outdoor air. Radon can enter buildings from the ground and accumulate in enclosed spaces, posing potential health risks.

Thoron Gas: Thoron is another radioactive gas produced by the successive decay of thorium in the Earth's crust. Similar to radon, thoron can contribute to indoor air radioactivity and varies in concentration based on geological factors.

Decay Products: Radon and thoron undergo radioactive decay, producing a series of short-lived and long-lived decay products known as radon and thoron progeny. These decay products can attach to airborne particles and can be transported by air currents, contributing to natural radioactivity.

Cosmic Radiation: Cosmic radiation from space is another natural source of ionizing radiation in the atmosphere. High-energy particles, such as protons and other cosmic particles interact with atmospheric molecules, producing secondary particles and contributing to the overall background radiation.

Terrestrial Radiation: Radioactive isotopes present in the Earth's crust, such as potassium-40, contribute to natural background radiation in the air. Emanations from soil, rocks, and building materials can release radioactive particles into the air.

2.8.2 Natural radioactivity in soil

Natural radioactivity in soil is primarily a result of the presence of radioactive isotopes and their decay products within the Earth's crust (***Quindos et al. 1994; Abojassim and Rasheed 2021***). These radioactive elements contribute to the background radiation that surrounds us. Here are some key aspects of natural radioactivity in soil:

Uranium and Thorium and decay products: Uranium-238 (U-238) and thorium-232 (Th-232) are two naturally occurring radioactive elements found in varying concentrations in the Earth's crust. These elements undergo radioactive decay, producing a series of daughter isotopes, some of which are also radioactive. The decay products of uranium and thorium contribute significantly to natural radioactivity in soil. For example, radium, radon, and lead are some of the decay products that can be present in soil, influencing its radioactivity.

Potassium: Potassium-40 (K-40) is another radioactive isotope that contributes to natural radioactivity in soil. It is a naturally occurring isotope of potassium and undergoes both beta decay and electron capture.

Cosmic Radiation: Cosmic rays from space contribute to the production of certain radionuclides in the atmosphere, which eventually settle into the soil. The interaction of cosmic radiation with atmospheric gases and elements in the soil leads to the production of radionuclides like carbon-14.

Radon Gas: Radon, a radioactive noble gas, is produced as a series decay product of uranium. It can migrate from the soil to the air and can accumulate in enclosed spaces, posing potential health risks when inhaled.

Geological Variation: The geological composition of a region significantly influences the concentration of radioactive elements in the soil. Certain geological formations may have higher concentrations of uranium, thorium, or other radioactive elements, leading to variations in soil radioactivity.

2.8.3 The natural radioactivity in the ocean

The natural radioactivity in the ocean is primarily a result of the presence of certain radioactive isotopes that occur naturally in the Earth's crust and are released into the

ocean environment through various processes (***Livingston and Povinec 2000; Buesseler 2014***). Here are key contributors to natural radioactivity in the ocean:

Uranium and Thorium Series: Uranium-238 (U-238) and thorium-232 (Th-232) are naturally occurring radioactive elements found in the Earth's crust. These elements undergo radioactive decay, leading to the release of radionuclides into the environment, including the ocean.

Radium and Radon: Radium-226 (Ra-226) and radium-228 (Ra-228) are decay products of uranium and thorium, and they can be found in ocean water. Radon gas (Rn-222), another decay product, can be released from the ocean into the atmosphere.

Polonium: Polonium-210 is a successive decay product of Uranium-238 and is found in seawater. It can accumulate in marine organisms, particularly in the tissues of fish.

Potassium: Potassium-40 is a naturally occurring radioactive isotope that is part of the potassium found in seawater. It contributes to the overall radioactivity in the ocean.

Cosmic Radiation: Cosmic radiation from space can produce radionuclides in the atmosphere, which then enter the ocean through precipitation and atmospheric deposition.

Anthropogenic Contributions: While natural radioactivity dominates, human activities, such as nuclear weapons testing and accidents, may introduce artificial radionuclides into the ocean.

Sediment and Seabed Radioactivity: Radioactive isotopes can accumulate in marine sediments and the seabed over time. Some radionuclides present in the ocean may be adsorbed onto suspended particles and deposited on the ocean floor.

Oceanographic Processes: Ocean currents, mixing, and circulation play a role in distributing and redistributing radioactive substances in the ocean. Certain areas may exhibit higher concentrations due to localized geological and oceanographic conditions.

2.8.4 Radioactivity in Human body

Human body is naturally radioactive due to the presence of trace amounts of radioactive isotopes (***ICRP 1979; Rao 2012***). These isotopes are typically acquired through natural processes, such as ingestion, inhalation, and absorption from the environment. The primary radioactive isotopes found in the human body include:

Potassium: Potassium is an essential element for the body, and a small fraction of naturally occurring potassium is radioactive potassium-40. K-40 undergoes beta decay, contributing to the overall radioactivity within the body.

Carbon: Carbon is a fundamental element in organic molecules, and a small fraction of carbon in the atmosphere is radioactive carbon-14. Humans acquire C-14 through the consumption of plants and animals, and it becomes part of the body's carbon pool.

Other Radionuclides: Trace amounts of other radioactive isotopes, such as radon progeny, uranium, thorium, lead-210, polonium-210, and tritium, may also be present in the human body, acquired through various pathways.

While the human body is naturally radioactive, the levels of radioactivity are relatively low, and the associated radiation exposure is generally considered to be minimal and not harmful. The body has natural mechanisms to regulate and excrete certain radioactive materials. The overall radioactivity of the human body is often referred to as "background radiation.

Below are the approximated concentrations of radionuclides computed for a 70 kg adult, derived from data outlined in ICRP (International Commission on Radiological Protection) publication 30.

Table 2.1 Natural Radioactivity in human body (***ICRP 1979***)

Nuclide	Total mass of nuclide found in the body	Total activity of nuclide found in the body	Daily intake of nuclides
Uranium	90 µg	30 pCi (1.1 Bq)	1.9 µg
Thorium	30 µg	3 pCi (0.11 Bq)	3 µg
Potassium 40	17 mg	120 nCi (4.4 kBq)	0.39 mg
Radium	31 pg	30 pCi (1.1 Bq)	2.3 pg
Carbon 14	22 ng	0.1 µCi (3.7 kBq)	1.8 ng
Tritium	0.06 pg	0.6 nCi (23 Bq)	0.003 pg
Polonium	0.2 pg	1 nCi (37 Bq)	~0.6 fg

2.9 Radioactivity in other natural materials

2.9.1 Natural radioactivity in food

Natural radioactivity in food is primarily a result of the presence of radioactive isotopes that occur naturally in the environment (***Abojassim et al. 2016; Caridi et al. 2019; Yang et al 2021***). These isotopes can be absorbed by plants and animals through soil, water, and air, leading to varying levels of radioactivity in different food items. Here are some key points regarding natural radioactivity in food:

Potassium: Potassium (K-40) is an essential element for plants and animals, and potassium-40 is a naturally occurring radioactive isotope. K-40 is present in soil, water, and, consequently, in plants and animals. It contributes to the overall natural radioactivity in food.

Radionuclides in Soil: Radioactive elements like uranium, thorium, and radium present in soil can be absorbed by plant roots and incorporated into the food chain. Radionuclides from the soil can also accumulate in animals that graze or feed on plants.

Radon Gas: Radon, a radioactive noble gas, can be released from the soil and water and can dissolve into foods during processing or cooking. In particular, certain beverages, such as groundwater and natural spring water, may contain radon.

Cosmic Radiation: Cosmic radiation from space contributes to the natural radioactivity in the environment. Certain radionuclides produced by cosmic rays can settle on crops and become part of the food supply.

Seafood and Marine Products: Certain seafood and marine products may contain higher levels of natural radioactivity due to the presence of radionuclides in ocean water. For example, iodine-131 may be present in seaweed, and polonium-210 can be found in certain fish species.

2.9.2 Natural radioactivity in building materials

Natural radioactivity in building materials is primarily due to the presence of radioactive isotopes in the Earth's crust, which can be incorporated into various construction materials. These materials can emit ionizing radiation, contributing to the overall background radiation in indoor environments. Here are key points regarding natural radioactivity in building materials:

Uranium and Thorium Series: Uranium-238 (U-238) and thorium-232 (Th-232) are two naturally occurring radioactive elements found in the Earth's crust. These elements, along with their decay products, contribute to natural radioactivity in rocks, soils, and minerals used in building materials.

Radon Gas Emanation: Radon, a radioactive noble gas, is produced as a decay product of uranium and thorium. Building materials made from rocks or minerals with higher concentrations of uranium and thorium can release radon gas into indoor air, potentially leading to increased indoor radon levels.

Concrete and Bricks: Concrete and bricks are common building materials that may contain natural radionuclides. Aggregates used in concrete, such as limestone and granite, can have elevated levels of uranium, thorium, and their decay products.

Granite and Marble: Granite and marble, often used for countertops and flooring, can contain varying levels of radioactive isotopes. The concentration of natural radionuclides like uranium, thorium, and their radioactive decay products in these materials depends on the specific geological source.

Tiles and Ceramics: Tiles and ceramics may contain minerals, such as zircon, which can have higher concentrations of uranium and thorium. Glaze materials used in ceramics can also contribute to natural radioactivity.

Plasterboard and Gypsum: Some construction materials, including plasterboard and gypsum, may contain phosphogypsum as a byproduct of phosphate mining. Phosphogypsum can contain elevated levels of natural radionuclides, mostly uranium and radium.

2.9.3 Natural radioactivity in Fertilizers

Natural radioactivity in fertilizers can occur due to the presence of radioactive elements in the raw materials used to manufacture the fertilizers. The most common radioactive elements found in fertilizers are uranium (^{238}U), thorium (^{232}Th), and potassium-40 (^{40}K). These elements are naturally occurring and can be present in varying concentrations in minerals and rocks.

Uranium (^{238}U): Uranium is a radioactive element that can be present in phosphate rock, which is a common raw material for manufacturing phosphate fertilizers. The concentration of uranium in fertilizers depends on the source of the phosphate rock used.

Thorium (^{232}Th): Thorium is another radioactive element that can be found in some phosphate deposits. Like uranium, its presence in fertilizers is linked to the composition of the raw materials.

Potassium-40 (^{40}K): Potassium is an essential nutrient for plants, and potassium-containing fertilizers may contain a naturally occurring radioactive isotope, potassium-40. However, the radioactivity from K-40 is generally lower compared to uranium and thorium.

2.10 Radiation exposure to the Public

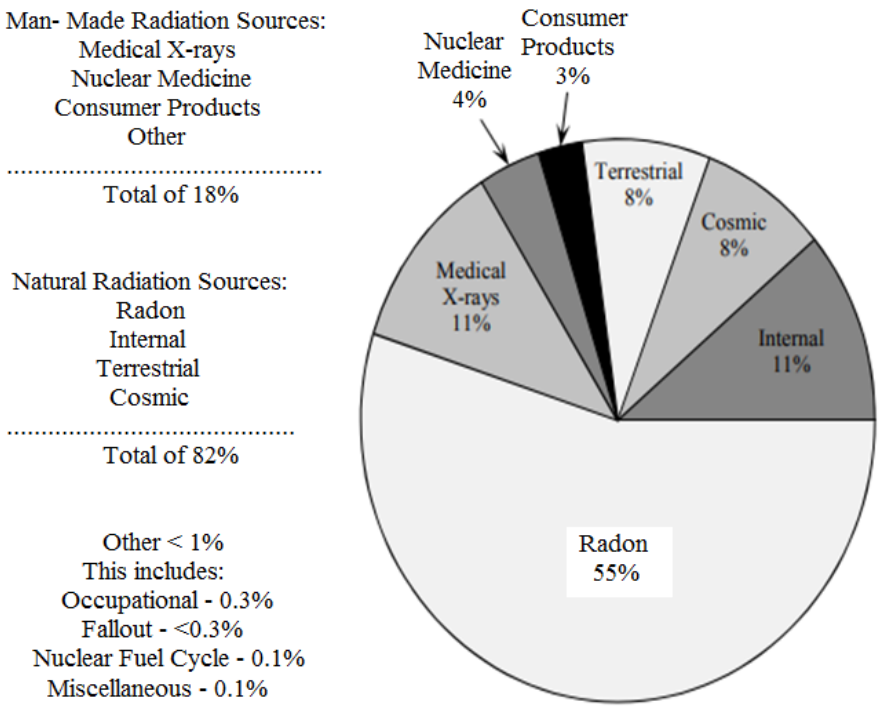

Fig. 2.4 Radiation exposure from various sources

2.11 Biophysical effects of radioactivity

The biophysical effects of radioactivity refer to the interactions between ionizing radiation and living tissues, encompassing a range of biological responses at the cellular and molecular levels. These effects can have significant implications for human health. Here are key biophysical effects of radioactivity:

The health effects of ionizing radiation are typically categorized into deterministic and stochastic effects.

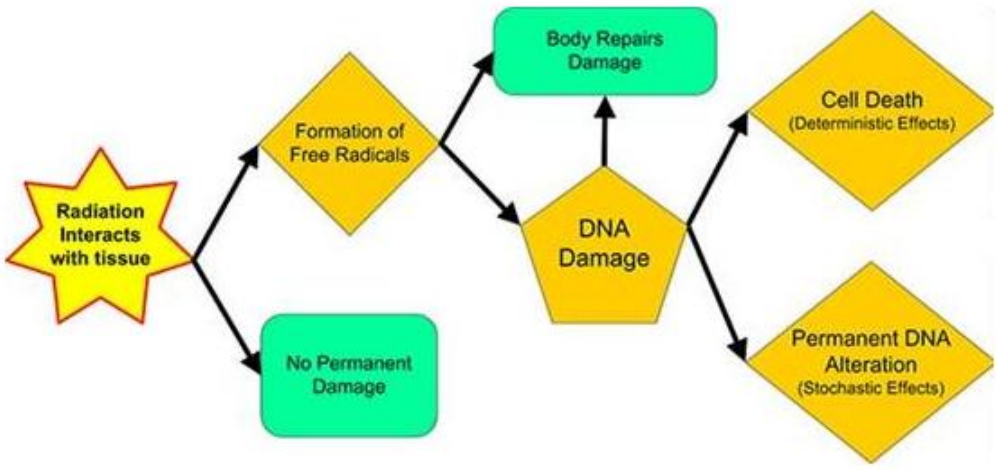

Fig. 2.5 Radiation – Deterministic and Stochastic Effects (***Peck and Samei 2017***)

2.11.1 Deterministic effect

A deterministic effect is a health impact that necessitates a particular level of exposure to ionizing radiation for it to manifest. The intensity of a deterministic effect escalates with the increase in exposure dose and involves a minimum threshold below which no clinically detectable effects occur. This category of effect is both predictable and reproducible, exemplified by consistent biological outcomes when certain body parts receive escalating localized doses. These effects stem from severe cell damage or death, and individuals encounter the physical repercussions when the cell demise reaches a magnitude sufficient to induce significant impairment in tissues or organs. They manifest as short-term adverse reactions in tissues, resulting from exposure doses significantly high enough to harm living tissues. For instance, administering increasing doses to specific areas of the body consistently leads to well-understood biological effects.

Some examples of deterministic effects include: Radiation-induced skin burns, Acute radiation syndrome, Radiation sickness, Cataracts, Sterility, Tumor Necrosis, Even death.

2.11.2 Stochastic effects

Stochastic effects encompass random occurrences with a probability factor. A particularly uncommon stochastic effect involves the emergence of cancer in a region or tissue exposed to radiation. The likelihood of this event is generally proportionate to the received dosage. Stochastic effects manifest even years after radiation exposure, having a latent period, with the severity unrelated to the original dosage. Given the presence of various environmental agents recognized as carcinogens, it is challenging in most instances to directly observed cancer cases to radiation exposure. When a population receives a single dose of ionizing radiation, predicting which individuals within that group might develop cancer, if at all, becomes impractical. It is also difficult to ascertain whether those who do develop cancer did so due to the ionizing radiation or other lifestyle factors, such as smoking.

Examples of stochastic effects include: Cancer, Heritable or genetic changes.

Understanding these biophysical effects is crucial for establishing radiation protection standards, developing medical radiation therapies, and managing environmental radiation exposure. Regulatory measures and safety practices aim to minimize the potential harmful effects of radioactivity on human health.

2.12 Radiation dose

Radiation damage is estimated by the quantity radiation dose. Dose basically refers to the amount of energy absorbed per unit mass of the exposed object. Different

dosimetric quantities have been defined for proper estimation of biological damage caused by radiation.

2.12.1 Absorbed dose

The absorbed dose (D) represents the amount of energy absorbed per unit mass of the irradiated object. Absorbed dose serves as a dose metric, quantifying the energy deposited in a substance by ionizing radiation per unit mass. Different materials exposed to the same radiation may absorb varying amounts of energy. This measure is pivotal in assessing dose absorption within living tissues, contributing to endeavors in radiation protection to mitigate adverse effects and in radiology, where potential benefits such as cancer treatment are explored. Additionally, absorbed dose finds utility in directly evaluating the impact of radiation on non-living entities, as exemplified in applications like radiation hardening. However, it does not encompass the biological effects of diverse radiations.

Rad: The rad serves as CGS unit for measuring absorbed dose, defined as the absorption of 100 ergs per gram of material. One rad represents the actual energy absorbed in any material, applicable to all types of radiation.

Gray (Gy): SI unit of absorbed dose is gray and equals 1 Joule/kg. It measures the actual energy absorbed in any material for any radiation type. While applicable to diverse radiations, it does not account for their varied biological effects. Frequently expressed in centi-gray, one gray is equivalent to 100 rads.

2.12.2 Equivalent dose

The equivalent dose (H_T) is based on the average absorbed dose in a tissue or organ (D_T), weighted by the radiation weighting factor (w_R) for the radiation(s) affecting the body, including radiation emitted by internal sources. It is calculated as the product of the absorbed dose ($D_{T,R}$) averaged over a tissue or organ (T) and the radiation weighting factor (w_R) for each radiation (***Equation 2.4***).

$$\boldsymbol{H_T = \sum_R w_R . D_{T,R}} \qquad 2.4$$

For practical purposes of assessing and regulating the hazards of ionizing radiation to workers and the general population, weighting factors are used. A radiation weighting factor is an estimate of the effectiveness per unit dose of the given radiation relative to low-LET standard. Radiation weighting factors are dimensionless multiplicative factors used to convert physical dose (Gy) to equivalent dose (Sv); i.e., to place biological effects from exposure to different types of radiation on a common scale (***Valentin 2003***).

Table 2.2 Radiation weighting factors (***ICRP 1991***)

Radiation Type and Energy Range	**Radiation Weighting Factor, W_R**
X and γ rays, all energies	1
Electrons positrons and muons, all energies	1
Neutrons:	
< 10 keV	5
10 keV to 100 keV	10
> 100 keV to 2 MeV	20
> 2 MeV to 20 MeV	10
> 20 MeV	5
Protons, (other than recoil protons) and energy > 2 MeV,	2-5
α particles, fission fragments, heavy nuclei	20

Rem: The rem is a unit of equivalent dose, often expressed in mrem. For gamma rays and beta particles, 1 rad of exposure results in 1 rem of dose.

Sievert (Sv): Represented as 1 Sv = 1 Gray × w_R, the sievert is a SI unit of equivalent dose, relating absorbed dose in human tissue to the radiation's effective biological damage. One sievert is equivalent to 100 rem.

2.12.3 Effective dose

The effective dose represents the calculated whole-body equivalent dose with the same stochastic risk as irradiation of individual organs of varying radio -sensitivity. It has units of Sv or rem and is defined by the following relationship:

$$\boldsymbol{E = \sum_T w_T . H_T} \qquad 2.5$$

w_T is the tissue weighting factor. The weighting factors are designed so that this effective dose supposedly represents the dose that the body could receive (uniformly) that would give the same stochastic risk as various organs getting different doses.

Table 2.3 Tissue weighting factors for different organs

Organs	**Tissue weighting factors (w_T)**		
	ICRP (1979)	***ICRP (1991)***	***ICRP (2008)***
Gonads	0.25	0.2	0.08
Red bone marrow	0.12	0.12	0.12
Colon	-	0.12	0.12
Lung	0.12	0.12	0.12

Stomach	0.15	0.12	0.12
Bladder	-	0.05	0.04
Breast	0.15	0.05	0.12
Liver	-	0.05	0.04
Oesophagus	-	0.05	0.04
Thyroid	0.03	0.05	0.04
Skin	-	0.01	0.01
Bone surfaces	0.03	0.01	0.01
Salivary glands	-	-	0.01
Brain	-	-	0.01
Remainder of body	0.3	0.05	0.12

2.12.4 Committed equivalent dose

To address ongoing irradiation of organs and tissues post-intake, the committed dose concept introduces the committed equivalent dose, H_T (τ) as the time integral of the equivalent dose-rate in a specific tissue (T).

$$\boldsymbol{H_T(\tau) = \int_{t_0}^{t_0+\tau} H_T(t)dt} \qquad 2.6$$

Where; t_0 is the time of intake, $H_T(t)$ is the equivalent dose rate at time t in organ or tissue T and τ is the time elapsed after an intake of radioactive substances. When τ is not specified, it will be taken to be 50 years for adults and to age 70 years for intakes by children.

2.12.5 Committed effective dose

The committed effective dose E(τ) for each internally deposited radionuclide is then calculated by summing the products of committed equivalent doses and appropriate w_T values for all irradiated tissues.

$$\boldsymbol{E(\tau) = \sum w_T . H_T(\tau)} \qquad 2.7$$

It's important to note that radiation exposure can have different effects depending on the type of radiation, the duration of exposure, and the specific tissues that are exposed. The dose and dose equivalent units described above are used to help quantify the potential risks associated with radiation exposure.

2.13 Radiation measurement detectors

Radiation measurement detectors are devices designed to detect and measure ionizing radiation. These detectors play a crucial role in various fields, including medicine, nuclear power, environmental monitoring, and occupational safety. There are different

types of radiation detectors, each with its specific characteristics and applications. Here are some common types of radiation measurement detectors:

Geiger-Muller Counters

Principle: Gas-filled detector that produces an electrical pulse when ionizing radiation interacts with the gas.

Applications: General radiation surveys, environmental monitoring, and detecting radioactive contamination.

Ionization Chambers

Principle: Measures the electrical charge produced by ionization of gas when radiation interacts with it.

Applications: Dosimetry in medical and industrial settings, as well as environmental monitoring.

Proportional Counters

Principle: Gas-filled detector that operates in the proportional region, providing information on the energy of the incident radiation.

Applications: Research in nuclear physics, radiation protection, and environmental monitoring.

Solid-State Detectors

Principle: Utilizes semiconductors to measure ionization caused by radiation.

Applications: Medical imaging, nuclear physics research, and radiation therapy.

Scintillation Detectors

Principle: Uses crystals or liquids that emit light (scintillation) when struck by ionizing radiation, and this light is then detected.

Applications: Medical imaging, environmental monitoring, and identifying specific radionuclides.

Dosimeters

Principle: Portable devices worn by individuals to measure personal radiation exposure over time.

Applications: Occupational radiation monitoring, especially for workers in nuclear facilities and medical settings.

Neutron Detectors

Principle: Detects neutrons, which are uncharged particles, using materials that undergo nuclear reactions with neutrons.

Applications: Nuclear power plants, neutron scattering experiments, and security screening.

Thermoluminescent Dosimeters (TLD)

Principle: Measures the light emitted when certain crystals are heated after being exposed to ionizing radiation.

Applications: Personal and environmental dosimetry, medical dosimetry, and radiation protection.

Optically Stimulated Luminescence (OSL) Detectors

Principle: Similar to TLD but uses light stimulation to measure stored energy.

Applications: Dosimetry in medical radiography, radiation therapy, and environmental monitoring.

These detectors are essential tools for ensuring safety in environments where ionizing radiation is present. They help monitor exposure levels, identify sources of radiation, and protect individuals from potential health risks associated with ionizing radiation. The choice of detector depends on the specific application, the type of radiation being measured, and the desired level of accuracy and sensitivity.

Table 2.4 List of detectors for analysis of environmental radionuclides

Emitted Radiation	Detector type
Alpha	(1) Silicon detector (2) Liquid scintillator (3) Ionization chamber (4) Proportional counter (5) GM counter (6) SSNTD (plastic detector)
Beta	(1) Gas-filled (air/Ar/Kr/Xe)detector (2) Liquid scintillator (3) Silicon detector (4) Crystal scintillator
	(1) Crystal scintillator

Gamma	(2) Germanium detector (3) GM counter

References

Abojassim, A. A., & Rasheed, L. H. (2021). Natural radioactivity of soil in the Baghdad governorate. Environmental Earth Sciences, 80, 1-13.

Akinloye, M. K., Isola, G. A., Olasunkanmi, S. K., & Okunade, D. A. (2015). Irradiation as a Food Preservation Method in Nigeria: Prospects and Problems. Int. J. Res. Appl. Sci. Eng. Technol, 3, 85-96.

Atwood, D. A. (Ed.). (2013). Radionuclides in the Environment. John Wiley & Sons.

Beaugelin-Seiller, K., Howard, B. J., & Garnier-Laplace, J. (2019). An approach to identifying the relative importance of different radionuclides in ecological radiological risk assessment: Application to nuclear power plant releases. Journal of environmental radioactivity, 197, 116-126.

Blifford, I. H., Lockhart Jr, L. B., & Rosenstock, H. B. (1952). On the natural radioactivity in the air. Journal of Geophysical Research, 57(4), 499-509.

Buesseler, K. O. (2014). Fukushima and ocean radioactivity. Oceanography, 27(1), 92-105.

Espinosa, G., & Moreno, A. (1980). Alpha detection by SSNTD's. In Solid State Nuclear Track Detectors (pp. 777-784). Pergamon.

ICRP (1979). Limits for intakes of radionuclides by workers. ICRP Publication 30 (Part 1). Ann. ICRP 2(3/4).

ICRP (1991). 1990 Recommendations of the International Commission on Radiological Protection. ICRP Publication 60. Ann. ICRP 21(1–3).

ICRP (2008). Radiation dose to patients from radiopharmaceuticals – Addendum 3 to ICRP Publication 53. ICRP Publication 106. Ann. ICRP 38(1/2).

Irvine Jr, J. W. (1949). Industrial Applications of Radionuclides. Analytical Chemistry, 21(3), 364-368.

Kamen, M. D. (2013). Radioactive tracers in biology: An introduction to tracer methodology (Vol. 1). Elsevier.

Livingston, H. D., & Povinec, P. P. (2000). Anthropogenic marine radioactivity. Ocean & Coastal Management, 43(8-9), 689-712.

Mathew, S., Rajagopalan, M., Abraham, J. P., Balakrishnan, D., & Umadevi, A. G. (2012). Natural radioactivity content in soil and indoor air of Chellanam. Radiation protection dosimetry, 152(1-3), 80-83.

Naftz, D., Morrison, S. J., Fuller, C. C., & Davis, J. A. (Eds.). (2002). Handbook of groundwater remediation using permeable reactive barriers: applications to radionuclides, trace metals, and nutrients. Academic Press.

Peck, D. J., & Samei, E. (2017). How to understand and communicate radiation risk. Image Wisely.

Qaim, S. M. (2017). Nuclear data for production and medical application of radionuclides: present status and future needs. Nuclear medicine and biology, 44, 31-49.

Quindos, L. S., Fernandez, P. L., Soto, J., Rodenas, C., & Gomez, J. (1994). Natural radioactivity in Spanish soils. Health physics, 66(2), 194-200.

Rama, M., & Honda, M. (1961). Natural radioactivity in the atmosphere. Journal of Geophysical Research, 66(10), 3227-3231.

Rao, D. D. (2012). Radioactivity in human body and its detection. Radiation Protection and Environment, 35(2), 57-58.

Sanchez-Torres, A. (2011). Radioisotope power systems for space applications. Radioisotopes Application in Physical Sciences, 1, 457-471.

Valentin, J. (2003). Relative biological effectiveness (RBE), quality factor (Q), and radiation weighting factor (wR): ICRP Publication 92. Annals of the ICRP, 33(4), 1-121.

Chapter – 3

Environmental Radioactivity: Experimental Studies

Environmental radioactivity in different materials: An experimental survey

Radioactivity measurements have been conducted on various materials, emphasizing the imminent threat to human society. The following sections delve into some of the important studies.

3.1 Building materials

Samples of natural and manufactured building materials collected from Algeria by Amrani and Tahtat (***2001***), are used to determine the concentrations of ^{226}Ra, ^{232}Th and ^{40}K in those materials. The specific concentrations of ^{226}Ra, ^{232}Th and ^{40}K of materials exhibited ranges of 12–65 Bq/kg, 7–51 Bq/kg and 36–675 Bq/kg respectively. To evaluate potential radiation hazards associated with using these materials in construction, radium-equivalent activities are computed for the analyzed samples.

This study presents the measurement of radioactivity levels of various building materials such as gypsum, ceramic, marble, and granite, either imported from neighboring countries in South Eastern Europe (Macedonia, Greece, and Bulgaria) or produced in Serbia Krstić et al. (***2007***). The measurements are conducted using an HpGe detector and a multichannel analyzer. The activity concentration index is calculated for each examined sample. For Macedonian and Bulgarian gypsum, the activity index ranges from 0.0297 to 1.2545 and 0.0376 to 0.1521 respectively. Regarding marble the activity index values for Macedonian, Greek, and Bulgarian samples are ranged from 0.0124 to 0.6245, 0.0104 to 1.2089 and 0.0162 to 0.6747 respectively. Additionally, for Greek ceramic and granite the activity index ranges between 0.3508 to 1.0152 and 0.0438 to 1.0062 respectively.

Mavi and Akkurt (***2010***) conducted a study to assess the radioactivity levels in building materials used in the Isparta region of Turkey. Using γ-ray spectrometry equipped with a NaI(Tl) detector connected to MCA, the radioactivity of specific building materials in this region is measured. The specific activity values for ^{226}Ra, ^{232}Th and ^{40}K in the selected building materials ranged from 17.91 to 58.88 Bq/kg, 6.77 to 19.49 Bq/kg and 65.72 to 248.76 Bq/kg respectively. To evaluate the radiation hazard posed by natural radioactivity in these materials, parameters such as absorbed dose rate in air (D), annual effective dose (AED), radium equivalent activities (R_{aeq}), and external hazard index (H_{ex}) are calculated.

3.2 Milk

Powdered infant milk, commonly known as infant formula, serves as a convenient and nutrient-rich alternative to human breast milk in numerous countries, constituting a fundamental source of essential minerals and proteins crucial for infant growth and

development. Despite its widespread use, there exists limited global data on the levels of radioactivity in infant powdered milk, necessitating a comprehensive evaluation of radiological health risks.

This paper presents the findings of radioactivity measurements for ^{90}Sr, ^{137}Cs, and ^{40}K in milk diet samples collected from 1965 to 1990 in Bombay, India by Shukla et al. (***1994***). The study reveals that the activity levels of ^{40}K in milk remained relatively constant. Regarding fallout radionuclides (^{90}Sr and ^{137}Cs), in milk samples showed average concentration levels ranging from <0.005 to 0.442 Bq/l.

In Malaysia, Uwatse et al. (***2015***) conducted a study aimed to assess radioactivity levels and associated doses in commonly consumed powdered infant milk. Four key radionuclides ^{226}Ra, ^{232}Th, ^{40}K, and ^{137}C are analyzed across 14 brands of powdered milk available to Malaysian infants, sourced from various regions worldwide. The mean activity concentrations for ^{226}Ra, ^{232}Th, ^{40}K, and ^{137}Cs are determined as 3.05 ± 1.84, 2.55 ± 2.48, 99.1 ± 69.5, and 0.27 ± 0.19 Bq/kg, respectively. Among the examined milk samples, the brand from the Philippines (Lactogen) exhibited a low level of radioactivity, while a Singaporean brand (S26 SMA Gold) showed the highest levels. The artificial radionuclide, ^{137}Cs, is nearly undetectable in the majority of the brands investigated. Estimated mean annual effective doses resulting from powdered milk consumption are 635.13 and 111.45 μSv/year for infants aged ≤1 year and 1–2 years, respectively. Notably, the obtained dose for infants ≤1 year old is significantly higher, while for infants aged 1–2 years, it is lower.

Thirty-three samples of powdered milk and thirteen samples of liquid milk, predominantly sourced from various countries, are obtained from the local market in Saudi Arabia by Alharshan et al. (***2017***). The purpose is to assess the levels of artificial and natural radionuclides and determine the safety of milk consumption for humans. Employing spectrometric analysis with the HPGe detector, the study revealed that the activity concentration of ^{40}K in powdered milk varied from 130 ± 7 to 595 ± 32 Bq/kg, with an average of 285 ± 29 Bq/kg. The ^{137}Cs activity concentration in powdered milk ranged between 0.05 ± 0.02 and 1.3 ± 0.2 Bq/kg. In the case of liquid milk, the activity concentration of ^{40}K ranged from 40 ± 2 to 98 ± 5 Bq/l, averaging 66 ± 4 Bq/l. Meanwhile, the concentration of ^{137}Cs in liquid milk is determined to be 0.12 ± 0.03 Bq/l.

3.3 Plant

The link between cigarette smoke and cancer has long been established. Smokers are ten times at greater risk of developing lung cancer than that of non-smokers. Tobacco fields and plants also have higher concentration of uranium and consequently large contents of ^{210}Po and ^{210}Pb belonging to uranium and radium decay series. These radionuclides have long association with tobacco plants. The alpha radioactivity of the leaves of the tobacco plants is measured using plastic track detectors LR-115 Type-II at

Inter University Accelerator Center (IUAC), New Delhi, India by Nain et al. (***2010***). This study reveals that the track density due to alpha particles is higher at bottom face as compared to top face of the leaves.

The concentrations of naturally occurring radioactive materials, including ^{226}Ra, ^{238}U, ^{232}Th, ^{40}K and ^{137}Cs are determined by Thabayneh and Jazzar (***2013***) in 44 plant samples collected from various locations in the northwestern region of the West Bank, Palestine. High-resolution gamma ray spectroscopy is employed for measurement. The activity concentrations of radionuclides in the examined plant samples varied, ranging from 7.5 to 157.6 Bq/kg with average of 48.3 Bq/kg for ^{226}Ra, 7.5 to 66.1 Bq/kg with average of 26.5 Bq/kg for ^{238}U, 1.8 to 48.5 Bq/kg with average of 10.1 Bq/kg for ^{232}Th, 14.3 to 1622 Bq/kg with average of 288.0 Bq/kg for ^{40}K and <0.1 to 4.7 Bq/kg with average of 2.2 Bq/kg for ^{137}Cs.

In this investigation, Kareem et al. (***2016***) assessed the inherent radiation levels in specific medicinal plants found in Iraq. Their aim is to ascertain the activity concentration, radium equivalent, and internal hazard index attributable to naturally occurring radionuclides ^{238}U, ^{232}Th, and ^{40}K. Gamma-ray spectroscopy is employed to determine the activity concentration. The results reveal that the concentrations for Uranium-238, Thorium-232, and Potassium-40 in the medicinal plants are 4.953 ± 0.37, 2.916 ± 0.12 and 219.134 ± 2.24 Bq/kg respectively. Radium equivalent values ranged from 6.081 ± 0.09 to 44.608 ± 0.46 Bq/kg, averaging 20.278 ± 0.38 Bq/kg. Furthermore, the internal hazard index values ranged from 0.016 to 0.135, with an average of 0.060.

The assessment of natural radioactivity concentration in rice serves as a crucial factor in gauging the potential population exposure resulting from the habitual consumption of food containing natural radionuclides. Various food types, including rice, inherently contain discernible levels of natural radioactivity, which subsequently enter the human body through the ingestion pathway. As rice is the predominant cultivated crop in Bangladesh and a staple in the Bangladeshi diet, investigations have been conducted by Nahar et al. (***2018***) to evaluate the natural radioactivity in rice. These study employed gamma-ray spectrometry to quantify radiation hazards associated with rice consumption. The average activity levels of natural radionuclides, namely ^{226}Ra, ^{228}Ra and ^{40}K in the rice samples are determined to be 1.09 ± 0.31, 0.17 ± 0.21 and 4.70 ± 1.59 Bq/kg respectively. The resulting estimated effective doses attributable to the consumption of rice for these respective radionuclides are 43.69, 16.39 and 4.15 μSv/y.

3.4 Coal ash

Coal ash is a byproduct of burning coal in power plants. The two primary types of coal ash are fly ash and bottom ash. The combustion of coal leads to the emission of a notable quantity of naturally occurring radionuclides into the atmosphere. Many

research efforts have focused on assessing the impact of Coal-fired Power Plants (CPPs) on atmospheric radioactive pollution.

Coal, including lignite, is gaining significance in meeting Turkey's growing energy demands. Gamma-ray spectroscopic techniques are employed by Aycik and Ercan (***1997***) to ascertain the levels of uranium, thorium, and potassium in coal and fly ash samples originating from the southwestern region of Turkey. For the lignite burned by Combined Power Plants (CPPs) in Yatağan and Milas (Muğla), the concentrations ranged from 4 to 25 ppm with an average of 16 ppm, 3 to 16 ppm with an average of 10 ppm and 218 to 596 ppm with an average of 49 ppm for uranium, thorium, and potassium respectively. In the ash fraction passing through the electrostatic precipitators, the concentrations varied from 21 to 43 ppm with an average of 35 ppm, 10 to 31 ppm with an average of 18 ppm, and 252 to 936 ppm with an average of 774 ppm for uranium, thorium, and potassium respectively. The concentration range for Radium-226 in lignite and fly ash samples is determined to be 2.3 to 14.0 pCi/g with an average of 9.1 pCi/g and 13 to 21 pCi/g with an average of 18 pCi/g, respectively.

The Figueira coal-fired power plant (CFPP) is identified among Brazilian CFPPs with elevated uranium concentrations. Gamma-ray spectrometry is employed to assess the contents of ^{238}U, ^{226}Ra, ^{210}Pb, ^{232}Th and ^{40}K in samples of pulverized coal, furnace bottom ash and fly ash by Flues et al. (***2006***). Concentrations of natural radionuclides in pulverized coal ranged from 813 to 2609 Bq/kg for the U series and 22 to 40 Bq/kg for ^{232}Th. Fly ash exhibited concentrations ranging from 1442 to 14641 Bq/kg for the uranium series, with a consistent enrichment factor observed for ^{238}U, ^{226}Ra and ^{232}Th.

The levels and behavior of naturally occurring primordial radionuclides, including ^{238}U, ^{226}Ra, ^{210}Pb, ^{232}Th, ^{228}Ra, and ^{40}K, in coals and fly ashes are measured by Papastefanou (***2008***). The activity concentrations of the examined coals from Greek coal mines ranged from 117 to 435 Bq/kg for ^{238}U, 44 to 255 Bq/kg for ^{226}Ra, 59 to 205 Bq/kg for ^{210}Pb, 9 to 41 Bq/kg for ^{228}Ra and 59 to 227 Bq/kg for ^{40}K. For the examined fly ashes produced in Greek coal-fired power plants, concentrations ranged from 263 to 950 Bq/kg for ^{238}U, 142 to 605 Bq/kg for ^{226}Ra, 133 to 428 Bq/kg for ^{210}Pb, 27 to 68 Bq/kg for ^{228}Ra and 204 to 382 Bq/kg for ^{40}K. The results indicate an enrichment of radionuclides in fly ash relative to the input coal during the combustion process, with enrichment factors (EF) ranging from 0.60 to 0.76 for ^{238}U, 0.69 to 1.07 for ^{226}Ra, 0.57 to 0.75 for ^{210}Pb, 0.86 to 1.11 for ^{228}Ra and 0.95 to 1.10 for ^{40}K.

Gamma spectrometry was employed to measure the natural radioactivity in coal fly ash and natural pozzolan Portland cement samples manufactured in Spain by Sanjuán et al. (***2020***). The activity concentrations of ^{226}Ra, ^{232}Th and ^{40}K varied between 15.7 to 88.3 Bq/kg, 12.8 to 81.0 Bq/ kg, and 37.0 to 678.0 Bq/kg respectively. Assessments of radiological hazards stemming from the natural radioactivity are conducted through the determination of the activity concentration index (I), absorbed dose rate (D_{ext}), and annual effective dose (E_p). The calculated values fell within the range of 0.20 mSv to

0.87 mSv for coal-cement and 0.18 mSv to 0.50 mSv for pozzolan-cement, satisfying the threshold criterion of ≤ 1 mSv.

3.5 Chemical fertilizer

The concentrations of radioactivity in various chemical fertilizers—triple superphosphate (TSP), single superphosphate (SSP), diammonium phosphate (DAP), phosphogypsum, muriate of potash (MOP), urea, zinc sulfate, and zinc oxysulfate—utilized in the agricultural soil of Bangladesh are assessed through gamma spectrometry employing a high purity germanium (HPGe) detector by Alam et al. (***1997***). In the analyzed fertilizer samples, ^{226}Ra exhibited a range of 4.8 ± 0.8 to 323.8 ± 24.4 Bq/kg, ^{228}Th ranged from 3.4 ± 1.7 to 22.0 ± 2.8 Bq/kg and ^{40}K ranged from 7.9 ± 2.4 to 12,628.5 ± 169.0 Bq/kg. The study also determined the radium-to-thorium ratio, with the ^{226}Ra/^{228}Th ratio spanning from 0.237 to 18.69.

Kim and Cho (***2022***) conducted a research to study e radioactive concentrations in fertilizers of nitrogen, calcium, sulfur, phosphate acid, and potassium chloride fertilizers which are the most widely used fertilizers in Korea. In the nitrogen fertilizer, concentrations of ^{137}Cs, ^{134}Cs, and ^{40}K were found to be 3.49 ± 5.71 Bq/kg, 34.43 ± 7.61 Bq/kg, and 569.16 ± 91.15 Bq/kg, respectively, with no detection of ^{131}I. The calcium fertilizer exhibited the highest concentration of ^{137}Cs at 5.74 ± 4.40 Bq/kg, along with 22.37 ± 5.39 Bq/kg of ^{134}Cs and 433.67 ± 64.24 Bq/kg of ^{40}K, while ^{131}I is not detected. The sulfur fertilizer showed concentrations of ^{40}K, ^{134}Cs, ^{137}Cs and ^{131}I at 347.31 ± 55.73 Bq/kg, 19.42 ± 4.53 Bq/kg, 2.21 ± 3.49 Bq/kg and 0.04 ± 0.22 Bq/kg respectively. In the phosphoric acid fertilizer, the highest concentration of ^{40}K is observed at 70,007.34 ± 844.18 Bq/kg, along with 46.07 ± 70.40 Bq/kg of ^{134}Cs, while neither ^{137}Cs nor ^{131}I is detected. Potassium chloride fertilizer showed concentrations of ^{40}K and ^{134}Cs at 12,827.92 ± 1542.19 Bq/kg and 94.76 ± 128.79 Bq/kg, respectively, with no detection of ^{137}Cs or ^{131}I.

3.6 Food

Food items may contain traces of radioactive materials, both from natural sources and potential nuclear emergencies. Radioactive substances may adhere to vegetables and fruits through deposition from the air or rainwater. Abojassim et al. (***2016***) aimed to assess the specific activity and annual effective dose resulting from the consumption of vegetables and fruits obtained from the local market in Najaf governorate, Iraq. The natural radioactivity of the samples is measured using a gamma ray spectrometer. The findings revealed that the average specific activities in vegetable samples for ^{238}U, ^{232}Th, and ^{40}K are 5.21, 4.76, and 186.15 Bq/kg, respectively. In fruit samples, the average specific activities for ^{232}Th and ^{40}K are 2.53 and 211.64 Bq/kg, respectively. The estimated total average annual effective doses in vegetable samples for adults, children (10 years old), and infants are 0.117, 0.122, and 0.179 mSv/y, respectively. For fruit

samples, the total average annual effective dose for adults, children (10 years old), and infants are 0.141, 0.295, and 0.388 mSv/y, respectively.

This article presents a thorough investigation conducted to assess the levels of natural radioactivity in a variety of food sources in Italy by Caridi et al. (***2019***)., including animal and plant-based items such as meat, fish, milk and derivatives, legumes, cereals and derivatives, fruits, vegetables, and vegetable oils. The study focuses on different feeding regimes and is targeted at individuals aged 17 years and above. A total of 85 samples of Italian origin are subjected to HPGe gamma spectrometry, sourced from major retailers in the years 2014, 2015, and 2016. The investigation focused on the specific activity of ^{40}K, yielding the following mean values: (106.3 ± 6.9) Bq/kg for bovine, swine, and sheep meat; (116.5 ± 9.7) Bq/kg for fish; (52.9 ± 3.1) Bq/kg for milk and derivatives; (271.9 ± 16.7) Bq/kg for legumes; (67.2 ± 4.7) Bq/kg for cereals and derivatives; (52.7 ± 4.4) Bq/kg for fruit; (72.9 ± 5.6) Bq/kg for vegetables; (83.9 ± 6.5) Bq/kg for hortalizas; all lower than the minimum detectable activity for vegetable oils. Among animal foods, fish exhibited the highest mean ^{40}K activity concentration, while among vegetable foods, legumes displayed the highest concentration. An assessment of dose levels associated with typical Mediterranean, Vegetarian, and Vegan diets is conducted, revealing annual effective doses of 0.16 mSv/y, 0.41 mSv/y, and 0.54 mSv/y, respectively.

To assess the radiological hazard to human health associated with the consumption of radionuclides in food, various plant-based foods cultivated in the mining region are gathered and subjected to analysis in China (***Yang et al. 2021***). Findings revealed that concentration level of ^{210}Pb varies between 8.1–150 Bq/kg and concentration level of ^{228}Ra varies between 0.3–4.2 Bq/kg) in local foods. The annual committed effective doses for children (3.1 mSv/y) and adults (1.3 mSv/y) from the ingestion of these local foods may surpass the recommended reference threshold of 1 mSv/y (***UNSCEAR 2000***).

In this thesis radioactivity measurement has been performed on soil, air and water. So, special emphasis has been given on the discussion of radioactivity analysis of soil, air and water.

3.7 Water and its radiological pollution

Water, the essence of life, is a remarkable and indispensable substance that plays an integral role in shaping our planet and sustaining all forms of life. Comprising two hydrogen atoms bonded to a single oxygen atom (H_2O), water's simple molecular structure belies its complex and diverse properties. Water is a universal solvent, capable of dissolving a wide range of substances, making it an essential agent in various chemical and biological processes. Its polarity results in hydrogen bonding, which contributes to its high surface tension and remarkable cohesive and adhesive properties. These qualities enable capillary action, allowing water to defy gravity as it climbs through narrow channels in plants and soil. The three primary states of water—solid (ice), liquid, and gas (vapor)—facilitate an intricate cycle known as the water cycle

or hydrologic cycle. This cycle encompasses processes such as evaporation, condensation, precipitation, and runoff, which collectively redistribute water across the Earth's surface, replenishing ecosystems, filling aquifers, and powering the intricate mechanisms of weather patterns. Water has a profound impact on climate regulation. Oceans, with their vast heat-absorbing capacity, help regulate global temperatures by absorbing and releasing heat over time. This mitigates extreme temperature fluctuations, creating more hospitable conditions for life. The abundance of water on Earth is striking, with about 71% of the planet's surface covered by oceans, seas, lakes, and rivers. However, freshwater, which accounts for only about 2.5% of this water, is the critical resource that sustains terrestrial life. The availability of freshwater varies across regions and is influenced by factors such as precipitation patterns, geological formations, and human activities. Unfortunately, water resources are under increasing pressure due to population growth, industrialization, agriculture, and climate change. Ensuring access to clean and safe drinking water for all has become a global challenge, with many regions facing scarcity and contamination issues.

3.7.1 Source of water

Water sources are essential components of our planet's ecosystem, providing the life-sustaining resource that is vital for the existence of all living organisms. These sources encompass a wide range of natural reservoirs from which we obtain water for various purposes, including drinking, irrigation, industrial processes, and recreation. Here, we'll explore some of the primary types of water sources:

3.7.1.1 Surface water bodies

Rivers and Streams: Rivers and streams, flowing bodies of water that originate from various sources such as springs, snowmelt, and rainfall, serve as important sources of freshwater for communities and ecosystems. They are also often utilized for transportation and energy generation through hydropower.

Lakes and Ponds: These are larger standing bodies of freshwater formed through various geological processes, including tectonic activity, glacial activity, and volcanic activity. Lakes and ponds can serve as reservoirs for drinking water, provide habitat for diverse aquatic life, and offer recreational opportunities.

Reservoirs: Reservoirs are artificially created bodies of water formed by damming rivers for purposes like water supply, flood control, and energy generation. Reservoirs store water that can be released as needed to meet various demands.

3.7.1.2 Groundwater sources

Aquifers: Underground layers of porous rock or sediment that hold significant amounts of water from aquifers. Rainwater infiltrates through the soil and accumulates in these

underground reservoirs. Aquifers are tapped through wells for drinking water and irrigation.

Underground Springs: Springs are natural sources of water that emerge from the ground, often originating from aquifers. They can be a reliable source of freshwater for both human and ecological needs.

3.7.1.3 Glaciers and Ice Caps

Glaciers and ice caps store a massive amount of Earth's freshwater in the form of ice. As ice melts, it contributes to surface water bodies and groundwater systems, sustaining water availability during dry seasons.

3.7.1.4 Rainwater

Rainwater is a direct source of freshwater that falls from the atmosphere to the ground. It can be collected and stored for various uses, especially in regions with limited access to other water sources. Collecting and storing rainwater for immediate or future use is a practice that dates back centuries. Rainwater harvesting systems can range from simple containers to complex catchment systems.

3.7.1.5 Desalination

Desalination is the process of converting seawater into freshwater through methods like distillation or reverse osmosis. It's a critical source of water in regions where freshwater scarcity is a pressing issue.

3.7.1.6 Atmospheric Water

Atmospheric moisture can be captured using technologies like fog collectors or dew condensers, providing a localized source of freshwater in certain climates.

Safeguarding and managing these water sources is of paramount importance for sustaining ecosystems, supporting human populations, and ensuring water security. Pollution, over-extraction, and climate change pose significant challenges to the availability and quality of these water sources. Sustainable water management practices, conservation efforts, and technological innovations are crucial for maintaining the health of our planet's water sources for generations to come.

3.7.2 Aquifer

We mostly use ground water derived from aquifers. Beneath the Earth's surface lies a hidden world of interconnected underground reservoirs known as aquifers. These vast geological formations serve as natural storage units for water, playing a crucial role in sustaining ecosystems, communities, and industries worldwide. Aquifers are layers of permeable rock or sediment that have the ability to store and transmit water. These

formations can range in size from relatively small pockets to massive underground expanses. The porosity and permeability of the materials within an aquifer dictate its capacity to hold and allow water to flow through. Porosity refers to the volume of void spaces within the rock or sediment, while permeability indicates the ease with which water can move through those spaces. Visual representation of groundwater presence in rock formations is given in **Figure 3.1**.

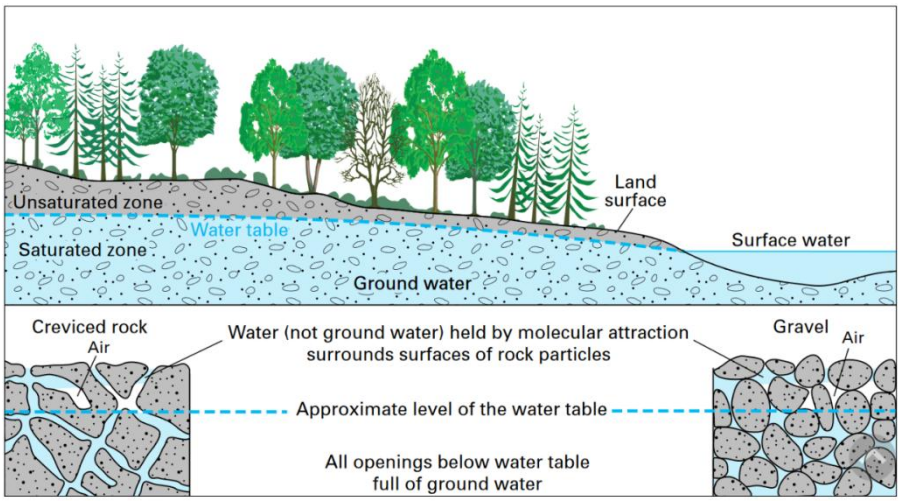

Fig. 3.1 Presence of Groundwater within Rock Formations (modified after ***USGS 2019***)

Types of Aquifers: There are two primary types of aquifers: unconfined and confined. Unconfined aquifers, often found near the surface, have an open upper boundary that is influenced by factors like precipitation and evaporation. Confined aquifers, on the other hand, are surrounded by impermeable layers that restrict the movement of water into or out of the aquifer. The pressure within confined aquifers can be substantial, causing water to rise in wells without any pumping—a phenomenon known as artesian flow.

Role and Importance: Aquifers play a vital role in maintaining water availability, especially in regions where surface water sources like rivers and lakes may be scarce or unreliable. They store significant amount of freshwater that accumulate over time through processes like precipitation and infiltration. This stored water is gradually released to springs, streams, wells, and other surface water bodies, ensuring a consistent flow of water even during dry periods. Communities rely on aquifers for various purposes, including drinking water supply, irrigation for agriculture, and industrial processes. Proper management of aquifers is essential to prevent over-extraction, which can lead to groundwater depletion, land subsidence, and other environmental issues. Monitoring and understanding the recharge rates of aquifers are critical for sustainable water management.

Challenges and Concerns: As human populations grow and water demand increases, aquifers face new challenges. An aquifer is defined as a rock capable of effectively transmitting water to wells and springs. Wells can be drilled into aquifers to extract

water. Over time, precipitation contributes water (recharge) into the porous rock of the aquifer. However, the rate of recharge isn't uniform across all aquifers, and this aspect must be taken into account when drawing water from a well. Climate change can impact precipitation patterns, affecting the recharge rates of aquifers. Extracting water too rapidly from an aquifer depletes its water content, causing the well's water yield to diminish progressively and even potentially run dry. Interestingly, excessive pumping from one's well could even impact the neighbor's well if they both rely on the same aquifer. Pollution from agricultural runoff, industrial activities, and urban development can contaminate groundwater, rendering it unsafe for consumption. Additionally, over-pumping of aquifers in coastal areas can lead to the lowering of the water table and the intrusion of saltwater into freshwater aquifers—a phenomenon known as saltwater intrusion.

3.7.3 Radiological water pollution

Radiological water pollution, also known as radiological contamination of water, refers to the presence of radioactive materials in natural water sources such as rivers, lakes, groundwater, and oceans. This type of pollution occurs when radioactive substances, which emit ionizing radiation, are released into the environment and find their way into aquatic ecosystems. Radiological pollution can have significant environmental, human health, and socio-economic consequences, making it a matter of considerable concern and regulatory attention.

Key aspects of radiological water pollution:

Sources of Contamination: Radiological contamination of water can originate from various sources, including nuclear power plants, nuclear weapons testing, industrial facilities handling radioactive materials, nuclear accidents, and the improper disposal of radioactive waste. Natural sources, such as radon gas from underground rock formations, can also contribute to radiological contamination.

Radioactive Substances: The radioactive materials that can potentially contaminate water include various radioactive isotopes of elements such as uranium, thorium, radium, and radon. These substances can enter water bodies through natural processes or human activities. These radioactive materials emit ionizing radiation, which can damage living organisms and pose health risks.

Environmental Impact: Radiological pollution can harm aquatic ecosystems by disrupting the balance of life in water bodies. It can negatively affect aquatic plants, animals, and microorganisms, potentially leading to the loss of biodiversity. Contaminated water can also impact the food chain, as radioactive materials may accumulate in aquatic organisms and be transferred to higher trophic levels.

Human Health Concerns: Human exposure to radiologically contaminated water can occur through consumption of contaminated seafood, drinking water, and even through

recreational activities like swimming or boating. Prolonged exposure to radiation can increase the risk of various health problems, including cancer, genetic mutations, and other radiation-related illnesses. Governments and international organizations have established strict regulations and guidelines to monitor and control radiological contamination of water. These measures include regular testing of water quality, setting permissible limits for radioactive substances, and implementing emergency response plans in case of nuclear accidents or other incidents. Addressing of radiological contamination in water often involves remediation efforts, such as the removal of contaminated sediments, the construction of containment structures, and the treatment of water to reduce radiation levels. Cleanup can be a complex and costly process, requiring long-term monitoring and management. Raising public awareness about the risks associated with radiological water pollution is crucial. Education campaigns help individuals understand the importance of water quality and encourage responsible practices in handling and disposing of radioactive materials.

In conclusion, radiological water pollution poses a multifaceted challenge that impacts ecosystems, human health, and the environment. Effective monitoring, regulation, and remediation efforts are essential to mitigate its adverse effects and protect both aquatic ecosystems and human populations from the hazards of radioactive contamination in water.

3.7.4 Measurement of radon concentration in groundwater: A survey

Radon is most often found as contaminant of water we use. Elevated level of radon in water can cause several health hazards including cancer. Numerous studies have assessed radon concentration in groundwater on a global scale over decades. Some of these investigations carried out in the last 25years or so are discussed here.

In Jordan, Al-Bataina et al. (***1997***) conducted a research regarding the concentration of radon in various natural water sources. The ^{222}Rn concentrations spans from 3.3 to 10.7 Bq/l in cold spring water, 3.2 to 5.5 Bq/l in hot spring water, 3.1 to 5.7 Bq/l in well water, 2.5 to 4.7 Bq/l in drinking water, and 4.3 to 6.3 Bq/l in sea water. Importantly, the observed radon levels in Jordanian water fall within the United States Environmental Protection Agency recommended MCL of 11.1 Bq/l (***USEPA 1991***), indicating no unusual concentrations.

In their study, Amrani et al. (***2000***) investigated the levels of ^{222}Rn in 25 groundwater samples gathered from various locations in Tassili, Algeria. The ^{222}Rn content in these samples varied from 0.50 to 19.37 Bq/l. Notably, only one sample surpassed the USEPA recommended MCL of 11.1 Bq/l. Interestingly, the analysis revealed no discernible linear correlation between radon concentrations in the samples and the respective temperatures or well depths.

Horvath et al. (***2000***) conducted a research to assess radon concentration in thermal water samples from the northern region of Venezuela. The determined concentrations ranged from 1 to 560 Bq/l. Dose calculations indicated that regular consumption of the measured water samples could result in an additional radiation dose of up to 4 mSv/y.

In 2003, D'Alessandro and Vita conducted a study focusing on radon level measurements in 119 groundwater samples within the volcanic region of Mount Etna, situated on the eastern coast of Sicily. They utilized a portable scintillation chamber for their research and found that the radon concentration in these samples varied from 1.8 to 52.7 Bq/l. What's noteworthy is that approximately 40% of these samples exceeded the USEPA proposed MCL of 11.1 Bq/l. Interestingly, the highest concentrations of radon are discovered in the eastern sector of the volcano, which is seismically active, while the south-western sector, also seismically active and prone to magmatic degassing, exhibited lower radon levels. The researchers noted that the concentration of ^{222}Rn is positively correlated with the content of the parent elements in aquifer rocks.

In another study conducted by Choubey et al. in 2003, they conducted a radon measurement survey in groundwater within the Doon Valley, located in the Outer Himalayas of India. Their primary objective is to understand how radon concentration in groundwater is influenced by various factors, including hydrodynamic conditions, the presence of radium in underlying rocks, soil porosity, and permeability. They collected 34 groundwater samples from hand-pumps and tube-wells located in three distinct hydrogeological regions within the eastern segment of the Doon Valley. The radon measurements in tube-wells and hand-pumps ranged from 25.4 ± 1.8 to 92.5 ± 3.4 Bq/l, with an average concentration of 53.5 ± 2.6 Bq/l. All the samples have exceeded the USEPA proposed MCL of 11.1 Bq/l. Notably, they observed a significant positive correlation between radon concentration and well depth in the Doiwala-Dudhli and Jolleygrant areas. This suggests that radon concentration tends to increase with drilling depth in areas primarily composed of younger Doon gravels. Conversely, samples from the Ganga catchment exhibited a negative correlation, indicating higher radon levels at shallower depths in the Ganga catchment, which comprises alluvial terraces of the Ganga basin. This suggests the presence of uranium-rich sediments at these shallow depths. They have also revealed that elevated radon concentrations in well water can impact indoor radon levels when used as a household water source.

Sonkawade et al. (***2004***) conducted a study at the Nuclear Science Centre (NSC) in Delhi, India premises to assess radon levels in indoor air and tube-well water samples, which are used for drinking by NSC residents. They employed AlphaGuard to quantify radon concentrations. The measured radon levels in all water samples remained relatively consistent, ranging from 1645 Bq/m^3 to 3869 Bq/m^3. Even after de-ionization, radon concentrations in the water samples remained in the range of 1569 Bq/m^3 to 2213 Bq/m^3. Although the pH values of the water samples are measured, there is no observable correlation between radon concentration and water pH. Importantly, all measured radon levels in drinking water are found to be well below the recommended

levels by The United Nations Scientific Committee on the Effects of Atomic Radiation of 40 Bq/l (***UNSCEAR 2000***), ensuring minimal health risks to NSC residents.

A groundwater radon concentration measurement in Extremadura, Spain has been conducted by Galan et al. (***2004***). The samples are categorized based on their source, including wells, springs, or spas. Radon levels exhibit a broad spectrum, ranging from 0.151 - 1168 Bq/l. All samples surpassed the Minimum Detectable Activity (MDA), with spa samples displaying the highest radon levels. Alarmingly, nearly 33% of Extremadura's analyzed waters exceeded the WHO recommended reference level of 100 Bq/l. An examination of the hydrogeological characteristics of each sampling site revealed that approximately 72% of samples surpassing the WHO recommended reference level, are associated with granitic areas. This study suggests a strong correlation between radon concentrations and granite.

This study presents the measurements of radon activities in various types of natural waters in the Santos region of Brazil (***Marques et al. 2004***). A Makrofol E polycarbonate plastic detector was utilized for this purpose. The measured radon concentrations exhibited a range of 0.95 to 36.00 Bq/l for ground waters, 0.30 to 0.54 Bq/l for sea waters, 0.39 to 0.47 Bq/l for tap waters, 0.43 to 2.40 Bq/l for river waters. Additionally, for water from the Santos/São Vicente public water supply the determined radon concentration is 2.35 Bq/l.

Villalba et al. (***2005***) presented findings from a study on the concentrations of ^{222}Rn in ground and drinking water in nine cities located in Chihuahua State, Mexico. Among the 114 wells sampled, approximately 50% exhibited ^{222}Rn concentrations exceeding the USEPA prposed MCL of 11.1 Bq/l. Additionally, around 48% of tap water samples collected from 255 households showed radon concentrations surpassing the MCL. Interestingly, the study revealed a noticeable correlation between the levels of total dissolved solids and radon concentration in groundwater. These elevated levels of ^{222}Rn are attributed to the geological composition of the aquifer rocks.

A study conducted by Xinwei in 2006 presents findings from measurements of radon concentrations in drinking water sourced from both the municipal water supply system and private wells located in Baoji, China. A total of 69 samples are collected and analyzed. The average radon concentration in tap water is 12 kBq/m^3, with a maximum recorded value of 18 kBq/m^3. In contrast, well water showed a higher average radon concentration of 41 kBq/m^3, with a maximum value of 127 kBq/m^3. Further investigation revealed variations in radon concentrations in well water based on the depth of the wells. Specifically, shallow wells (with depths less than 10 meters) had an average radon concentration of 24 kBq/m^3, middle wells (with depths ranging from 10 to 30 meters) showed an average of 34 kBq/m^3, and deep wells exhibited the highest average radon concentration at 56 kBq/m^3. The observed radon concentrations in drinking water are found to contribute to indoor radon levels within the range of 2.8% to 13.2% of the average indoor radon concentration in Shaanxi. Additionally, the

estimated effective dose to individuals from inhaling radon released from household water ranged from 0.03 to 0.14 mSv/yr.

Yalim et al. (***2007***) have conducted a study to assess the concentrations of ^{222}Rn in well waters located near the Afyonkarahisar fault zone and its surrounding areas. Afyonkarahisar is situated in the mid-western region of Anatolia, Turkey, in proximity to the Akşehir fault zone. This region, characterized by its geological activity, has been known to experience earthquakes ranging from 3.0 to 7.1 on the Richter scale. Samples are meticulously analyzed using a Packard Tri-Carb 2770TR/SL model liquid scintillation analyzer. The results of this analysis revealed ^{222}Rn concentrations ranging from 0.7 to 31.7 Bq/l.

A significant portion of Lebanon's population depends on springs and wells as their primary sources of drinking water. Considering this dependency Abdallah et al. (***2007***) investigated variations in dissolved radon levels in water supplies, primarily focusing on potential radiation-related health risks. The research utilized the E-PERM method to measure ^{222}Rn levels in water from various locations across Lebanon, ranging from sea level to 1200 meters above sea level and spanning diverse geological formations. The findings revealed a wide range of dissolved radon concentrations, with the lowest recorded at 0.91 Bq/l in a coastal well and the highest at 49.6 Bq/l in a spring located in a mountainous area. Among the 20 sampled sites, only five exhibited radon levels exceeding the MCL level of 11.1 Bq/l, primarily concentrated in regions near well-known geological fault zones. A preliminary estimate of the national average radon level is approximately 11.4 Bq/l. Overall, the study concluded that the determined radon concentrations fell well below the reference level of 100 Bq/l proposed by World Health Organization (***WHO 2004***).

Shiva et al. (***2007***) conducted a research focused on assessing the concentrations of ^{222}Rn in potable waters sourced from different locations in the Bangalore, India using the emanometry method. A total of 94 groundwater (bore well) samples are scrutinized, revealing ^{222}Rn concentrations ranging from 5.3 to 283.4 Bq/l, with a mean value of 87 Bq/l. The effective dose varied between 42.6 and 2280.2 μSv/y, with an average of 702.5 μSv/y.

A study conducted by Cosma et al. in 2008 focuses on radon concentration measurements in natural waters within Romania's Transylvania region. The measurements employed the LUK-VR system, which utilizes a Lucas cell to measure radon gas. Due to the substantial number of water samples collected (1511 samples) for analysis, a brief counting time was necessary, resulting in measurements taken during a non-equilibrium state between radon and its decay products. The results indicate that radon concentrations fall within the range of 0.5 to 129.3 kBq/m^3, with an average concentration of 15.4 kBq/m^3 across all water types examined in this survey.

Radon and thoron concentrations are assessed in the soil gas, ground water, and indoor air within the Budhakedar region of Tehri Garhwal, India by Prasad et al. (***2008***). Observed radon levels in groundwater are ranging from 8 - 3005 Bq/l.

This study presents findings on both passive and active radon levels in indoor air and drinking water across Cyprus and Greece, specifically in Attica and Crete (***Nikolopoulos*** and ***Louizi 2008***). The investigation includes exposure–dose estimations. In Cyprus, radon concentrations in drinking water varied from 0.3 - 20 Bq/l, while in Greece, they ranged between 0.8 - 23 Bq/l. This study revealed that radon emerges as the primary contributor to exposure and dose in both the Greek and Cypriot populations.

In 2009 Oner et al. conducted a study to find out the levels of radon concentrations in both drinking water and river water. The research focused on water samples collected within the city of Amasya, located in the inland regions of the Middle Black Sea area in Turkey, as well as from the Yeşilırmak River flowing through the center of Amasya city. The analysis revealed that the concentrations of radon in Amasya's tap water, spring water, and the Yeşilırmak River water ranged from 0.42 ± 0.14 to 2.4 ± 0.32 Bq/l, 0.39 ± 0.19 to 1.17 ± 0.21 Bq/l and 0.28 ± 0.04 to 1.08 ± 0.30 Bq/l, respectively. Based on this data, the estimated average effective dose equivalent from radon in tap water is 5.87 μSv/y.

Ramsar stands as one of the world's most prominent regions characterized by elevated background radiation levels. This heightened natural radioactivity primarily stems from the presence of the ^{238}U natural series and its subsequent decay products, notably ^{226}Ra and ^{220}Rn, which have been brought to the surface through the hot springs water. A research done by Mowlavi et al. (***2009***), focused on quantifying the radon concentration in 14 drinking water sources within the Ramsar area, utilizing the PRASSI system for measurement. The findings indicate that all of the examined water sources exhibit radon concentrations exceeding 10 kBq/m^3. Additionally, an assessment is conducted to estimate the average annual radiation dose incurred by the public due to radon in water.

The study focused on evaluating the levels of uranium and radon in water samples obtained from hand pumps, natural sources, and wells in specific regions of Upper Siwaliks, Northern India (***Singh et al. 2009***). The α-scintillometry method is utilized to estimate radon concentrations in the water samples, resulting in values ranging from 0.87 ± 0.29 to 32.10 ± 1.79 Bq/l. Despite these individual assessments, no direct correlation was identified between the uranium and radon concentrations in the water samples from Upper Siwaliks.

A study about the effect of meteorological parameters on radon concentration in borehole air and water have been conducted by Smetanová et al. (***2010***) at Modra-Piesok, Slovakia. The research focused on investigating the fluctuations in the concentration of ^{222}Rn in both borehole air and water within a borehole drilled in

cracked quartzite. The study also explored the potential correlations with meteorological parameters. This paper presents the results of a comprehensive investigation spanning two and a half years, shedding light on the dynamic behavior of radon in borehole water under various meteorological conditions. Notably, rainfall had a significant impact on radon concentration in water within the borehole. This effect was particularly pronounced during the spring and summer months. The decrease in radon content in borehole water adhered exclusively to the radioactive decay law during the spring and summer.

A research done by Khattak et al. (***2011***) focused on the analysis of 36 drinking water samples obtained from various sources, including taps, boreholes, and deep tube wells, within the University of Peshawar's Main Campus and its adjacent areas in Pakistan. Radon content in these water samples is determined using the RAD7 electronic device. The study revealed that these water samples exhibited an average radon concentration of 8.8 ± 0.8 Bq/l, with a maximum value of 18.2 ± 1.0 Bq/l and a minimum value of 1.6 ± 0.3 Bq/l. Of particular concern, 11 of the analyzed drinking water samples exceeded the USEPA proposed MCL of 11.1 Bq/l. Furthermore, this study estimated the annual effective dose resulting from radon exposure in water through both ingestion and inhalation for individuals. Importantly, all samples in this study exhibited annual effective doses lower than the WHO recommended reference level of 0.1 mSv/yr. Additionally, the research identified a positive correlation between radon levels and the depth of the water sources within the region.

Yalcin et al. in 2011 have measured radon concentration in drinking water samples at Kastamonu, Turkey .The study involved assessing the levels of ^{222}Rn in natural spring and tap water samples collected from, during both spring and summer seasons. The primary objectives are to create a geographical representation of radon concentrations in the region's water sources and to evaluate any potential radiological risks to the local population. Radon measurements are conducted using an AlphaGUARD radon gas analyzer. For natural springs, radon concentrations in spring ranged from 0.39±0.02 to 12.73±0.39 Bq/l and in summer ranged from 0.50±0.09 to 19.21±1.00 Bq/l. For tap water, radon concentrations in spring ranged from 0.36±0.04 to 9.29±0.45 Bq/l and in summer ranged from 0.31±0.03 to 13.14±0.38 Bq/l. Additionally, this study also involved calculating the radiation doses resulting from the consumption of these water sources. The estimated effective dose equivalents, attributed to the ingestion of ^{222}Rn present in these waters ranged between 0.80 to 49.09 μSv/y in spring and 0.93 to 32.54 μSv/y in summer.

Radon measurements are carried out by Akar et al. (***2012***) on water samples obtained from 27 wells and 19 taps supplied by these wells within the city of Bursa, Turkey. The analysis is conducted using the AlphaGUARD PQ 2000 PRO radon gas analyzer, covering various geological formations in the region. The recorded radon concentrations exhibited a range of 1.46 to 53.64 Bq/l for well water and 0.91 to 12.58 Bq/l for tap water. Among all of the samples, only 7 exceeded the USEPA recommended MCL of 11.1

Bq/l. Generally, all measured concentrations remained significantly below the WHO proposed reference level of 100 Bq/l. Additionally, assessments are made to determine the doses resulting from the consumption of water with these radon levels. The calculated annual mean effective doses associated with ^{222}Rn intake through water consumption ranged from 0.02 μSv/y as a minimum to 1.11 μSv/y as a maximum.

In Novi Sad, Serbia Todorovic et al. (***2012***) provide an analysis of radon activity measurements in water samples collected from various sources, including public drinking fountains, bottled drinking water, and tap water. The measurements are conducted utilizing the RAD 7 radon detector, a product manufactured by DURRIDGE COMPANY Inc. Notably, one of the water samples yielded a corrected radon concentration value that exceeded the WHO recommended reference level of 100 Bq/l.

Al Zabadi et al. (***2012***) have assessed radon levels in drinking water sources within Nablus city, with the goal of informing a comprehensive water management policy for Palestine. Water samples collected from four wells and five springs that supply water to the residents of Nablus city. Additionally, within the city's seven regions, three samples collected from tap in each residential area. In the case of the old city, ten samples are collected. Radon concentration measurements are conducted using the RAD 7 device produced by Durridge Company. The determined radon concentration in the water sources (well and spring) are ranging from 1.5 to 23.4 Bq/l with an average of 6.9 Bq/l. For residential tap water across the seven regions, the radon concentrations are ranging from 0.9 to 1.3 Bq/l with an average of 1.0 Bq/l. In the case of the old city, the radon concentration values are ranging from 0.9 to 3.9 Bq/l with an average of 2.3 Bq/l.

Radon concentrations in water from springs and hand pumps in the Kumaun Himalaya region of India were quantified using the radon emanometry technique by Bourai et al. (***2012***). The measured radon concentrations ranged from 1 to 392 Bq/l, with an average concentration of 50 Bq/l in groundwater across various lithotectonic units. It was observed that radon levels were higher in areas characterized by granite, quartz porphyry, schist, and phyllites, whereas the lowest radon levels were recorded in regions dominated by sedimentary rocks, particularly quartzite formations.

An extensive investigation is conducted on groundwater and soil samples collected from diverse locations in the vicinity of Mysore city, India by Chandrashekara et al. (***2012***). The analysis revealed that the ^{222}Rn concentration in groundwater exhibited variations between 4.25 and 435 Bq/l, with an average of 25.9 Bq/l. The estimated mean values for inhalation and ingestion doses resulting from ^{222}Rn in water are determined to be 65.2 and 5.43 μSv/y, respectively.

Rani et al. (***2013***) conducted a study, specifically for investigate radon concentration in groundwater samples (intended for drinking purposes) from hand pumps in various districts of northern Rajasthan, India including Sri Ganganagar, Hanumangarh, Sikar, and Churu. Results indicated that radon concentrations in the sampled groundwater

ranged from 0.5 ± 0.3 Bq/l (Chimanpura) to 85.7±4.9 Bq/l (Khandela), with an average value of 9.03±1.03 Bq/l. Almost 89% of the samples exhibited radon concentrations well below the USEPA proposed MCL. Furthermore, the research evaluated the annual effective dose in the stomach and lungs per person. The estimated total annual effective dose for adults ranged from 1.34 to 229.68 μSv/y. Notably, the total annual effective dose from three locations in the studied area exceeded the WHO recommended reference dose limit of 0.1 mSv/y.

Radon levels are assessed in water samples obtained from the Hanumangarh district in Rajasthan, India by Duggal et al. (***2013***). Utilizing the RAD7, an electronic radon detector manufactured by Durridge Company Inc., measurements are conducted. The radon concentrations in these samples exhibited a range from 1.6 ± 0.6 to 5.4 ± 0.7 Bq/l, with a mean value of 3.3 ± 1.1 Bq/l. The recorded radon concentration values are observed to fall well within the USEPA proposed MCL of 11.1 Bq/l. Additionally, this research encompassed an evaluation of the annual effective dose for both ingestion and inhalation. The estimated total effective dose spanned from 4.29 to 14.47 μSv/y. Importantly, the total effective dose across all locations within the studied area is found to remain within the WHO recommended reference limit of 0.1 mSv/y.

Erdogan et al. (***2013***) conducted an assessment of radon concentration measurement in16 well water samples representing various depths and aquifer types in the city center of Konya, located in Central Turkey. The radon concentrations of the well water samples, collected during the spring and summer seasons of 2012, are determined using a radon gas analyzer (AlphaGUARD PQ 2000PRO). For the spring season, radon concentrations ranged from 2.29±0.17 to 27.25±1.07 Bq/l, while for the summer season, they ranged from 1.44±0.18 to 27.45±1.25 Bq/l. The findings indicate that radon concentration levels in the water are seasonally dependent and exhibit slight variations with depth. Among the 16 well water samples, 11 had radon concentration levels below the USEPA proposed MCL of 11.1 Bq/l. Importantly, all measured radon concentration levels are well below the WHO proposed reference limit of 100 Bq/l. To assess the potential health impact of consuming this water, effective doses are calculated. The calculated effective doses ranged from a minimum of 0.29 μSv/y to a maximum of 5.49 μSv/y.

Concentrations of ^{222}Rn in drinking water samples collected from Beijing City, China, are determined using a straightforward method involving continuous radon monitoring by Wu et al. (***2014***). This method utilized a radon-in-air monitor combined with an air-water exchanger. In total, 89 water samples are collected and subjected to analysis for their Rn content. The recorded radon levels spanned from the detection limit to as high as 49 Bq/L with an average of 5.87 Bq/l. The average annual effective dose resulting from the ingestion of radon in drinking water is found to be 2.78 μSv/y, while the inhalation of radon emanating from water accounted for 28.5 μSv/y. This study concludes that the significant radiological hazard does not primarily arise from the

ingestion of waterborne radon but rather from the inhalation of radon gas escaping from the water.

Elevated levels of radon in water pose an increased risk to human health. To assess this risk, concentrations of ^{222}Rn are analyzed in 56 samples of drinking water from areas adjacent to the Rafsanjan fault, Iran during the autumn of 2013 by Malakootian et al. (***2014***). The recorded radon concentrations ranged from 0 to 18.480 Bq/l. For adults and children, the highest annual effective doses were 181.5 μSv/y and 248.95 μSv/y respectively, while the lowest recorded doses were zero for both age groups. Notably, radon concentration is observed to be greater on the right side of the fault compared to the left side. As a mitigation measure, they have recommended to ventilate the water before use in order to lower radon concentration levels.

An investigation is performed by Krishan et al. (***2015***) to determine the distribution of radon concentration within groundwater samples collected from the East coast of West Bengal, India. The ^{222}Rn levels in 20 groundwater samples are assessed using the Durridge RAD-7 instrument, revealing values ranging from 1.9 ± 0.78 to 9.0 ± 1.13 Bq/l, with an average concentration of 5.0 ± 0.83 Bq/l. It is noteworthy that these measurements fall comfortably below the USEPA proposed MCL of 11.1 Bq/l.

Srinivasa et al. (***2015***) have conducted a radon measurement study to analyze radon concentration in 27 water samples from Hassan district in Karnataka, India using emanometry technique, and the physicochemical parameters were assessed using standard methods. The concentrations of ^{222}Rn in the water sapmples ranged from 0.85 ± 0.2 to 60.74 ± 2.5 Bq/l, with an average concentration of 26.5 ± 1.65 Bq/l. This investigation reveals that 66% of the water samples exceeded the MCL of 11.1 Bq/l. Furthermore, there is no significant correlation observed between radon concentration and the physicochemical parameters. Importantly, the average annual effective ingestion doses from all the samples are below the WHO proposed dose limit of 0.1 mSv/y.

A research work done by Rangaswamy et al. (***2016***) presents the distribution of radon activity concentration in drinking water samples and their annual effective dose exposure in Shimoga district in Karnataka, India. The radon concentrations in 38 drinking water samples are measured by using Emanometry technique. The measured radon concentration in drinking water samples ranged between 3.10 ± 0.25 and 38.50 ± 1.54 Bq/l with an average value of 13.60 ± 1.12 Bq/l. This study reveals that 44.8 % drinking water samples analyzed have radon levels in excess of the MCL of 11.1 Bq/l. The total mean annual effective doses of all the samples are significantly lower than the WHO proposed reference level of 0.1 mSv/y.

Al-jnaby (***2016***) conducted a research to assess the radon level in drinking water originating from various regions in Hilla, the central region of Babylon, Iraq, using a RAD7 detector. Measured radon levels are varied between 0.0361 ± 0.00014 to 0.193 ±

0.0211 Bq/l with a mean of 0.115 ± 0.048 Bq/l. The estimated average annual effective dose is 0.413 mSv/y.

Radon concentration measurements are conducted by Inácio et al. (***2017***) on 33 water samples collected from wells at various depths and types of aquifers in Covilhã's County, Portugal, using the DURRIDGE RAD7 radon gas analyzer. Out of the total samples 23 yielded values exceeding 100 Bq/l, with the highest measured value reaching 1690 Bq/l.

Radon concentrations were assessed in 95 groundwater samples gathered from 28 villages and towns within the Hisar district of Haryana, India (***Sharma et al. 2017***). The measurements are conducted using RAD7, an electronic solid-state alpha detector produced by Durridge Company Inc. The recorded mean radon concentrations in the water samples varied between 1.4 ± 0.3 and 13.3 ± 4.1 Bq/l. Notably, the mean radon levels at three locations surpassed the MCL of 11 Bq/l. Additionally, this research also included an evaluation of the annual effective dose resulting from ingestion and inhalation. The total annual effective dose stemming from the ingestion and inhalation of radon in drinking water ranged from 13.7 to 130.3 μSv/y.

Radon levels are assessed in 59 groundwater samples gathered within the Fatehabad district of Haryana, India by Duggal et al. (***2017***). The measurements are conducted using the RAD7. The recorded radon concentrations spanned from 1.4 to 22.6 Bq/l. Notably, 14% of the groundwater samples exceeded the MCL of 11.1 Bq/l. Furthermore, this study also examined the annual effective dose resulting from radon ingestion and inhalation. The cumulative annual effective dose due to both radon ingestion and inhalation from drinking water ranged between 14.1 to 221.8 μSv/y.

In this research, Moreno et al. (***2018***) conducted measurements of indoor air and tap water radon (^{222}Rn) levels across various locations on the Giresun University campus, Turkey. Radon concentrations in tap water samples are observed within the range of 0.98 Bq/l to 27.28 Bq/l. It is noteworthy that the measured radon levels are found to be well below the WHO recommended reference level of 100 Bq/l. The calculated effective dose values fell within the ranges of 9.9–150.4 μSv/y for ingestion and 0.97–14.84 μSv/y for inhalation. Moreover, the assessment of excess lifetime cancer risk (ELCR) yielded an estimated value of 0.54%.

The concentration of natural radioactivity, including isotopes such as ^{226}Ra, ^{232}Th, ^{40}K, as well as radon (^{222}Rn), has been investigated in drinking water samples collected from the Baling area of Kedah, Malaysia (***Ahmad et al. 2018***). The analysis of radon concentration was carried out using a RAD-7 detector, encompassing 10 tap water samples and 7 well water samples. The observed ^{222}Rn concentration varied between a minimum and maximum range of 1.9 ± 0.31 Bq/l and 11.9 ± 1.1 Bq/l, respectively, with an average value of 5.7 ± 0.68 Bq/l. Notably, the highest radon concentration was detected in well water, while the lowest was found in tap water. It is noteworthy that

only 2 out of the sampled water sources exhibited radon concentrations below the USEPA proposed MCL of 11.1 Bq/l. Furthermore, an analysis of the data revealed a strong positive correlation, with an R^2 value of 0.87, between the concentration of radium and radon in these drinking water samples. When estimating the age-dependent annual effective dose resulting from ^{222}Rn exposure, the findings indicated that the values were lower than the WHO recommended reference limit of 0.1 mSv/y. This study underscores the potential vulnerability of infants and children compared to adults due to their more active bone growth processes.

Ravikumar and Somashekar (***2018***) conducted a study to know the distribution of radon in ground water. 65 groundwater samples from selected parts of Bangalore, India were collected and analyzed for radon activity using RAD7 radon monitor. The radon activity is in the range of 3.05–696 Bq/l with a mean of 91.39 Bq/l and 92.31% of the groundwater samples recorded elevated radon concentration above the USEPA proposed MCL value of 11.1 Bq/L. The mean annual effective dose contribution of people falling under different age groups (viz., infants, children, teens: males and females, adults: males and females, pregnant and lactating women) due to ingestion of water-borne ^{222}Rn ranged from 0.082 to 0.444 mSv/y.

In the Jazan area of Saudi Arabia, concentrations of dissolved radon in drinking and ground water were assessed using the sealed cup technique (***El-Araby et al. 2019***). A total of 110 water samples are collected from 11 different locations. The mean values for radon levels in drinking and ground water are determined to be 2.47 ± 0.14 and 2.95 ± 0.22 Bq/l, respectively. Additionally, the mean of the total annual effective doses resulting from the ingestion and inhalation of drinking and ground water are calculated as 24.25 ± 1.33 and 28.99 ± 2.12 μSv/y, respectively. Importantly, these values are found to be below the WHO proposed refrence limit of 0.1 mSv/y.

Di Carlo et al. (***2019***) conducted a comprehensive study on 33 mineral spring waters in Lazio, a region in Central Italy, to determine if self-bottled mineral waters could pose a public health risk. Two different methods were employed to sample the waters to assess the impact of bottling on radon levels. Samples are collected from 20 distinct spring sources, with six samples taken from each source. The findings revealed that 2 out of the 20 (10%) measured mineral spring waters exceeded the reference limit of 100 Bq/l.

The concentration of naturally occurring Radium (^{226}Ra) and Radon (^{222}Rn) in drinking water samples collected from 20 villages in the Jalandhar and Kapurthla districts of Punjab was assessed for potential health risks, as reported by Jakhu et al. in (***2020***). In the examined water samples, the ^{222}Rn concentration ranged from 1.42 to 5.26 Bq/l, with an average concentration of 3.51 Bq/l. The annual average doses resulting from the inhalation and ingestion of ^{222}Rn in the water in this studied area were found to be 0.89 nSv/y and 0.74 μSv/y, respectively. The total annual effective dose attributable to ^{222}Rn in the water varied between 0.3 and 28.01 μSv/y, with an average of 19.46 μSv/y. It is worth noting that the total annual effective dose due to ^{222}Rn in the water samples

from the study area falls below the WHO proposed reference dose level of 0.1 mSv/y. Consequently, the authors anticipate that the associated health risks related to these radionuclides are minimal.

Isinkaye and Ajiboye (***2020***) have studied correlations between ^{226}Ra and ^{222}Rn activity concentrations in surface soil and groundwater samples. Water samples are randomly collected from 100 different ground water sources in southwest Nigeria. The levels of ^{222}Rn concentration in groundwater samples range from 0.9 to 472.0 Bq/l with an average of 34.7 ± 55.5 Bq/l. Notably, 5% of the groundwater samples exceed the WHO prescribed limit of 100 Bq/l for ^{222}Rn in drinking water. This study reveals that ^{226}Ra content of the water did not significantly contribute to the radon activity concentration of the groundwater. The estimated annual effective dose equivalent (AEDE) resulting from groundwater ^{222}Rn range from 0.2 - 120.6 μSv/yr, with an average of 8.9 μSv/yr. The average dose value remain below the WHO proposed limit of 0.1 mSv/yr.

In 2021 Rani et al. conducted a radiological risk assessment for the first time in the Barnala district of Punjab, India, focusing on the presence of radon isotopes in drinking water. This assessment utilized a scintillation-based radiation detector. To ensure comprehensive coverage, they collected a total of 100 water samples from various sources, including canal and underground water, obtained from 25 villages. In-situ measurements are conducted to determine the concentration of Rn-222 in these water samples. The recorded values ranged from 0.17 ± 0.01 to 9.84 ± 0.59 Bq/l, with an average value of 3.37 ± 0.29 Bq/l. Notably, these measurements fell well below the WHO recommended reference limit of 100 Bq/l.

Ismail et al. (***2021***) conducted a study to assess radon concentrations in water sources located in the southwestern coastal region of Peninsular Malaysia. A total of 27 water samples are collected from diverse sources, including groundwater, hot springs, lakes, rivers, seawater, and tap water. Radon concentrations were quantified using a portable RAD7 radon detector. The recorded radon concentrations ranged from 0.07 ± 0.12 to 187 ± 12 Bq/l, with an average of 21 ± 12 Bq/l. The highest average concentration is detected in hot spring water, measuring 99 ± 6 Bq/l, while the lowest is observed in tap water, with an average concentration of 1.95 ± 0.61 Bq/l. Notably, the average radon concentrations in all water categories fell below the WHO recommended limit of 100 Bq/l. The total effective dose arising from both inhaled and ingested radon in water is determined. The study found an average effective dose of 4.45 μSv/y, which is comfortably below the WHO proposed reference level of 0.1 mSv/y.

In this investigation, a total of 42 water samples were gathered from Karasu and Pinarbasi, the two primary sources supplying drinking water to the Kahramanmaras city center water distribution network, Turkey by Küçükönder and Gümbür (***2022***). These samples are collected from sixteen cisterns directly fed by these water sources and twenty-four taps connected to these cisterns. Radon concentrations in these water samples were quantified using CR-39 passive trace detectors. For natural spring water

samples, the radon concentrations are found to vary, with concentrations ranging from 174.7 ± 18.7 Bq/m^3 to 211.7 ± 30.7 Bq/m^3. In cistern water samples, the observed radon concentrations spanned from 80.6 ± 3.9 Bq/m^3 to 303.0 ± 21.8 Bq/m^3. Similarly, in tap water samples, radon concentrations varied between 99.3 ± 5.5 Bq/m^3 and 305.8 ± 10.7 Bq/m^3. The results indicate that the radon levels in the samples are significantly lower than the recommended safe limits for drinking water.

With the objective of evaluating the potential public impact of radon, Damla et al. (***2022***) conducted investigations on drinking water samples in the city of Batman, situated in the southeastern region of Turkey. The results of their study revealed that radon concentrations ranged from 0.19 to 0.93 Bq/l, with an average concentration of 0.48 Bq/l. To assess the associated health risks for individuals of different age groups, the authors estimated the annual effective doses for both ingestion and inhalation. The findings suggest that the calculated values for annual effective doses fall well below the WHO recommended limit of 0.1 mSv/y. Furthermore, the study investigated the spatial distribution of radon in water samples from undisturbed areas and utilized this data to generate interpolated radiological maps.

A radon measurement study in water has been organized by Kumar et al. in 2022 at Dadri, India. A total of 25 villages in the vicinity of the National Capital Power Cooperation (NTPC), provided water samples for this assessment. Continuous monitoring equipment (SMART RnDuo) is employed to assess radon levels in household water sourced from hand pumps. Radon concentrations are found to range from 17±1 to 68±3 Bq/l, with an average concentration of 33±13 Bq/l. All recorded radon concentrations in the collected samples fall comfortably within the WHO established limit of 100 Bq/l. The calculated mean annual effective dose attributable to radon ingestion and inhalation from water sources is 84±33 μSv/y and 167±65 μSv/y, respectively. Additionally, the mean total annual effective dose is 167±65 μSv/y, exceeds the reference dose level of 0.1 mSv/y recommended by WHO. Moreover, the mean annual effective doses for the lungs and stomach are 9.9±3.9 μSv and 10.1±3.9 μSv, respectively.

To assess the presence of radon in commercial bottled water within Dhaka city and deep well water samples from the University of Dhaka campus, Bangladesh Al Mahmud et al. (***2023***) employed the RAD7 radon monitoring system. The radon concentration in bottled water ranged from 0.11 Bq/l to 1.30 Bq/l, with an average of 0.59 Bq/l. The deep well water displayed an average radon concentration of 4.88 Bq/l, within a range of 3.02 Bq/l to 5.98 Bq/l. It is noteworthy that all 25 water samples fell within the recommended limits established by USEPA and WHO for radon levels. The mean annual effective doses resulting from radon in bottled water and deep well water are estimated to be 0.126 μSv/y and 12.481 μSv/y, respectively.

In an effort to quantify radon levels in and around Areekode Region, Kerala, India a smart radon monitor (SRM) developed by the Baba Atomic Research Centre (BARC) in

Mumbai is employed by Ravi et al. (***2023***). The study revealed that the concentration of ^{222}Rn in groundwater and bore well water in this region ranged from 0.37±0.03 Bq/l to 3.53±0.10 Bq/l. It's worth noting that all of the samples are well below the USEPA proposed MCL limit of 11.1 Bq/l.

3.8 Air pollution by radioactive materials

Air pollution by radioactive materials poses serious risks to human health and the environment. Radioactive materials emit ionizing radiation, which can have harmful effects on living organisms when released into the air. Sources of radioactive air pollution include nuclear power plants, industrial activities, accidents, and improper disposal of radioactive waste.

One of the main concerns with radioactive air pollution is the potential for long-term health effects. Ionizing radiation can damage cells and DNA, leading to an increased risk of cancer and other illnesses. The extent of the health impact depends on factors such as the type of radioactive material released, the amount released, and the duration of exposure.

Nuclear power plants are significant contributors to airborne radioactive pollution. Although these facilities are designed with safety measures to prevent releases of radioactive materials, accidents or malfunctions can still occur. The Chernobyl disaster in 1986 (***Lundin et al. 1993***) and the Fukushima Daiichi nuclear disaster in 2011 (***Thielen 2012***) are two notable examples of accidents that resulted in the release of radioactive materials into the air, causing widespread contamination and health concerns.

Industrial activities such as mining, processing, and manufacturing involving radioactive materials can also contribute to airborne pollution. Improper handling and disposal of radioactive waste pose additional risks, as leaks or spills can release radioactive substances into the air.

Efforts to mitigate air pollution by radioactive materials involve strict regulations, monitoring, and proper disposal practices. Nuclear facilities must adhere to safety guidelines to prevent accidents, and emergency response plans should be in place to address any unforeseen events. Proper disposal of radioactive waste is essential to prevent the release of harmful substances into the air.

Public awareness and education are crucial components of addressing the risks associated with radioactive air pollution. Communities living near nuclear facilities or in areas with a history of radioactive contamination should be informed about potential risks and safety measures. Regular monitoring of air quality and public health assessments can help identify and address issues promptly.

In conclusion, air pollution by radioactive materials poses significant challenges to human health and the environment. Proper safety measures, regulatory oversight, and

public awareness are essential to minimize the risks associated with the release of radioactive substances into the air. Continued research and advancements in technology are also critical to developing cleaner and safer methods for handling and managing radioactive materials.

3.8.1 Air Radon

Radon in indoor air refers to the presence of radon gas, specifically ^{222}Rn, within the confines of a building or enclosed space. It can seep into buildings through cracks in foundations, gaps in construction materials, or openings in the ground, and it can accumulate to potentially hazardous levels when proper ventilation is lacking. Exposure to elevated levels of indoor radon can pose significant health risks, as it decays into radioactive particles that can be inhaled and can damage lung tissue, increasing the risk of lung cancer. Therefore, it is essential to monitor and mitigate indoor radon levels to protect the health and safety of the occupants of a building.

3.8.1.1 Air radon concentration studies: An overview

The primary source of natural radiation exposure for the population stems from inhaling radon and its derivative products. Therefore many researchers have done the air radon measurement study around the world.

To conduct a comprehensive ecological survey, Marenny et al. (***1996***) assessed radon and its daughter product concentrations in 62 regions of Russia, including the St Petersburg Region, the Central Territories, and the Altay Territory. Utilizing cost-effective dosimeters based on track-etch and activated-charcoal detectors, they measured environmental radon concentrations. Indoor measurements are conducted in over 1000 residences, public spaces, and industrial buildings across 21 towns and villages. The track chambers are exposed for approximately 2–3 months, while charcoal detectors are deployed for 6–10 days, predominantly during the summer. Measured indoor radon concentrations ranged between 8-1554 Bq/m^3.

In 2003-2004, a comprehensive study was conducted in China, spanning 23 cities, utilizing solid-state nuclear detectors to assess the radon concentrations in 234 underground structures by Li et al. (***2006***). This investigation encompassed all seasons, including spring, summer, and winter. The results revealed an annual radon concentration spectrum ranging from 14.9 to 2482 Bq/m^3, with an average of 247 Bq/m^3. When analyzing the data on a city-by-city basis, Fuzhou and Baotou stood out with notably higher radon levels at 714 $Bq/m^3$and 705 Bq/m^3, respectively. Conversely, Guangzhou and Shanghai exhibited comparatively lower radon levels, recording 71.1 Bq/m^3 and 72.6 Bq/m^3, respectively. It is also determined that people working in these cities received an average annual effective dose of 1.6 mSv due to radon exposure. Notably, the study highlighted a seasonal variation, with radon levels being at their lowest during the winter months and reaching their peak during the summer.

In this research, Bouzarjomehri and Ehrampoosh (***2008***) conducted an assessment of the air radon levels in 84 basement dwellings located in various regions of Yazd, Iran. Their investigation involved the use of a portable radon gas surveyor, employing an active measurement approach. This device enabled them to measure the α radiation in each basement over a 24-hour period using a solid-state detector. The radon concentrations in these basements ranged from 5.55 to 747.4 Bq/m^3, with an average concentration of 137.36 Bq/m^3. The mean radon concentration did not significantly differ from the mitigation recommendation level provided by the Environmental Protection Agency (EPA), which stands at 148 Bq/m^3. However, it's noteworthy that over 30% of the basements exceeded the EPA's recommended guideline for radon concentration.

A survey is conducted to measure indoor radon levels in 105 workplaces across the Rawalpindi region and Islamabad Capital Territory, Pakistan (***Rahman et al. 2010***). CR-39 based radon detectors are utilized for this purpose. Results from the survey indicated that the measured indoor radon concentrations in the surveyed buildings varied from 12 ± 5 to 293 ± 19 Bq/m^3, with an overall mean value of 64 ± 32 Bq/m^3. Notably, offices located in basements of Rawalpindi city exhibited the highest mean radon concentration, reaching 113 ± 48 Bq/m^3. The overall average annual effective dose in the examined workplaces is calculated to be 0.61 ± 0.30 mSv/y. Further analysis revealed that the mean annual effective doses for basements, ground floors, and first floors are 0.87 ± 0.34 mSv/y, 0.55 ± 0.28 mSv/y, and 0.47 ± 0.29 mSv/y, respectively.

Jayanthi et al. (***2011***) conducted a study to investigate radiation exposure and effective dose due to air radon in residents of 10 villages within the Natural High Background Radiation Areas (NHBRA) of the coastal regions of Kanyakumari District and Tamil Nadu, India. Measured radon level varies from 13 to 52.5 Bq/m^3. Additionally this research focused on two exposure routes: external and internal through inhalation. The analysis revealed that the average total annual effective dose varied from 2.59 to 8.76 mSv/yr.

.A series of measurements were conducted in 56 residential homes across 14 different areas within Alexandria city, Egypt by Abd-Elzaher (***2013***). The measurements utilized LR-115 (Type II) alpha track detectors configured in a "closed-can" design. These detectors are strategically placed in bedrooms, living rooms, and kitchens of each dwelling. Additionally, for the purpose of comparison, detectors are also deployed in basements, ground floors, and first floors of the homes. The findings revealed a range of indoor radon concentrations, spanning from 15 to 132 Bq/m^3. Specifically, the average radon concentrations are as follows: in living rooms, bedrooms, and kitchens located in basements, the averages are 39 ± 10, 63 ± 15, and 81 ± 25 Bq/m^3, respectively. On the ground floor, the average concentrations are 35 ± 9, 44 ± 6, and 56 ± 10 Bq/m^3 for living rooms, bedrooms, and kitchens, respectively. On the first floor, these averages are 29 ± 8, 34 ± 7, and 45 ± 8 Bq/m^3, respectively. When considering all the surveyed districts, the overall mean radon concentration is determined to be 44 ± 16 Bq/m^3. Furthermore,

an estimation of the mean annual effective dose received by residents in the study area amounted to 0.75 mSv/y.

To investigate seasonal variations in indoor radon levels among houses in Northern Rajasthan, India, Duggal et al (***2014***) conducted measurements in 100 different households. They employed LR-115-type II plastic track detectors across four consecutive three-month periods: winter, spring, summer, and autumn. The average indoor radon concentrations for each season were as follows: 176 Bq/m^3 (winter), 131 Bq/m^3 (spring), 120 Bq/m^3 (summer), and 151 Bq/m^3 (autumn). The yearly average indoor radon concentrations in these homes ranged from 117 to 215 Bq/m^3, with an overall mean of 144 Bq/m^3. Approximately 10% of the residences exhibited indoor radon activity concentration values within the action level range (200–300 Bq/m^3) recommended by the International Commission on Radiological Protection. Residents in the study area received an annual effective radiation dose ranging from 2.0 to 3.67 mSv, with an average of 2.46 mSv. Seasonal trends in indoor radon levels indicated the highest values in winter and the lowest in summer. The study also examined the impact of building characteristics on radon measurements.

In Hamirpur district of Himachal Pradesh, India a comprehensive study is conducted to measure radon levels in both indoor air and soil gas simultaneously, utilizing the RAD7 solid-state alpha detector (***Mehra and Bala 2014***). The primary objective of this research was to assess the radon concentration and the annual effective dose associated with indoor air quality. Various locations across the Hamirpur region were carefully selected for the investigation, revealing a range of radon concentrations in indoor air from 35 Bq/ m^3 to 956 Bq/m^3 with an average of 189.43 Bq/m^3. The calculation of the total annual effective dose from indoor air measurements yielded values ranging from 0.88 mSv/ y to 24.09 mSv/ y, with a mean of 4.77 mSv/y.

To enhance the design of a national survey focused on assessing radon exposure among schoolchildren in Serbia, a preliminary investigation was conducted across all 334 primary schools situated in 13 municipalities in Southern Serbia by Bochicchio et al. (***2014***). Analyzing data gathered from passive measurements, it is determined that approximately 5% of these schools have rooms with an annual radon concentration exceeding 300 Bq/m^3. The weighted mean annual radon concentration, considering the number of students, stood at 73 Bq/m^3, which marked a 39% reduction compared to the unweighted average concentration of 119 Bq/m^3. Notably, it is probable that the actual average radon concentration in classrooms when children are present is even lower.

A preliminary study aimed to assess indoor radon concentrations in public primary schools, identify the primary factors influencing these levels, and estimate the radiation exposure for students and teachers is conducted by Madureira et al. (***2016***). Radon levels were measured in 45 classrooms across 13 public primary schools in Porto, northeastern Portugal using CR-39 passive radon detectors over a two-month period. In

all the schools, radon concentrations ranged from 56 to 889 Bq/m^3, with a mean of 197 Bq/m^3. Alarmingly, 92% of the measurements exceeded the WHO indoor air quality guideline of 100 Bq/m^3, and 8% exceeded the national legislation limit of 400 Bq/m^3. Additionally, the average annual effective dose was calculated at 1.25 mSv/y, varying from 0.58 to 3.07 mSv/y, which is below the action level of 3–10 mSv. The significant variation in radon concentrations observed between and within different floors underscores the necessity of monitoring radon levels in multiple rooms on each floor.

In this research, Yousef and Zimami (***2019***) aimed to assess indoor radon concentrations and investigate the seasonal variations of radon levels to gauge the annual effective dose experienced by residents in Al-Kharj, Saudi Arabia. They selected 84 households for this study and employed the RAD 7 detector to measure cumulative radon exposure from September 2014 to November 2017. Their findings unveiled notable disparities in radon concentration, with higher levels observed during winter (24.33 ± 11.10 Bq/m^3) compared to summer (14.54 ± 5.50 Bq/m^3). Conversely, radon concentration in spring and autumn closely approximated the average annual radon concentration (19.23 ± 8.13 Bq/m^3). The average annual effective dose was determined to be 0.49 mSv/year.

Mirdoraghi et al. (***2020***) conducted a research work to assess air radon levels in Tehran city, Iran. To achieve these goals, the study involved the placement of 800 Alpha Track detectors in homes across 22 regions of Tehran city. These detectors are retrieved after three months, with measurements repeated in spring, summer, and autumn. The study employed standard equations to evaluate the annual effective dose and lung cancer risk, and the data are subjected to analysis using SPSS 20. Results revealed a range of radon concentrations, with the lowest recorded in Ghalee-kobra (0.13 Bq/m^3) and the highest in the Charbagh-ponak district (661.11 Bq/m^3). Notably, no discernible correlation is observed between radon levels and house type, structural integrity, or construction materials. Storehouses and basements exhibited significantly higher radon concentrations (P = 0.016) compared to occupied rooms. The estimated annual effective dose ranged from 0.65 to 2.03 mSv.

D'Avino et al. (***2021***) conducted a research focused on assessing the annual radon concentration in 62 bank buildings distributed across the Campania region in Southern Italy. The measurements are conducted in 136 confined spaces, with 127 located on underground floors and 9 on ground floors, commonly frequented by workers and the general public. The analysis considered several parameters, including the type of flooring, wall materials, the number of openings, and the duration of door/window openings for air exchange. The results revealed radon levels ranging from 17 to 680 Bq/m^3, with an average concentration of 130 Bq/m^3. Approximately 7% of the findings exceeded the established limit of 300 Bq/m3. Notably, the study identified that the floor level and air exchange played the most substantial roles in influencing radon levels. This study underscores the critical importance of assessing indoor radon levels, particularly in work environments, to safeguard the health of both employees and the public against radon-induced health risks.

In this comprehensive study conducted by Reste et al. 2022 at the state level, a significant portion of Latvia's territory is covered, encompassing 941 radon measurements using Radtrack2. These measurements are taken over a span of 4 to 6 months in a wide range of locations, including public offices, educational institutions, and healthcare facilities. The study's findings revealed that a substantial 94.7% of the sampled locations do not surpass the national permissible limit of 200 Bq/m^3, a threshold at which preventative actions must be taken. Slightly higher radon concentrations are observed in well-insulated locations with plastic windows and limited air exchange, primarily in educational facilities, such as schools (59 Bq/m^3 with a range of 36 to 109 Bq/m^3) and kindergartens (48 Bq/m^3 with a range of 32 to 79 Bq/m^3). Surprisingly, industrial workplaces exhibited lower radon levels (28 Bq/m^3 with a range of 16 to 55 Bq/m^3).

3.9. Environmental radioactivity in soil

Environmental radioactivity in soil refers to the presence of radioactive substances in the Earth's soil. These substances can originate from natural sources, such as radionuclides present in rocks and minerals, as well as from human activities, including nuclear power plants, industrial processes, and fallout from nuclear weapon testing. Monitoring and assessing environmental radioactivity in soil are crucial for understanding potential risks to ecosystems and human health, as well as for implementing appropriate measures to mitigate and manage any adverse impacts. However, measurement of radioactivity in soil also plays a very crucial role to mankind for other positive purposes.

3.9.1 Soil Radon

Soil radon gas, often referred to simply as radon, is a naturally occurring radioactive gas found in the Earth's crust. Radon levels in the soil can vary significantly from one location to another. Geology, soil composition, and the presence of uranium and thorium in the ground all influence radon concentrations. As a result, radon levels can differ greatly even within a small geographic area. Radon can migrate from the soil into buildings through cracks in foundations, gaps around pipes, and other openings. Inadequate ventilation and insulation can lead to the accumulation of radon indoors, increasing the risk to occupants.

3.9.1.1 Influence of meteorological parameters on soil radon concentration: A summary

To understand the influence of meteorological parameters on radon emissions many researchers have conducted studies worldwide. Some of them are discussed here.

The present work done by Kovach (***1945***), focuses on the time-frame spanning from May 17, 1944, to March 25, 1945, and aims to explore the meteorological factors impacting the radon content within the soil-gas, including changes in barometric pressure, wind

velocity effects, and temperature variations. During this investigation period, they examined four soil depths: 25, 75, 150, and 200 cm. Over 177 days of active research, encompassing 642 individual measurements, they quantified the radon content of soil-gas using ionization chambers connected to a Wulf bifilar electrometer. In dry soil conditions, the radon content remains relatively constant at each depth and increases with greater depth. Extended periods of snow and ice coverage on the ground lead all soil depths to converge towards similar values. Frozen ground exhibits the highest radon content throughout the year. Barometric pressure, particularly up to a depth of 200 cm, induces variations in radon content. Increasing pressure tends to reduce radon content, while decreasing pressure results in an increase. This effect is most pronounced at the 25- and 75-cm depths. Sustained high wind velocity over several hours notably diminishes the radon content in the upper layers of the soil. Changes in ground temperature appear to have minimal impact on the radon content in soil-gas.

Fujiyoshi et al. (***2006***) continuously monitored ^{222}Rn concentration in soil gas Since November 22, 2004, the observation revealed fluctuations in radon concentration over time in the natural woods located on the campus of Hokkaido University in Sapporo, Japan. Among the various factors influencing soil radon levels and their variability, temperature was identified as the predominant factor during three seasons. During these seasons ^{222}Rn concentrations exhibited a daily high and nightly low, with the transition occurring around 10 o'clock in the morning. This pattern was occasionally disrupted by low-pressure fronts and accompanying rain. As soil temperatures gradually decreased from late November to mid-December, the activity levels also decreased. Once the ground surface is entirely covered with snow, the soil radon levels remained low with minimal fluctuation. Winter, however, see several peaks in the ^{222}Rn time-series chart, with some of these peaks in early winter and early spring being influenced by meteorological parameters. In a few instances, the radon activity experienced sudden increases, coinciding with elevated pressure at a depth of 10 cm in the soil. This phenomenon may be linked to subsurface events, including seismic activity in the area.

Sundal et al. (***2008***) conducted a study to examine the impact of various meteorological factors on soil radon levels in a permeable ice-marginal deposit in Kinsarvik, Norway. This investigation involved continuous monitoring of soil radon concentrations, as well as parameters like temperature, precipitation, wind speed, wind direction, air pressure, and soil moisture content for duration of 10 months. The findings indicate that soil radon concentrations exhibit noticeable seasonal and daily fluctuations primarily driven by changes in air temperature. These fluctuations result from air movements between areas with varying elevations within the ice-marginal deposit, which are caused by differences in temperature between soil air and the surrounding atmosphere. Interestingly, the study recorded abrupt changes in air flow direction when the atmospheric air temperature approached the average annual air temperature. Furthermore, the study revealed that air pressure was the second most influential

factor affecting soil radon concentrations. Notably, no discernible impact of factors such as precipitation, wind speed, wind direction, or soil moisture on soil radon levels was observed.

Anomalies in radon content within the soil gas of three boreholes at the Orlica fault in the Krško basin, Slovenia, have been measured by Torkar et al. (***2010***). To discern anomalies arising from environmental factors (such as air and soil temperature, barometric and soil air pressure, and rainfall) from those exclusively linked to seismic activity, a two-step methodology is employed. Initially, seismic activity data are removed from the dataset, and an artificial neural network (ANN) is trained using standard back propagation, with five inputs representing environmental parameters and a single output indicating radon concentration. Subsequently, predictions of radon concentrations (Cp) generated by this ANN for the entire dataset are compared to actual measurements (Cm). The analysis of the signal |Cm/Cp − 1| revealed three types of anomalies (CA — correct anomaly, FA — false anomaly, and NA — no anomaly), with the detection parameters for an anomaly being varied within predefined intervals. An exhaustive search is conducted among results to identify the optimal set of parameters. Additionally, an attempt is made to streamline the search process by training another ANN, using the numbers of anomalies of each type as inputs and five anomaly detection parameters as outputs. This study revealed that through these methodologies, the correct prediction of 10 out of 13 seismic events within a 2-year period is achieved.

Almayahi et al. (***2013***) conducted a research centred on examining the correlation between the concentrations of ^{222}Rn and ^{220}Rn in soil and various meteorological factors (including temperature, pressure, humidity, and terrestrial gamma radiation) in Northern Peninsular Malaysia. They conducted on-site measurements of both ^{222}Rn and ^{220}Rn concentrations in surface air and at a depth of 50 cm using two active monitoring techniques: the RAD7 radon detector and the radon continuous monitor from Sun Nuclear Corporation. At the 50 cm depth, the soil radon concentrations spanned from minimum of 133 Bq/m^3 to a maximum of 143,059 Bq/m^3. The study revealed weak positive and negative correlations between the concentrations of ^{222}Rn and the various meteorological parameters.

The soil radon (Rn^{222}) and thoron (Rn^{220}) concentrations at the Badargadh and Desalpar observatories in Gujarat, India, are studied to investigate the sources of radon emissions, their potential as earthquake precursors, and the impact of meteorological conditions on radon release by Sahoo et al. (***2018***). Radon and meteorological data are collected using the Radon Monitor RMT 1688-2 at these two stations during specific time periods. The results showed that at Desalpar, radon concentrations ranged from 781 to 4320 Bq/m^3, with an average of 2499 Bq/m^3. At Badargadh, radon concentrations ranged from 264 to 2221 Bq/m^3, with an average of 1135.4 Bq/m^3. To understand the influence of meteorological parameters on radon emissions linear regression analysis was conducted, revealing a negative correlation between radon and temperature, and positive correlations between radon and humidity and pressure.

In this investigation Seyis et al. (***2022***) conducted an extensive analysis of soil radon concentration variations and the potential factors influencing these fluctuations. The study involved continuous in-situ measurements with high temporal resolution over an extended time frame, aimed at unveiling the relationships between soil radon levels and various controlling parameters. To accomplish this objective, they established a network of six monitoring stations across three different sites in Western Turkey: four stations in Gebze, one in Armutlu, and one in Sarıköy. Over a span of 18 months, from April 2008 to November 2010, they meticulously recorded data on eight distinct parameters, including soil radon, soil temperature, soil moisture, air temperature, air pressure, precipitation, wind speed, and wind direction. Soil radon measurements are collected at 15-minute intervals, while the other parameters were logged hourly. To extract valuable insights from the collected data, they subjected the time series of each parameter to Empirical Mode Decomposition (EMD) analysis to identify different frequency signals. Ultimately, they computed correlation coefficients between these parameters to identify potential connections and associations. Their study underscores the importance of long-term, continuous, and synchronous monitoring of multiple parameters, with a duration exceeding one year, to gain a deeper understanding of soil radon behavior. In particular, it highlights the significance of concurrently measuring and interpreting soil moisture and temperature alongside soil radon concentrations. Such an approach enhances the reliability of soil radon time series data, making it more valuable for earthquake forecasting research and indoor radon risk mitigation efforts.

References

Abdallah, S. M., Habib, R. R., Nuwayhid, R. Y., Chatila, M., & Katul, G. (2007). Radon measurements in well and spring water in Lebanon. Radiation measurements, 42(2), 298-303.

Abd-Elzaher, M. (2013). Measurement of indoor radon concentration and assessment of doses in different districts of Alexandria city, Egypt. Environmental geochemistry and health, 35, 299-309.

Ahmad, N., Rehman, J. U., Rafique, M., & Nasir, T. (2018). Age-dependent annual effective dose estimations of 226Ra, 232Th, 40K and 222Rn from drinking water in Baling, Malaysia. Water Science and Technology: Water Supply, 18(1), 32-39.

Akar Tarim, U., Gurler, O. R. H. A. N., Akkaya, G. İ. Z. E. M., Kilic, N., Yalcin, S., Kaynak, G., & Gundogdu, O. (2012). Evaluation of radon concentration in well and tap waters in Bursa, Turkey. Radiation protection dosimetry, 150(2), 207-212.

Al Mahmud, J., Siraz, M. M., Alam, M. S., Das, S. C., Bradley, D. A., Khandaker, M. U., ... & Yeasmin, S. (2023). A study into the long-overlooked carcinogenic radon in bottled water and deep well water in Dhaka, Bangladesh. International journal of environmental analytical chemistry, 1-13.

Al Zabadi, H., Musmar, S., Issa, S., Dwaikat, N., & Saffarini, G. (2012). Exposure assessment of radon in the drinking water supplies: a descriptive study in Palestine. BMC research notes, 5, 1-8.

Alam, M. N., Chowdhury, M. I., Kamal, M., Ghose, S., Banu, H., & Chakraborty, D. (1997). Radioactivity in chemical fertilizers used in Bangladesh. Applied Radiation and Isotopes, 48(8), 1165-1168.

Alharshan, G. A., Aloraini, D. A., Al-Ghamdi, H., Almuqrin, A. H., El-Azony, K. M., & Alsalamah, A. S. (2017). Measuring the radioactivity concentration of 40 K and 137 Cs and calculating the annual internal doses from ingesting liquid and powdered milk. radiochemistry, 59, 98-103.

Al-jnaby, M. K. M. (2016). Radon Concentration in Drinking Water Samples at Hilla city, Iraq. World Scientific News, (52), 130-142.

Almayahi, B. A., Tajuddin, A. A., & Jaafar, M. S. (2013). In situ soil 222Rn and 220Rn and their relationship with meteorological parameters in tropical Northern Peninsular Malaysia. Radiation Physics and Chemistry, 90, 11-20.

Amrani, D., & Tahtat, M. (2001). Natural radioactivity in Algerian building materials. Applied Radiation and Isotopes, 54(4), 687-689.

Aycik, G. A., & Ercan, A. (1997). Radioactivity measurements of coals and ashes from coalfired power plants in the southwestern part of Turkey. Journal of Environmental Radioactivity, 35(1), 23-35.

Bochicchio, F., Žunić, Z. S., Carpentieri, C., Antignani, S., Venoso, G., Carelli, V., ... & Bossew, P. (2014). Radon in indoor air of primary schools: a systematic survey to evaluate factors affecting radon concentration levels and their variability. Indoor air, 24(3), 315-326.

Bourai, A. A., Gusain, G. S., Rautela, B. S., Joshi, V., Prasad, G., & Ramola, R. C. (2012). Variations in radon concentration in groundwater of Kumaon Himalaya, India. Radiation protection dosimetry, 152(1-3), 55-57.

Bouzarjomehri, F., & Ehrampoosh, M. H. (2008). Radon level in dwellings basement of Yazd-Iran. Iranian journal of radiation research, 6(3), 141-144.

Chandrashekara, M. S., Veda, S. M., & Paramesh, L. (2012). Studies on radiation dose due to radioactive elements present in ground water and soil samples around Mysore city, India. Radiation protection dosimetry, 149(3), 315-320.

Cosma, C., Moldovan, M., Dicu, T., & Kovacs, T. (2008). Radon in water from Transylvania (Romania). Radiation Measurements, 43(8), 1423-1428.

D'Alessandro, W., & Vita, F. (2003). Groundwater radon measurements in the Mt. Etna area. Journal of environmental radioactivity, 65(2), 187-201.

D'Avino, V., Pugliese, M., Ambrosino, F., Bifulco, M., La Commara, M., Roca, V., ... & La Verde, G. (2021). Radon survey in bank buildings of campania region according to the italian transposition of euratom 59/2013. Life, 11(6), 533.

Damla, N., Alp, M. S., Yesilkanat, C. M., & Isık, U. (2022). Evaluation and analysis of the spatial distribution of radiation risks caused by radon in drinking water of Batman, Türkiye. Journal of Radioanalytical and Nuclear Chemistry, 331(12), 5859-5868.

Di Carlo, C., Lepore, L., Venoso, G., Ampollini, M., Carpentieri, C., Tannino, A., ... & Bochicchio, F. (2019). Radon concentration in self-bottled mineral spring waters as a possible public health issue. Scientific reports, 9(1), 14252.

Duggal, V., Mehra, R., & Rani, A. (2013). Analysis of radon concentration in drinking water in Hanumangarh district of Rajasthan, India. Radiation Protection and Environment, 36(2), 65.

Duggal, V., Rani, A., & Mehra, R. (2014). Measurement of indoor radon concentration and assessment of doses in different districts of Northern Rajasthan, India. Indoor and Built Environment, 23(8), 1142-1150.

Duggal, V., Sharma, S., & Mehra, R. (2017). Radon levels in drinking water of Fatehabad district of Haryana, India. Applied Radiation and Isotopes, 123, 36-40.

Erdogan, M., Eren, N., Demirel, S., & Zedef, V. (2013). Determination of radon concentration levels in well water in Konya, Turkey. Radiation protection dosimetry, 156(4), 489-494.

Flues, M., Camargo, I. M. C., Silva, P. S. C., & Mazzilli, B. P. (2006). Radioactivity of coal and ashes from Figueira coal power plant in Brazil. Journal of Radioanalytical and Nuclear Chemistry, 270(3), 597-602.

Fujiyoshi, R., Sakamoto, K., Imanishi, T., Sumiyoshi, T., Sawamura, S., Vaupotic, J., & Kobal, I. (2006). Meteorological parameters contributing to variability in 222Rn activity concentrations in soil gas at a site in Sapporo, Japan. Science of the total environment, 370(1), 224-234.

Galan Lopez, M., Martin Sanchez, A., & Gómez Escobar, V. (2004). Application of ultra-low level liquid scintillation to the determination of 222 Rn in groundwater. Journal of Radioanalytical and Nuclear Chemistry, 261, 631-636.

Groundwater is the saturated zone of soil/rock below the land surface. U.S. Geological Survey's (USGS) Water Science School 1999.

Horvath, A., Bohus, L. O., Urbani, F., Marx, G., Piroth, A., & Greaves, E. D. (2000). Radon concentrations in hot spring waters in northern Venezuela. Journal of environmental radioactivity, 47(2), 127-133.

Inácio, M., Soares, S., & Almeida, P. (2017). Radon concentration assessment in water sources of public drinking of Covilhã's county, Portugal. Journal of Radiation Research and Applied Sciences, 10(2), 135-139.

Isinkaye, M. O., & Ajiboye, Y. (2020). Correlations of 226 Ra and 222 Rn activity concentrations in surface soil and groundwater of basement complex geological area of southwest Nigeria. SN Applied Sciences, 2, 1-8.

Ismail, N. F., Hashim, S., Sanusi, M. S. M., Abdul Rahman, A. T., & Bradley, D. A. (2021). Radon levels of water sources in the southwest coastal region of Peninsular Malaysia. Applied Sciences, 11(15), 6842.

Jayanthi, D. D., Maniyan, C. G., & Perumal, S. (2011). Assessment of indoor radiation dose received by the residents of natural high background radiation areas of coastal villages of Kanyakumari district, Tamil Nadu, India. Radiation Physics and Chemistry, 80(7), 782-785.

Kareem, A. A., Hady, H. N., & Abojassim, A. A. (2016). Measurement of natural radioactivity in selected samples of medical plants in Iraq. International Journal of Physical Sciences, 11(14), 178-182.

Khattak, N., Khan, M., Shah, M., & Javed, M. (2011). Radon concentration in drinking water sources of the Main Campus of the University of Peshawar and surrounding areas, Khyber Pakhtunkhwa, Pakistan. Journal of Radioanalytical and Nuclear Chemistry, 290(2), 493-505.

Kovach, E. M. (1945). Meteorological influences upon the radon-content of soil-gas. Eos, Transactions American Geophysical Union, 26(2), 241-248.

Krishan, G., Rao, M. S., Kumar, C. P., & Semwal, P. (2015). Radon concentration in groundwater of east coast of West Bengal, India. Journal of Radioanalytical and Nuclear Chemistry, 303, 2221-2225.

Krstić, D., Nikezić, D., Stevanović, N., & Vučić, D. (2007). Radioactivity of some domestic and imported building materials from South Eastern Europe. Radiation Measurements, 42(10), 1731-1736.

Küçükönder, E., & Gümbür, S. (2022). Radon gas measurement in water samples in Kahramanmaras province of Turkey. Water, Air, & Soil Pollution, 233(5), 175.

Kumar, M., Kumar, P., Agrawal, A., & Sahoo, B. K. (2022). Radon concentration measurement and effective dose assessment in drinking groundwater for the adult population in the surrounding area of a thermal power plant. Journal of Water and Health, 20(3), 551-559.

Li, X., Zheng, B., Wang, Y., & Wang, X. (2006). A survey of radon level in underground buildings in China. Environment international, 32(5), 600-605.

Lundin, T., Mårdberg, B., & Otto, U. (1993). Chernobyl: nuclear threat as disaster. International handbook of traumatic stress syndromes, 431-439.

Madureira, J., Paciência, I., Rufo, J., Moreira, A., de Oliveira Fernandes, E., & Pereira, A. (2016). Radon in indoor air of primary schools: determinant factors, their variability and effective dose. Environmental Geochemistry and Health, 38, 523-533.

Malakootian, M., Khashi, Z., Iranmanesh, F., & Rahimi, M. (2014). Radon concentration in drinking water in villages nearby Rafsanjan fault and evaluation the annual effective dose. Journal of Radioanalytical and Nuclear Chemistry, 302, 1167-1176.

Marenny, A. M., Vorozhtsov, A. S., Nefedov, N. A., & Orlova, O. A. (1996). Results of radon concentration measurements in some regions of Russia. Radiation Measurements, 26(1), 43-48.

Marques, A. L., Dos Santos, W., & Geraldo, L. P. (2004). Direct measurements of radon activity in water from various natural sources using nuclear track detectors. Applied radiation and isotopes, 60(6), 801-804.

Mavi, B., & Akkurt, I. (2010). Natural radioactivity and radiation hazards in some building materials used in Isparta, Turkey. Radiation Physics and Chemistry, 79(9), 933-937.

Mehra, R., & Bala, P. (2014). Estimation of annual effective dose due to radon level in indoor air and soil gas in Hamirpur district of Himachal Pradesh. Journal of Geochemical Exploration, 142, 16-20.

Mirdoraghi, M., Einor, D., Baghal Asghari, F., Esrafili, A., Heidari, N., Mohammadi, A. A., & Yousefi, M. (2020). Assess the annual effective dose and contribute to risk of lung cancer caused by internal radon 222 in 22 regions of Tehran, Iran using geographic information system. Journal of Environmental Health Science and Engineering, 18, 211-220.

Moreno, V., Bach, J., Zarroca, M., Font, L., Roqué, C., & Linares, R. (2018). Characterization of radon levels in soil and groundwater in the North Maladeta Fault area (Central Pyrenees) and their effects on indoor radon concentration in a thermal spa. Journal of environmental radioactivity, 189, 1-13.

Mowlavi, A. A., Shahbahrami, A., & Binesh, A. (2009). Dose evaluation and measurement of radon concentration in some drinking water sources of the Ramsar region in Iran. Isotopes in environmental and Health Studies, 45(3), 269-272.

Nahar, A., Asaduzzaman, K., Islam, M. M., Rahman, M. M., & Begum, M. (2018). Assessment of natural radioactivity in rice and their associated population dose estimation. Radiation Effects and Defects in Solids, 173(11-12), 1105-1114.

Nain, M., Gupta, M., Chauhan, R. P., Kant, K., Sonkawade, R. G., & Chakarvarti, S. K. (2010). Estimation of radioactivity in tobacco.

Nikolopoulos, D., & Louizi, A. (2008). Study of indoor radon and radon in drinking water in Greece and Cyprus: implications to exposure and dose. Radiation Measurements, 43(7), 1305-1314.

Oner, F., Yalim, H. A., Akkurt, A., & Orbay, M. (2009). The measurements of radon concentrations in drinking water and the Yeşilırmak River water in the area of Amasya in Turkey. Radiation protection dosimetry, 133(4), 223-226.

Papastefanou, C. (2008). Radioactivity of coals and fly ashes. Journal of radioanalytical and nuclear chemistry, 275(1), 29-35.

Prasad, G., Prasad, Y., Gusain, G. S., & Ramola, R. C. (2008). Measurement of radon and thoron levels in soil, water and indoor atmosphere of Budhakedar in Garhwal Himalaya, India. Radiation Measurements, 43, S375-S379.

Rahman, S. U., Rafique, M., & Anwar, J. (2010). Radon measurement studies in workplace buildings of the Rawalpindi region and Islamabad Capital area, Pakistan. Building and environment, 45(2), 421-426.

Rangaswamy, D. R., Srinivasa, E., Srilatha, M. C., & Sannappa, J. (2016). Measurement of radon concentration in drinking water of Shimoga district, Karnataka, India. Journal of Radioanalytical and Nuclear Chemistry, 307, 907-916.

Rani, S., Kansal, S., Singla, A. K., & Mehra, R. (2021). Radiological risk assessment to the public due to the presence of radon in water of Barnala district, Punjab, India. Environmental Geochemistry and Health, 43(12), 5011-5024.

Ravi, H. R., Sajan, C. P., Bapat, P. N., Madhukumar, D. M., Ghalib, W. A. M., & Mansoor, A. M. (2023). Determination of Radon Concentration in Groundwater of Areekode Region, Kerala, India—A Case Study. Journal of the Geological Society of India, 99(2), 281-286.

Ravikumar, P., & Somashekar, R. K. (2018). Distribution of 222Rn in groundwater and estimation of resulting radiation dose to different age groups: a case study from Bangalore City. Human and Ecological Risk Assessment: An International Journal, 24(1), 174-185.

Reste, J., Pavlovska, I., Martinsone, Z., Romans, A., Martinsone, I., & Vanadzins, I. (2022). Indoor air radon concentration in premises of public companies and workplaces in Latvia. International Journal of Environmental Research and Public Health, 19(4), 1993.

Sahoo, S. K., Katlamudi, M., Shaji, J. P., Murali Krishna, K. S., & Udaya Lakshmi, G. (2018). Influence of meteorological parameters on the soil radon (Rn 222) emanation in Kutch, Gujarat, India. Environmental monitoring and assessment, 190, 1-20.

Sanjuán, M. Á., Suárez-Navarro, J. A., Argiz, C., & Mora, P. (2020). Assessment of natural radioactivity and radiation hazards owing to coal fly ash and natural pozzolan Portland cements. Journal of Radioanalytical and Nuclear Chemistry, 325, 381-390.

Seyis, C., İnan, S., & Yalçın, M. N. (2022). Major factors affecting soil radon emanation. Natural Hazards, 114(2), 2139-2162.

Sharma, S., Duggal, V., Srivastava, A. K., & Mehra, R. (2017). Assessment of radiation dose from exposure to radon in drinking water from Western Haryana, India. International Journal of Environmental Research, 11, 141-147.

Shiva Prasad, N. G., Nagaiah, N., Ashok, G. V., & Mahesh, H. M. (2007). Radiation dose from dissolved radon in potable waters of the Bangalore environment, South India. International journal of environmental studies, 64(1), 83-92.

Shukla, V. K., Menon, M. R., Ramachandran, T. V., Sathe, A. P., & Hingorani, S. B. (1994). Natural and fallout radioactivity in milk and diet samples in Bombay and population dose rate estimates. Journal of environmental radioactivity, 25(3), 229-237.

Singh, J., Singh, H., Singh, S., & Bajwa, B. S. (2009). Estimation of uranium and radon concentration in some drinking water samples of Upper Siwaliks, India. Environmental monitoring and assessment, 154, 15-22.

Smetanová, I., Holý, K., Müllerová, M., & Polášková, A. (2010). The effect of meteorological parameters on radon concentration in borehole air and water. Journal of radioanalytical and nuclear chemistry, 283(1), 101-109.

Sonkawade, R. G., Ram, R., Kanjilal, D. K., & Ramola, R. C. (2004). Radon in tube-well drinking water and indoor air. Indoor and Built Environment, 13(5), 383-385.

Srinivasa, E., Rangaswamy, D. R., & Sannappa, J. (2015). Determination of radon activity concentration in drinking water and evaluation of the annual effective dose in Hassan district, Karnataka state, India. Journal of Radioanalytical and Nuclear Chemistry, 305, 665-673.

Sundal, A. V., Valen, V., Soldal, O., & Strand, T. (2008). The influence of meteorological parameters on soil radon levels in permeable glacial sediments. Science of the total environment, 389(2-3), 418-428.

Thabayneh, K. M., & Jazzar, M. M. (2013). Radioactivity levels in plant samples in Tulkarem district, Palestine and its impact on human health. Radiation protection dosimetry, 153(4), 467-474.

Thielen, H. (2012). The Fukushima Daiichi nuclear accident—an overview. Health physics, 103(2), 169-174.

Todorovic, N., Nikolov, J., Forkapic, S., Bikit, I., Mrdja, D., Krmar, M., & Veskovic, M. (2012). Public exposure to radon in drinking water in Serbia. Applied Radiation and Isotopes, 70(3), 543-549.

Torkar, D., Zmazek, B., Vaupotič, J., & Kobal, I. (2010). Application of artificial neural networks in simulating radon levels in soil gas. Chemical Geology, 270(1-4), 1-8.

Uwatse, O. B., Olatunji, M. A., Khandaker, M. U., Amin, Y. M., Bradley, D. A., Alkhorayef, M., & Alzimami, K. (2015). Measurement of natural and artificial radioactivity in infant powdered milk and estimation of the corresponding annual effective dose. Environmental Engineering Science, 32(10), 838-846.

Villalba, L., Sujo, L. C., Cabrera, M. M., Jiménez, A. C., Villalobos, M. R., Mendoza, C. D., ... & Peraza, E. H. (2005). Radon concentrations in ground and drinking water in the state of Chihuahua, Mexico. Journal of environmental radioactivity, 80(2), 139-151.

Wu, Y. Y., Ma, Y. Z., Cui, H. X., Liu, J. X., Sun, Y. R., Shang, B., & Su, X. (2014). Radon concentrations in drinking water in Beijing City, China and contribution to radiation dose. International journal of environmental research and public health, 11(11), 11121-11131.

Xinwei, L. (2006). Analysis of radon concentration in drinking water in Baoji (China) and the associated health effects. Radiation protection dosimetry, 121(4), 452-455.

Yalcin, S., Gurler, O., Akar, U. T., Incirci, F., Kaynak, G., & Gundogdu, O. (2011). Measurements of radon concentration in drinking water samples from Kastamonu (Turkey). Isotopes in environmental and health studies, 47(4), 438-445.

Yalim, H. A., Sandıkcıoğlu, A., Ünal, R., & Orhun, Ö. (2007). Measurements of radon concentrations in well waters near the Akşehir fault zone in Afyonkarahisar, Turkey. Radiation Measurements, 42(3), 505-508.

Yousef, A. M. M., & Zimami, K. (2019). Indoor radon levels, influencing factors and annual effective doses in dwellings of Al-Kharj City, Saudi Arabia. Journal of Radiation Research and Applied Sciences, 12(1), 460-467.

Kim, G. H., & Cho, J. H. (2022). Radioactive concentrations in chemical fertilizers. Journal of Radiation Protection and Research, 47(4), 195-203.

USGS (2019). United States Geological Survey. Aquifers and Groundwater. Water Science School October 16, 2019.

Al-Bataina, B. A., Ismail, A. M., Kullab, M. K., Abumurad, K. M., & Mustafa, H. (1997). Radon measurements in different types of natural waters in Jordan. Radiation Measurements, 28(1-6), 591-594.

Choubey, V. M., Bartarya, S. K., & Ramola, R. C. (2003). Radon in groundwater of eastern Doon valley, Outer Himalaya. Radiation measurements, 36(1-6), 401-405.

WHO (2004).World Health Organization. Guidelines for third edition recommendations drinking-water quality.

USEPA (1991). United States Environmental Protection Agency. National primary drinking water regulations: radio nuclides; proposed rules. Federal register, 56(138), 33050.

Rani, A., Mehra, R., & Duggal, V. (2013). Radon monitoring in groundwater samples from some areas of Northern Rajasthan, India, using a RAD7 detector. Radiation protection dosimetry, 153(4), 496-501.

El-Araby, E. H., Soliman, H. A., & Abo-Elmagd, M. (2019). Measurement of radon levels in water and the associated health hazards in Jazan, Saudi Arabia. Journal of radiation research and applied sciences, 12(1), 31-36.

Isinkaye, M. O., & Ajiboye, Y. (2020). Correlations of 226 Ra and 222 Rn activity concentrations in surface soil and groundwater of basement complex geological area of southwest Nigeria. SN Applied Sciences, 2, 1-8.

Jakhu, R., Mehra, R., & Bangotra, P. (2020). Risk assessment of 226 Ra and 222 Rn from the drinking water in the Jalandhar and Kapurthla districts of Punjab. SN Applied Sciences, 2, 1-8.

Caridi, F., Marguccio, S., Belvedere, A., DAgostino, M., & Belmusto, G. (2019). The natural radioactivity in food: a comparison between different feeding regimes. Current Nutrition & Food Science, 15(5), 493-499.

Yang, B., Zhou, Q., Zhang, J., Li, Z., & Tuo, F. (2021). Evaluation of the natural radioactivity in food and soil around uranium mining region. Journal of Radioanalytical and Nuclear Chemistry, 329, 127-133.

Abojassim, A. A., Hady, H. N., & Mohammed, Z. B. (2016). Natural radioactivity levels in some vegetables and fruits commonly used in Najaf Governorate, Iraq. Journal of bioenergy and food science, 3(3), 113-123.

Chapter – 4

Experimental Set-Up For Radon Measurement In Different Media

Radon Measurement In Air, Water And Soil

For the thesis work we have measured radon concentration in water, air and soil gas. AlphaGUARD PQ2000 PRO monitor has been utilized to measure radon in air and water, whereas soil radon has been measured using Barasol BMC2 probe.

4.1 AlphaGUARD PQ2000 PRO Monitor

Among the different radon detecting systems, AlphaGUARD PQ2000 PRO seems to come close to an "ideal" radon monitor due to its high sensitivity and outstanding accuracy and capability of measuring radon gas in extreme atmospheric conditions. AlphaGUARD PQ2000 PRO is a portable radon monitor utilizes the established concept of pulse ionization chamber (alpha spectroscopy) in combination with digital signal processing (DSP) technology. It can detect radon concentrations in the range of 1.85-1998000Bq/m^3, with a precision of 0.37 Bq/m^3. It can be operate in the temperature range of -10°C to +50°C (***Instruments 1998***). It has a radon detector with a 0.62 litre volume (active volume of 0.56 liter). It gives quick responses to radon concentration gradients with very high detection efficiency. To operate the cylindrical ionization chamber of the AlphaGUARD PQ2000 PRO, a 750 volt DC power supply is required. During the measurement procedure, ^{222}Rn gas gets into the ionization chamber through a vast glass fiber filter, a diffusion process occurs. Glass fiber filter prevents the radon progeny products from entering the ionization chamber and allows the gaseous radon (^{222}Rn) to pass (***Instruments 1998***). Additionally, the filter serves as a barrier, preventing dust particles from contaminating the interior of the chamber. When radon gas emits alpha particles, these particles ionize the air inside the ionization chamber. The cathode draws in positively charged particles, while the anode attracts the negatively charged ones. Through this process ionization current flows through the whole circuit which is proportional to the number of emitted alpha particles (***Adrovic and Dedic 2008***). The ionisation chamber's design remains largely conventional. Referencing **Figure 4.1**, intricate details of the detector's construction are depicted. Serving as the standard tool for professional radon monitoring, this radon detector ensures precise on-site measurements. Beyond assessing radon concentrations in the air, the AlphaGUARD PQ2000 PRO device concurrently captures and logs ambient temperature, relative humidity, and atmospheric pressure through integrated sensors. The AlphaGUARD PQ2000 PRO functions autonomously via its rechargeable battery, allowing for 10 to 15 days of operation without reliance on mains power. Additionally, the device can be powered directly from the mains when needed. Schematic diagram of inner design of an AlphaGUARD PQ2000 PRO is depicted in **Figure 4.1**.

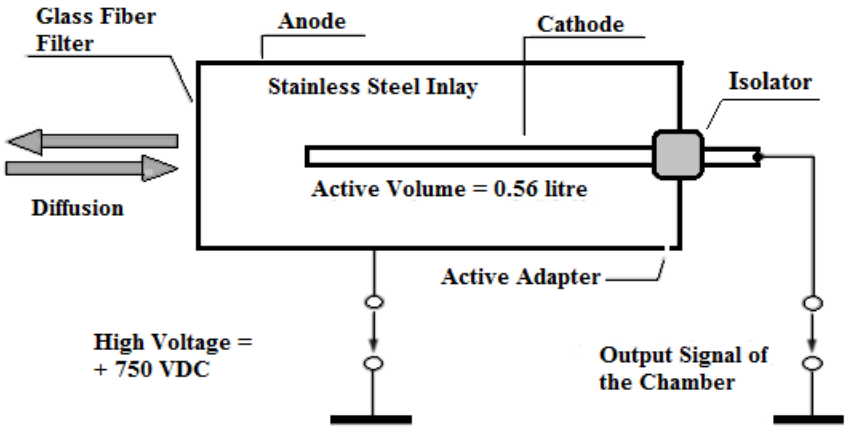

Fig. 4.1 Diagram illustrating the internal structure of an AlphaGUARD PQ2000 PRO (***Instruments 1998***)

Despite the well-established limitations inherent in measuring extremely low currents within ionisation chambers, the incorporation of DSP (Digital Signal Processing) technologies enables the utilization of a large detector volume. In DSP, there exist three distinct signal processing channels, with each channel being linked to a dedicated analog-to-digital converter integrated into the network framework. This architectural arrangement enables the simultaneous analysis of incoming signals from preamplifiers based on three distinct sets of characteristics. Block diagram of digital signal processing is depicted in **Figure 4.2.**

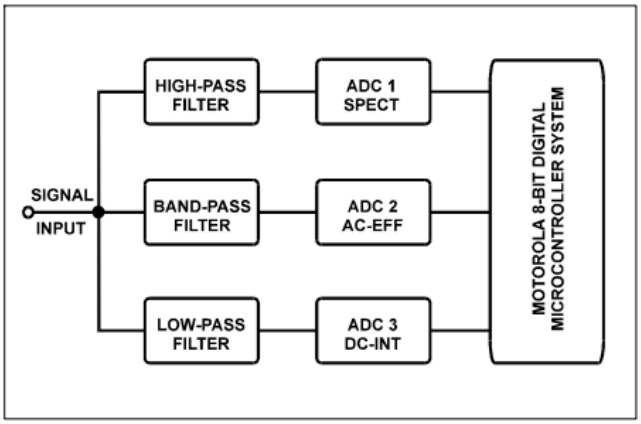

Fig. 4.2 Block diagram of digital signal processing (***Instruments 1998***)

Within the AlphaGUARD PQ2000 PRO system Channel 1 serves as the spectrometric channel. In this channel, signal analysis extends beyond merely characterizing pulse depth; it also involves categorizing pulses based on their waveforms. This pulse analysis results in a three-dimensional spectrum. Along the X-axis, pulse depth is classified, typically in relation to the energy of adjacent alpha particles. The Y-coordinate represents the pulse count per unit of time, while the Z-coordinate denotes different pulse waveform categories.

The intricate pulse characterization employed here allows for an exceptionally efficient distinction between authentic alpha particle events and various forms of interference (such as microphonic phenomena). Channel 2 handles signal processing solely under higher radon concentration circumstances. The chosen band-pass filter design ensures that the signal noise level amplitudes maintain a direct proportional relationship with the square root of the total ionization current under high pulse densities. By judiciously utilizing this correlation, precise measurements in the pico-ampere range are achievable (***Instruments 1998***). Moreover, this approach eliminates a common source of errors, namely the drift in preamplifier offset resulting from the temperature-sensitive FET structure of the preamplifier. Channel 3 is reserved for a conventional direct current measurement approach, to be employed when encountering exceptionally high radon concentrations. This channel also contributes to the system's robustness against excessive feedback. These three signal attributes collectively serve as the basis for six distinct analysis algorithms. Ultimately, an optimized density procedure is employed to derive the actual radon concentration from these attributes. As a result, each radon value displayed by the AlphaGUARD PQ2000 PRO system emerges as the final outcome of approximately 50,000,000 computational operations (***Instruments 1998***). Achieving this computational efficiency necessitates the utilization of cutting-edge semiconductor technology, which enables the AlphaGUARD PQ2000 PRO's energy consumption to be maintained at a low level of 3 mA, even when processing such voluminous data loads.

A user operating the AlphaGUARD PQ2000 PRO has the option to select either the 10-minute cycle or the 60-minute cycle. In the 10-minute cycle, the data storage capacity is sufficient for approximately 550 hours (about 3 weeks) of continuous recording. On the other hand, the 60-minute cycle allows for extended measurements, with a recording capacity of approximately 3400 hours (around 4 months).

In addition to the aforementioned cycles, the AlphaGUARD PQ2000 PRO offers two additional measuring cycles known as the flow-through mode (Flow-Mode). These modes have been specifically designed to accurately capture and present strong concentration gradients when conducting flow-through measurements.

Different measuring modes are displayed in **Figure 4.3 (a** & **b)**.

Fig. 4.3a Different diffusion modes

Fig. 4.3b Different flow modes

On the display panel the upper line displays the measured radon concentration in Bq/m^3, accompanied by its associated statistical error bar. The lower line indicates the current air temperature in °C with a range from -10°C to +50°C, the relative humidity in % rH with a range spanning from 0% rH to 95% rH and the barometric pressure is shown in hPa, with a range extending from 700 mbar to 1100 mbar. Example of one measured radon concentration value is displayed in **Figure 4.4.**

Fig. 4.4 Display showing radon concentration and other parameters

Calibration of AlphaGUARD PQ2000 PRO

The AlphaGUARD PQ2000 PRO is calibrated to meet the rigorous standards of various international radon measurement organizations, including esteemed institutions such as the National Institute of Standards and Technology (NIST) in the United States, the National Physical Laboratory (NPL) in the United Kingdom (UK), and the Physikalisch-Technische Bundesanstalt (PTB) in Germany. This system is versatile, allowing for both instantaneous radon activity measurements across various geographical points and continuous radon monitoring at a specific location over extended periods. The AlphaGUARD PQ2000 PRO has an instrumental calibration error of ± 3% for ^{222}Rn concentration measurement (***Instruments 1998***). This instrument is known for its very high calibration stability and for this reason it is used in many international calibration verification laboratories. Also, this long-term maintenance-free radon monitor delivers reliable measurement values in extreme air humidity and is insensitive to both vibrations and shocks.

4.1.1 Measurement of indoor and outdoor

Radon gas concentration, whether indoors or outdoors, can be measured directly using the diffusion mode of the AlphaGUARD PQ2000 PRO. The device has to position in the area where the activity of radon gas is to be assessed. During the measurement procedure the equipment has been operated in a 10-minute diffusion mode. Following each 10-minute interval, the recorded radon level, along with air temperature, pressure, and relative humidity, can be collected either manually or by extracting the data from the instrument. **Figure 4.5** provides a depiction of an indoor radon gas measurement scenario.

Fig. 4.5 Measurement of indoor air radon concentration

4.1.2 Measurement of water radon concentration

To measure water radon concentration, one needs the AquaKIT and AlphaPUMP in addition to the AlphaGUARD PQ2000 PRO. Its integration with AlphaGUARD PQ2000 PRO and AlphaPUMP, AquaKIT empowers us to accurately assess the concentration of radon in water samples. The essential elements within AquaKIT utilized for the purpose of water radon analysis encompass a glass degassing vessel, a glass security vessel, and several interconnecting tubes.

Tap positions for sample injection and radon concentration measurement are shown in **Figure 4.6 (a** & **b)**.

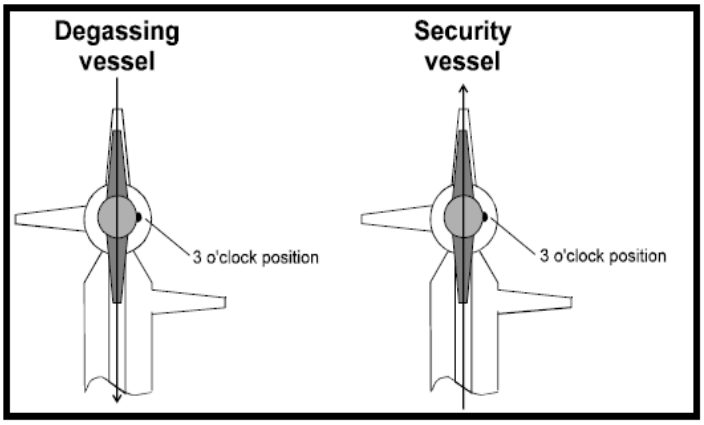

Fig. 4.6a Schematic diagram of tap position during sample injection

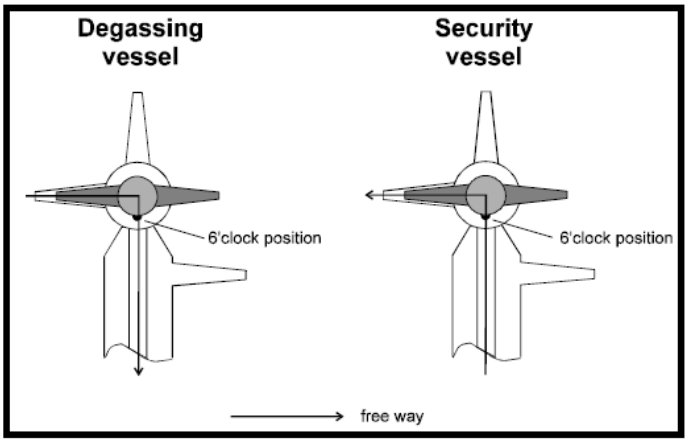

Fig. 4.6b Schematic diagram illustrating the position of the tap for measuring radon concentration

In a closed gas cycle as shown in **Figure 4.7**, the AlphaPUMP serves the purpose of purging dissolved radon from water samples stored within the degassing vessel. To prevent water vapor from entering the AlphaGUARD PQ2000 PRO, a security vessel is connected downstream of the degassing vessel's outlet. This arrangement ensures that any water vapor introduced into the gas cycle during the degassing procedure is collected within the security vessel, thereby reducing the chance for water vapor to reach the AlphaGUARD PQ2000 PRO. The AlphaPUMP, as depicted in **Figure 4.7**, is used to maintain the directional flow of air and radon within the measurement system.

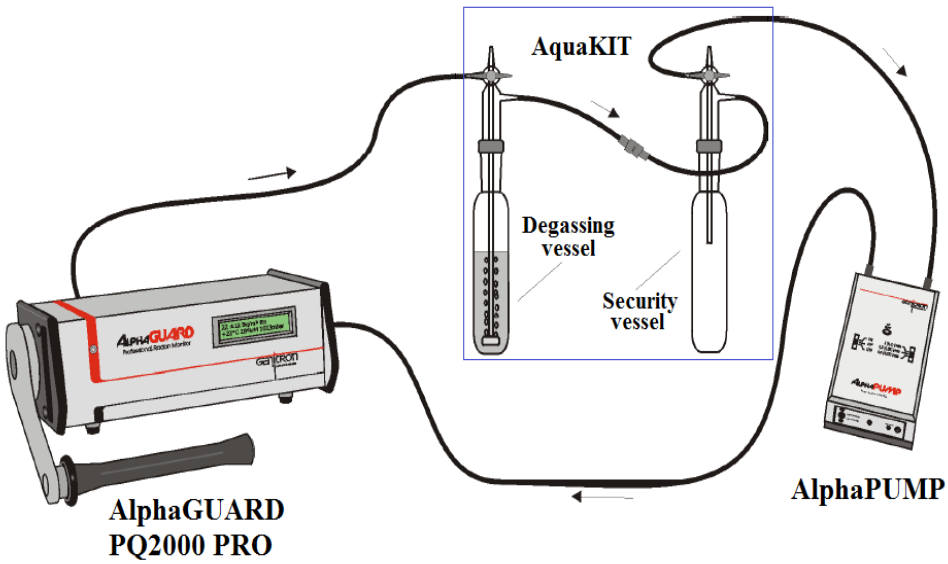

Fig. 4.7 Schematic diagram of the experimental set-up used for measurement of water radon (***Instruments 1998***)

An image depicting the laboratory setup for measuring water radon is presented in the following **Figure 4.8**.

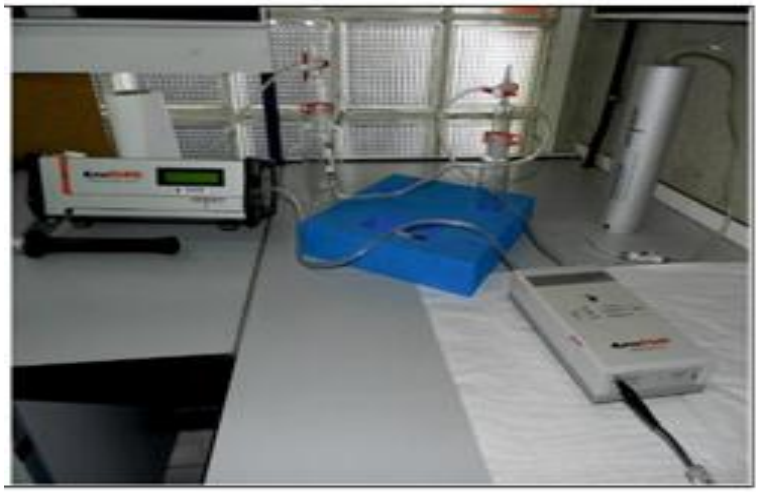

Fig. 4.8 Water radon measurement set-up

For proper measurements, it is necessary to ensure that the air within the experimental arrangement is free of radon before experiment. This entails achieving a "zero level" of radon concentration before introducing water samples into degassing vessel (***Instruments 1998***). Ordinarily, radon concentration in ambient air is quite minimal. Hence, prior to commencing the estimation of water radon concentration, the measurement setup is purged with ambient air to effectively reduce radon levels if they exist in the AlphaGUARD PQ2000 PRO device. Subsequently, we added an activated charcoal filter cartridge in the sealed circuit to reduce the concentration levels of radon (< 5 Bq/m^3) within the measurement setup. This method of measuring at the zero level is crucial before analyzing new water samples that might possess potentially low radon concentrations. However, for quick measurements, the "zero level" protocol can be omitted provided the samples are anticipated to have considerably high radon concentrations (exceeding several kBq/m^3).

To ensure accurate measurement of radon concentration, the residual ^{222}Rn level was reduced to zero using an active coal filter cartridge (***Figure 4.9***) before taking readings for the next sample

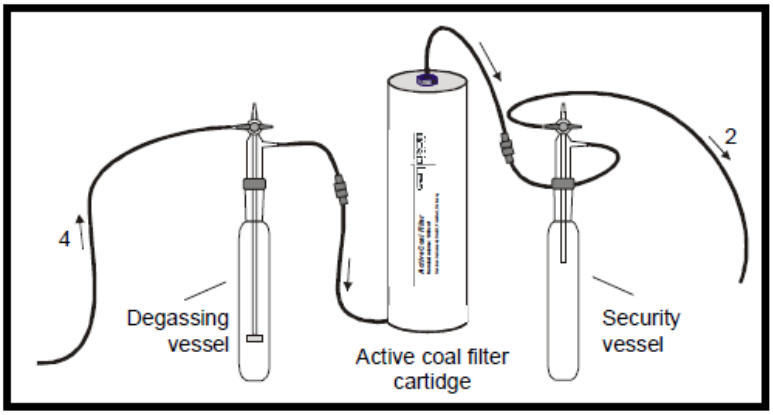

Fig. 4.9 Configuration for achieving a zero level using an active coal filter cartridge

The water radon levels are assessed using the quick measurement procedure recommended by the manufacturer (***Instruments 1998***). Before assessing the radon concentration in each sample, the background concentration of radon in the vacant arrangement is determined over a brief period. Using a plastic syringe, 100 ml of each water sample is injected into the degassing vessel. Subsequently, the AlphaGUARD PQ2000 PRO monitor is activated with the "1min FLOW" measuring mode, and the AlphaPUMP's pumping rate is set to 0.3 liters/min in accordance with the manufacturer's quick measurement guidelines (***Instruments 1998***).

Following a 10 minute interval, the AlphaPUMP is turned off, while the AlphaGUARD continued to operate for an additional 20 minutes. Throughout this entire process, after every minute radon concentration of each sample is recorded via Data Expert software provided with the AlphaGUARD PQ2000 PRO. The recorded values are then averaged to obtain the final radon concentration in the concerned air (C_{Air}) for each sample. ^{222}Rn concentration in the water sample is estimated from C_{Air} using the following equation (***Instruments 1998***):

$$\boldsymbol{C_{Water} = \frac{C_{Air} \times \left(\frac{V_{System} - V_{Sample}}{V_{Sample}} + k\right) - C_0}{1000}} \quad (4.1)$$

Where; C_{Water} represents the concentration of ^{222}Rn in the water sample (Bq/l), C_{Air} is the air ^{222}Rn concentration in the measurement setup after injecting water sample (Bq/m^3), C_0 represents the initial radon level within the measurement setup before injecting water sample (Bq/m^3), V_{System} corresponds to the interior volume of the measurement setup (ml), V_{Sample} is the volume of water sample (ml) and k denotes the diffusion coefficient of ^{222}Rn.

The determination of radon level of the samples relies on the ^{222}Rn concentration as indicated by the AlphaGUARD PQ2000 PRO. Nevertheless, it's crucial to emphasize that the measurement value at hand does not accurately reflect the actual radon concentration within the water sample. This discrepancy arises from the fact that a portion of the radon remains diluted within the aqueous phase (***Instruments 1998***). To accurately account for this dilution effect, precise knowledge of the internal volume of the measurement setup, denoted as V_{System} is necessary.

The temperature-dependent behavior of water dissolved radon is characterized by the diffusion coefficient k. It is expressed as the relationship between the concentrations of radon in the liquid phase compared to its concentration in the gas phase (***Instruments 1998***). Utilizing the value of k one can calculate the amount of radon that present within the water sample after the dilution process.

The expression for the diffusion coefficient 'k' is as follows (***Clever 1979***):

$$\boldsymbol{k = 0.105 + 0.405\, e^{(-0.0502T)}} \quad (4.2)$$

Where; T is temperature of water sample (˚C).

Temperature dependency of the radon diffusion coefficient factor k is depicted in **Fig. 4.10**.

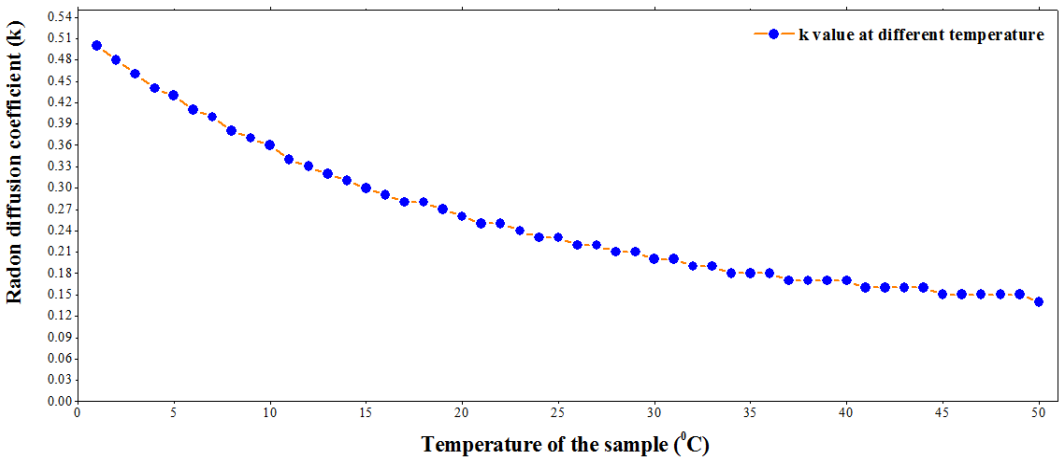

Fig. 4.10 Variation of diffusion coefficient values with temperature

Fig. 4.10 illustrates that within the temperature range of 20 - 30 °C the impact of temperature on k is minimum. The quick measurements rely on the provided relationship, where the volume of air enclosed in the setup compared to the measuring water sample is approximately 10:1. As a consequence, 'k' introduces an error of ≤ ± 2 into the final results under typical room temperature conditions (25 - 30 °C) (***Instruments 1998***). Nonetheless, for measurements involving significant temperature fluctuations, precise determination of the diffusion coefficient 'k' becomes imperative to ensure the accuracy of the ultimate outcomes.

Given the specified conditions by the AlphaGUARD PQ2000 PRO manufacturer for quick measurement using the AlphaPUMP, it is possible to simplify **Equation 4.1** as follows (***Instruments 1998***):

$$C_{Water} = \frac{C_{Air} \times (10.02 + k) + C_0}{1000} \quad (4.3)$$

Where; V_{System}= 1102 ml and V_{Sample}= 100 ml (for our measurement set-up).

During the measurement process, the temperature of the water samples is recorded, and the corresponding k values are determined using **Equation 4.2**.

4.2 BARASOL BMC2 probe

The Algade-manufactured BARASOL BMC2 radon probe can be used for continuous monitoring of radon levels, as well as temperature and pressure within soil gas. Soil radon concentration is the amount of radon in a given volume of soil gas, and it is measured by detecting the radioactive decay of radon in soil gas. This probe

incorporates a radon sensor equipped with a silicon alpha-sensitive detector that has a sensitive area of 400 mm^2 and a depletion depth of 100 μm. This detector records the influx of radon gas into its detection chamber. The sensor is shielded from light through an aluminum layer and has an added layer of cellulose varnish for extra mechanical protection. Within a cylindrical chamber measuring 6 cm in diameter and 57 cm in length, emissions of α-particles from radon are detected by the silicon detector. The chamber's lower section is equipped with three layers of 20 μm thick cellulose filters, allowing only radon gas to pass while capturing solid daughter products. A front-facing energy cut-off window in front of the silicon detector enables the detection of α-particles within the energy range of 1.5 MeV to 6 MeV. To prevent soil particles and insects from entering the exposed bottom of the cylindrical steel casing that encases the detector material, a lattice made of stainless steel is in position. Measuring the soil radon concentration is achieved through an energy spectrometer connected to the silicon device.

The adjustable radioactive detector is capable of measuring within a customizable time frame of 1 to 240 minutes. Its measurement capabilities encompass a spectrum from 100 Bq/m^3 - 1 GBq/m^3, demonstrating a precision of 1 Bq/m^3. Operational versatility extends to temperatures ranging from -20°C to 70°C. Complementing the radon detection functionality, this apparatus is equipped with a platinum resistance thermometer designed to gauge soil temperatures within the range of -20°C to 100°C. Furthermore, it incorporates a silicon-based pressure sensor dedicated to tracking atmospheric pressure, with measurements spanning from 500 mbar to 1.5 bar.

BMC2 probe has three main components: a detection unit, electronics, and a battery unit. These components are housed within a cylindrical tube made of fibre glass and corrosion-resistant stainless steel. This tube has a diameter of 62 mm and a length of 489 mm. Interconnection and control for the probe are facilitated by an 8-pin connector, which, when covered by a cap, offers an IP68 rating for airtight and watertight sealing. The battery unit accommodates two 1.5 V alkaline batteries. A pair of high-quality alkaline batteries bestows the probe with over 6 months of independent operational capability. The memory of the probe can store data for up to one year.

4.2.1 Method of measurement

For continuous monitoring of radon gas in soil, the radon monitor BARASOL BMC2 installed vertically in a borehole at a depth of 1 m beneath the ground surface at the monitoring site. There is an exponential increase of soil radon activity up to a depth around 80 cm where it attains an asymptotic value (***Mittal et al. 2016, Chowdhury et al. 2022***). Hence, radon activity should be fairly constant below this depth and dependent only on geological and local meteorological factors (***Chowdhury et al. 2022***). It would ease the detection of sudden fluctuations in soil radon activity. The borehole wall is protected with a polyvinyl chloride (PVC) pipe. The pipe is approximately 1 meter in length and 10 centimetres in diameter. The detector is situated at the lower extremity of the pipe,

which is open at the bottom while sealed airtight at the top by a plastic cap (see ***Figure 4.11***). Apart from the detection of radon activity, the instrument can also record variations of the soil temperature and soil pressure. Data collection procedure is performed at the rate of 1 measurement per hour. The time series data are recorded by the RnView2 software. Experimental setup for the soil radon measurement study is presented in **Figure 4.11**.

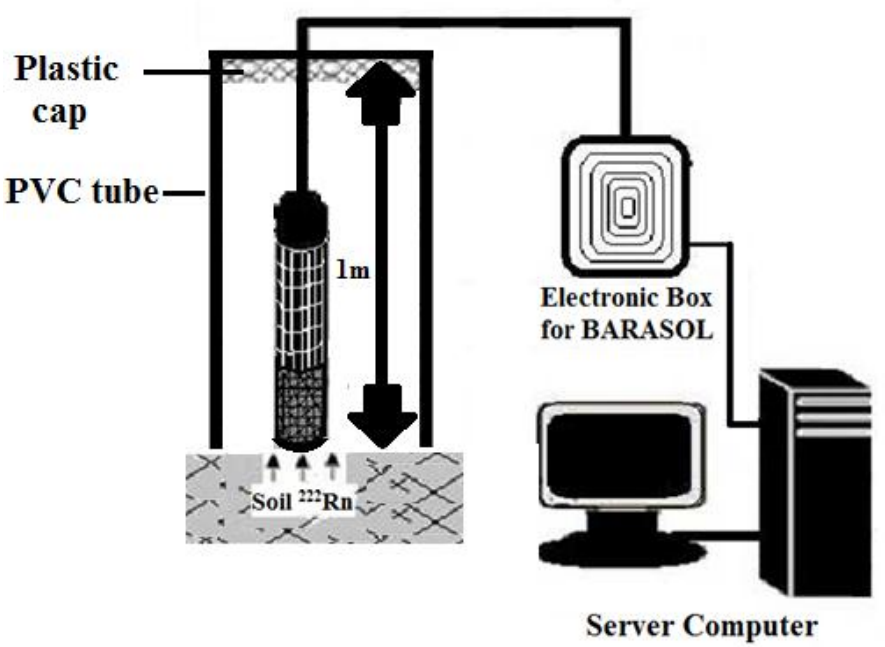

Fig. 4.11 Schematic diagram of experimental setup for soil ^{222}Rn measurement with BARASOL BMC2 probe

References

Adrovic, F., & Dedic, A. (2008). Investigation of Radon in drinking water from wells of the North-Eastern region of Bosnia and Herzegovina.

Chowdhury, S., Deb, A., Barman, C., Nurujjaman, M., & Bora, D. K. (2022). Simultaneous monitoring of soil 222Rn in the Eastern Himalayas and the geothermal region of eastern India: an earthquake precursor. Natural Hazards, 112(2), 1477-1502.

Clever, H. L. (1979). Krypton, xenon and radon-gas solubilities. Solubility Data Series.

Instruments G (1998). AlphaGUARD portable radon monitors user manual. Germany.

Mahur, A. K., Kumar, R., Jojo, P. J., Kumar, A., Singh, A. K., Varshney, A. K., & Prasad, R. (2006). Radon levels in dwellings of some Indian cities. Asian Journal of Chemistry, 18(5), 3371.

Mittal, S., Rani, A., & Mehra, R. (2016). Radon levels in drinking water and soil samples of Jodhpur and Nagaur districts of Rajasthan, India. Applied Radiation and Isotopes, 113, 53-59.

Vaupotič, J., Gregorič, A., Kobal, I., Žvab, P., Kozak, K., Mazur, J., ... & Grządziel, D. (2010). Radon concentration in soil gas and radon exhalation rate at the Ravne Fault in NW Slovenia. Natural hazards and earth system sciences, 10(4), 895-899.

Chapter – 5

Underground Air Radon Exposure In And Around Kolkata Municipal Corporation Area: An Exhaustive Study

5.1 Introduction

The contemporary issue of health hazards arising from exposure to various toxic elements is a matter of significant concern (***McKenzie et al. 2012; Eaton and Groopman 2013; Naujokas et al. 2013***). Radon (^{222}Rn), a radioactive byproduct of the ^{238}U chain resulting from the alpha decay of radium (^{226}Ra), stands out as a major contributor to radiation exposure in the human population. Identified as a carcinogenic gas (***Field et al. 2001***), radon poses a substantial risk of causing lung cancer (***Miles 1998; Wenjie et al. 1999***) and cancers affecting other organs, such as the stomach and spleen (***Kendall and Smith 2002***).

Given the ubiquitous presence of ^{238}U in soil and rock worldwide, radon exposure is pervasive. Nevertheless, the concentration of radon in the air exhibits considerable variability depending on the location, primarily influenced by the radon exhalation rate from the soil (***Ielsch et al. 2001***). Notably, higher concentrations are observed in underground spaces, with the expectation of diffusion to the atmosphere where concentrations are lower. Numerous homes globally exhibit elevated levels of ^{222}Rn concentration (***Gesell 1983; Langroo et al. 1991; Doi et al. 1994***). Factors influencing radon concentration in indoor spaces include the emanation power of the ground, radon diffusion to the air, and various construction-related elements (***Dixon et al. 1996; Durrani and Ilic 1997; Li et al. 2006; Oikawa et al. 2006; Rahman et al. 2008***), such as construction materials (e.g., cements, ceramics, marble chips), wall porosity and thickness, radium concentration in subsoil, geological structure beneath built-up areas, and air ventilation pathways.

The measurement of indoor radon concentration is crucial, considering that over 50% of the radiation dose received by the human population from natural sources comes from radon and its progeny (***Ahmed et al. 1997; Kullab et al. 1997; UNSCEAR 2000***). Typically, basements and various underground spaces, being in direct contact with soil and often having inadequate ventilation systems, exhibit elevated radon levels (***Anastasiou et al. 2003***).

The possible sources of basement or indoor radon gas are demonstrated in **Figure 5.1**.

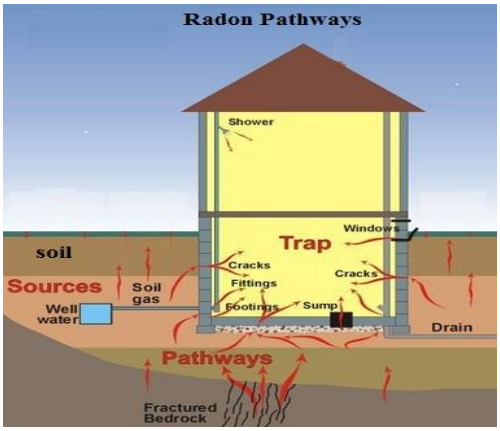

Fig. 5.1 Possible sources of indoor radon gas

The action level is the defined threshold of radon concentration that triggers the implementation of remedial or protective measures. Various agencies and countries have established their own safety guidelines for indoor air radon gas concentration (***Franklin and Fuoss et al. 1995; Choubey and Ramola 1997; Fuoss et al. 1999; Ramola 2005; Prasad et al. 2008; Jayanthi et al. 2011***), typically around 200 Bq/m^3 in most cases.

To fully utilize basements and underground spaces without compromising safety, it is essential to assess radon concentration levels in these areas. Such assessments are conducted globally, with studies by Field et al. (***2000***) exploring residential radon exposure and its lung cancer risk in the USA. Li et al. (***2006***) measured radon concentrations in Chinese basements, ranging from 14.9 Bq/m^3 to 2482 Bq/m^3. Rahman et al. (***2010***) surveyed radon levels in the Rawalpindi region and Islamabad Capital Territory of Pakistan, revealing concentrations ranging from 12 ± 5 Bq/m^3 to 293 ± 19 Bq/m^3. In Yazd, Iran, the mean radon concentration in dwelling basements was found to be 137.36 Bq/m^3 (***Bouzarjomehri and Ehrampoosh 2008***).

Similar measurements have been conducted in various parts of India, such as Delhi (***Gupta et al. 2011***), Tamilnadu (***Jayanthi et al. 2011***), and certain Himalayan locations (***Choubey and Ramola 1997; Ramola et al. 2005; Prasad et al. 2008***). Numerous references, including Franklin and Fuoss (***1995***) and Fuoss et al. (***1999***), underscore the importance of radon measurement in underground spaces. However, there is no existing report on radon measurements in Kolkata, a densely populated metropolitan city. With a population of approximately 45 lakhs and a density of 24,252/km^2 according to the provisional results of the 2011 national Census, Kolkata sees migration from other districts of West Bengal and nearby states due to its developing economy. As skyscraper basements are increasingly repurposed for various uses, including supermarkets, clinics, restaurants, entertainment venues, garages, or parking spaces, it is imperative to assess ^{222}Rn concentration levels before use and implement necessary measures if levels are elevated.

5.1.1 Objective of the study

Main objective of this study is to measure the radon (^{222}Rn) concentration in basements and subways in the different parts of Kolkata city and its nearby areas. Radon concentrations have been measured in 36 different basements and 14 underground subways (which are continuously being used by common people or passengers). For assessing the effect of the radon exposure on the health of the concerned people, we have estimated the annual effective dose consumed by the persons working or staying in the basements. This type of investigation is carried out for the first time in Kolkata city and around and hope will add new information regarding indoor radon exposure and its effect in this part of the world.

5.2 Location and extent of the study area

Kolkata Municipal Corporation (KMC) area, the focus of the present investigation, is the second largest urban agglomeration in India bounded by latitude 22°27'–22°40' N and longitude 88°18'–88°28' E (***Mohanty et al. 2013***). Its elevation is 1.5 – 9.0 m (5-30 ft) and is over the Bengal Basin. Kolkata, the capital of West Bengal state, is one of the oldest industrial cities in India and is a major industrial and commercial hub in the eastern and north-eastern region of India. The boundary area of KMC covers an extent of 187.33 sq. km (***Jha and Bairagya 2011, Nath et al. 2014***). The observation sites within the boundary area of KMC and its surrounding areas are shown in the **Figure 5.2**.

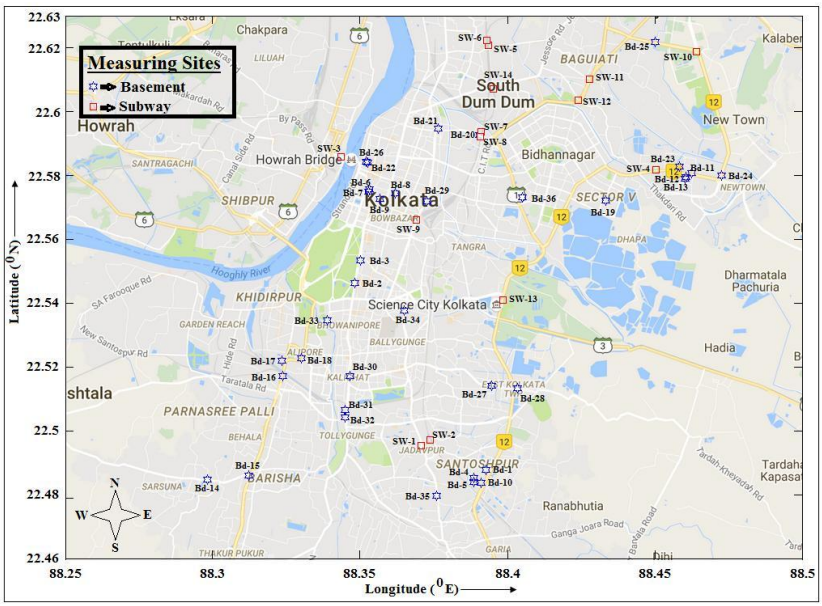

Fig. 5.2 A map showing the measurement sites in KMC and its surrounding areas

Originally the city of Kolkata grew in the North-South direction over the natural level of the east bank of Hooghly River for over a length of 50 km. But due to enormous population pressure it has encroached into the back swamp and marshy land to the east by way of filling up extensive areas, especially in the Salt Lake and Rajarhat areas.

5.3 Measurement techniques and analysis procedure

5.3.1 Radon concentration measurement procedure

Air radon concentration has been measured using AlphaGuard radon monitor in 10 minutes diffusion mode. A detail about the measurement process is given in **Chapter 4 Section 4.1.1**. The instrument was placed at different locations of the basements and underground subways and readings were noted until equilibrium state was reached. After measuring the basement or subway ^{222}Rn concentrations, the radon monitor was placed on the nearby open ground space for measuring Background (BG) ^{222}Rn concentration. The Background radon concentrations were measured on the same day under same weather condition and it was ensured that there was no concrete structure

within 10 ft of the measuring point. The latitude and longitude of the places were also noted using a GPS meter.

5.3.2 Annual effective dose

To evaluate the annual effective dose received by the persons (workers and security guards etc.) staying in the basement for a significant period of time, we have used **relation 5.1** as suggested in ICRP (1993) and UNSCEAR (2000). Effective dose ($E_{T,R}$) is defined as the sum of the weighted equivalent doses in all the tissues and organs of the body and is given by:

$$\boldsymbol{E_{T,R} = C_{Rn} \times D \times F_{Rn} \times T_{Rn}} \qquad (\mathbf{5.1})$$

where, C_{Rn} is the ^{222}Rn concentration in Bq/m^3. D is conversion coefficient whose value is taken as 9 x10^{-6} mSv/h/Bq/m^3 (***UNSCEAR 2000***). F_{Rn}, the indoor ^{222}Rn equilibrium factor, is a measure of degree of radioactive equilibrium between radon and its decay products. F_{Rn} is taken to be 0.4 (***UNSCEAR 2000***). T_{Rn}, the indoor occupancy time, is the total hour spent within the indoor in a year. For dose calculation average occupation time per day is considered to be 9 hours.

5.4 Results and discussions

5.4.1 Radon concentration study

We conducted measurements of radon gas concentrations in the basements of various buildings and subways in the KMC area and its surroundings using an alpha guard radon monitor. Radon concentrations were assessed multiple times at each site, and the reported values represent the averages. The radon concentration data for all basements are presented in **Table 5.1**, and for subways in **Table 5.2**, with 'Bd' denoting buildings and 'SW' representing subways. Some buildings have multiple basement levels, with a maximum of three levels (BL1, BL2, and BL3 for basement levels one, two, and three, respectively). The average depths of BL1, BL2, BL3, and SW are 8 ft, 20 ft, 32 ft, and 12 ft, respectively. **Table 5.1** and **Table 5.2** also include the latitude and longitude coordinates of the corresponding sites. The basements and subways exhibit varying air circulation conditions, with some relying on natural circulation and others employing a man-made circulation system

Table 5.1: Measured radon concentration level for the basements of different buildings and corresponding Background (BG) values

Sl. No.	Building Code	Latitude/ Longitude	Basement Level	^{222}Rn Concentration (Bq/m^3)	BG. ^{222}Rn Concentration (Bq/m^3)
1	Bd-1	22.48767°N 88.39268°E	BL1	17.57±3.03	18.25±1.73

2	Bd-2	22.54631°N 88.34832°E	BL1	22.20±3.71	22.75±2.09
3	Bd-3	22.55342°N 88.35013°E	BL1	21.90±3.26	21.50±2.38
4	Bd-4	22.48387° N 88.38871° E	BL1	15.12±2.62	17.30±4.02
6	Bd-6	22.57566° N 88.35317° E	BL1	15.25±1.73	30.5±13.43
7	Bd-7	22.57492° N 88.35301° E	BL1	24.16±6.08	11.00±1.22
8	Bd-8	22.57447° N 88.36185° E	BL1	24.33±1.77	12.66±0.81
9	Bd-9	22.57266° N 88.35667° E	BL1	19.83±4.36	12.66±0.81
10	Bd-10	22.48363° N 88.39102° E	BL1	16.17±2.21	17.00±5.33
11	Bd-11	22.58081° N 88.46250° E	BL2	21.85±2.22	
			BL1	18.75±4.38	18.75±4.38
12	Bd-12	22.57952° N 88.46070° E	BL3	21.00±1.82	
			BL2	25.50±5.38	
			BL1	18.99±3.25	19.33±2.03
13	Bd-13	22.57891° N 88.46021° E	BL1	18.42±2.06	24.25±1.18
14	Bd-14	22.48472° N 88.29833° E	BL1	20.00±3.50	29.50±5.62
15	Bd-15	22.48603°N 88.31212° E	BL1	17.60±1.85	29.50±5.62
16	Bd-16	22.51712°N 88.32363° E	BL1	15.20±0.82	7.67±2.67
17	Bd-17	22.52197°N 88.32352° E	BL1	18.25±2.88	7.50±0.71
18	Bd-18	22.52276° N 88.33012° E	BL1	8.50±3.14	7.50±0.71
19	Bd-19	22.57223°N 88.43334° E	BL3	21.67±3.60	
			BL2	20.43±2.68	
			BL1	25.40±5.29	23.50±3.02
20	Bd-20	22.59273°N 88.39062° E	BL1	14.25±0.87	22.50±4.93
21	Bd-21	22.59454° N 88.37653° E	BL1	25.75±5.72	26.33±3.18
22	Bd-22	22.58403°N 88.35272° E	BL1	18.00±3.74	22.50±2.84
23	Bd-23	22.58271°N 88.45843° E	BL1	25.57±2.77	22.60±4.53

		22.57991° N	BL2	24.60±4.63	
24	Bd-24	88.47262° E	BL1	22.53±2.64	19.20±4.35
			BL3	26.10±3.44	
		22.62177° N	BL2	18.20±0.81	
25	Bd-25	88.45002° E	BL1	18.25±3.81	19.00±1.00
		22.58422°N			
26	Bd-26	88.35203° E	BL1	22.57±2.35	22.25±3.97
		22.51398°N	BL2	18.67±2.35	
27	Bd-27	88.39461° E	BL1	20.86±2.89	16.33±2.03
		22.51332°N			
28	Bd-28	88.40353° E	BL1	16.67±2.54	16.33±2.03
		22.57173°N			
29	Bd-29	88.37272° E	BL1	24.75±2.84	11.50±3.10
		22.51722°N			
30	Bd-30	88.34661° E	BL1	37.50±8.49	25.00±4.89
		22.50644°N			
31	Bd-31	88.34494° E	BL1	59.00±7.18	28.33±2.48
		22.50410°N			
32	Bd-32	88.34484° E	BL1	37.00±2.55	21.66±7.82
		22.53466°N			
33	Bd-33	88.33884° E	BL1	27.50±7.40	25.00±3.54
		22.53756°N			
34	Bd-34	88.36494° E	BL1	34.33±2.86	23.67±1.79
		22.47971°N			
35	Bd-35	88.37597°E	BL1	26.75±4.51	14.00±2.55
		22.57317°N			
36	Bd-36	88.40544°E	BL1	33.33±5.89	15.33±1.78
Total = 36		**Avg. value**		**22.70 ± 1.21**	**19.44 ± 1.06**

Table 5.1 shows that basement 31(Bd-31) has the highest radon concentration (59.00 ± 7.18) Bq/m^3 while basement 18 (Bd-18) has the lowest radon concentration (8.50 ± 3.14) Bq/m^3, with an average of (22.70 ± 1.21) Bq/m^3 for all the basements. Basement to basement variation of radon concentration has been presented in **Figure 5.3** for all the BL1s.

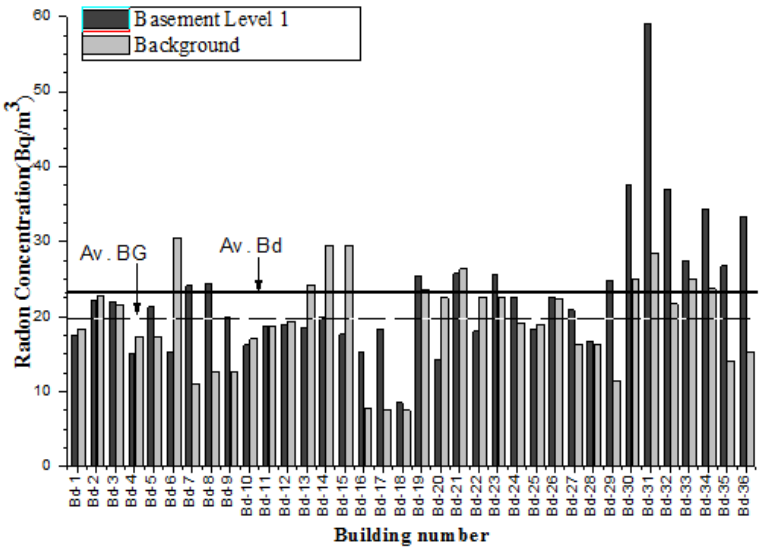

Fig. 5.3 A bar chart of building no. and corresponding Radon concentration both in basement level 1 & Background

Highest radon concentration has been observed in Tollygunge area (**22.50644° N, 88.34494° E**).

Figure 5.4 compares radon concentration of the different basement levels for those buildings having multiple basement levels.

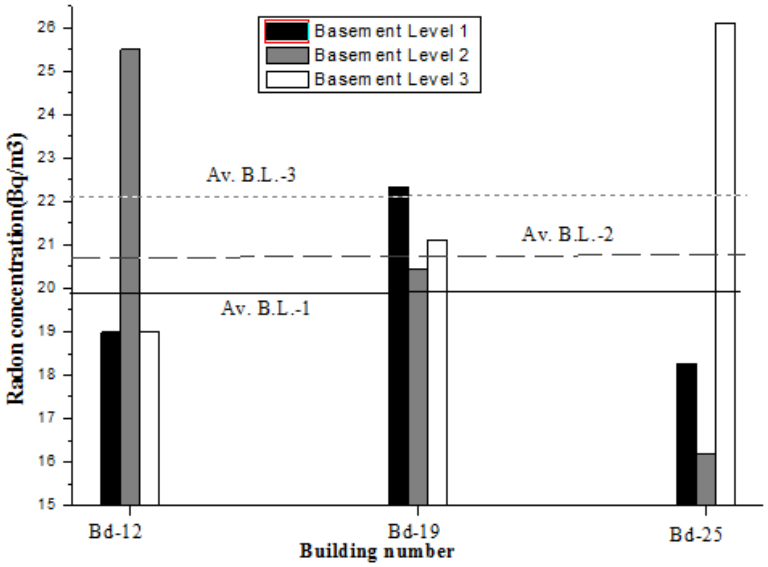

Fig. 5.4 Bar chart showing comparative radon level in basement level 1, 2 and 3

From this plot we observe that radon concentration does not follow any specific pattern for the different basement levels of a particular building.

Table 5.2 Measured radon concentration level both in the subways and corresponding background values

Sl. No.	Subway Code	Latitude / Longitude	^{222}Rn Concentration(Bq/m^3)	BG. ^{222}Rn Concentration(Bq/m^3)
1	SW-1	22.49531° N 88.37082° E	17.64 ± 2.07	13.40 ± 2.76
2	SW-2	22.49723° N 88.37382° E	18.66 ± 2.49	9.45 ± 2.30
3	SW-3	22.58573° N 88.34361° E	18.00 ± 2.30	21.86 ± 2.84
4	SW-4	22.58165° N 88.45052° E	19.40 ± 3.09	19.33 ± 2.03
5	SW-5	22.62069° N 88.39352° E	39.00 ± 1.24	21.00 ± 0.66
6	SW-6	22.62217° N 88.39307° E	17.44 ± 1.18	21.00 ± 0.66
7	SW-7	22.59364° N 88.39112° E	22.67 ± 4.22	16.2.0 ± 2.38
8	SW-8	22.59202° N 88.39080° E	26.50 ± 1.57	16.2.0 ± 2.36
9	SW-9	22.56610° N 88.36923° E	20.25 ± 4.24	18.00 ± 1.24
10	SW-10	22.61881° N 88.46402° E	25.28 ± 2.46	20.83 ± 1.68
11	SW-11	22.61003° N 88.42784° E	19.83 ± 2.78	22.67 ± 4.02
12	SW-12	22.60362° N 88.42413° E	17.00 ± 2.70	23.00 ± 7.38
13	SW-13	22.54082° N 88.39843° E	13.50 ± 1.78	14.50 ± 6.36
14	SW-14	22.60714° N 88.39508° E	47.50 ± 7.19	22.67 ± 6.68
Total = 14	**Avg. value**		**23.05 ± 2.59**	**18.58 ± 1.14**

Table 5.2 manifests that subway-14 (SW-14) has the maximum radon concentration (47.50 ± 7.19) Bq/m^3 while subway-13 (SW-13) has the lowest radon level (13.50 ± 1.78) Bq/m^3, average being (23.05 ± 2.59) Bq/m^3 for the subways. The variation of radon concentration level for different subways has been shown in **Figure 5.5**.

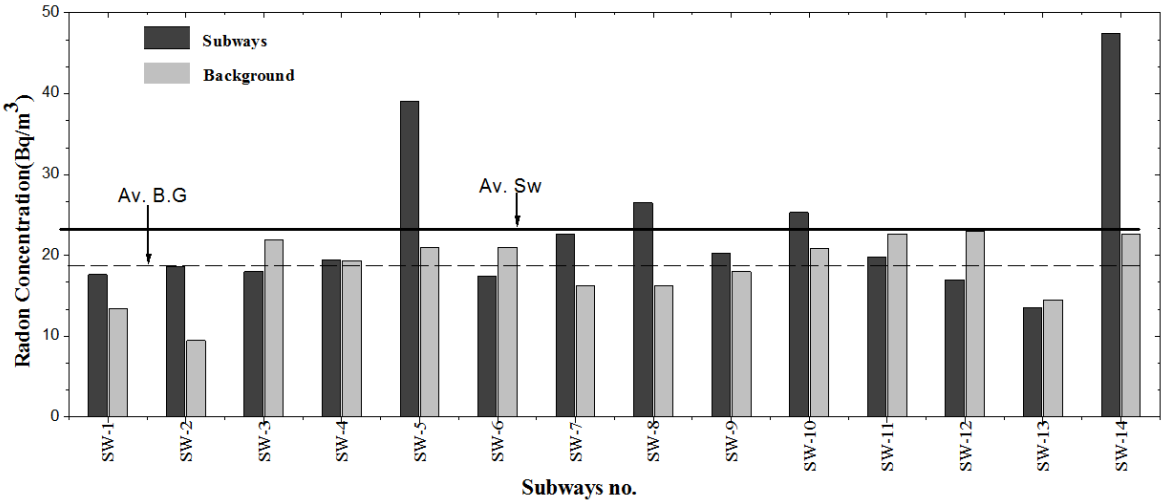

Fig. 5.5 Radon concentration for subways and corresponding B.G

The average radon concentration in background levels is noted to be just slightly below that in both basements and subways. The difference is minimal, with some instances where the background radon concentration surpasses that in basements. This observation can be attributed to the primary source of radon in these underground spaces, which is the emanation of radon from building materials rather than soil radon originating from the earth's crust beneath. Additionally, these constructions are designed to be situated on low radon-emitting soil and are unlikely to experience radon leakage through cracks, particularly given that most of them are recent constructions.

To provide a comprehensive understanding of the radon concentration profile across the entire survey area, we present a 3-D scatter plot (**Figure 5.6**) depicting the radon activity at various sites, encompassing both basements and subways, in relation to their spatial locations.

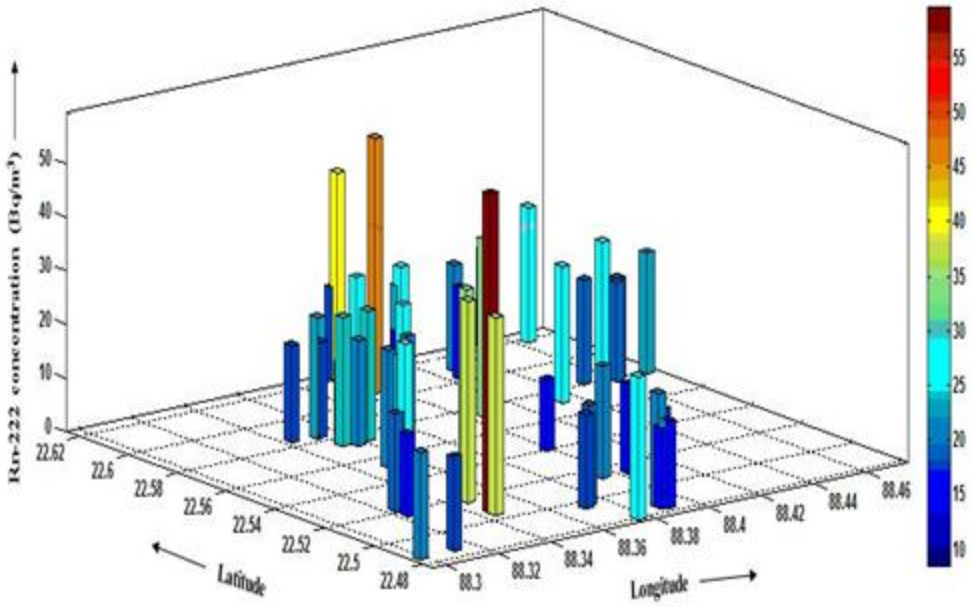

Fig. 5.6 A 3-D scatter plot of Radon activity at different basements and subways

From this investigation it is clear that for all the basements and subways the measured radon concentration level is well below the recommended reference levels (***Franklin and Fuoss et al. 1995; Choubey and Ramola 1997; Fuoss et al. 1999; Ramola 2005; Prasad et al. 2008; Jha and Bairagya 2011; Mohanty et al. 2013***). Overall well maintained ventilation systems are also the cause for low radon activity in the measured underground places.

5.4.2 Dose estimation study

For dose estimation we have only considered the workers of the basements, because the time taken for crossing the subways is not very much long and long-time staying in these subways is not allowed. These underground spaces (basements) serve diverse functions such as housing hotels and restaurants, providing parking facilities, hosting shopping malls and markets, accommodating doctors' clinics, featuring radiotherapy departments, and serving as rest areas for security guards. Many individuals spend extended periods working or residing in these basements. Despite the relatively low levels of radon activity, it is crucial to determine the annual effective dose received by these individuals. The average radon concentrations and annual effective doses for basements at levels 1, 2, and 3 are detailed separately in **Table 5.3**. The average annual effective dose is computed using **Equation 5.1** for individuals like security guards and shopkeepers who spend over 8 hours per day in basements. This calculation is performed considering two scenarios: i) 6 working days per week and ii) 7 working days per week. For type ii) workers, the indoor occupancy time is 9 hours × 365 days = 3285 hours per year, while for type i) workers, it is 9 hours × 331 days = 2817 hours per year. The resulting estimated dose values are presented in **Table 5.3.**

Table 5.3 Average radon concentration in basements and corresponding annual equivalent and effective dose for the persons working there.

Building Code	Basement Level	^{222}Rn Concentration Bq/m^3	Annual effective dose (mSv/y)	
			For 6 working days/week	For 7 working days/week
Bd-1	BL1	17.57	0.18	0.21
Bd-2	BL1	22.20	0.23	0.26
Bd-3	BL1	21.90	0.22	0.26
Bd-4	BL1	15.12	0.15	0.18
Bd-5	BL1	21.28	0.22	0.25
Bd-6	BL1	15.25	0.15	0.18
Bd-7	BL1	24.16	0.25	0.29
Bd-8	BL1	24.33	0.25	0.29
Bd-9	BL1	19.83	0.20	0.23
Bd-10	BL1	16.17	0.16	0.19
Bd-11	BL2	21.85	0.22	0.26
	BL1	18.75	0.19	0.22
Bd-12	BL3	21.00	0.21	0.25
	BL2	25.50	0.26	0.30

	BL1	18.99	0.19	0.22
Bd-13	BL1	18.42	0.19	0.22
Bd-14	BL1	20.00	0.20	0.24
Bd-15	BL1	17.60	0.18	0.21
Bd-16	BL1	15.20	0.15	0.18
Bd-17	BL1	18.25	0.19	0.22
Bd-18	BL1	8.50	0.09	0.10
Bd-19	BL3	21.67	0.22	0.26
	BL2	20.43	0.21	0.24
	BL1	25.40	0.26	0.30
Bd-20	BL1	14.25	0.14	0.17
Bd-21	BL1	25.75	0.26	0.30
Bd-22	BL1	18.00	0.18	0.21
Bd-23	BL1	25.57	0.26	0.30
Bd-24	BL2	24.60	0.25	0.29
	BL1	22.53	0.23	0.27
Bd-25	BL3	26.10	0.26	0.31
	BL2	18.20	0.18	0.22
	BL1	18.25	0.19	0.22
Bd-26	BL1	22.57	0.23	0.27
Bd-27	BL2	18.67	0.19	0.22
	BL1	20.86	0.21	0.25
Bd-28	BL1	16.67	0.17	0.20
Bd-29	BL1	24.75	0.25	0.29
Bd-30	BL1	37.50	0.38	0.44
Bd-31	BL1	59.00	0.61	0.71
Bd-32	BL1	37.00	0.38	0.44
Bd-33	BL1	27.50	0.28	0.33
Bd-34	BL1	34.33	0.35	0.41
Bd-35	BL1	26.75	0.27	0.32
Bd-36	BL1	33.33	0.34	0.39
Total =36	**Avg. value**	**22.70 ± 1.21**	**0.23 ± 0.01**	**0.27 ± 0.02**

Basement 31 has highest effective dose for basement level 1. The highest value of dose is 0.71 mSv/y. The variation of calculated values of annual effective dose for basement level 1 is displayed in the **Figure 5.7**.

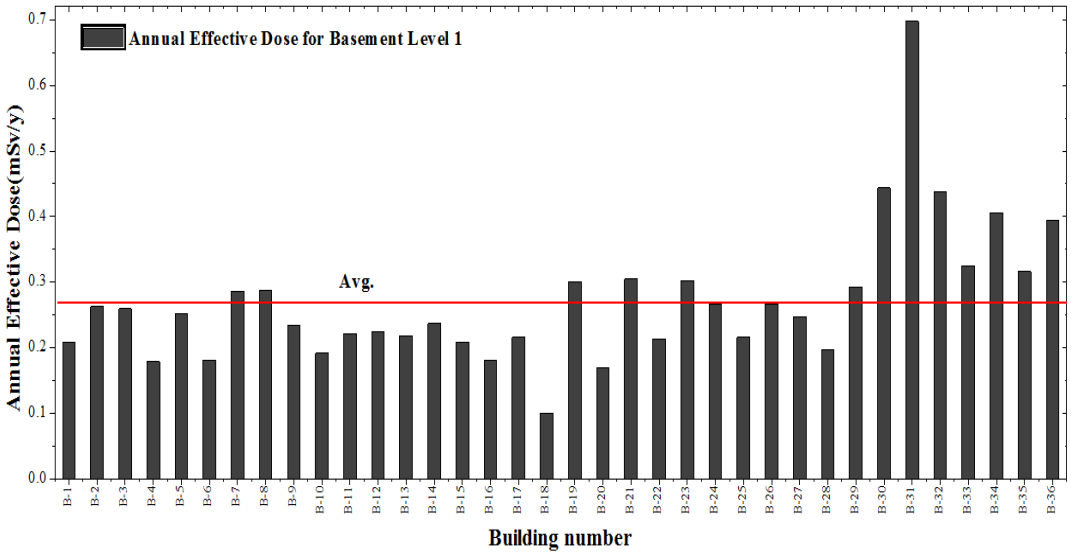

Fig. 5.7 A bar chart of different building's annual effective dose in basement level 1

The dose estimation shows that the workers are safe from any kind of health hazards due to radon exposure.

5.5 Conclusions

This study assesses the concentration of radon gas in the basements of various skyscrapers and other significant underground locations, such as commonly used subways. The measurements were predominantly taken in and around the Kolkata Municipal Corporation area. The average concentration of ^{222}Rn was found to be 22.70 ± 1.21 Bq/m^3 for basements and 23.05 ± 2.59 Bq/m^3 for subways. The mean annual effective dose for basements was (0.27 ± 0.02) mSv/y and (0.23 ± 0.01) mSv/y for 7 working days/week and 6 working days/week, respectively. This investigation concludes that underground spaces like basements and subways in the Kolkata Municipal Corporation area and its vicinity are deemed safe for regular use in terms of radon hazards.

References

Ahmad, N., & Khatibeh, A. J. A. H. (1997). Indoor radon levels and natural radioactivity in Jordanian soils. Radiation Protection Dosimetry, 71(3), 231-233.

Anastasiou, T., Tsertos, H., Christofides, S., & Christodoulides, G. (2003). Indoor radon (222Rn) concentration measurements in Cyprus using high-sensitivity portable detectors. Journal of Environmental Radioactivity, 68(2), 159-169.

Bouzarjomehri, F., & Ehrampoosh, M. H. (2008). Radon level in dwellings basement of Yazd-Iran. Iranian journal of radiation research, 6(3), 141-144.

Census (2011). Census of India.

Choubey, V. M., & Ramola, R. C. (1997). Correlation between geology and radon levels in groundwater, soil and indoor air in Bhilangana Valley, Garhwal Himalaya, India. Environmental Geology, 32, 258-262.

Dixon, D. W., Gooding, T. D., & McCready-Shea, S. (1996). Evaluation and significance of radon exposures in British workplace buildings. Environment International, 22, 1079-1082.

Doi, M., Fujimoto, K., Kobayashi, S., & Yonehara, H. (1994). Spatial distribution of thoron and radon concentrations in the indoor air of a traditional Japanese wooden house. Health Physics, 66(1), 43-49.

Durrani, S. A., & Ilic, R. (Eds.). (1997). Radon measurements by etched track detectors-applications in radiation protection, earth sciences. World Scientific.

Eaton, D. L., & Groopman, J. D. (Eds.). (2013). The toxicology of aflatoxins: human health, veterinary, and agricultural significance. Elsevier.

Field, R. W., Steck, D. J., Smith, B. J., Brus, C. P., Fisher, E. L., Neuberger, J. S., ... & Lynch, C. F. (2000). Residential radon gas exposure and lung cancer: the Iowa Radon Lung Cancer Study. American Journal of Epidemiology, 151(11), 1091-1102.

Field, R. W., Steck, D. J., Smith, B. J., Brus, C. P., Fisher, E. L., Neuberger, J. S., & Lynch, C. F. (2001). The Iowa radon lung cancer study—phase I: residential radon gas exposure and lung cancer. Science of the total environment, 272(1-3), 67-72.

Franklin, E. M., & Fuoss, S. (1995). Occupant radon exposure in houses with basements (No. CONF-950999-). American Association of Radon Scientists and Technologists, Cottonwood, AZ (United States).

Fuoss, S., Bode, M., & Franklin, E. M. (1999). Exposure to Radon in basement spaces of Minnesota homes. Housing and Society, 26(1-3), 4-15.

Gesell, T. F. (1983). Background atmospheric 222Rn concentrations outdoors and indoors: a review. Health Physics, 45(2), 289-302.

Gupta, M., Mahur, A. K., Sonkawade, R. G., & Verma, K. D. (2011). Monitoring of indoor radon and its progeny in dwellings of Delhi using SSNTDs. relation, 6(7).

Ielsch, G., Thieblemont, D., Labed, V., Richon, P., Tymen, G., Ferry, C., ... & Bechennec, F. (2001). Radon (222Rn) level variations on a regional scale: influence of the basement trace element (U, Th) geochemistry on radon exhalation rates. Journal of environmental radioactivity, 53(1), 75-90.

Jayanthi, D. D., Maniyan, C. G., & Perumal, S. (2011). Assessment of indoor radiation dose received by the residents of natural high background radiation areas of coastal villages of Kanyakumari district, Tamil Nadu, India. Radiation Physics and Chemistry, 80(7), 782-785.

Jha, V. C., & Bairagya, H. P. (2011). Flood plain evaluation in the Ganga-Brahmaputra Delta: a tectonic review. Ethiopian Journal of Environmental Studies and Management, 4(3), 12-24.

Kendall, G. M., & Smith, T. J. (2002). Doses to organs and tissues from radon and its decay products. Journal of Radiological Protection, 22(4), 389.

Kullab, M. K., Al-Bataina, B. A., Ismail, A. M., Abumurad, K. M., & Ghaith, A. (1997). Study of radon-222 concentration levels inside kindergartens in Amman. Radiation measurements, 28(1-6), 699-702.

Langroo, M. K., Wise, K. N., Duggleby, J. C., & Kotler, L. H. (1991). A nationwide survey of 222Rn and gamma radiation levels in Australian homes. Health Physics, 61(6), 753-761.

Li, X., Zheng, B., Wang, Y., & Wang, X. (2006). A survey of radon level in underground buildings in China. Environment international, 32(5), 600-605.

McKenzie, L. M., Witter, R. Z., Newman, L. S., & Adgate, J. L. (2012). Human health risk assessment of air emissions from development of unconventional natural gas resources. Science of the Total Environment, 424, 79-87.

Miles, J. (1998). Development of maps of radon-prone areas using radon measurements in houses. Journal of Hazardous Materials, 61(1-3), 53-58.

Mohanty, W. K., Verma, A. K., Vaccari, F., & Panza, G. F. (2013). Influence of epicentral distance on local seismic response in Kolkata City, India. Journal of Earth System Science, 122, 321-338.

Nath, S. K., Adhikari, M. D., Maiti, S. K., Devaraj, N., Srivastava, N., & Mohapatra, L. D. (2014). Earthquake scenario in West Bengal with emphasis on seismic hazard

microzonation of the city of Kolkata, India. Natural Hazards and Earth System Sciences, 14(9), 2549-2575.

Naujokas, M. F., Anderson, B., Ahsan, H., Aposhian, H. V., Graziano, J. H., Thompson, C., & Suk, W. A. (2013). The broad scope of health effects from chronic arsenic exposure: update on a worldwide public health problem. Environmental health perspectives, 121(3), 295-302.

Oikawa, S., Kanno, N., Sanada, T., Abukawa, J., & Higuchi, H. (2006). A survey of indoor workplace radon concentration in Japan. Journal of Environmental Radioactivity, 87(3), 239-245.

Prasad, Y., Prasad, G., Gusain, G. S., Choubey, V. M., & Ramola, R. C. (2008). Radon exhalation rate from soil samples of South Kumaun Lesser Himalayas, India. Radiation Measurements, 43, S369-S374.

Rahman, S. U., & Anwar, J. (2008). Measurement of indoor radon concentration levels in Islamabad, Pakistan. Radiation measurements, 43, S401-S404.

Rahman, S. U., Rafique, M., & Anwar, J. (2010). Radon measurement studies in workplace buildings of the Rawalpindi region and Islamabad Capital area, Pakistan. Building and environment, 45(2), 421-426.

Ramola, R. C. (2005, February). Levels of indoor radon, thoron, and their progeny in Himalaya. In International Congress Series (Vol. 1276, pp. 215-216). Elsevier.

UNSCEAR (2000). United Nations Scientific Committee on the effects of atomic radiations. The General Assembly with Scientific Annex, New York.

Wenjie, Y., Yang, L., Yufeng, L., Hongtao, L., Wang, S., & Weiquan, L. (1999). Measuring 222Rn level in underground space by SSNTD'S. Chinese Journal of Health, 3: 93, 115.

ICRP (1993). International Commission On Radiological Protection. Principles for intervention for protection of the public in a radiological emergency. Annals of the ICRP, 63(22), 4.

Chapter 6

Estimation Of Underground Water Radon Danger In Bakreswar And Tantloi Geothermal Region, India

6.1 Introduction

Radiation is a natural part of our environment. Human beings are likely to be exposed daily from a number of natural radioactive series sources like uranium (^{238}U), thorium (^{232}Th), actinium (^{227}Ac) and their daughter radionuclides and also from non-series radioactive materials like potassium (^{40}K), carbon (^{14}C) and ruthenium (^{44}Ru) etc.. This type of natural radiation is called terrestrial radiation, divided into internal and external categories. However, globally major attention is given to the radionuclide radon (^{222}Rn) owing to its larger contribution both through unknowing ingestion as well as inhalation and far in excess cancer risks than the other terrestrial radionuclides (***NCRP 1984; UNSCEAR 2008; WHO 2011***).

Radon (^{222}Rn) is the naturally occurring heaviest radioactive gas with a mass number of 222 and is potentially the most hazardous among all of the radon isotopes (including actinon and thoron) (***WHO 2009; ICRP 2010***). Alpha emitter ^{222}Rn is a water soluble noble gas with a half-life of 3.82 days. In the uranium-238 decay series ^{222}Rn is produced due to the decay of radium-226. It is highly mobile and can be found everywhere in environment. ^{222}Rn continuously enters into the water aquifers after being produced in earth crust rocks. It can be transported to large distances through soil by ground water (***Wanty and Gundersen 1998***). Normally radon is found in ground water sources with wide range of concentration levels (***Hess et al. 1985***). Radon concentration depend on the local geological factors like type of rocks (***Michel 1990; Choubey and Ramola 1997***), presence of faults (***Ball et al. 1991; Banwell and Parizek 1988***), porosity - permeability and type of minerals present in the rock (***Lawrence et al. 1991***), and other aquifer parameters (***Bonotto and Caprioglio 2002; Hoehn and Von Gunten 1989***). Ground water from granite and sedimentary aquifers usually contain high ^{222}Rn concentrations (***Brutsaert et al. 1981; Andrews & Wood 1972***).

The routes of human exposure from water ^{222}Rn are direct ingestion of radon contaminated water and inhalation of water-borne air radon. During ingestion radon remains in the stomach for several minutes and before passing to the small intestine radon contributes 97% radiation dose to stomach cell lining (***Kendall & Smith 2002***). Through diffusion in small intestine radon is mixed with blood and the dissolved radon circulates through different veins and capillaries and exposes whole body **(*Khursheed 2000; Gazi et al. 2022***). Even drinking of water with low radon level for long time period may lead to various serious health problems including cancer (***USNRC 1999; Zhuo et al. 2001; Kendall & Smith 2002***). During other daily household activities like cooking, bathing and washing clothes etc. radon easily mixes with the indoor air from water. ^{222}Rn disintegrates through short lived decay products of ^{218}Po, ^{214}Pb, ^{214}Bi and ^{214}Po which stay suspended in air. When someone breathes in indoor air they easily enter into our respiratory system and expose it by small to large amounts of radiation. This radiation may damage the lining cells of the lungs and increase the chance of lung cancer (***Samet 1989***). The risk of occurrence of cancer due to inhalation of radon is higher for those

who live in a radon-contaminated house for a long term. The World Health Organization (WHO) has acclaimed in their recent reports that this carcinogenic gas is the second leading cause of lung cancer after tobacco smoking (***WHO 2009***). It has been estimated that radon causes up to 15% of lung cancers worldwide and smokers are estimated to be 25 times more at risk from radon exposure than non-smokers (***WHO 2009***). The risk of lung cancer increases by about 16% per 100 Bq/m^3 increase in long time average of indoor radon activity (***WHO 2011***). The United States Environmental Protection Agency (USEPA) reported cancer deaths from water radon – almost 89% of total cancer deaths are due to lung cancer caused by breathing of water-borne indoor air radon and rest 11 % of cancer deaths are due to stomach cancer caused by ingestion of radon containing water (***USEPA 2018***). However, in outdoors radon quickly mixes with the open air and dilutes to a very low concentration. Therefore, outdoor radon is generally not a big problem for the human beings as far as radon hazard is concerned (***Somlai et al. 2007***).

Radon in water may be used for positive purposes also. Due to the radioactive disequilibrium ^{222}Rn permits age dating of groundwater which has resided in the subsurface for up to 15 days (***Hoehn and Von 1989***). Radon in water is also used to trace the groundwater residence time which is the length of time water spends in the groundwater portion of the hydrologic cycle (***Treutler et al. 2007***).

Due to its immense potential for causing fatal health disorders, radon in ground water is monitored throughout the World (***Horvath et al. 2000; Choubey et al. 2003; Galan et al. 2004; Marques et al. 2004; Xinwei 2006; Shiva et al. 2007; Abdallah et al. 2007; Prasad et al. 2008; Cosma et al. 2008; Nikolopoulos and Louizi 2008; Singh et al. 2009; Przylibski 2011; Chandrashekara 2012; Duggal et al. 2013; Rani et al. 2013; Krishan et al. 2015; Sethy et al. 2015***). Detailed discussion about this has been presented in **Chapter 3 Section 3.7.4**. To compare groundwater radon concentrations in different geologies, aquifers have been classified into two main groups depending on lithology – crystalline and sedimentary (***Michel 1990***). The crystalline aquifers contain igneous and metamorphic rocks like granite and gneiss in which ground water flows through fractures. Water originating from or coming in contact with such granitic or gneissic formations are expected to be associated with elevated levels of radon (***Michel 1990***). In sedimentary aquifers, groundwater flows through interconnected pore spaces, and radon concentration is generally low (***Michel 1990***). Hence, groundwater with elevated levels of radon may be expected to be found in regions with crystalline aquifers, which are generally present in regions where volcanic or orogenic activities have taken place.

6.1.1 Motivation of the present study

In the present work, ^{222}Rn activities have been measured in groundwater samples collected from deep tube wells at several locations in and around Bakreswar and Tantloi geothermal area which owes its origin to the now extinct Rajmahal Volcanism, located close to the shear zones within Precambrian crystalline rocks. The mineralized

rocks of this Archaean metamorphosed region constitute the bedrocks of crystalline aquifers making it an attractive region of study for radon in ground water.

Few studies have been carried out in this region. Ghose et al. (***2002***) and Singh et al. (***2015***) have reported that the thermal springs of Bakreswar geothermal region are flowing through Precambrian granites and they have found that the thermal springs water are enriched in radioactive elements like uranium, thorium, radium, radon and potassium. According to Chaudhuri et al. (***2010***) the observed helium and uranium concentrations in spring water have showed very high values. These results further provoked us for an in depth study of radon contamination in ground water of this region.

Aim of this study is to develop a map of radon concentrations in deep tube-well water of Bakreswar and Tantloi study area which will enable us to assess the associated health risk of the common people of this area due to usage of water.

6.2 Description of the study area

This study was carried out in different locations in and around Bakreswar ($23^0 52' 30'' N$, $87^0 22' 30'' E$) in Birbhum district of West Bengal and Tantloi ($24^0 2' 27'' N$, $87^0 16' 58'' E$) in Dumka district of Jharkhand, India. Geological map of the study area is presented in **Fig. 6.1**.

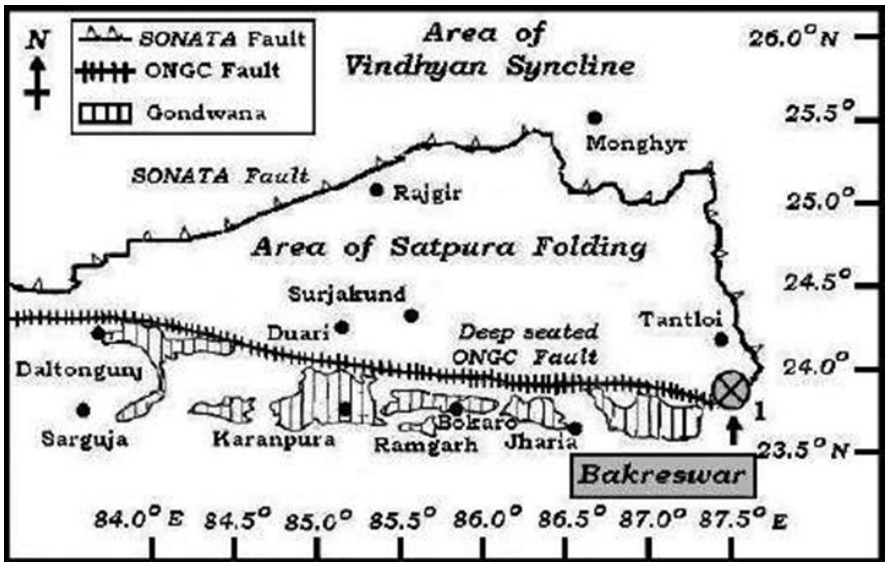

Fig. 6.1 Geological settings of Bakreswar-Tantloi geothermal region

In **Figure 6.1** it can be observed that the Bakreswar - Tantloi geothermal field connects the eastern fringes of two major fault systems – Son-Narmada-Tapti (SONATA) and Oil and Natural Gas Corporation Limited (ONGC) faults – that cut across northern and central parts of India (***Majumdar et al. 2005; Shanker 1988***). Geologically, it belongs to the Chhotanagpur Gneissic Complex (CGC) of the eastern part of peninsular India and consists of Archaean gneisses and schists (***GSI 1991***). The basement rocks are

Precambrian granites and gneisses transected by a large number of dolerite and amphibolite dykes. Highly porous and permeable subsurface of earth in this region is created due to the presence of faulted/fractured granitic rocks in the crust (***Nagar 1996***). A 1.4 km long silicified and brecciated shear zone trending north-south and linked to the extinct Rajmahal volcanism is extended from Gohaliara to Tantipara in Bakreswar region (***Majumdar 2005***). A cluster of hot springs with different temperatures ranging between 35°C and 72°C (***Majumdar 2000***) and having almost similar chemical composition (***Deb and Mukherjee 1969***) is located along this N-S trending regional fault. Almost all the hot springs of Bakreswar are alkaline (pH ~ 9) in nature and rich in SiO_2 (50-150 ppm), Na+ (30-100 ppm), Cl- (30-100 ppm) and F- (~ 13 ppm) (***Deb and Mukherjee 1969; Ghose et al. 2002; Majumdar 2010; Mukhopadhyay and Sarolkar 2012***).

In the absence of any provision for adequate water supply management, the primary source of water for drinking and household use in this region is groundwater. Consequently, an analysis of the radon concentration in the groundwater samples has been conducted. The locations of water collection within the study area are marked in **Figure 6.2**.

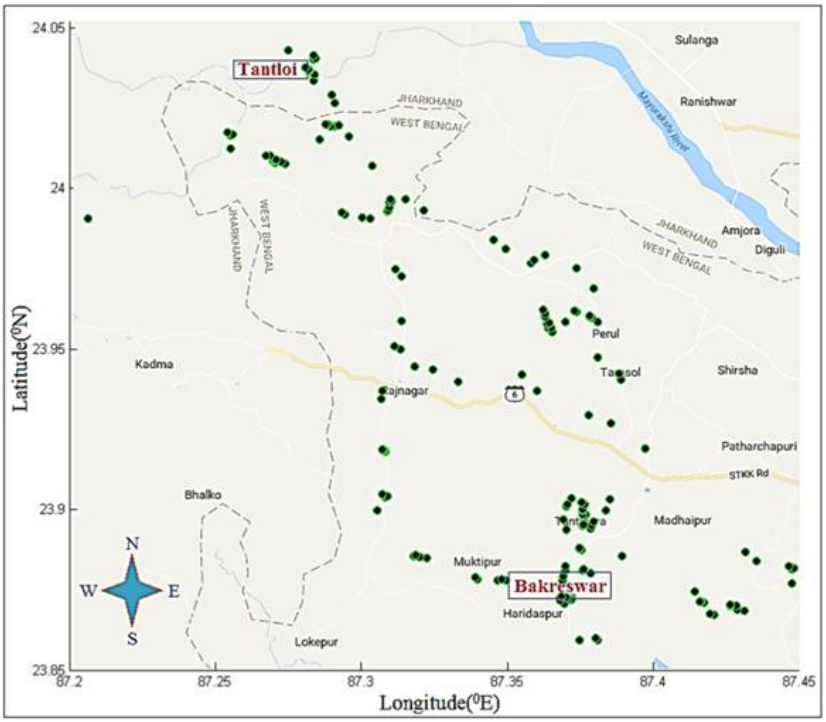

Fig. 6.2 Locations of the collected water samples

The extinct Rajmahal volcano is located in the Rajmahal hill area of Santhal Pargana district of Jharkhand. The exact location of the volcano cannot be ascertained at present because the Rajmahal volcanism originally consisted of multiple fissure eruptions. The Chotanagpur Plateau region of West Bengal and Jharkhand is created due to these fissure eruptions during the Jurassic period. Locations of the Rajmahal hill and study area are presented in **Figure 6.3**.

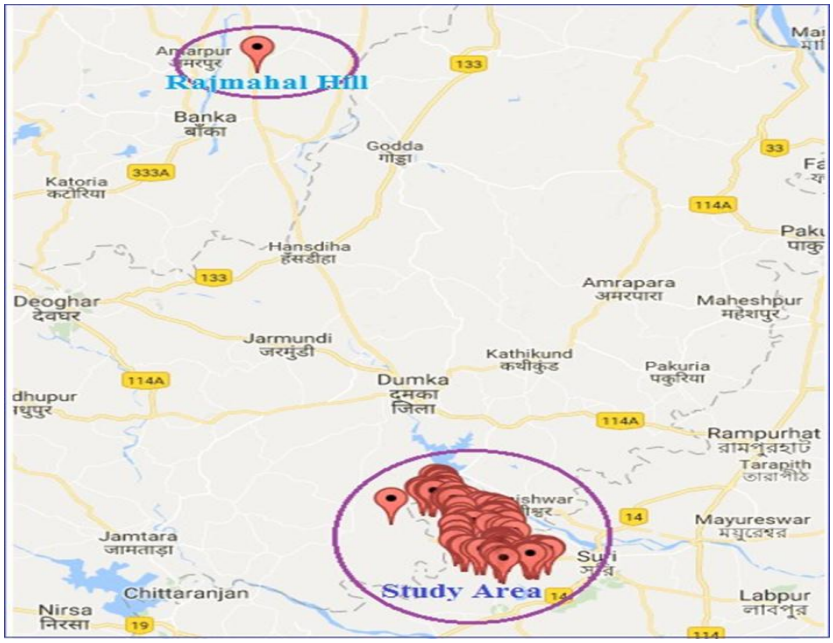

Fig. 6.3 Locations of Rajmahal hill and sample collection sites of the study area in Chotanagpur Plateau

6.3 Sampling Procedures

During the period of March 2015 to December 2016, water samples are collected from randomly selected drilled tube wells with various depths ranging from 24 m to 76 m. This water is primarily used for drinking. To study the radon activity in water, all groundwater samples are collected using properly leveled 250 ml leak-tight plastic bottles that were specifically designed for this purpose. Water samples are taken in bottles after pumping every tube-well for about 5 minutes until fresh water came from deep (***Choubey et al. 2003; Jobaggy et al. 2017***). In general, the residents of the area collect drinking water after pumping tube-wells for a few minutes. In order to assess the potential health risks associated with consuming this water, we collected samples after 5 minutes of pumping. Each bottle was filled to maximum capacity directly, with care taken to prevent any air bubbles from entering, before being sealed to ensured minimum radon loss by degassing.

To accurately determine the location of the tube-wells, their corresponding latitudes and longitudes were recorded using a global positioning system (GPS) meter.

6.4 Measurement and Methods

6.4.1 Measurement of radon concentration

Radon concentration of all samples have been analysed using AquaKit supplied with radon monitoring system AlphaGuard, details of which is discussed in **Chapter 4 Section 4.1.2**.

6.4.2 Estimation of dose due to radon

Radiation dose is a more suitable parameter than radon concentration to estimate the health risk caused by radon in drinking water. Therefore, we have estimated the total annual effective dose due to inhalation of water-borne radon and ingestion of radon containing water. The dose exposures due to water-borne radon have been calculated following by the parameters given in the UNSCEAR reports (***UNSCEAR 2000, 2008***).

6.4.2.1 Ingestion dose

Estimation of annual effective ingestion dose from the water sample has been obtained by the following relation (***UNSCEAR 2000***):

$$\boldsymbol{D_{Ingestion} = C_{RnW} \times C_W \times EDC} \quad (6.1)$$

Where; $D_{Ingestion}$ = annual effective ingestion dose from water radon (μSv/yr), C_{RnW} = ^{222}Rn concentration in water (Bq/l), C_W = annual average water consumption by an individual (l/yr), EDC = effective dose coefficient for ingestion of water radon (3.5 nSv/Bq, ***UNSCEAR 2000***).

6.4.2.2 Inhalation dose

The annual effective inhalation dose due to water-borne radon has been estimated by the following relation (***UNSCEAR 2000***):

$$\boldsymbol{D_{Inhalation} = C_{RnW} \times DCF \times T \times F \times I} \quad (6.2)$$

Where; $D_{Inhalation}$ = annual effective inhalation dose of indoor radon (μSv/yr), C_{RnW} = ^{222}Rn concentration in water (kBq/m^3), DCF = dose coefficient factor for inhalation of water-borne radon (9nSv/h/Bq/m^3, ***ICRP 1993; UNSCEAR 2000***), T = transfer factor of radon in indoor air from water (10^{-4}, ***Nazaroff et al. 1985; USNRC 1999; UNSCEAR 2000***), F = indoor radon equilibrium factor (0.4, ***UNSCEAR 2000***), I = annual average indoor occupancy time (7000 h/yr, ***UNSCEAR 2000***).

6.4.2.3 Total annual effective dose

The total annual effective dose from water radon exposure has been estimated by adding the inhalation dose and ingestion dose of the water samples as follows (***UNSCEAR 2000***):

$$\boldsymbol{D_{Total} = D_{Inhalation} + D_{Ingestion}} \quad (6.3)$$

6.5 Water radon reference levels

High concentration of ^{222}Rn in drinking water is of great concern as its exposure may pose life threatening health risks like cancer. The average life-time probability of occurrence of cancer from ^{222}Rn is higher than any other natural or human induced water dissolved contaminant (***Cothern & Marcus 1984; Vitz 1991***). Therefore, depending on the radiological risk posed by water dissolved radon, many international and national agencies have proposed different reference levels for radon in drinking water and also advised to take immediate actions as and when required to reduce the exposure due to water dissolved ^{222}Rn.

The United States Environmental Protection Agency (USEPA) has proposed in their recent report (***USEPA 2018***) that radon activity level in drinking water should not exceeds the reference level of 148 Bq/l (4000 pCi/l), only if drinking water suppliers reduce the indoor air radon as prescribed by USEPA enhanced indoor air programs. Otherwise action should be taken to reduce radon levels in drinking water to bring it down below the maximum contamination level (MCL) of 11.1 Bq/l (300 pCi/l) (***USEPA 1991; USEPA 2018***). United Nations Scientific Committee on the Effects of Atomic Radiation (UNSCEAR) has recommended that if radon concentrations in drinking water have not exceeded the range of 4 - 40 Bq/l, no action is required to reduce the water radon levels (***UNSCEAR 2008***). Besides these recommendations the World Health Organization (WHO) and the European Union Commission have also suggested that screening levels for radon in drinking water have to be set based on the national reference levels, otherwise they have recommended the local agencies to take some remedial actions if radon level in drinking water rises above the reference level of 100 Bq/l (***EU 2001; WHO 2011***). Considering these recommendation levels some European countries like Denmark, Finland, Germany, Greece, Ireland, Sweden and Czech Republic have set their own reference levels in the range between 20 - 1000 Bq/l for dissolved radon in drinking water (***WHO 2004***). Till now the regulatory authority in India has not set any reference level for radon in drinking water supply.

As there is no national recommended reference level of radon in drinking water and no indoor air radon reduction program in this study area. Therefore, in view of the recommendations we have considered both the reference levels of 11.1 Bq/l (***USEPA 1991***) and 100 Bq/l (***WHO 2009***) for this study as are done by many workers in India and abroad (***Charoensri et al. 2015; Rangaswamy et al. 2016***).

6.6 Results and discussions

6.6.1 Radon Concentration Study

We have measured ^{222}Rn concentration levels in groundwater samples collected from 173 different tube-wells around Bakreswar and Tantloi region. Positions of the tube-

wells with their corresponding water radon concentration level have been tabulated in **Table 6.1**.

Table 6.1 ^{222}Rn concentration level of the water samples

Sample No.	Position of Tube-well		Radon Conc. (Bq/l)
	Longitude (°N)	Latitude (°E)	
SL-1	87.20609	23.99107	165.81
SL-2	87.25469	24.01698	216.89
SL-3	87.25512	24.01709	261.01
SL-4	87.25547	24.01656	130.63
SL-5	87.25603	24.0115	50.60
SL-6	87.26737	24.01025	146.34
SL-7	87.2688	24.00997	69.54
SL-8	87.26971	24.00837	75.15
SL-9	87.2704	24.00873	52.22
SL-10	87.27048	24.00854	41.90
SL-11	87.27055	24.00797	48.12
SL-12	87.27092	24.00874	141.79
SL-13	87.27249	24.00823	109.09
SL-14	87.27392	24.0077	62.79
SL-15	87.27429	24.04318	232.74
SL-16	87.27633	24.0404	777.47
SL-17	87.27802	24.04008	803.84
SL-18	87.2809	24.03741	24.12
SL-19	87.2818	24.03692	37.57
SL-20	87.28191	24.0365	57.54
SL-21	87.28233	24.0365	59.14
SL-22	87.28345	24.03355	376.41
SL-23	87.28353	24.04134	270.47
SL-24	87.28363	24.04017	39.84
SL-25	87.28388	24.0353	68.69
SL-26	87.28419	24.04053	21.17
SL-27	87.28578	24.01502	133.66
SL-28	87.28768	24.01995	40.60
SL-29	87.28862	24.01975	109.41
SL-30	87.28968	24.0194	61.99
SL-31	87.28975	24.02899	104.43
SL-32	87.29095	24.01928	95.70
SL-33	87.29102	24.02655	119.53
SL-34	87.29237	24.01952	199.90
SL-35	87.29315	23.99249	116.19
SL-36	87.29435	23.99189	204.61
SL-37	87.2959	24.01617	173.82
SL-38	87.30025	23.9907	113.76

SL-39	87.30309	23.99059	68.89
SL-40	87.30363	24.00687	74.67
SL-41	87.30538	23.89957	50.51
SL-42	87.30666	23.9344	88.80
SL-43	87.30675	23.93447	60.06
SL-44	87.3071	23.91856	76.87
SL-45	87.30716	23.93686	85.33
SL-46	87.30719	23.90485	84.05
SL-47	87.30735	23.91854	3.30
SL-48	87.30795	23.91845	81.18
SL-49	87.3082	23.90388	40.50
SL-50	87.30832	23.91783	62.28
SL-51	87.30877	23.90418	40.27
SL-52	87.30888	23.9927	184.47
SL-53	87.30939	23.99293	69.00
SL-54	87.30954	23.99569	180.82
SL-55	87.30967	23.99405	89.98
SL-56	87.30995	23.99668	37.96
SL-57	87.31035	23.99603	169.65
SL-58	87.3112	23.95084	22.52
SL-59	87.31183	23.97484	165.82
SL-60	87.31355	23.94994	80.26
SL-61	87.31359	23.95876	133.95
SL-62	87.31382	23.97249	76.09
SL-63	87.31523	23.9964	59.04
SL-64	87.3178	23.88537	98.88
SL-65	87.31832	23.94443	71.57
SL-66	87.31844	23.8858	107.84
SL-67	87.32009	23.88517	70.45
SL-68	87.32131	23.99302	43.54
SL-69	87.32251	23.88476	74.86
SL-70	87.32442	23.94358	69.05
SL-71	87.33313	23.93987	61.26
SL-72	87.33902	23.87873	53.47
SL-73	87.33963	23.87827	52.79
SL-74	87.3453	23.98377	47.19
SL-75	87.34665	23.87801	45.99
SL-76	87.34787	23.87821	18.49
SL-77	87.34942	23.98103	31.12
SL-78	87.34958	23.87805	26.17
SL-79	87.35484	23.94191	89.98
SL-80	87.35816	23.97651	81.70
SL-81	87.35908	23.97757	63.56
SL-82	87.36011	23.93679	133.11

SL-83	87.36221	23.96209	132.63
SL-84	87.36281	23.9791	12.47
SL-85	87.36283	23.96093	153.31
SL-86	87.36293	23.95991	28.99
SL-87	87.36357	23.95786	164.83
SL-88	87.36384	23.95768	19.07
SL-89	87.36395	23.95636	24.61
SL-90	87.3644	23.958	277.86
SL-91	87.3651	23.95648	113.38
SL-92	87.36534	23.9553	192.11
SL-93	87.36825	23.87152	86.44
SL-94	87.36856	23.87275	55.67
SL-95	87.36867	23.87765	70.31
SL-96	87.36867	23.87787	100.64
SL-97	87.36903	23.87915	74.15
SL-98	87.3691	23.89695	108.73
SL-99	87.36957	23.87067	99.81
SL-100	87.36971	23.95842	117.94
SL-101	87.3698	23.88108	26.58
SL-102	87.37001	23.88226	28.75
SL-103	87.37005	23.87263	177.08
SL-104	87.37012	23.90094	78.31
SL-105	87.37015	23.90091	114.55
SL-106	87.37029	23.89359	38.45
SL-107	87.37067	23.90165	111.36
SL-108	87.37068	23.90162	48.54
SL-109	87.37077	23.87232	175.65
SL-110	87.3714	23.87203	130.37
SL-111	87.37175	23.9034	70.19
SL-112	87.37202	23.87207	112.40
SL-113	87.37283	23.96192	137.98
SL-114	87.37368	23.96159	22.75
SL-115	87.37378	23.97495	63.22
SL-116	87.37474	23.88795	36.99
SL-117	87.37486	23.88775	56.02
SL-118	87.37517	23.85972	65.15
SL-119	87.3753	23.88737	113.50
SL-120	87.37542	23.90229	47.45
SL-121	87.37563	23.88115	31.29
SL-122	87.37567	23.88117	44.90
SL-123	87.3757	23.89995	176.44
SL-124	87.37571	23.8812	36.46
SL-125	87.37572	23.8985	34.15
SL-126	87.37572	23.89502	75.35

SL-127	87.37575	23.8996	167.90
SL-128	87.37606	23.88128	4.12
SL-129	87.37618	23.88105	11.65
SL-130	87.37619	23.8954	58.03
SL-131	87.37623	23.88137	10.83
SL-132	87.37629	23.90169	208.01
SL-133	87.3768	23.89837	98.16
SL-134	87.37767	23.92936	52.74
SL-135	87.37826	23.96002	84.14
SL-136	87.37829	23.96034	43.98
SL-137	87.37849	23.88009	56.87
SL-138	87.37867	23.8941	298.71
SL-139	87.37889	23.95952	78.83
SL-140	87.37889	23.895	158.14
SL-141	87.37917	23.8594	83.52
SL-142	87.37927	23.8603	73.10
SL-143	87.3796	23.8962	111.83
SL-144	87.37968	23.96862	22.53
SL-145	87.38081	23.95822	82.75
SL-146	87.381	23.94743	46.45
SL-147	87.38374	23.89962	150.75
SL-148	87.38494	23.90315	355.22
SL-149	87.38537	23.92674	8.57
SL-150	87.38836	23.94239	151.87
SL-151	87.38904	23.94028	330.49
SL-152	87.38906	23.88535	36.21
SL-153	87.38927	23.88545	127.75
SL-154	87.39719	23.91877	90.50
SL-155	87.41406	23.87459	438.70
SL-156	87.41605	23.87135	84.60
SL-157	87.41641	23.87128	143.79
SL-158	87.41736	23.87102	121.99
SL-159	87.41824	23.86858	626.05
SL-160	87.41939	23.8675	101.47
SL-161	87.42066	23.86722	165.95
SL-162	87.42623	23.87026	275.14
SL-163	87.42645	23.87008	196.03
SL-164	87.42845	23.86994	29.10
SL-165	87.42876	23.86884	123.48
SL-166	87.43098	23.86832	178.45
SL-167	87.43159	23.88672	142.86
SL-168	87.43545	23.884	43.13
SL-169	87.44633	23.88284	267.01
SL-170	87.44725	23.8792	345.10

SL-171	87.44728	23.88141	352.25
SL-172	87.4479	23.88109	357.95
SL-173	87.44819	23.88154	334.87

It is observed from **Table 6.1** that the obtained ^{222}Rn concentrations are widely varying between 3.3 Bq/l to 803.8 Bq/l. Radon concentration profile of the 170 samples is shown in **Figure 6.4a**; and the same for 3 samples having very high Radon concentration is shown in **Figure 6.4b**.

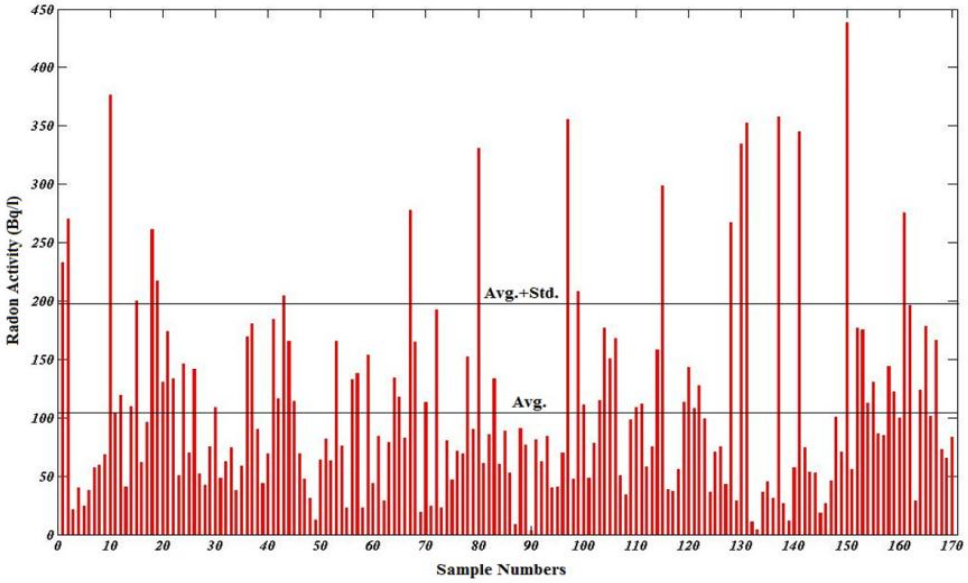

Fig. 6.4a

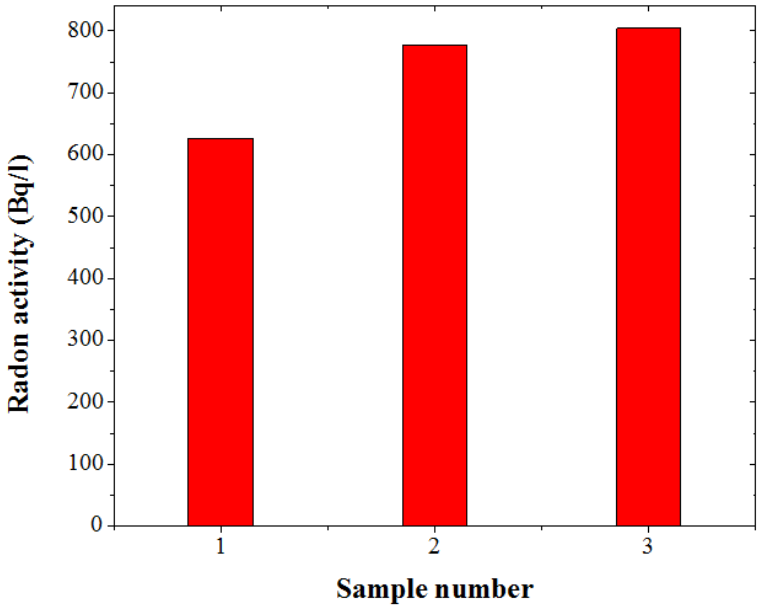

Fig. 6.4b

Fig. 6.4 Radon concentrations in underground water **a**) ^{222}Rn concentration profile of 170 samples; **b**) ^{222}Rn concentration profile of three samples having vary having very high radon concentration

Radon concentration distribution of the 170 samples excluding the 3 samples with very concentrations is represented in **Figure 6.5**.

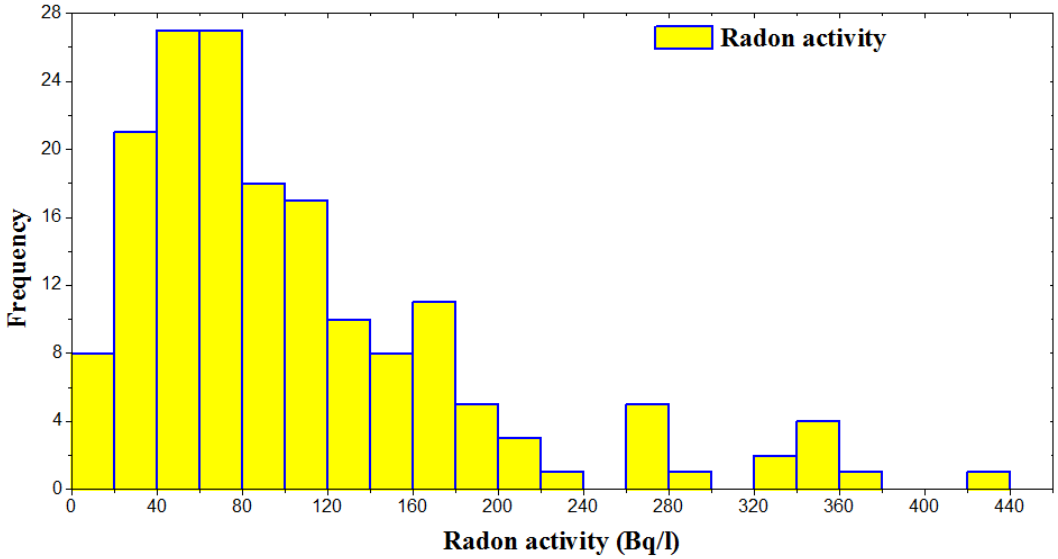

Fig. 6.5 Distribution of ^{222}Rn concentration of the groundwater samples

It shows that the distribution is highly asymmetric with a long tail. Considering the 170 inputs of the distribution of radon concentration we have calculated the statistical parameters using the conventional formulae (***Hopkins and Weeks 1990; Press et al. 1992***) and the parameters are tabulated in **Table 6.2**.

Table 6.2 Descriptive statistics of the data of the present study

Statistical Parameters	Value (Bq/l)
Sample Size	170
Range	3.30 - 435.40 (Bq/l)
Mean	106.78 (Bq/l)
Median	81.43 (Bq/l)
Variance	6972.80
Std. Deviation	83.50 (Bq/l)
Coefficient of Variation	0.78
Std. Error	6.40
Skewness	1.60
Excess Kurtosis	2.64

*In Statistical analyses three very high values are excluded

Three samples have very high concentrations. If we include the 3 very high value samples the statistical parameters will largely depend on these 3 values which will not reflect the real situation. That is why we have excluded these 3 values. The values of skewness and excess kurtosis factor presented in **Table 6.2**, indicates that the distribution of radon concentration follows a log-normal pattern (***Press et al. 1992***). The wide variation of radon concentration in ground water of the study area may be caused

due to the critical geological formation of the region like the presence of two major faults and one 1.4 km long shear zone in the earth crust and also may be due to the large variation in bore-hole depth of the tube-wells. Several faults and cracks crisscross the crust in this region, but the exact subsurface lithospheric structure is not known. It may be possible that the tube-wells inserted into the ground at these three locations where radon concentrations are very high lie exactly on some fault line. Hence, radon gas issuing out of the fault dissolves into the groundwater that is coming out of these tube-wells.

Among 173 samples 72 samples (42%) exceed the proposed reference level of 100 Bq/l recommended by the EU Commission and the WHO (***EU 2001; WHO 2011***). However if we consider the Maximum Contamination Level (MCL) of 11.1 Bq/l proposed by USEPA (***1991***), 169 samples (98%) have radon concentration above it. High radon concentrations (>200 Bq/l) are verified atleast twice. Results never vary more than 10%. For an example 2 water samples having concentration value of 777 Bq/l and 803 Bq/l have measured for the first time during 19th -20th March, 2015 and then repeated the measurement during 25th February, 2016 and the obtained results are 738.54 Bq/l and 767.54 Bq/l.

To have a comprehensive view of the spatial variation in radon concentration in our present study area, a 3-D scatter plot and a contour map are presented respectively in **Figure 6.6** (***a*** and ***b***).

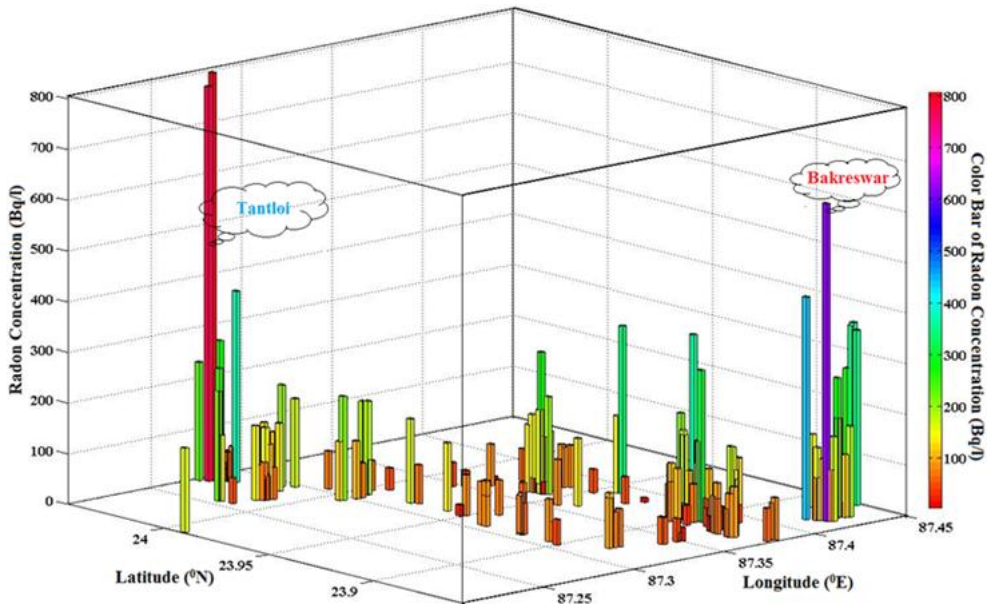

Fig. 6.6a

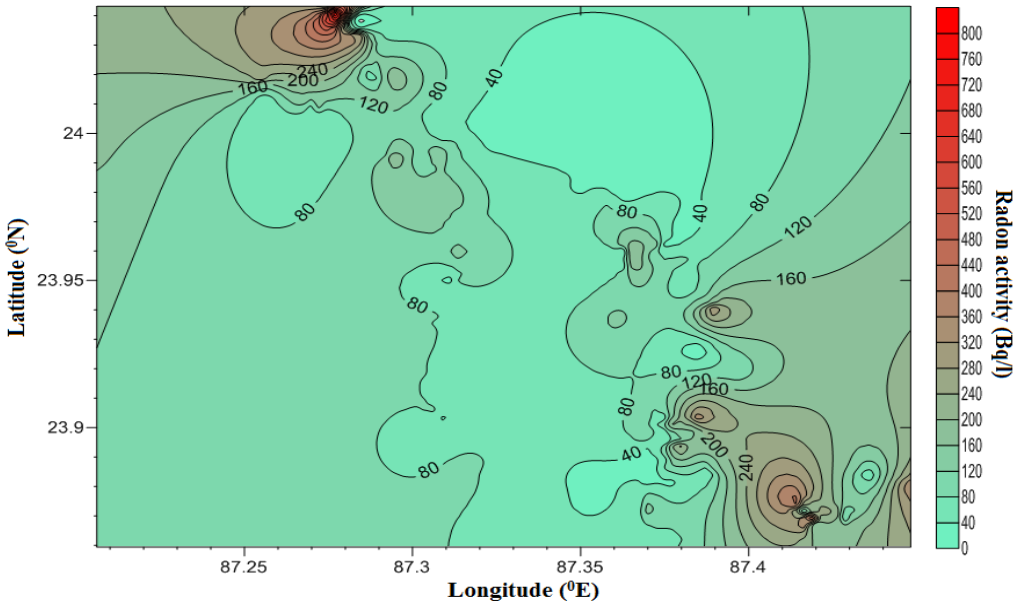

Fig. 6.6b

Fig. 6.6 Spatial variation in radon concentration in the present study area: **a**) 3-D Scatter plot of groundwater ^{222}Rn conccentrations with positions; **b**) Contour map of radon concentration in drinking water samples

It is evident that significantly high radon concentrations have been observed in tube-well water taken from Tantipara, Jamtholia near Bakreswar and Tongra near Tantloi.

The observed values of radon concentration in groundwater samples in this region have been compared with the results reported by other investigators from different parts of the world and are presented in **Table 6.3**.

Table 6.3 Dissolved Radon concentration in groundwater in different parts of the world

Region	Source/Usage	Rn^{222} Concentration			Reference
		Min	Max	Mean	
El Castano, Venezuela	Tap, hot-spring water	1.00	560.00	-	***Horvath et al. 2000***
Eastern Doon Valley, outer Himalaya, Ramnagar and Tumkur, India	Shallow, hand-pump water	2.96	299.06	54.53	***Choubey et al. 2003***
Extremadura, Spain	Spring, spa, well water	0.15	1200.00	98.00	***Galan et al. 2004***
Santos Region, Brazil	Ground water	0.95	36.00	-	***Marques et al. 2004***
Baoji, China	Tap-water	8.00	18.00	12.00	

	Well water	6.00	127.00	41.00	
Bangalore region, India	Bore-well water	5.30	283.40	87.00	***Shiva et al. 2007***
AniIbil, Lebanon	Well, hot spring	0.91	49.60	-	***Abdallah et al. 2007***
Greece and Cyprus	Drinking water	0.80	24.00	5.40	***Nikolopoulos and Louizi 2008***
Transylvania, Romania	Surface, well, spring water	0.50	126.30	15.40	***Cosma et al. 2008***
Upper Siwaliks, India	Hand-pump, well, natural sources water	0.87	32.10	-	***Singh et al. 2009***
Sudetes uranium region, Poland	Ground water	5.50	215.70	47.42	***Przylibski 2011***
Bore well Mysore, India	Bore-well water	0.10	643.90	25.07	***Chandrashekara et al. 2012***
Bathinda, India	Tube-well water	0.90	5.10	2.63	***Duggal et al. 2013***
Northern rajasthan, India	Well water	0.50	85.70	9.00	***Rani et al. 2013***
Jaduguda, India	Ground-water	7.50	389.60	123.50	***Sethy et al. 2015***
East Cost of West Bengal, India	Ground water	1.90	9.00	5.00	***Krishan et al. 2015***
Bakreswar and Tantloi Region, India	Tube-well water	3.30	803.80	117.69	***Present Study***

From this **Table 6.3** it is manifested that the average groundwater radon concentration of the present study area is higher than that reported by all other studies except the values presented by the investigator of Jaduguda Uranium Mines and Garhwali Himalaya (mountain area) of India (***Prasad et al. 2008; Sethy et al. 2015***). Hence, it may be inferred that besides rock structures and mineralization of the study area, detailed fault fracture structures may be considered as important attribute to radon concentration in ground water of the study area.

6.6.2 Study of annual effective dose

To assess the probable health risk we have estimated the annual effective dose for the people who are using radon contaminated water of the study region. Such water is a source of radiation dose through ingestion of water as well as inhalation of indoor air.

To estimate ingestion dose most of the investigators of different parts of the World have considered 730 l/y water consumption proposed by WHO and ICRP in case of reservoir water intake (***WHO 2009; ICRP 2010***). However, considering only direct tap water intake, some investigators have taken 60 l/y water consumption as proposed by UNSCEAR (***2000***). Due to this controversy, in this study we have considered both the water consumption quantities to estimate ingestion dose.

The annual effective doses corresponding to the collected water samples are calculated using **Formulae 6.1-6.3**, by considering 60 litre and 730 litre of annual water intake and tabulated in **Table 6.4**.

Table 6.4 Annual effective dose values of the water samples for different water consumption levels

Sample No.	Inhalation Dose (μSv/y)	Ingestion Dose (μSv/y)		Total Annual Effective Dose (μSv/y)	
		for 60 l/yr	for 730 l/yr	for 60 l/yr	for 730 l/yr
SL-1	8.32	0.70	8.44	9.02	17.46
SL-2	10.36	0.87	10.51	11.23	21.74
SL-3	21.60	1.80	21.90	23.40	45.30
SL-4	27.28	2.28	27.66	29.56	57.22
SL-5	29.36	2.45	29.77	31.81	61.58
SL-6	31.43	2.62	31.87	34.05	65.92
SL-7	46.6	3.89	47.25	50.49	97.74
SL-8	48.06	4.01	48.73	52.07	100.8
SL-9	53.34	4.45	54.08	57.79	111.87
SL-10	56.76	4.73	57.54	61.49	119.03
SL-11	56.78	4.74	57.57	61.52	119.09
SL-12	57.33	4.78	58.13	62.11	120.24
SL-13	60.79	5.07	61.63	65.86	127.49
SL-14	62.02	5.17	62.88	67.19	130.07
SL-15	65.95	5.50	66.87	71.45	138.32
SL-16	66.97	5.59	67.90	72.56	140.46
SL-17	72.45	6.04	73.46	78.49	151.95
SL-18	73.06	6.09	74.07	79.15	153.22
SL-19	73.34	6.12	74.36	79.46	153.82
SL-20	78.43	6.54	79.52	84.97	164.49
SL-21	78.86	6.58	79.95	85.44	165.39
SL-22	86.06	7.18	87.26	93.24	180.50
SL-23	91.25	7.61	92.52	98.86	191.38
SL-24	91.86	7.66	93.14	99.52	192.66
SL-25	93.22	7.77	94.51	100.99	195.50
SL-26	94.67	7.89	95.98	102.56	198.54
SL-27	95.66	7.98	96.99	103.64	200.63
SL-28	96.90	8.08	98.24	104.98	203.22

SL-29	100.40	8.37	101.79	108.77	210.56
SL-30	101.49	8.46	102.89	109.95	212.84
SL-31	102.06	8.51	103.48	110.57	214.05
SL-32	102.32	8.53	103.74	110.85	214.59
SL-33	105.58	8.80	107.05	114.38	221.43
SL-34	108.69	9.06	110.20	117.75	227.95
SL-35	109.72	9.15	111.24	118.87	230.11
SL-36	110.83	9.24	112.37	120.07	232.44
SL-37	113.15	9.43	114.72	122.58	237.30
SL-38	115.9	9.66	117.51	125.56	243.07
SL-39	117.06	9.76	118.68	126.82	245.5
SL-40	118.92	9.91	120.57	128.83	249.40
SL-41	119.58	9.97	121.24	129.55	250.79
SL-42	121.27	10.11	122.95	131.38	254.33
SL-43	122.31	10.20	124.01	132.51	256.52
SL-44	127.29	10.61	129.06	137.9	266.96
SL-45	127.5	10.63	129.27	138.13	267.4
SL-46	131.60	10.97	133.43	142.57	276.00
SL-47	132.91	11.08	134.76	143.99	278.75
SL-48	133.04	11.09	134.88	144.13	279.01
SL-49	134.75	11.23	136.62	145.98	282.60
SL-50	140.29	11.70	142.24	151.99	294.23
SL-51	141.18	11.77	143.14	152.95	296.09
SL-52	143.32	11.95	145.31	155.27	300.58
SL-53	144.99	12.09	147.01	157.08	304.09
SL-54	146.24	12.19	148.27	158.43	306.70
SL-55	148.78	12.40	150.85	161.18	312.03
SL-56	149.04	12.42	151.11	161.46	312.57
SL-57	151.36	12.62	153.46	163.98	317.44
SL-58	154.38	12.87	156.52	167.25	323.77
SL-59	156.21	13.02	158.38	169.23	327.61
SL-60	156.95	13.08	159.13	170.03	329.16
SL-61	158.24	13.19	160.43	171.43	331.86
SL-62	159.32	13.28	161.53	172.60	334.13
SL-63	160.18	13.35	162.40	173.53	335.93
SL-64	164.18	13.69	166.46	177.87	344.33
SL-65	173.10	14.43	175.51	187.53	363.04
SL-66	173.61	14.47	176.02	188.08	364.1
SL-67	173.88	14.49	176.30	188.37	364.67
SL-68	174.01	14.51	176.43	188.52	364.95
SL-69	175.25	14.61	177.68	189.86	367.54
SL-70	176.88	14.74	179.34	191.62	370.96
SL-71	177.19	14.77	179.65	191.96	371.61
SL-72	177.54	14.80	180.00	192.34	372.34
SL-73	180.36	15.03	182.87	195.39	378.26

SL-74	184.22	15.36	186.78	199.58	386.36
SL-75	186.85	15.58	189.45	202.43	391.88
SL-76	188.17	15.69	190.79	203.86	394.65
SL-77	188.65	15.73	191.27	204.38	395.65
SL-78	189.37	15.79	192.00	205.16	397.16
SL-79	189.89	15.83	192.52	205.72	398.24
SL-80	191.75	15.98	194.41	207.73	402.14
SL-81	193.70	16.15	196.39	209.85	406.24
SL-82	197.35	16.45	200.09	213.80	413.89
SL-83	198.66	16.56	201.42	215.22	416.64
SL-84	202.26	16.86	205.07	219.12	424.19
SL-85	204.58	17.05	207.42	221.63	429.05
SL-86	205.89	17.16	208.75	223.05	431.8
SL-87	208.53	17.38	211.43	225.91	437.34
SL-88	210.46	17.54	213.39	228	441.39
SL-89	211.81	17.66	214.75	229.47	444.22
SL-90	212.04	17.67	214.98	229.71	444.69
SL-91	213.20	17.77	216.16	230.97	447.13
SL-92	215.02	17.92	218.01	232.94	450.95
SL-93	217.83	18.16	220.86	235.99	456.85
SL-94	223.77	18.65	226.88	242.42	469.3
SL-95	226.75	18.90	229.90	245.65	475.55
SL-96	226.75	18.90	229.90	245.65	475.55
SL-97	228.06	19.01	231.23	247.07	478.3
SL-98	241.16	20.10	244.51	261.26	505.77
SL-99	247.37	20.62	250.8	267.99	518.79
SL-100	249.18	20.77	252.64	269.95	522.59
SL-101	251.53	20.97	255.02	272.50	527.52
SL-102	253.62	21.14	257.14	274.76	531.9
SL-103	255.71	21.31	259.26	277.02	536.28
SL-104	263.17	21.94	266.82	285.11	551.93
SL-105	271.76	22.65	275.54	294.41	569.95
SL-106	274.00	22.84	277.81	296.84	574.65
SL-107	274.91	22.91	278.73	297.82	576.55
SL-108	275.71	22.98	279.54	298.69	578.23
SL-109	280.63	23.39	284.53	304.02	588.55
SL-110	281.82	23.49	285.73	305.31	591.04
SL-111	283.25	23.61	287.19	306.86	594.05
SL-112	285.72	23.81	289.69	309.53	599.22
SL-113	286.02	23.84	290.00	309.86	599.86
SL-114	286.68	23.89	290.66	310.57	601.23
SL-115	288.67	24.06	292.68	312.73	605.41
SL-116	292.80	24.40	296.87	317.20	614.07
SL-117	297.21	24.77	301.34	321.98	623.32
SL-118	301.20	25.10	305.38	326.30	631.68

SL-119	307.42	25.62	311.69	333.04	644.73
SL-120	311.17	25.94	315.50	337.11	652.61
SL-121	321.93	26.83	326.41	348.76	675.17
SL-122	328.54	27.38	333.10	355.92	689.02
SL-123	329.19	27.44	333.76	356.63	690.39
SL-124	334.23	27.86	338.87	362.09	700.96
SL-125	335.44	27.96	340.10	363.40	703.50
SL-126	336.83	28.07	341.51	364.90	706.41
SL-127	337.56	28.13	342.25	365.69	707.94
SL-128	347.71	28.98	352.54	376.69	729.23
SL-129	357.32	29.78	362.28	387.10	749.38
SL-130	360.01	30.01	365.01	390.02	755.03
SL-131	362.36	30.20	367.39	392.56	759.95
SL-132	368.78	30.74	373.9	399.52	773.42
SL-133	379.89	31.66	385.17	411.55	796.72
SL-134	382.72	31.90	388.03	414.62	802.65
SL-135	386.35	32.20	391.71	418.55	810.26
SL-136	398.52	33.21	404.05	431.73	835.78
SL-137	415.38	34.62	421.15	450.00	871.15
SL-138	417.85	34.83	423.65	452.68	876.33
SL-139	417.87	34.83	423.68	452.7	876.38
SL-140	418.20	34.85	424.01	453.05	877.06
SL-141	423.11	35.26	428.99	458.37	887.36
SL-142	427.52	35.63	433.46	463.15	896.61
SL-143	438.03	36.51	444.12	474.54	918.66
SL-144	442.64	36.89	448.79	479.53	928.32
SL-145	444.63	37.06	450.81	481.69	932.5
SL-146	446.25	37.19	452.44	483.44	935.88
SL-147	449.70	37.48	455.94	487.18	943.12
SL-148	455.67	37.98	462.00	493.65	955.65
SL-149	464.87	38.74	471.33	503.61	974.94
SL-150	484.12	40.35	490.85	524.47	1015.32
SL-151	494	41.17	500.86	535.17	1036.03
SL-152	503.75	41.98	510.74	545.73	1056.47
SL-153	515.62	42.97	522.78	558.59	1081.37
SL-154	524.19	43.69	531.47	567.88	1099.35
SL-155	546.57	45.55	554.16	592.12	1146.28
SL-156	586.51	48.88	594.66	635.39	1230.05
SL-157	657.75	54.82	666.89	712.57	1379.46
SL-158	672.87	56.08	682.22	728.95	1411.17
SL-159	681.59	56.8	691.06	738.39	1429.45
SL-160	693.36	57.78	702.99	751.14	1454.13
SL-161	700.21	58.36	709.94	758.57	1468.51
SL-162	752.75	62.73	763.21	815.48	1578.69
SL-163	832.84	69.41	844.41	902.25	1746.66

SL-164	843.88	70.33	855.60	914.21	1769.81
SL-165	869.66	72.48	881.74	942.14	1823.88
SL-166	887.67	73.98	900.00	961.65	1861.65
SL-167	895.16	74.60	907.59	969.76	1877.35
SL-168	902.04	75.17	914.57	977.21	1891.78
SL-169	948.55	79.05	961.73	1027.60	1989.33
SL-170	1105.53	92.13	1120.88	1197.66	2318.54
SL-171	1577.65	131.48	1599.56	1709.13	3308.69
SL-172	1959.23	163.27	1986.44	2122.50	4108.94
SL-173	2025.68	168.81	2053.82	2194.49	4248.31

From **Table 6.4** it can be observed that the estimated doses due to inhalation of indoor air vary between 8.32 µSv/y to 1577.63 µSv/y with an average of 269.08 µSv/y. The estimated ingestion doses vary between 8.40 µSv/y to 1599.72 µSv/y with an average value of 272.83 µSv/y in case of annual intake of water 730 litre and if we consider 60 litre annual water intake then the estimated ingestion doses vary between 0.69 µSv/y to 130.90 µSv/y with an average value of 22.42 µSv/y. For average calculation three very high values are excluded for all the cases. The study reveals that inhalation dose is a significant contributor for radon exposure from ground water and it is the main source if we consider 60 litre annual intake of water.

The profile of total annual effective dose is presented in **Figure 6.7** (***a*** and ***b***).

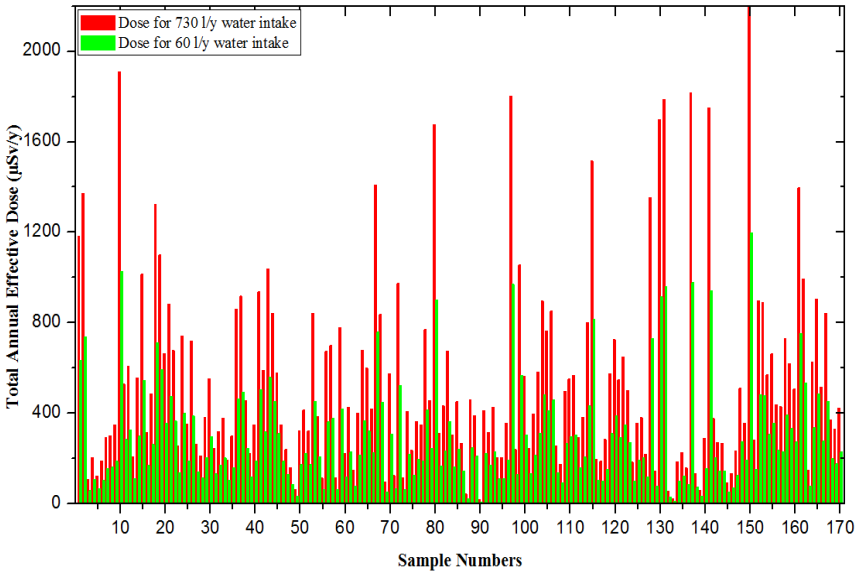

Fig. 6.7a

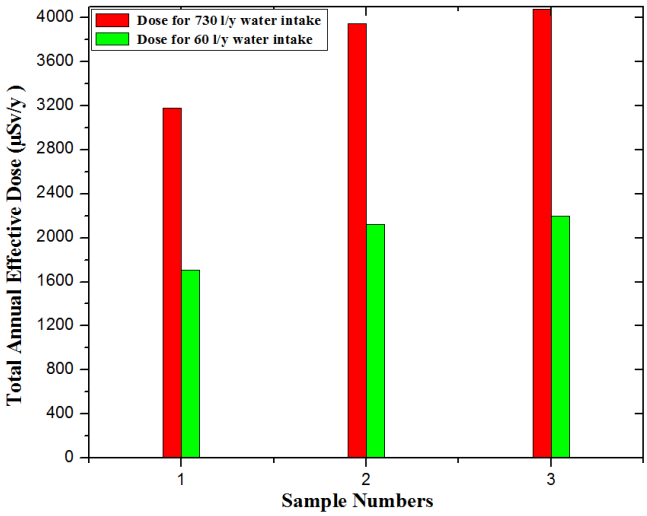

Fig. 6.7b

Fig. 6.7 Profile of total annual effective doses of radon in the study area: **a)** doses of radon in 170 groundwater samples; **b)** doses of radon in three groundwater samples with high radon concentration

From **Figure 6.7** (***a*** and ***b***) it is clear that the estimated total annual effective dose due to inhaled and ingested radon varies between 9.01 μSv/y to 2197.37 μSv/y with a mean value of 291.51 μSv/y (intake 60 l/y) and 16.72 μSv/y to 4079.47 μSv/y with an average value of 541.92 μSv/y (intake 730 l/y). The recommended value of the safe limit by WHO and EU Commission for the total annual effective dose received from drinking water is 100 μSv/y (***WHO 2004; EU 2001, 2005***). The total annual effective dose from 162 samples (about 95%) exceed the safe limit for 730 l/y intake and 147 samples (about 85%) exceed this limit if we consider 60 litre annual water intake.

6.7 Conclusions

The present study has revealed that 42% of the samples collected from Bakreswar and Tantloi and adjacent areas have radon concentration above WHO and EU Commission recommended reference level of 100 Bq/l. Even the average radon concentration of the ground water samples of this area is above the reference level. So, this Bakreswar and Tantloi area may be designated as ground water radon prone zone.

Both inhalation and ingestion doses are important, so far radiation exposure from radon in ground water is concerned. If we consider annual intake of water (730 l/y) about 95% samples exceed the reference limit of 100 μSv/y proposed by WHO and EU Commission for drinking water. Even if conservative approach of water intake (60 l/y), 85% of the samples cause higher exposure compared to the recommended dose limit.

Considering the gravity of the situation continuous monitoring of radon concentration level in water is required. If the radon concentration in drinking water is higher than the reference limit, radon reduction may be implemented using USEPA suggested Granular Activated Carbon (GAC) method or Aeration technique (***USEPA 2016***). Moreover,

it is also suggested to boil or stir the tube-well water before direct intake. However to reduce the indoor radon concentration it is also very important to make sure that the living rooms are well ventilated with air filter, fan and sufficient air passing windows.

Areas with high radon concentrations need special attention and further investigations are required not only for health hazard aspect but also for initiation of other research activities like harnessing of Helium, geothermal energy etc. (***Ghose et al. 2002; Khattak et al. 2011; Gurav et al. 2015***).

References

Abdallah, S. M., Habib, R. R., Nuwayhid, R. Y., Chatila, M., & Katul, G. (2007). Radon measurements in well and spring water in Lebanon. Radiation measurements, 42(2), 298-303.

Andrews, J. N., & Wood, D. F. (1972). Mechanism of radon release in rock matrices and entry into groundwaters. Bath Univ. of Tech., Eng..

Ball, T. K., Cameron, D. G., Colman, T. B., & Roberts, P. D. (1991). Behaviour of radon in the geological environment: a review. Quarterly Journal of Engineering Geology and Hydrogeology, 24(2), 169-182.

Banwell, G. M., & Parizek, R. R. (1988). Helium 4 and radon 222 concentrations in groundwater and soil gas as indicators of zones of fracture concentration in unexposed rock. Journal of Geophysical Research: Solid Earth, 93(B1), 355-366.

Bonotto, D. M., & Caprioglio, L. (2002). Radon in groundwaters from Guarany aquifer, South America: environmental and exploration implications. Applied radiation and isotopes, 57(6), 931-940.

Brutsaert, W. F., Norton, S. A., Hess, C. T., & Williams, J. S. (1981). Geologic and hydrologic factors controlling radon-222 in ground water in Maine. Groundwater, 19(4), 407-417.

Chandrashekara, M. S., Veda, S. M., & Paramesh, L. (2012). Studies on radiation dose due to radioactive elements present in ground water and soil samples around Mysore city, India. Radiation protection dosimetry, 149(3), 315-320.

Charoensri, A., Siriboonprapob, S., & Sastri, N. (2015, April). Analysis of radon in shallow-well water: a case study at Phichit subdistrict in Songkhla province, Thailand. In Journal of Physics: Conference Series (Vol. 611, No. 1, p. 012025). IOP Publishing.

Chaudhuri, H., Das, N. K., Bhandari, R. K., Sen, P., & Sinha, B. (2010). Radon activity measurements around Bakreswar thermal springs. Radiation Measurements, 45(1), 143-146.

Choubey, V. M., & Ramola, R. C. (1997). Correlation between geology and radon levels in groundwater, soil and indoor air in Bhilangana Valley, Garhwal Himalaya, India. Environmental Geology, 32, 258-262.

Choubey, V. M., Bartarya, S. K., & Ramola, R. C. (2003). Radon in groundwater of eastern Doon valley, Outer Himalaya. Radiation measurements, 36(1-6), 401-405.

Cosma, C., Moldovan, M., Dicu, T., & Kovacs, T. (2008). Radon in water from Transylvania (Romania). Radiation Measurements, 43(8), 1423-1428.

Cothern, C. R., & Marcus, W. L. (1984). Estimating risk for carcinogenic environmental contaminants and its impact on regulatory decision making. Regulatory toxicology and pharmacology, 4(3), 265-274.

Deb, S., & Mukherjee, A. L. (1969). On the genesis of a few groups of thermal springs in the Chotanagpur Gneissic Complex, India. J. Geochem. Soc. India, 4, 1-9.

Duggal, V., Mehra, R., & Rani, A. (2013). Determination of ^{222}Rn level in groundwater using a RAD7 detector in the Bathinda district of Punjab, India. Radiation Protection Dosimetry, 156(2), 239-245.

EU (2001). European Union Commission. Recommendation on the protection of the public against exposure to radon in drinking water supplies. Office Journal of the European Community, 85-88.

EU (2005). European Union Commission. Progress Report. Brussels, 9 November 2005. SEC (2005) 1426.

Galan Lopez, M., Martin Sanchez, A., & Gómez Escobar, V. (2004). Application of ultra-low level liquid scintillation to the determination of 222 Rn in groundwater. Journal of Radioanalytical and Nuclear Chemistry, 261, 631-636.

Gazi, M., Naskar, A. K., Mondal, M., & Deb, A. (2022). Radiological safety assessment of drinking water in Darjeeling hill and foothill areas: An experimental finding. Water Supply, 22(8), 6504-6515.

Ghose, D., Chowdhury, D. P., & Sinha, B. (2002). Large-scale helium escape from earth surface around Bakreswar–Tantloi geothermal area in Birbhum district, West Bengal, and Dumka district, Jharkhand, India. Current Science, 993-996.

GSI, Kolkata (1991). Geological Survey of India. Geothermal Atlas of India, Spl. Publ. 19, pp. 110–113

Gurav, T., Chandrasekharam, D., & Singh, H. K. (2015, April). Trace element and REE concentrations in the thermal waters, West Coast Geothermal Province, India. In Proceedings World Geothermal Congress, Melbourne (pp. 1-9).

Hess, C. T., Vietti, M. A., & Mage, D. T. (1987). Radon from drinking water—evaluation of water-borne transfer into house air. Environmental Geochemistry and Health, 9, 68-73.

Hoehn, E., & Von Gunten, H. R. (1989). Radon in groundwater: A tool to assess infiltration from surface waters to aquifers. Water resources research, 25(8), 1795-1803.

Hopkins, K. D., & Weeks, D. L. (1990). Tests for normality and measures of skewness and kurtosis: Their place in research reporting. Educational and psychological measurement, 50(4), 717-729.

Horvath, A., Bohus, L. O., Urbani, F., Marx, G., Piroth, A., & Greaves, E. D. (2000). Radon concentrations in hot spring waters in northern Venezuela. Journal of environmental radioactivity, 47(2), 127-133.

ICRP (1993). International Commission On Radiological Protection. Principles for intervention for protection of the public in a radiological emergency. Annals of the ICRP, 63(22), 4.

International Commission on Radiological Protection. ICRP (2010). Lung cancer risk from radon and progeny. Publication 115. Ann ICRP 40(1),1–64.

Jobbágy, V., Altzitzoglou, T., Malo, P., Tanner, V., & Hult, M. (2017). A brief overview on radon measurements in drinking water. Journal of environmental radioactivity, 173, 18-24.

Kendall, G. M., & Smith, T. J. (2002). Doses to organs and tissues from radon and its decay products. Journal of Radiological Protection, 22(4), 389.

Khattak, N. U., Khan, M. A., Ali, N., & Abbas, S. M. (2011). Radon monitoring for geological exploration: a review. Journal of Himalayan Earth Sciences, 44(2), 91-102.

Khursheed, A. (2000). Doses to systemic tissues from radon gas. Radiation Protection Dosimetry, 88.

Krishan, G., Rao, M. S., Kumar, C. P., & Semwal, P. (2015). Radon concentration in groundwater of east coast of West Bengal, India. Journal of Radioanalytical and Nuclear Chemistry, 303, 2221-2225.

Lawrence, E., Poeter, E., & Wanty, R. (1991). Geohydrologic, geochemical, and geologic controls on the occurrence of radon in ground water near Conifer, Colorado, USA. Journal of Hydrology, 127(1-4), 367-386.

Majumdar, N., Majumdar, R. K., Mukherjee, A. L., Bhattacharya, S. K., & Jani, R. A. (2005). Seasonal variations in the isotopes of oxygen and hydrogen in geothermal waters from Bakreswar and Tantloi, Eastern India: implications for groundwater characterization. Journal of Asian Earth Sciences, 25(2), 269-278.

Majumdar, R. K., Majumdar, N., & Mukherjee, A. L. (2000). Geoelectric investigations in Bakreswar geothermal area, West Bengal, India. Journal of Applied Geophysics, 45(3), 187-202.

Majumdar, R. K., Majumdar, N., & Mukherjee, A. L. (2010, February). Geological, geochemical and geoelectric studies for hydrological characterization and assessment of Bakreswar thermal springs in hard rock areas of Birbhum district, West Bengal, India. In Proceedings of 8th Biennial international conference and exposition on petroleum geophysics, Hyderabad, India.

Marques, A. L., Dos Santos, W., & Geraldo, L. P. (2004). Direct measurements of radon activity in water from various natural sources using nuclear track detectors. Applied radiation and isotopes, 60(6), 801-804.

Michel, J. (1990). Relationship of radium and radon with geological formations. Radon, radium and uranium in drinking water, 7, 83-95.

Mukhopadhyay, D. K., & Sarolkar, P. B. (2012, January). Geochemical appraisal of Bakreshwar–Tantloi hot springs, West Bengal and Jharkhand, India. In Proceedings, Thirty-Seventh Workshop on Geothermal Reservoir Engineering, Stanford University, Stanford, California (pp. 1-5).

Nagar, R. K. (1996). Geological, geophysical and geochemical investigations in Bakreswar-Tantloi th ermal field, Birbhum and Santhal Paragana districts, West Bengal and Bihar, India, Geothermal Energy in India. Geol. Surv. India Spl. Pub., 45, 349-360.

Nazaroff, W. W., Feustel, H., Nero, A. V., Revzan, K. L., Grimsrud, D. T., Essling, M. A., & Toohey, R. E. (1985). Radon transport into a detached one-story house with a basement. Atmospheric Environment (1967), 19(1), 31-46.

NCRP. (1984). Exposures from the uranium series with emphasis on radon and its daughters. NCRP Report No. 77.

Nikolopoulos, D., & Louizi, A. (2008). Study of indoor radon and radon in drinking water in Greece and Cyprus: implications to exposure and dose. Radiation Measurements, 43(7), 1305-1314.

Prasad, G., Prasad, Y., Gusain, G. S., & Ramola, R. C. (2008). Measurement of radon and thoron levels in soil, water and indoor atmosphere of Budhakedar in Garhwal Himalaya, India. Radiation Measurements, 43, S375-S379.

Press, W. H., Teukolsky, S. A., Vetterling, W. T., & Flannery, B. P. (1992). Numerical recipes in C (pp. I-XXVI). Cambridge: Cambridge university press.

Przylibski, T. A. (2011). Shallow circulation groundwater-the main type of water containing hazardous radon concentration. Natural Hazards and Earth System 428 Sciences, 11(6), 1695.

Rangaswamy, D. R., Srinivasa, E., Srilatha, M. C., & Sannappa, J. (2016). Measurement of radon concentration in drinking water of Shimoga district, Karnataka, India. Journal of Radioanalytical and Nuclear Chemistry, 307, 907-916.

Rani, A., Mehra, R., & Duggal, V. (2013). Radon monitoring in groundwater samples from some areas of Northern Rajasthan, India, using a RAD7 detector. Radiation protection dosimetry, 153(4), 496-501.

Samet, J. M. (1989). Radon and lung cancer. JNCI: Journal of the National Cancer Institute, 81(10), 745-758.

Sethy, N. K., Jha, V. N., Ravi, P. M., & Tripathi, R. M. (2015). Assessment of human exposure to dissolved radon in groundwater around the uranium industry of Jaduguda, Jharkhand, India. Current Science, 1855-1860.

Shanker, R. (1988). Heat flow map of India and discussion on its geological and economic significance. Indian Minerals, 42, 89-110.

Shiva Prasad, N. G., Nagaiah, N., Ashok, G. V., & Mahesh, H. M. (2007). Radiation dose from dissolved radon in potable waters of the Bangalore environment, South India. International journal of environmental studies, 64(1), 83-92.

Singh, H. K., Chandrasekharam, D., Trupti, G., & Singh, B. (2015, April). Geochemical characteristics of Bakreswar and Tantloi geothermal province, India. In Proceedings world geothermal congress (pp. 1-5).

Singh, J., Singh, H., Singh, S., & Bajwa, B. S. (2009). Estimation of uranium and radon concentration in some drinking water samples of Upper Siwaliks, India. Environmental monitoring and assessment, 154, 15-22.

Somlai, K., Tokonami, S., Ishikawa, T., Vancsura, P., Gáspár, M., Jobbágy, V., ... & Kovács, T. (2007). 222Rn concentrations of water in the Balaton Highland and in the southern part of Hungary, and the assessment of the resulting dose. Radiation Measurements, 42(3), 491-495.

Treutler, H., Just, G., Schubert, M., & Weiss, H. (2007). Radon as a tracer to determine the mean residence times of groundwater in decontamination reactors. Journal of radioanalytical and nuclear chemistry, 272(3), 583-588.

UNSCEAR (2000). United Nations Scientific Committee on the effects of atomic radiations. The General Assembly with Scientific Annex, New York.

UNSCEAR (2008). United Nations Scientific Committee on the Effects of Atomic Radiation. Report to the General Assembly 56. session (10-18 July 2008). Official Records: 63. session, suppl. no. 46 (A/63/46) (No. INIS-XU--09N0015). UN, New York.

USEPA (1991). United States Environmental Protection Agency. National primary drinking water regulations; radionuclides; proposed rules. Federal Register, 56(138), 33050.

USEPA (2016). United States Environmental Protection Agency. Consumer's Guide to Radon Reduction: How to Fix Your Home. (DOI EPA 402/K-10/005 | 2016 | www.epa.gov/radon)

USEPA (2018). Edition of the Drinking Water Standards and Health Advisories Tables (EPA 822-F-18-001).

USNRC (1999). United States National Research Council. Risk assessment of radon in drinking water. Committee on risk assessment of exposure to radon in drinking water, board on radiation effects research, commission on life sciences, National Research Council.

Vitz, E. (1991). Toward a standard method for determining waterborne radon. Health Physics, 60(6), 817-829.

Wanty, R. B., & Gundersen, L. C. (1988). Groundwater geochemistry and radon-222 distribution in two sites on the Reading Prong, Eastern Pennsylvania. Missouri Department of Natural Resouces Special Pub, 4, 147-156.

World Health Organization. (2004). Guidelines for drinking-water quality (Vol. 1). World Health Organization.

World Health Organization. (2009). WHO handbook on indoor radon: a public health perspective. World Health Organization.

WHO (2011). World Health Organization. Guidelines for drinking-water quality. Chapter 9. Radiological aspects. 4. Geneva.

Xinwei, L. (2006). Analysis of radon concentration in drinking water in Baoji (China) and the associated health effects. Radiation protection dosimetry, 121(4), 452-455.

Zhuo W, Iida T, Yang X (2001) Occurrence of ^{222}Rn, ^{226}Ra, ^{228}Ra and U in groundwater in Fujian Province, China. Journal of environmental radioactivity 53(1): 111-120

Chapter – 7

Water Radon Risk in Susunia Hill Area: An Assessment in Terms of Radiation Dose

7.1 Introduction

Radioactivity is a natural part of our environment. Approximately 80% of human exposure to radioactivity is natural, and 55-70% of this comes from radon and its daughters (***UNSCEAR 2000***). Radon (^{222}Rn) is an alpha-emitter, water soluble, colourless and odourless noble gas produced by alpha decay of radium (^{226}Ra) in the uranium (^{238}U) decay series. Radon gas generally originates from the rocks and soils under the earth crust (***Evans 1969***). After emanating from these sources radon can easily mix with the groundwater (***Wanty and Gundersen 1998***) by diffusion process. Due to high water solubility (0.000125 mole fraction at 37 ˚C, 15 times higher than that of helium or neon) ^{222}Rn activity in water can be significantly higher than that of the other natural radionuclides (***Fonollosa et al. 2016***). During showering, cooking, washing and other household activities the dissolved radon gas escapes from the water and gets into the indoor air (***UNSCEAR 2000***). Therefore, measurement of radon in drinking water is very essential for public health. A detailed discussion about it is given in our previous chapter (**Chapter 6 Section 6.1**).

In this present work we have chosen Susunia hill area of southern West Bengal, India where elevated radon activity in groundwater is expected due to its geological settings. Because of no other source of water supply in this area, almost all of the water requirement for household activities and drinking is fed by tube-wells. Radon in water might be a big concern for public health of this area if the tube-well water contains high radon activity. There is no previous reporting in literature regarding the radon content in groundwater of this hill area. Hence, this study aims at investigating the radon activity level in ground water (tube-well) of Susunia hill area and around and to estimate the inhalation and ingestion dose of the waterborne radon. Such studies are considered very important so far public health is concerned.

7.2 Study Area

Susunia hill area (around 23^{0}23′39′′N, 86^{0}59′11′′E) is an important Stone Age archaeological site in Bankura district, West Bengal, India. It is also a famous tourist spot in Bankura district and well known for its holy springs and flora**.** This region is located at the south-western limits of the Archaean Chotanagpur plateau, containing a varied topographical characteristics stretching from hilly zones to alluvial plains with undulating lands and rocky patches in the middle (***Biswas 2014***).The presence of sillimanite, kyanite-bearing schist and quartzite on the surrounding area of the Susunia hill indicates the evidence of shearing zones (***Mahapatra and Chakrabarty 2011***). It has been observed that water-rock ratios are comparatively high in fracture-enhanced porous zones formed by shearing (***Mahapatra and Chakrabarty 2011***).This area is enriched with dumortierite and tourmaline like minerals. Several rock layers like granite, granitic gneiss, micaschist, anorthosite, shale, quartzite, sandstone, limestone etc. are found in the earth crust of this region (***Das 2017***).

Bankura district is elevated towards north-west and the overall inclination of the surface travels from north-west to south-east, therefore almost all of the rivers run towards south-east. This high hilly region is covered by crystalline rocks of Precambrian age and located in the north-western part of the district. Depending upon the impulse of earthquakes the Bureau of Indian Standards (BIS) categorized that Susunia hill region falls under seismic zone III (***BIS 1893***). Tectonically this region is highly disordered due to disposition of different types of rock layers. Formational disturbance of this area is caused by the existence of extensive nature of fold, faults, lineament and shear zones (***Chakrabarti and Bhattacharya 2013***).

From geological point of view, compositions of rocks and soils of this area show evidence of shearing and high mineral deposition (***Mahapatra and Chakrabarty 2011***) which may elevate the radon activity in groundwater (***Otton 1992***) of this area.

Location of Susunia hill in Bankura district is presented in **Figure 7.1**.

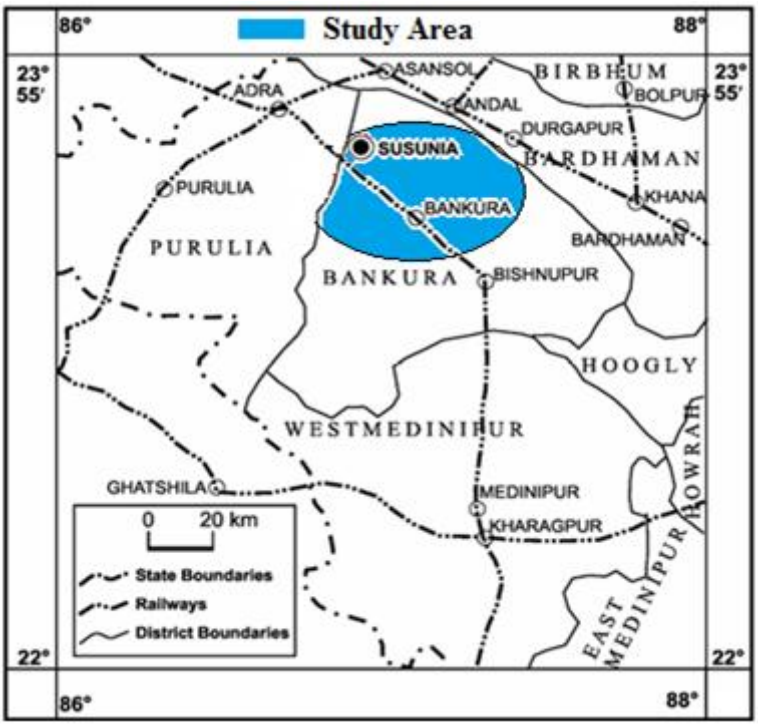

Fig. 7.1 Map of the study area

The locations (obtained by GPS meter) of the tube-well water sampling sites in Susunia hill and its surrounding area are shown in **Figure 7.2**.

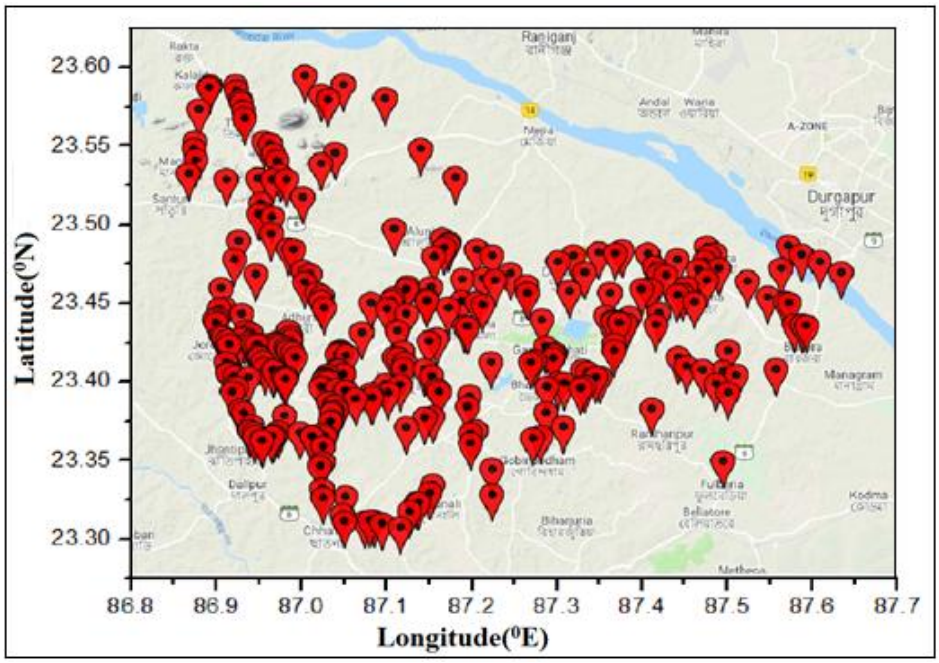

Fig. 7.2 Water sample collection sites

The area is basically hot and humid with small period of winter and rainy months. Because of lack of rain fall and non-existence of other water sources or reservoirs people use tube-well water for drinking as well as other daily house hold activities like cooking, bathing etc.

Fine combination of alluvial plains and undulating hilly terrain along with vast stretches of trees like sal, mohua, palash, eucalyptus, etc. all over the region offers a famous tourist destination to visitors from all over India which may raise its importance for radiological aspect.

7.3 Material and experimental methods

7.3.1 Groundwater sampling

A total of 316 water samples have been collected from drilled tube-wells with borehole depth ranging from 9 m to 122 m. distributed within the study area. The sampling was conducted during 25th December, 2018 - 2nd February, 2020. We have considered only those tube-wells which are situated in highly populated villages and are mainly used for drinking. Sampling procedure has been discussed in **Chapter 6 Section 6.3**. The actual location of the sampling sites were assigned by noting the corresponding latitude and longitude of each and every tube well using a global position system (GPS) meter.

7.3.2 Water radon activity measurement procedure

The samples collected in a day were brought to the measuring site immediately and the radon activities were measured by AlphaGUARD radon monitor within 1-3 hours of collection to minimize the radon loss due to decay. Details about the water radon

measurement procedure have been discussed in **Chapter 4 Section 4.1.2**. pH values of the water samples have been measured by pH meter. Information regarding the depth of the tube-wells have been gathered as far as possible.

7.3.3 Dose estimation

In consideration of the health risk of the local people caused by the water-borne radon exposure, it is essential to estimate the annual effective dose inflicted upon the local people of these areas due to ingestion as well as inhalation of radon from water. A detail about the dose estimation procedure is discussed in **Chapter 6 Section 6.4.2**.

Indoor occupancy time

In this present study for inhalation dose calculation we have not used the UNSCEAR (**2000**) proposed 7000 hr/yr indoor occupancy time. Reason behind it is, in this study area the main source of income of the local people is agricultural work. Because of which every day local people spend 8 - 10 hours on farmland and on an average they stay at indoor for 15 hours. Considering the local condition we have taken the annual average indoor occupancy time (I) of 5475 (15 × 365) hours for this study.

Annual water intake

For ingestion dose estimation daily water intake is needed. According to World Health Organization (WHO) the daily water intake is 2 litre per day for humans (***WHO 2009***). Also many researchers have taken 1liter daily water consumption according to meteorological conditions of their study area (***Zhuo et al. 2001; Rangaswamy et al. 2016***). However, majority of water is usually not consumed directly from tap and as a result radon is readily lost. Therefore more realistic value of 60 litre for the weighed direct annual consumption of tap water has been proposed in UNSCEAR (***2000***) report**.**

We came to know from local people of Susunia hill area that due to the hot and humid weather the adults and children of this area directly drinks 3-4 l/d and 2-3 l/d tube-well water respectively. Additionally they consume more water indirectly. Hence, the daily direct water intake of the local people from the tube wells is 3 l/d considering the average water consumptions of adults and children of this area.

In view of the controversies regarding annual water intake in this present study we have measured the ingestion doses considering both the annual water intake of 60 litre as prescribed by UNSCEAR and 1095 (3 × 365) litre as informed by the local people.

7.4 Results and discussions

7.4.1 Radon activity measurement

For this study radon activity has been measured in 316 tube-well water samples

collected from various locations in and around Susunia hill area in Bankura district of West Bengal, India. Recorded data are presented in **Table 7.1**.

Table 7.1 Recorded data of radon activity, pH of the tube-well water and depth of the tube-wells

Sample Id	Latitude (°N)	Longitude (°E)	Activity (Bq/l)	pH	Depth (m)
TW - 1	23.5225	86.87158	101.02	7.4	
TW - 2	23.42888	87.15787	195.98	7.7	52
TW - 3	23.58459	86.94977	11.89	8.1	
TW - 4	23.45792	86.9528	232.38	6.4	
TW - 5	23.35468	86.95419	108.5	8.1	
TW - 6	23.35469	86.95405	170.79	6.6	68
TW - 7	23.44653	86.95777	34.92	7.2	
TW - 8	23.33616	86.96018	18.55	7.2	
TW - 9	23.52867	86.96042	45.33	6.9	31
TW - 10	23.57264	86.96061	12.84	0.1	14
TW - 11	23.38647	86.9033	12.48	6.9	
TW - 12	23.44137	86.96077	118.1	8	
TW - 13	23.4275	86.89004	267.71	6.3	65
TW - 14	23.44148	86.96085	115.35	6.8	34
TW - 15	23.44438	86.96131	114.81	6.8	
TW - 16	23.32117	86.96134	120.4	7.1	
TW - 17	23.31555	86.96165	124.26	8.3	
TW - 18	23.34849	86.96175	102.84	7.1	
TW - 19	23.33871	86.96189	2228.98	8	106
TW - 20	23.35645	86.96225	204.94	8.3	
TW - 21	23.43651	86.8952	130.2	6.2	
TW - 22	23.39075	86.9626	152.86	6.9	
TW - 23	23.39196	86.96339	10.37	7.5	
TW - 24	23.43068	86.8905	257.18	6.2	
TW - 25	23.35483	86.9636	200	6.8	
TW - 26	23.39424	86.96443	127.78	6.7	
TW - 27	23.39068	86.96459	67.63	7.2	
TW - 28	23.56974	86.96523	6.46	8.3	
TW - 29	23.39022	86.96527	87.91	6.7	33
TW - 30	23.37699	86.96569	20.66	7.9	
TW - 31	23.3643	86.9666	67.58	7.4	
TW - 32	23.36945	86.96746	55	8.1	
TW - 33	23.37066	86.96796	403.72	7	
TW - 34	23.36503	86.96809	253.96	7.9	
TW - 35	23.43645	86.89188	780.22	8.2	85
TW - 36	23.37461	86.9698	50.2	6.2	
TW - 37	23.37464	86.96984	61.64	6.8	
TW - 38	23.53543	86.9704	33.24	8.3	20

TW - 39	23.38481	86.97123	65.12	6.5	
TW - 40	23.40736	86.97133	47.48	7.4	
TW - 41	23.37153	86.97156	8.83	8.1	
TW - 42	23.39752	86.97184	252.35	7.6	61
TW - 43	23.39701	86.92861	552.86	8.3	
TW - 44	23.40992	86.97381	128.97	8.3	41
TW - 45	23.40767	86.97426	63.32	7.2	
TW - 46	23.44921	86.89331	11.1	6.9	13
TW - 47	23.40924	86.97451	53.77	8.3	
TW - 48	23.39458	86.97518	248.24	6.8	46
TW - 49	23.30499	86.97523	126.82	7.3	
TW - 50	23.57888	86.97537	18.16	8.2	15
TW - 51	23.39473	86.97573	91.87	7.6	27
TW - 52	23.30041	86.97611	400.42	8.3	
TW - 53	23.3166	86.97688	383.61	7.6	
TW - 54	23.38368	86.97698	45	8.2	14
TW - 55	23.38371	86.97698	55.96	7.4	
TW - 56	23.40685	86.9775	23.23	6.4	
TW - 57	23.41891	86.89352	141.81	8.3	
TW - 58	23.37906	86.98381	37.21	7.1	18
TW - 59	23.4212	86.98799	28.45	7.6	
TW - 60	23.30093	86.98986	203.29	7.3	
TW - 61	23.30137	86.99365	74.18	6.8	
TW - 62	23.44014	86.99403	81.32	7.6	30
TW - 63	23.38206	86.99447	59.77	7.9	53
TW - 64	23.37955	86.99508	87.41	8.3	58
TW - 65	23.30157	86.99616	100	7.9	
TW - 66	23.29963	87.00171	55.21	7.3	
TW - 67	23.38829	87.00364	143.17	8.3	43
TW - 68	23.41763	86.89475	151.51	6.3	47
TW - 69	23.57	87.00405	22.59	7.4	26
TW - 70	23.43644	87.0053	112.78	6.1	
TW - 71	23.38256	87.23541	5.81	6.5	
TW - 72	23.44131	87.00795	39.12	7.4	18
TW - 73	23.44292	87.00939	237.93	8.3	
TW - 74	23.40542	87.01031	153.42	8.3	48
TW - 75	23.48711	87.01034	63.67	6.5	24
TW - 76	23.42218	86.91075	20.47	8.2	18
TW - 77	23.40444	87.01274	283.16	8.3	
TW - 78	23.29709	87.01423	959.05	6.3	96
TW - 79	23.43648	86.96258	344.88	7.8	
TW - 80	23.38751	87.01433	59.35	6.4	23
TW - 81	23.40878	87.01579	23.89	7.3	11
TW - 82	23.39853	87.01646	45.08	7	17
TW - 83	23.4024	86.89696	53.29	7.9	25

TW - 84	23.43315	87.0179	408.36	6.3	
TW - 85	23.44907	87.01802	80.29	7.8	52
TW - 86	23.3604	87.01834	89.11	7.2	
TW - 87	23.45055	87.01891	28.91	7.9	17
TW - 88	23.30724	87.02014	181.84	7.6	
TW - 89	23.31243	87.02517	37.65	6.4	
TW - 90	23.51861	86.89683	12.04	6.1	
TW - 91	23.31252	87.02632	123.21	8.3	
TW - 92	23.53802	87.02767	14.08	7.8	44
TW - 93	23.39766	87.03037	40.15	8.1	
TW - 94	23.36703	87.03047	58.76	6.7	
TW - 95	23.44103	87.03219	89.36	6.2	
TW - 96	23.44236	87.0322	20.97	7.2	19
TW - 97	23.41535	87.03332	60.39	6.7	
TW - 98	23.31865	87.03404	95.12	6.2	
TW - 99	23.44976	87.03504	15	6.3	13
TW - 100	23.39306	87.03553	81.56	6.9	
TW - 101	23.40238	87.0167	97.12	8.3	60
TW - 102	23.36731	87.03616	43.88	6.7	
TW - 103	23.32366	87.03641	50.69	7.2	
TW - 104	23.46927	87.03709	115.89	6.9	38
TW - 105	23.38493	87.03901	52.5	7.4	
TW - 106	23.4171	87.03909	35.23	7.8	
TW - 107	23.38311	87.0399	224.54	8.2	
TW - 108	23.48067	87.04229	85.77	6.6	59
TW - 109	23.47531	87.0437	82	8.1	58
TW - 110	23.47717	87.04629	213.86	7.5	55
TW - 111	23.43668	87.04664	35.1	6.9	
TW - 112	23.53841	86.87449	16.73	7.6	
TW - 113	23.41573	86.89722	4.8	8.3	
TW - 114	23.42818	87.04666	2.6	8.1	
TW - 115	23.47811	87.04734	198.17	7.6	48
TW - 116	23.44877	87.04831	3.89	7.9	11
TW - 117	23.51963	87.05121	62.8	8.3	42
TW - 118	23.44133	87.05537	152.11	7.3	
TW - 119	23.45531	87.0561	124.03	6.5	40
TW - 120	23.42542	87.05713	74.81	7.5	
TW - 121	23.3737	87.05946	93.15	8.3	
TW - 122	23.42489	87.05961	10.85	7.4	
TW - 123	23.38069	87.06054	34.58	6.5	
TW - 124	23.39547	86.89795	479.26	7.3	75
TW - 125	23.35665	87.06149	100.61	6.9	
TW - 126	23.35036	87.06179	119.45	6.2	
TW - 127	23.35847	87.06495	54.87	6.2	
TW - 128	23.44078	87.06535	1083.41	7.2	

TW - 129	23.47407	87.06566	126.31	8.3	
TW - 130	23.45539	87.06946	105.46	6.8	61
TW - 131	23.4386	87.06954	74.12	6.1	
TW - 132	23.40205	87.10211	18.09	7.1	13
TW - 133	23.33385	87.07573	400	6.8	
TW - 134	23.31762	87.07576	168.43	7.3	
TW - 135	23.39572	86.89818	179.65	7.9	51
TW - 136	23.46987	87.07581	314.6	8.3	
TW - 137	23.45431	87.22096	134.4	8.3	46
TW - 138	23.45915	87.08805	148.75	7	48
TW - 139	23.31287	87.09144	2.77	8.1	
TW - 140	23.45152	87.09915	21.69	6.5	47
TW - 141	23.44616	87.09985	62.86	6.9	22
TW - 142	23.40207	87.0749	30	6.8	19
TW - 143	23.35331	87.10367	172.49	6.9	
TW - 144	23.4037	87.10447	30.56	6.2	19
TW - 145	23.35492	87.10867	45.16	6.6	
TW - 146	23.41321	86.89893	92.8	7.9	31
TW - 147	23.42908	87.10969	117.85	7.3	39
TW - 148	23.39381	87.11052	2.89	8.2	12
TW - 149	23.41248	87.11263	58.64	7.8	50
TW - 150	23.37023	87.11264	305.4	7.2	
TW - 151	23.38664	87.11291	13.33	8.1	11
TW - 152	23.40459	87.11685	22.22	7.8	
TW - 153	23.40651	87.11807	13.41	8.2	
TW - 154	23.40756	87.11846	26.3	7.2	18
TW - 155	23.3898	87.12064	73.42	7.4	23
TW - 156	23.46637	87.29673	23.7	7.8	19
TW - 157	23.39612	86.89917	333.93	8.3	
TW - 158	23.36111	87.12373	205.5	8.3	
TW - 159	23.38891	87.12479	426.21	8.1	71
TW - 160	23.4478	87.12791	357.28	6.8	46
TW - 161	23.47018	87.13062	19.53	6.8	
TW - 162	23.45121	87.13486	30.31	7.8	17
TW - 163	23.38545	87.13591	151.6	7.8	
TW - 164	23.39724	87.13669	15.87	7.9	
TW - 165	23.38698	87.13824	210.53	6.5	
TW - 166	23.45959	87.13841	41.33	7.5	22
TW - 167	23.3958	87.14075	27.02	8	20
TW - 168	23.38269	86.90071	680.32	6.5	76
TW - 169	23.39266	87.14611	71.75	6.9	
TW - 170	23.47186	87.14833	16.3	7.4	42
TW - 171	23.39294	87.14842	175.28	7.1	
TW - 172	23.43184	87.15299	124.88	6.8	43
TW - 173	23.44626	87.15531	77.5	6.7	27

TW - 174	23.47309	87.1568	4.35	7.6	
TW - 175	23.42801	87.15744	204.83	6.3	46
TW - 176	23.42894	86.88852	243.86	8.3	
TW - 177	23.4098	86.93827	59.23	8.2	
TW - 178	23.41401	87.15855	236.07	7.2	
TW - 179	23.38318	86.90109	3213.5	6.1	126
TW - 180	23.4712	87.15931	34.23	7.3	25
TW - 181	23.4272	87.1618	126.65	7	
TW - 182	23.42789	87.16194	261.93	7.3	
TW - 183	23.4732	87.1635	63.27	7.9	19
TW - 184	23.42677	87.16639	275.94	7.7	58
TW - 185	23.43129	87.16873	113.06	8.3	41
TW - 186	23.44854	87.17701	72.07	6.2	19
TW - 187	23.47134	87.18091	108.55	7.6	25
TW - 188	23.44937	87.18199	110.31	8.3	
TW - 189	23.4488	87.1833	64.82	7.6	24
TW - 190	23.38706	86.9012	18.41	8.2	14
TW - 191	23.3725	87.18405	38.19	6.5	20
TW - 192	23.46318	87.18533	58.11	6.4	
TW - 193	23.46324	87.18533	76.22	8.3	37
TW - 194	23.42624	87.1866	110.94	7.3	30
TW - 195	23.43358	87.18879	377	8.3	77
TW - 196	23.45886	87.18884	15.18	7.4	13
TW - 197	23.45759	87.19342	102.32	7.7	50
TW - 198	23.46792	87.201	152.7	8.3	46
TW - 199	23.44492	87.20103	155.32	6.3	44
TW - 200	23.40549	87.20191	160.84	6.6	46
TW - 201	23.46773	86.90195	19.32	7.6	14
TW - 202	23.44547	87.20404	74.33	6.4	23
TW - 203	23.45025	87.20676	41.92	6.4	18
TW - 204	23.4503	87.20702	184.41	8.2	49
TW - 205	23.39976	87.20713	135.19	8.3	49
TW - 206	23.44086	87.2125	192.64	7.7	55
TW - 207	23.46107	87.21525	51.18	7.2	24
TW - 208	23.39702	87.2181	152.78	7.5	56
TW - 209	23.4667	87.21941	22	6.7	16
TW - 210	23.45432	87.07767	44.08	7.9	25
TW - 211	23.47607	87.22103	101	8.3	27
TW - 212	23.39334	86.90223	18.18	8.1	
TW - 213	23.4703	87.22193	98.28	6.9	37
TW - 214	23.47174	87.2262	37.8	8	20
TW - 215	23.3882	87.22674	453.95	6.6	71
TW - 216	23.4617	87.22937	39.94	7.2	21
TW - 217	23.39659	87.23163	187.24	6.9	52
TW - 218	23.33929	87.23167	24.67	6.7	16

TW - 219	23.40983	87.23503	118.29	8.1	39
TW - 220	23.38258	87.00613	129.22	8.3	42
TW - 221	23.39403	87.24086	36.93	6.5	24
TW - 222	23.45354	87.24835	20.58	7.5	14
TW - 223	23.54228	86.8757	16.34	7.6	
TW - 224	23.57862	86.90271	50	7.7	
TW - 225	23.44355	87.26175	75.23	7.6	54
TW - 226	23.3976	87.26737	24.74	7.1	16
TW - 227	23.46204	87.27061	6.96	8.2	13
TW - 228	23.44055	87.27393	21.21	8.3	24
TW - 229	23.44273	87.27409	1.84	7.3	11
TW - 230	23.47664	87.2757	16.33	7.8	10
TW - 231	23.43984	87.27632	18.66	7.8	13
TW - 232	23.45581	87.27707	1.9	7.9	20
TW - 233	23.42609	87.27989	23.12	6.3	17
TW - 234	23.47076	87.28437	30.55	7.4	16
TW - 235	23.38646	86.96066	546.2	7.8	
TW - 236	23.42587	87.28531	37.11	8.3	25
TW - 237	23.42577	87.28552	51	8.1	23
TW - 238	23.42532	87.28801	13.92	6.3	11
TW - 239	23.43918	87.2907	1.78	7.9	10
TW - 240	23.46643	87.12068	10.84	8.3	12
TW - 241	23.45935	87.31157	8.53	7.6	13
TW - 242	23.3657	87.62727	66.7	6.9	
TW - 243	23.57563	86.90358	10.26	8.2	
TW - 244	23.47987	86.90509	115.79	6.5	40
TW - 245	23.56917	86.90607	16.92	7.5	
TW - 246	23.41709	86.90643	53.76	6.8	
TW - 247	23.3719	86.90646	219.57	6.3	
TW - 248	23.43309	86.90692	128.21	7.3	
TW - 249	23.56715	86.90716	21.19	6.5	
TW - 250	23.56223	86.90816	30.1	6.5	
TW - 251	23.53095	86.87612	136.56	8.3	
TW - 252	23.37001	86.90828	157.04	8.3	57
TW - 253	23.55766	86.90882	52.77	8.2	
TW - 254	23.41806	86.90889	169.6	6.5	
TW - 255	23.42215	87.0121	240.73	8.3	
TW - 256	23.39285	86.91195	32.81	7.8	
TW - 257	23.41533	86.91223	76.45	7.5	26
TW - 258	23.35875	86.91278	69.28	8.1	
TW - 259	23.42065	86.91336	384.85	8.3	
TW - 260	23.36191	86.91419	16.7	7.1	
TW - 261	23.41396	86.92056	202.64	8.3	
TW - 262	23.56316	86.87783	16.93	6.7	
TW - 263	23.3576	86.91529	73.2	7.9	

TW - 264	23.35511	86.91566	392.13	8.3	
TW - 265	23.45798	86.9168	92.24	8.3	60
TW - 266	23.4133	86.91758	144.38	8.3	51
TW - 267	23.51901	86.91826	12.64	7.4	
TW - 268	23.4065	86.91862	103.39	6.5	31
TW - 269	23.49689	86.91892	114.89	6.7	56
TW - 270	23.40559	86.91952	80.05	7.9	
TW - 271	23.50348	86.91979	17.4	6.4	
TW - 272	23.414	86.91474	374.45	8.1	71
TW - 273	23.56968	86.88175	2.7	8.2	
TW - 274	23.35224	86.92084	139.71	8.3	
TW - 275	23.35224	86.92081	139.71	8.3	
TW - 276	23.40255	86.92152	223.26	8.1	54
TW - 277	23.49708	86.92174	220.67	8.3	
TW - 278	23.54244	86.92234	18.19	7.9	
TW - 279	23.3983	86.92267	167.87	7.6	
TW - 280	23.5416	86.92612	41.33	7.6	
TW - 281	23.48399	86.92694	19.56	7.5	
TW - 282	23.49488	86.9273	118.6	7.6	
TW - 283	23.51868	86.92733	154.9	7.2	40
TW - 284	23.57747	86.88495	41.76	8.2	
TW - 285	23.35486	86.92748	107.15	7.2	49
TW - 286	23.53519	86.92858	31.56	6.7	
TW - 287	23.39699	86.97249	17.51	6.7	
TW - 288	23.35576	86.92867	88.26	8.3	
TW - 289	23.39707	86.92927	17.14	7.8	10
TW - 290	23.41477	86.92941	95.03	7.9	
TW - 291	23.53056	86.93102	34.41	6.3	
TW - 292	23.4141	86.93132	142.77	6.1	46
TW - 293	23.358	86.93177	53.37	7.1	
TW - 294	23.41297	86.93302	40.44	7.3	
TW - 295	23.57827	86.88545	4.42	7.5	
TW - 296	23.52203	86.93332	20.05	7.1	
TW - 297	23.3928	86.93534	22.12	7.9	18
TW - 298	23.36825	86.93588	136.32	8.3	
TW - 299	23.3913	86.93665	62.61	7.5	
TW - 300	23.39257	86.93714	81.88	8.2	60
TW - 301	23.41171	86.93723	63.88	7.2	
TW - 302	23.51843	86.93748	10.24	7.9	48
TW - 303	23.40975	87.15826	15.82	7.6	
TW - 304	23.40943	86.93832	17.78	6.3	16
TW - 305	23.42215	86.93851	39.04	7.8	
TW - 306	23.5826	86.88603	4.42	8.3	
TW - 307	23.4747	86.93858	11.81	8.2	
TW - 308	23.41868	86.93993	100	6.4	

TW - 309	23.41592	86.9401	136.24	8.3	
TW - 310	23.40821	86.94158	52.12	6.1	
TW - 311	23.47395	86.94193	12.38	6.2	
TW - 312	23.40517	86.94349	20.67	6.2	17
TW - 313	23.35735	86.94604	280.35	8.3	
TW - 314	23.5075	86.94807	8.29	7.9	12
TW - 315	23.46045	86.94851	42.05	6.7	
TW - 316	23.45338	86.94942	149.14	8.3	66

Radon activity profile of 308 samples with activity ranging between 1 – 500 Bq/l, is plotted in **Figure 7.3(a)** and the other 8 samples having very high activity (> 500 Bq/l) are presented separately in **Figure 7.3(b)** for better representation.

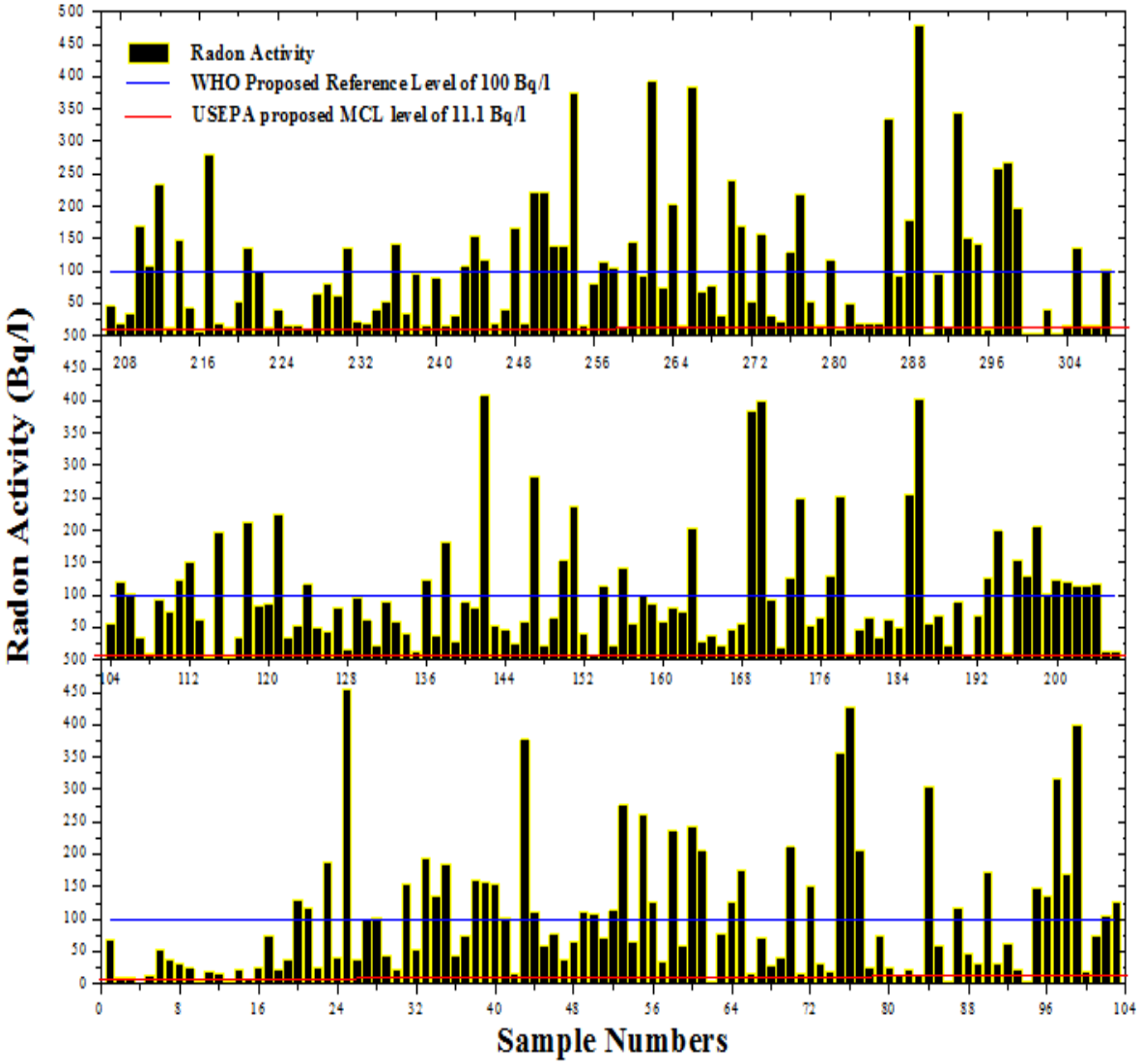

Fig. 7.3(a) Radon activity profile of the samples (< 500 Bq/l)

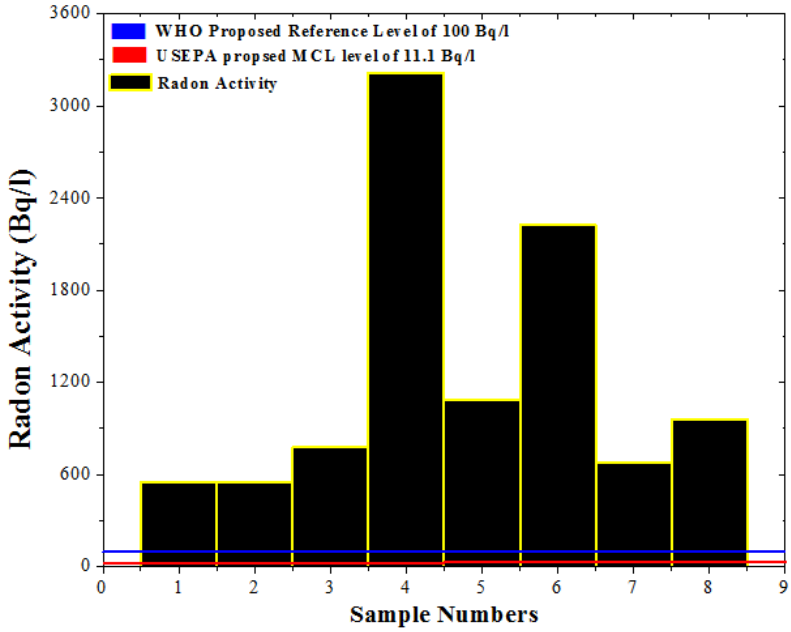

Fig. 7.3(b) Radon activity profile of the samples (> 500 Bq/l)

These two profiles show that the radon activity of the samples varies widely between 1.78 ± 0.07 – 3213.50 ± 77.32 Bq/l with an average of 128.30 ± 14.09 Bq/l.

The above average is for the total data set. However excluding the 8 samples with extremely high activity data (> 500 Bq/l) average activity level becomes 99.02 ± 5.51 Bq/l, which is just below the WHO and EU Council Directive prescribed reference level of 100 Bq/l (***WHO 2009; EURATOM 2013***). Results show that activities of 293 samples (about 93%) have exceeded the USEPA proposed MCL level of 11.1 Bq/l (***USEPA 1991***) and 127 samples (about 40%) have activities above the WHO and EU Council Directive proposed reference level of 100 Bq/l.

To demonstrate the overall variation pattern of radon activities of the samples we have shown the frequency distribution of radon activity in **Figure 7.4** (excluding the 8 samples with activity greater than 500 Bq/l).

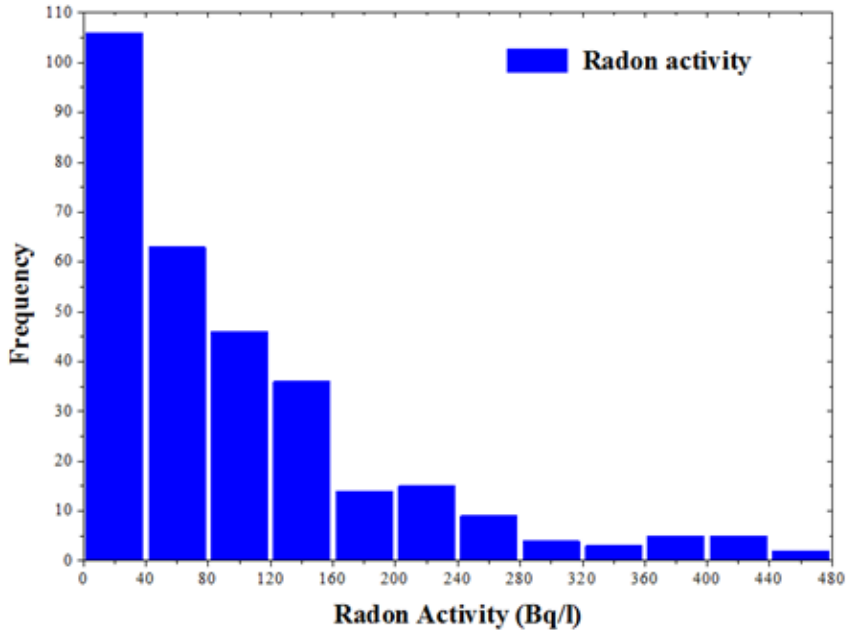

Fig. 7.4 Distribution of radon activities of the samples (< 500 Bq/l)

It is evident from **Figure 7.4** that the distribution is not symmetric in nature**.** The distribution peaks at the initial value and then decreases gradually. To understand the statistical properties of the data the important statistical parameters are determined using the conventional formulae (***Hopkins and Weeks 1990***). **Table 7.2** presents the summary of statistical parameters for radon activity of the 308 water samples.

Table 7.2 Statistical description of the water samples having radon activity < 500 Bq/l

Statistical Parameters	Value
Sample Size	308
Min	1.78 ± 0.07
Max	479.26 ± 12.23
Mean	99.02 ± 5.56
Variance	9362
Std. Deviation	96.76
Median	67.14
Skewness	1.62
Kurtosis	2.52

It can be observed from the **Table 7.2** that the arithmetic mean is slightly greater than the standard deviation, which indicates that the radon distribution fluctuates widely. The distribution is highly skewed with a skewness value of 1.62. The excess kurtosis value of 2.52 indicates that the distribution has flatter long tail with a sharp peak than the normal distribution. According to the skewness and excess kurtosis factor value it can be concluded that the distribution is not normal in nature (***Hopkins and Weeks 1990; Press 1992***).

A 3-D surface plot of all the samples is shown in **Figure 7.5** to highlight the geographical position of the very high radiation prone zones with radon activities above 500 Bq/l as well as to show the radon activity of the other areas.

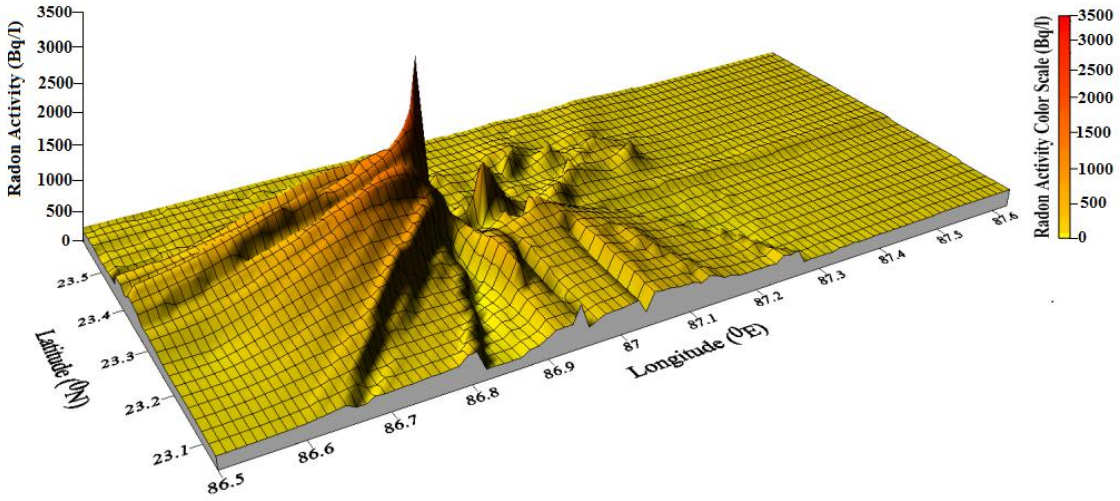

Fig. 7.5 3-D surface plot of radon activities of the water samples

We have measured the pH value of the samples and have investigated to unfold any correlation between radon activity and the pH values of the water samples. From **Table 7.1** it can be observed that the pH values of the water samples vary within the maximum of 8.3 and a minimum of 6.1, average being 7.4. The Pearson's correlation coefficient (***Weisstein 2006***) between pH and radon activity has a very low value of - 0.004 suggesting almost no correlation between them.

To search for possible correlation between the depth of the tube-wells and their radon activities, we have tried to gather information about the depth of the tube-wells. In case of 70 tube-wells we have found that their depths are written on them by the local authority. On the other hand, local people have been able to provide the data regarding the depth of 80 tube-wells. So, in total we have managed to collect the borehole depth data of 150 tube-wells out of 316. Tube-well depths of these 150 samples are only presented in **Table 7.1**.

In **Figure 7.6** we have shown the variation of water radon activity with depth of the tube-wells. The plot indicates correlation between radon activity and tube-well depths.

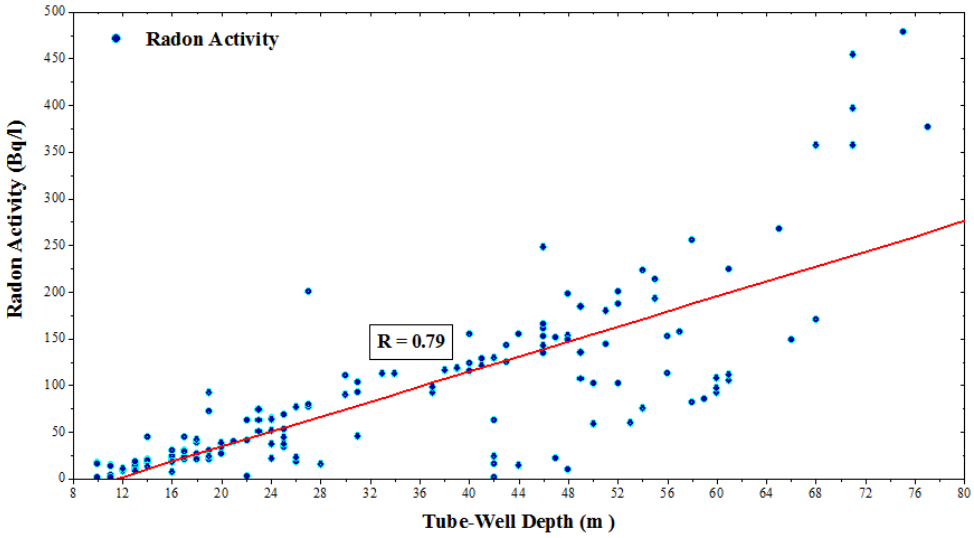

Fig. 7.6 Scatter plot of radon activity with tube-well depth

To have a quantitative estimate of the correlation, Pearson's correlation coefficient have been calculated. It reveals a fairly strong positive linear correlation with correlation factor of 0.79.

The water samples collected from Latiabani, Ethani, Gurputa, Pabradihi and Jirra areas have extremely high radon activities of 680.32 ± 13.47 Bq/l, 3213.50 ± 77.32 Bq/l, 2228.98 ± 49.27 Bq/l, 780.22 ± 13.26 Bq/l and 959.05 ± 16.58 Bq/l respectively.

It is also noted that the borehole depth of tube-wells of these 5 locations are 76 m, 126 m, 106 m, 85 m and 96 m respectively which are very high with respect to the other tube-wells. At greater depth presence of rocks containing uranium and radium may be comparatively high. Vicinity of fault or fracture zone may also be responsible for high radon activity.

Table 7.3 Study of water radon activity in different parts of the world

Sampling Site	Water Type	No of Samples	Activity Range (Bq/l)	Average Activity (Bq/l)	References
Garhwal Himalaya, India	Groundwater	150	8.00 – 3050.00	510.00	***Prasad et al. 2008***
Covilhã's county, Portugal	Groundwater	33	2.00 – 1690.00	354.00	***Inacio et al. 2017***
Susunia, India	Tube-well water	316	1.79 - 3237.89	128.27	***This Study***
Bakreswar and Tantloi, India	Tube-well water	173	3.30 – 803.00	117.69	***Naskar et al. 2018***

Bangalore, India	Groundwater	65	3.05 - 696.00	91.39	***Ravikumar and Somashekar 2018***
Sudetes uranium region, Poland	Groundwater	111	5.50 - 215.70	47.42	***Przylibski 2011***
South Catalonia, Spain	Spring and non-bottled mineral waters	15	1.40 - 104.90	20.31	***Fonollosa et al. 2016***
Songkhla, Thailand	Shallow well water	35	0.18 - 98.10	16.76	***Charoensri et al. 2014***
UK, Northern Ireland	Groundwater	26	5.80 - 36.60	16.30	***Gibbons and Kalin 1997***
Karnataka, India	Tap water, open well and bore-well	20	0.37 - 87.02	14.19	***Shilpa et al. 2017***
La Garrotxa, Spain	Well and spring water	53	0.80 - 26.0	11.40	***Moreno et al. 2014***
Balaton Highland, Hungary	Tap, well and spring water	120	0.31 - 24.30	5.56	***Somlai et al. 2007***
Kerman, Iran	Well, canal and storage water	32	1.20 - 9.88	5.14	***Malakootian and Nejhad 2017***
Rajasthan, India	Hand pumps and tube well water	20	0.50 - 22.00	4.42	***Mittal et al. 2016***
Karbala, Iran	Well Water	6	2.16 - 4.11	2.84	***Al-Alawy and Hasan 2018***
Jazan, Saudi Arabia	Ground and drinking water	110	1.65 - 3.82	2.00	***El-Araby et al. 2019***
Adıyaman, Turkey	Natural and domestic drinking water	16	0.39 - 0.71	0.49	***Aydin and Sogut 2019***

Table 6.3 (previous chapter) provides a comprehensive view of worldwide radon activity measurements in water, mainly used for drinking purposes. To have a more comprehensive view few more are presented in **Table 7.3.** When the results of this area are compared with other reported values presented in **Table 7.3 and Table 6.3**, it is clear that average radon activity in groundwater of Garhwal Himalaya and Covilhã's county is greater than the present study (***Prasad et al. 2008; Inacio et al. 2017***)**.** Also the average radon activity level of the present study is comparable with an earlier

investigation performed by our group in geothermal area of West Bengal and Jharkhand (***Naskar et al. 2018***) and also with the reported average radon level by the investigator of Jaduguda uranium mines (***Shety et al. 2015***)**.** However, the highest activity in Susunia Hill region is much higher than that of the previous study in Bakreswar and Tantloi area and also very high even in the context of global scenario.

7.4.2 Annual effective dose due to ^{222}Rn in water

The estimated radon dose values for the water samples are calculated using relation **6.1** to **6.3**, considering indoor occupancy time and annual water intake as discussed in **Section 7.3.3** and are presented in **Table 7.4**.

Table 7.4 Estimated annual effective dose values for the water samples

Sample Id	Annual effective dose (μSv/y)				
	Inhalation Dose	Ingestion Dose		Total Dose	
		for 60 l/y	for 3 l/d	for 60 l/y	for 3 l/d
TW - 1	199.12	21.22	387.16	220.33	586.27
TW - 2	32.98	3.52	64.12	36.49	97.1
TW - 3	32.21	3.44	62.63	35.64	94.83
TW - 4	269.16	28.68	523.37	297.84	792.53
TW - 5	33.37	3.56	64.89	36.93	98.26
TW - 6	5.33	0.57	10.35	5.89	15.67
TW - 7	82.31	8.77	160.05	91.08	242.36
TW - 8	8.72	0.93	16.94	9.65	25.66
TW - 9	8.72	0.93	16.94	9.65	25.66
TW - 10	386.28	41.16	751.10	427.44	1137.37
TW - 11	527.66	56.22	1026	583.88	1553.66
TW - 12	506.91	54.01	985.65	560.91	1492.55
TW - 13	1537.82	163.85	2990.2	1701.66	4528.01
TW - 14	21.88	2.34	42.55	24.21	64.42
TW - 15	279.51	29.79	543.49	309.29	823
TW - 16	298.63	31.82	580.67	330.45	879.29
TW - 17	679.76	72.43	1321.76	752.19	2001.52
TW - 18	23.74	2.53	46.15	26.26	69.88
TW - 19	191.43	20.40	372.22	211.82	563.64
TW - 20	9.47	1.01	18.40	10.47	27.86
TW - 21	944.63	100.65	1836.77	1045.27	2781.39
TW - 22	354.1	37.73	688.51	391.82	1042.6
TW - 23	182.91	19.49	355.66	202.4	538.57
TW - 24	658.18	70.13	1279.79	728.31	1937.97
TW - 25	1340.92	142.87	2607.33	1483.78	3948.24
TW - 26	6333.81	674.84	12315.7	7008.65	18649.6
TW - 27	36.29	3.87	70.56	40.16	106.85
TW - 28	38.08	4.06	74.05	42.14	112.13
TW - 29	35.84	3.82	69.68	39.66	105.51

TW - 30	98.55	10.5	191.63	109.05	290.18
TW - 31	1076.57	114.71	2093.32	1191.27	3169.88
TW - 32	20.23	2.16	39.33	22.38	59.55
TW - 33	228.23	24.32	443.77	252.54	671.99
TW - 34	33.35	3.56	64.85	36.91	98.2
TW - 35	105.97	11.29	206.04	117.26	312
TW - 36	432.78	46.11	841.51	478.89	1274.28
TW - 37	252.71	26.93	491.37	279.63	744.07
TW - 38	41.77	4.45	81.22	46.22	122.98
TW - 39	59.33	6.33	115.36	65.65	174.69
TW - 40	309.53	32.98	601.86	342.51	911.39
TW - 41	104.01	11.09	202.25	115.1	306.26
TW - 42	334.29	35.62	650.00	369.9	984.28
TW - 43	474.48	50.56	922.60	525.04	1397.08
TW - 44	64.67	6.9	125.75	71.56	190.42
TW - 45	150.69	16.06	293.00	166.74	443.68
TW - 46	136.56	14.55	265.52	151.10	402.07
TW - 47	758.54	80.82	1474.94	839.36	2233.48
TW - 48	32.92	3.51	64.01	36.43	96.92
TW - 49	399.41	42.56	776.62	441.96	1176.03
TW - 50	144.28	15.38	280.54	159.65	424.82
TW - 51	772.89	82.35	1502.84	855.24	2275.73
TW - 52	181.81	19.38	353.51	201.18	535.32
TW - 53	284.58	30.32	553.34	314.9	837.91
TW - 54	24.92	2.66	48.45	27.57	73.36
TW - 55	203.79	21.72	396.25	225.5	600.03
TW - 56	226.45	24.13	440.32	250.58	666.77
TW - 57	157.78	16.82	306.8	174.59	464.58
TW - 58	34.3	3.66	66.69	37.95	100.99
TW - 59	738.05	78.64	1435.08	816.68	2173.13
TW - 60	275.37	29.34	535.44	304.71	810.81
TW - 61	275.37	29.34	535.44	304.71	810.81
TW - 62	440.05	46.89	855.65	486.94	1295.69
TW - 63	434.95	46.35	845.72	481.29	1280.66
TW - 64	35.86	3.82	69.72	39.68	105.57
TW - 65	330.88	35.26	643.37	366.13	974.24
TW - 66	81.47	8.68	158.4	90.15	239.86
TW - 67	38.56	4.11	74.97	42.67	113.52
TW - 68	233.77	24.91	454.54	258.67	688.3
TW - 69	305.31	32.53	593.66	337.84	898.97
TW - 70	211.2	22.51	410.66	233.7	621.85
TW - 71	62.21	6.63	120.96	68.84	183.16
TW - 72	34.52	3.68	67.11	38.19	101.62
TW - 73	173.97	18.54	338.26	192.5	512.22
TW - 74	33.79	3.6	65.69	37.39	99.48

TW - 75	187.31	19.96	364.21	207.27	551.51
TW - 76	67.83	7.23	131.88	75.05	199.7
TW - 77	281.4	29.99	547.17	311.39	828.57
TW - 78	105.2	11.21	204.55	116.4	309.74
TW - 79	79.71	8.5	154.99	88.2	234.7
TW - 80	39.52	4.22	76.85	43.73	116.37
TW - 81	43.6	4.65	84.78	48.25	128.38
TW - 82	268.69	28.63	522.45	297.32	791.14
TW - 83	123.41	13.15	239.96	136.56	363.36
TW - 84	161.39	17.2	313.81	178.59	475.2
TW - 85	125.91	13.42	244.83	139.33	370.73
TW - 86	20.19	2.16	39.25	22.34	59.43
TW - 87	31.19	3.33	60.64	34.51	91.82
TW - 88	35.05	3.74	68.15	38.78	103.19
TW - 89	76.95	8.2	149.63	85.15	226.57
TW - 90	23.28	2.49	45.27	25.76	68.54
TW - 91	197.1	21	383.25	218.1	580.35
TW - 92	268.53	28.62	522.14	297.14	790.67
TW - 93	102.73	10.95	199.75	113.68	302.48
TW - 94	24.41	2.6	47.45	27.01	71.85
TW - 95	40.75	4.35	79.22	45.09	119.96
TW - 96	552.57	58.88	1074.45	611.45	1627.02
TW - 97	16.34	1.75	31.78	18.09	48.12
TW - 98	82.89	8.84	161.16	91.72	244.04
TW - 99	293.96	31.32	571.58	325.28	865.54
TW - 100	23.44	2.5	45.57	25.94	69.01
TW - 101	458.03	48.8	890.6	506.83	1348.62
TW - 102	213.86	22.79	415.83	236.64	629.68
TW - 103	336.63	35.87	654.56	372.5	991.18
TW - 104	68.83	7.34	133.84	76.17	202.66
TW - 105	36.57	3.9	71.1	40.46	107.66
TW - 106	89.35	9.52	173.73	98.87	263.08
TW - 107	25.31	2.7	49.21	28.01	74.52
TW - 108	24.6	2.63	47.83	27.22	72.43
TW - 109	232.78	24.81	452.62	257.58	685.4
TW - 110	227.36	24.23	442.08	251.58	669.44
TW - 111	226.3	24.12	440.01	250.41	666.3
TW - 112	237.31	25.29	461.44	262.6	698.75
TW - 113	244.92	26.1	476.23	271.02	721.15
TW - 114	202.7	21.6	394.14	224.3	596.84
TW - 115	4393.32	468.09	8542.57	4861.41	12935.9
TW - 116	403.94	43.04	785.44	446.98	1189.37
TW - 117	256.63	27.35	499	283.97	755.62
TW - 118	301.29	32.11	585.84	333.39	887.13
TW - 119	20.44	2.18	39.75	22.62	60.19

TW - 120	394.2	42	766.5	436.2	1160.7
TW - 121	251.86	26.84	489.72	278.69	741.58
TW - 122	133.3	14.21	259.2	147.51	392.5
TW - 123	12.74	1.36	24.76	14.09	37.5
TW - 124	173.28	18.47	336.92	191.74	510.19
TW - 125	40.73	4.34	79.18	45.06	119.91
TW - 126	133.21	14.2	259.01	147.4	392.21
TW - 127	108.41	11.55	210.79	119.96	319.2
TW - 128	795.74	84.79	1547.26	880.52	2342.99
TW - 129	500.56	53.34	973.31	553.89	1473.86
TW - 130	98.95	10.55	192.4	109.49	291.34
TW - 131	121.5	12.95	236.24	134.44	357.73
TW - 132	65.52	6.99	127.4	72.5	192.91
TW - 133	128.36	13.68	249.58	142.03	377.93
TW - 134	93.59	9.98	181.97	103.56	275.56
TW - 135	17.41	1.86	33.85	19.26	51.25
TW - 136	497.39	53	967.14	550.38	1464.52
TW - 137	1089.69	116.11	2118.84	1205.79	3208.53
TW - 138	254.2	27.09	494.28	281.29	748.48
TW - 139	124.81	13.3	242.68	138.11	367.48
TW - 140	105.99	11.3	206.08	117.28	312.06
TW - 141	489.29	52.14	951.38	541.42	1440.67
TW - 142	249.97	26.64	486.04	276.6	736
TW - 143	35.8	3.82	69.6	39.61	105.4
TW - 144	181.08	19.3	352.1	200.37	533.17
TW - 145	789.23	84.09	1534.61	873.32	2323.84
TW - 146	756.1	80.56	1470.19	836.66	2226.29
TW - 147	88.7	9.45	172.47	98.15	261.16
TW - 148	110.3	11.76	214.47	122.05	324.77
TW - 149	45.79	4.88	89.03	50.67	134.82
TW - 150	73.35	7.82	142.61	81.16	215.95
TW - 151	56.08	5.98	109.04	62.05	165.11
TW - 152	400.69	42.7	779.11	443.38	1179.8
TW - 153	146.21	15.58	284.3	161.79	430.51
TW - 154	160.29	17.08	311.66	177.36	471.95
TW - 155	117.81	12.56	229.07	130.36	346.88
TW - 156	172.29	18.36	335	190.65	507.29
TW - 157	197.1	21	383.25	218.1	580.35
TW - 158	108.82	11.6	211.6	120.42	320.42
TW - 159	282.19	30.07	548.7	312.26	830.89
TW - 160	44.53	4.75	86.58	49.27	131.11
TW - 161	222.29	23.69	432.23	245.98	654.52
TW - 162	11.46	1.23	22.27	12.68	33.72
TW - 163	77.11	8.22	149.93	85.33	227.04
TW - 164	468.97	49.97	911.87	518.93	1380.83

TW - 165	302.4	32.22	587.99	334.61	890.38
TW - 166	125.5	13.38	244.02	138.87	369.51
TW - 167	40.35	4.3	78.46	44.65	118.8
TW - 168	558.11	59.47	1085.22	617.58	1643.32
TW - 169	1890.29	201.41	3675.56	2091.69	5565.85
TW - 170	116.98	12.47	227.46	129.45	344.44
TW - 171	47.09	5.02	91.56	52.11	138.65
TW - 172	88.86	9.47	172.77	98.32	261.63
TW - 173	105.04	11.2	204.24	116.23	309.27
TW - 174	804.88	85.76	1565.04	890.64	2369.92
TW - 175	158.26	16.87	307.72	175.12	465.97
TW - 176	175.64	18.72	341.52	194.35	517.15
TW - 177	56.99	6.08	110.8	63.06	167.78
TW - 178	358.41	38.19	696.91	396.6	1055.31
TW - 179	74.21	7.91	144.3	82.12	218.51
TW - 180	242.85	25.88	472.21	268.73	715.05
TW - 181	27.76	2.96	53.97	30.71	81.72
TW - 182	79.14	8.44	153.88	87.57	233.02
TW - 183	115.82	12.34	225.2	128.16	341.02
TW - 184	176.13	18.77	342.48	194.9	518.61
TW - 185	41.34	4.41	80.37	45.74	121.7
TW - 186	119.03	12.69	231.45	131.72	350.48
TW - 187	187.49	19.98	364.55	207.46	552.03
TW - 188	29.57	3.15	57.49	32.72	87.06
TW - 189	160.76	17.13	312.58	177.89	473.34
TW - 190	86.49	9.22	168.18	95.71	254.66
TW - 191	99.91	10.65	194.27	110.56	294.18
TW - 192	228.42	24.34	444.15	252.76	672.57
TW - 193	103.48	11.03	201.21	114.51	304.69
TW - 194	69.44	7.4	135.02	76.84	204.46
TW - 195	442.57	47.16	860.55	489.73	1303.12
TW - 196	169.06	18.02	328.72	187.07	497.77
TW - 197	161.63	17.22	314.27	178.85	475.89
TW - 198	421.52	44.92	819.62	466.43	1241.14
TW - 199	69.19	7.38	134.53	76.56	203.71
TW - 200	5.13	0.55	9.97	5.68	15.09
TW - 201	390.6	41.62	759.49	432.21	1150.08
TW - 202	7.67	0.82	14.91	8.49	22.58
TW - 203	123.78	13.19	240.69	136.97	364.46
TW - 204	299.81	31.95	582.97	331.76	882.78
TW - 205	244.47	26.05	475.35	270.51	719.81
TW - 206	147.46	15.72	286.71	163.17	434.16
TW - 207	183.6	19.57	357	203.17	540.6
TW - 208	21.39	2.28	41.59	23.67	62.97
TW - 209	68.16	7.27	132.53	75.42	200.69

TW - 210	198.31	21.13	385.59	219.44	583.9
TW - 211	235.44	25.09	457.8	260.53	693.23
TW - 212	108.15	11.53	210.29	119.68	318.44
TW - 213	2135.41	227.52	4152.17	2362.92	6287.57
TW - 214	248.96	26.53	484.09	275.49	733.05
TW - 215	207.87	22.15	404.18	230.01	612.04
TW - 216	146.1	15.57	284.07	161.66	430.16
TW - 217	35.66	3.8	69.33	39.46	104.99
TW - 218	788.4	84	1533	872.4	2321.4
TW - 219	331.98	35.38	645.51	367.35	977.49
TW - 220	620.08	66.07	1205.71	686.15	1825.79
TW - 221	264.91	28.23	515.09	293.13	780
TW - 222	293.19	31.24	570.09	324.43	863.28
TW - 223	5.46	0.59	10.62	6.05	16.08
TW - 224	42.76	4.56	83.13	47.31	125.88
TW - 225	123.9	13.21	240.92	137.1	364.81
TW - 226	59.13	6.3	114.98	65.43	174.11
TW - 227	339.98	36.23	661.07	376.21	1001.05
TW - 228	60.24	6.42	117.13	66.66	177.36
TW - 229	89.02	9.49	173.08	98.5	262.09
TW - 230	232.29	24.75	451.67	257.04	683.95
TW - 231	5.7	0.61	11.08	6.31	16.78
TW - 232	115.58	12.32	224.74	127.9	340.32
TW - 233	601.95	64.14	1170.45	666.08	1772.39
TW - 234	26.28	2.8	51.09	29.08	77.37
TW - 235	43.8	4.67	85.16	48.47	128.96
TW - 236	26.44	2.82	51.4	29.25	77.83
TW - 237	51.84	5.53	100.8	57.37	152.64
TW - 238	144.72	15.42	281.39	160.13	426.1
TW - 239	46.72	4.98	90.84	51.69	137.55
TW - 240	405.05	43.16	787.58	448.2	1192.62
TW - 241	840.06	89.51	1633.45	929.57	2473.51
TW - 242	704.2	75.03	1369.28	779.23	2073.48
TW - 243	38.5	4.11	74.85	42.6	113.35
TW - 244	59.75	6.37	116.17	66.11	175.91
TW - 245	298.81	31.84	581.01	330.64	879.82
TW - 246	31.28	3.34	60.83	34.62	92.11
TW - 247	414.96	44.22	806.86	459.17	1221.82
TW - 248	81.47	8.68	158.4	90.15	239.86
TW - 249	53.26	5.68	103.56	58.94	156.82
TW - 250	141.42	15.07	274.99	156.49	416.41
TW - 251	32.13	3.43	62.47	35.56	94.6
TW - 252	345.48	36.81	671.77	382.29	1017.24
TW - 253	246.14	26.23	478.61	272.37	724.75
TW - 254	152.76	16.28	297.02	169.03	449.78

TW - 255	8.58	0.92	16.68	9.49	25.25
TW - 256	403.72	43.02	785.02	446.74	1188.74
TW - 257	480.65	51.22	934.6	531.86	1415.25
TW - 258	116.75	12.44	227	129.19	343.75
TW - 259	465.3	49.58	904.74	514.87	1370.04
TW - 260	67.47	7.19	131.19	74.66	198.66
TW - 261	249.63	26.6	485.39	276.23	735.02
TW - 262	516.27	55.01	1003.85	571.27	1520.12
TW - 263	124.71	13.29	242.49	138	367.19
TW - 264	543.88	57.95	1057.55	601.83	1601.42
TW - 265	222.85	23.75	433.31	246.59	656.15
TW - 266	142.05	15.14	276.21	157.19	418.26
TW - 267	213.96	22.8	416.02	236.75	629.97
TW - 268	217.43	23.17	422.77	240.59	640.19
TW - 269	127.77	13.62	248.43	141.38	376.19
TW - 270	75.28	8.02	146.37	83.3	221.64
TW - 271	114.54	12.21	222.71	126.74	337.25
TW - 272	150.23	16.01	292.12	166.24	442.35
TW - 273	218.67	23.3	425.18	241.97	643.85
TW - 274	743.07	79.17	1444.86	822.24	2187.92
TW - 275	29.92	3.19	58.18	33.11	88.1
TW - 276	201.68	21.49	392.15	223.16	593.82
TW - 277	300.98	32.07	585.23	333.04	886.2
TW - 278	306.14	32.62	595.27	338.76	901.4
TW - 279	317.02	33.78	616.42	350.8	933.44
TW - 280	146.51	15.61	284.87	162.12	431.38
TW - 281	82.63	8.81	160.66	91.43	243.29
TW - 282	363.48	38.73	706.76	402.2	1070.23
TW - 283	266.46	28.39	518.12	294.85	784.58
TW - 284	379.7	40.46	738.3	420.15	1117.99
TW - 285	100.88	10.75	196.15	111.63	297.03
TW - 286	301.13	32.09	585.53	333.22	886.66
TW - 287	43.37	4.62	84.32	47.99	127.68
TW - 288	86.89	9.26	168.94	96.14	255.82
TW - 289	199.08	21.21	387.09	220.29	586.16
TW - 290	193.71	20.64	376.66	214.35	570.37
TW - 291	74.51	7.94	144.87	82.45	219.38
TW - 292	894.74	95.33	1739.77	990.07	2634.5
TW - 293	78.73	8.39	153.08	87.11	231.8
TW - 294	369.06	39.33	717.6	408.38	1086.65
TW - 295	48.63	5.19	94.55	53.81	143.18
TW - 296	233.15	24.85	453.35	258	686.5
TW - 297	254.7	27.14	495.24	281.83	749.93
TW - 298	72.79	7.76	141.54	80.55	214.33
TW - 299	40.57	4.33	78.88	44.89	119.44

TW - 300	148.28	15.8	288.32	164.08	436.6
TW - 301	48.77	5.2	94.82	53.96	143.58
TW - 302	13.72	1.47	26.68	15.18	40.4
TW - 303	41.81	4.46	81.29	46.26	123.1
TW - 304	3.63	0.39	7.06	4.02	10.68
TW - 305	32.19	3.43	62.59	35.62	94.78
TW - 306	36.78	3.92	71.52	40.7	108.3
TW - 307	3.75	0.4	7.29	4.15	11.03
TW - 308	45.57	4.86	88.61	50.43	134.18
TW - 309	60.22	6.42	117.09	66.63	177.3
TW - 310	73.15	7.8	142.23	80.94	215.37
TW - 311	100.53	10.71	195.46	111.24	295.98
TW - 312	27.44	2.93	53.35	30.36	80.79
TW - 313	3.51	0.38	6.83	3.89	10.34
TW - 314	21.37	2.28	41.55	23.65	62.91
TW - 315	16.82	1.8	32.7	18.61	49.51
TW - 316	131.47	14.01	255.63	145.48	387.1

From **Table 7.4** we can see that the estimated inhalation dose due to waterborne radon varies between 3.51 - 6333.81 μS/y with an average value of 252.88 μS/y. However, inhalation dose may vary if transfer factor of radon from water to air fluctuates due to local conditions.

Considering the annual water intake of 1095 litre the estimated ingestion dose varies between 6.86 - 12315.74 μS/y with an average value of 491.71 μS/y. In case of annual water intake of 60 litre the estimated ingestion dose varies between 0.37 - 674.84 μS/y with an average value of 26.94 μS/y.

The total annual effective doses have range between 10.33 – 18649.55 μSv/y with an average value of 744.59 μSv/y considering water intake of 1095 l/y. On the other hand total annual effective doses vary between 3.90 – 7008.64 μSv/y with an average value of 279.82 μSv/y considering 60 l/y water intakes.

Such high average and standard deviation values may be attributed to the 8 samples which have extremely high dose values. Without considering these extreme values the average becomes 574.66 μSv/y with standard deviation 561.53 μSv/y (water intake 1095 l/y) and 215.96 μSv/y with standard deviation of 211.03 μSv/y (water intake 60 l/y) which still reflects high fluctuations in dose rate.

WHO and EU Council Directive have proposed that when the total annual effective dose received from drinking water exceeds the reference level of 100 μSv/y, possible remedial actions should be taken by the local regulatory system (***WHO 2011; EURATOM 2013***). According to these recommendations it has been felt that action needs to be

taken for the 269 tube-wells (about 85%) considering 1095 l/y water intake and for the 197 tube-wells (about 62%) considering 60 l/y water intake.

The results of total annual effective dose estimation affirms that if we accept the UNSCEAR recommended annual water intake of 60 litre for this study then exposure from inhalation of waterborne radon will be the main threat to the local people, on the other hand ingestion dose will be predominant if we consider 1095 l/y water intake.

7.5 Conclusions

In this study, we have reported for the first time the results of radon measurements in groundwater samples collected from 316 tube-wells in and around Susunia hill area, Bankura, West Bengal. Analysis on such large number of samples affirms the reliability of the results. The results show that the groundwater radon activity in almost 93% of the samples exceed the USEPA proposed MCL level of 11.1 Bq/l and almost 40% samples have higher activity than the reference level of 100 Bq/l recommended by WHO and EU Council Directive.

Estimation of the total annual effective dose from radon contaminated water, considering water intake of 1095 l/y per person as informed by the local people, shows that almost 85% samples exceed the reference level of 100 μSv/y prescribed by WHO and EU Council Directive. However, if we follow the UNSCEAR approach of 60 l/year per person water intake, almost 62% of the samples cause higher exposure compared to the recommended dose level. The above discussions reveal, whatever consideration we use, more than 50% of the samples cause higher dose than the recommended dose level.

Such high radon level may be attributed to the presence of faults, cracks and shear zones in the earth crust apart from rock structures and mineralization of the study area.

The study manifests that pH values of the water samples have no bearing on their radon activity. However data reveal strong correlation between radon activity and borehole depth which may be a manifestation of the fact that deeper earth crust contains greater concentration of uranium or radium bearing rocks.

For radiological safety, local people should be advised not to drink water directly from the tube wells. Deep tube-wells should be avoided as far as practicable. Boiling or even stirring are easy and effective ways of reducing radon activity in drinking water. However these should be performed outside the home premises to get rid of air radon. Moreover, they should also be asked not to store water inside their house just after collection from the tube wells.

References

Al-Alawy, I. T., & Hasan, A. A. (2018, May). Radon concentration and dose assessment in well water samples from Karbala Governorate of Iraq. In Journal of Physics: Conference Series (Vol. 1003, No. 1, p. 012117). IOP Publishing.

Aydin, M. F., & Söğüt, Ö. (2019). Measurement of radon gas activity concentrations in drinking water in the city center of Adıyaman, Turkey. Radiation Protection and Environment, 42(1 & 2), 10-14.

Biswas, A. (2014, January). Revisiting Susunia: a geomorphological perspectives. In Proceedings of the Indian History Congress (Vol. 75, pp. 1150-1155). Indian History Congress.

Chakrabarti, S., & Bhattacharya, H. N. (2013). Inferring the hydro-geochemistry of fluoride contamination in Bankura district, West Bengal: a case study. Journal of the Geological Society of India, 82, 379-391.

Charoensri, A., Siriboonprapob, S., & Sastri, N. (2015, April). Analysis of radon in shallow-well water: a case study at Phichit subdistrict in Songkhla province, Thailand. In Journal of Physics: Conference Series (Vol. 611, No. 1, p. 012025). IOP Publishing.

Council Directive 2013/51/EURATOM (2013). Laying down requirements for the protection of the health of the general public with regard to radioactive substances in water intended for human consumption. Official Journal of the European Union L (296):12-21.

Das, S. (2017). Delineation of groundwater potential zone in hard rock terrain in Gangajalghati block, Bankura district, India using remote sensing and GIS techniques. Modeling Earth Systems and Environment, 3(4), 1589-1599.

El-Araby, E. H., Soliman, H. A., & Abo-Elmagd, M. (2019). Measurement of radon levels in water and the associated health hazards in Jazan, Saudi Arabia. Journal of radiation research and applied sciences, 12(1), 31-36.

Evans, R. D. (1969). Engineers' guide to the elementary behavior of radon daughters. Health Physics, 17(2), 229-252.

Fonollosa, E., Peñalver, A., Borrull, F., & Aguilar, C. (2016). Radon in spring waters in the south of Catalonia. Journal of environmental radioactivity, 151, 275-281.

Gibbons, D., & Kalin, R. (1997). A Survey of Radon-222 in Ground Water from the Sherwood Sandstone Aquifer: Belfast and Newtownards, Northern Ireland. Groundwater Monitoring & Remediation, 17(2), 88-92.

Hopkins, K. D., & Weeks, D. L. (1990). Tests for normality and measures of skewness and kurtosis: Their place in research reporting. Educational and psychological measurement, 50(4), 717-729.

Inácio, M., Soares, S., & Almeida, P. (2017). Radon concentration assessment in water sources of public drinking of Covilhã's county, Portugal. Journal of Radiation Research and Applied Sciences, 10(2), 135-139.

Instruments G (1998). AlphaGUARD portable radon monitors user manual. Germany.

Mahapatra, S., & Chakrabarty, A. (2011). Dumortierite from Susunia Hill, Bankura District, West Bengal, India. Current Science, 100(3), 299-301.

Malakootian, M., & Nejhad, Y. S. (2017). Determination of radon concentration in drinking water of Bam villages and evaluation of the annual effective dose. International Journal of Radiation Research, 15(1), 81.

Mittal, S., Rani, A., & Mehra, R. (2016). Estimation of radon concentration in soil and groundwater samples of Northern Rajasthan, India. Journal of Radiation Research and Applied Sciences, 9(2), 125-130.

Moreno, V., Bach, J., Baixeras, C., & Font, L. (2014). Radon levels in groundwaters and natural radioactivity in soils of the volcanic region of La Garrotxa, Spain. Journal of environmental radioactivity, 128, 1-8.

Naskar, A. K., Gazi, M., Barman, C., Chowdhury, S., Mondal, M., Ghosh, D., ... & Deb, A. (2018). Estimation of underground water radon danger in Bakreswar and Tantloi Geothermal Region, India. Journal of Radioanalytical and Nuclear Chemistry, 315, 273-283.

Otton, J. K. (1992). The geology of radon. Washington: Government Printing Office.

Prasad, G., Prasad, Y., Gusain, G. S., & Ramola, R. C. (2008). Measurement of radon and thoron levels in soil, water and indoor atmosphere of Budhakedar in Garhwal Himalaya, India. Radiation Measurements, 43, S375-S379.

Press, W. H. (1992). Numerical recipes in Fortran 77: the art of scientific computing. Cambridge university press.

Przylibski, T. A. (2011). Shallow circulation groundwater–the main type of water containing hazardous radon concentration. Natural Hazards and Earth System Sciences, 11(6), 1695-1703.

Rangaswamy, D. R., Srinivasa, E., Srilatha, M. C., & Sannappa, J. (2016). Measurement of radon concentration in drinking water of Shimoga district, Karnataka, India. Journal of Radioanalytical and Nuclear Chemistry, 307, 907-916.

Ravikumar P, Somashekar RK (2018) Distribution of 222Rn in groundwater and estimation of resulting radiation dose to different age groups: a case study from Bangalore City. Journal of Human and Ecological Risk Assessment 24(1): 174-185

Sethy, N. K., Jha, V. N., Ravi, P. M., & Tripathi, R. M. (2015). Assessment of human exposure to dissolved radon in groundwater around the uranium industry of Jaduguda, Jharkhand, India. Current Science, 1855-1860.

Shilpa, G. M., Anandaram, B. N., & Mohankumari, T. L. (2017). Measurement of 222Rn concentration in drinking water in the environs of Thirthahalli taluk, Karnataka, India. Journal of Radiation Research and Applied Sciences, 10(3), 262-268.

Somlai, K., Tokonami, S., Ishikawa, T., Vancsura, P., Gáspár, M., Jobbágy, V., ... & Kovács, T. (2007). 222Rn concentrations of water in the Balaton Highland and in the southern part of Hungary, and the assessment of the resulting dose. Radiation measurements, 42(3), 491-495.

Standard, I. (1893). Criteria for earthquake resistant design of structures. Bureau of Indian Standards, Part, 1.

UNSCEAR (2000). United Nations Scientific Committee on the effects of atomic radiations. The General Assembly with Scientific Annex, New York.

USEPA (1991). United States Environmental Protection Agency. National primary drinking water regulations; radionuclides; proposed rules. Federal Register, 56(138), 33050.

Wanty, R. B., & Gundersen, L. C. (1988). Groundwater geochemistry and radon-222 distribution in two sites on the Reading Prong, Eastern Pennsylvania. Missouri Dept Natural Resour Special Pub, 4, 147-156.

Weisstein, E. W. (2006). Correlation coefficient. https://mathworld. wolfram. com/.

WHO (2011). Guidelines for drinking-water quality. World Health Organization 216: 303-304

World Health Organization. (2009). WHO handbook on indoor radon: a public health perspective. World Health Organization.

Zhuo, W., Iida, T., & Yang, X. (2001). Occurrence of 222Rn, 226Ra, 228Ra and U in groundwater in Fujian Province, China. Journal of environmental radioactivity, 53(1), 111-120.

Chapter – 8

Seasonal Variation of ^{222}Rn Concentration in Tube-well Water of Bankura District of West Bengal, India

8.1 Introduction

It has been discussed that radon in water can pose serious threat to human health which necessitates radon monitoring in water used for drinking as well as for other household activities. Radon concentration does not remain constant throughout the year. It has been reported that water radon concentrations may change as season changes. Similar studies have been done by Prasad et al. (***2009***), Smetanová et al. (***2010***) and Divya and Prakash (***2018***).

8.1.1 Objectives of the study

In our previous study (discussed in **Chapter 7)**, we observed that in Susunia hill and adjacent areas of the Bankura district local people mainly depend upon the tube well for their drinking water and also for other household activities. But radon levels of these tube-wells are generally very high compared to the worldwide water radon measurement studies (***Xinwei 2006; Rangaswamy et al. 2016; Inacio et al. 2017; Naskar et al. 2022***). It has been noticed that elevated radon levels in tube-well water could pose serious threats to the locals (***Xinwei 2006; Rangaswamy et al. 2016; Inacio et al. 2017***). Therefore, it is very important to know the variation of radon concentration in water with seasonal change and to identify the seasons when the radon level is maximum and minimum. The knowledge will help the local people to take remedial measures accordingly. In this area, no such survey has been carried out till now. Hence, this study aims to investigate the radon level in tube-well water of this area during the periods of winter, summer and monsoon separately in search of seasonal variation of radon in water.

8.1.2 Choice of tube-wells for the present study

For seasonal variation study we have chosen few tube-wells from the previous study (***Naskar et al. 2022***). Tube-wells are selected in such a way that the total set contain low, medium and high radon contaminated samples.

8.2 Study Area

Details about the geology of the study area is discussed in **Chapter 7.2**. The climate of this area is tropical with three prominent seasons; those are separated as - the very cold and dry winter, the very hot and humid summer and the monsoon with medium rainfall. The winter spreads over the month of November to February and the lowest temperature is met during the month of January. It is evident that a hot summer with high humidity and low rainfall is attained from the month of March to June. The monsoon starts at end of June and lasts up to mid of October. Therefore every year rainy season stays for a long period with moderate rainfall.

Hot summer with a lack of rainfall and dry winter with almost no rainfall causes serious water scarcity in this region (***Das and Mondal 2016, Goswami and Ghosal 2022***). In every year during summer all surface-water sources like ponds, lakes and rain-fed small rivers are dried up (***Das 2017***). Therefore, local people fully depend on these tube wells for drinking water as well as for other household activities and also for farming their agricultural lands (***Das 2017; Naskar et al. 2022***).

8.3 Sample Collection

In this recent study we have chosen a total of 90 tube-wells from our previous work (**Chapter 7)** in such a way that they may be equally divided into three categories namely Set-I, Set-II and Set- III considering their water radon concentration i.e. low (< 100 Bq/L), medium (100 - 300 Bq/L) and high (> 300 Bq/L) respectively. All these tube wells are identified according to their previously recorded corresponding latitudes and longitudes using a global position system (GPS) meter (**Chapter 7)**. Studies have been performed on these identified tube wells only.

The locations (obtained by GPS meter) of the groundwater sampling sites around the study area are presented in **Table 8.1**.

Table 8.1 Location of the tube-wells

Sample No	Latitude (°N)	Longitude (°E)	Sample No	Latitude (°N)	Longitude (°E)
1	23.40517	86.94349	46	23.45792	86.95280
2	23.39280	86.93534	47	23.42789	87.16194
3	23.46643	87.12068	48	23.35645	86.96225
4	23.41710	87.03909	49	23.42801	87.15744
5	23.39403	87.24086	50	23.41401	87.15855
6	23.47174	87.22620	51	23.42750	86.89004
7	23.41297	86.93302	52	23.44292	87.00939
8	23.39766	87.03037	53	23.49708	86.92174
9	23.52867	86.96042	54	23.43068	86.89050
10	23.46107	87.21525	55	23.38311	87.0399
11	23.38493	87.03901	56	23.42677	87.16639
12	23.40821	86.94158	57	23.39752	86.97184
13	23.40238	87.01670	58	23.42888	87.15787
14	23.41709	86.90643	59	23.37190	86.90646
15	23.36945	86.96746	60	23.36503	86.96809
16	23.51963	87.05121	61	23.37023	87.11264
17	23.38481	86.97123	62	23.39612	86.89917
18	23.41171	86.93723	63	23.44780	87.12791
19	23.44880	87.18330	64	23.41396	86.92056
20	23.36570	87.22727	65	23.43358	87.18879
21	23.37955	86.99508	66	23.43651	86.89520
22	23.44014	86.99403	67	23.35511	86.91566

23	23.39306	87.03553
24	23.44907	87.01802
25	23.54160	86.92612
26	23.47531	87.04370
27	23.39257	86.93714
28	23.41477	86.92941
29	23.40240	86.89696
30	23.31865	87.03404
31	23.43184	87.15299
32	23.41891	86.89352
33	23.46927	87.03709
34	23.44133	87.05537
35	23.40549	87.20191
36	23.39294	87.14842
37	23.41806	86.90889
38	23.35735	86.94604
39	23.30093	86.98986
40	23.39458	86.97518
41	23.47717	87.04629
42	23.36111	87.12373
43	23.35483	86.96360
44	23.38698	87.13824
45	23.41400	86.91474

68	23.33385	87.07573
69	23.30041	86.97611
70	23.3166	86.97688
71	23.37066	86.96796
72	23.43315	87.0179
73	23.38891	87.12479
74	23.39547	86.89795
75	23.38820	87.22674
76	23.39572	86.89818
77	23.35331	87.10367
78	23.42065	86.91336
79	23.46987	87.07581
80	23.38647	86.90330
81	23.44086	87.21250
82	23.39699	86.97249
83	23.29709	87.01423
84	23.43645	86.89188
85	23.30724	87.02014
86	23.44078	87.06535
87	23.38318	86.90109
88	23.42894	86.88852
89	23.38269	86.90071
90	23.33871	86.96189

Locations of the tube-wells in the study are shown in **Fig. 8.1**.

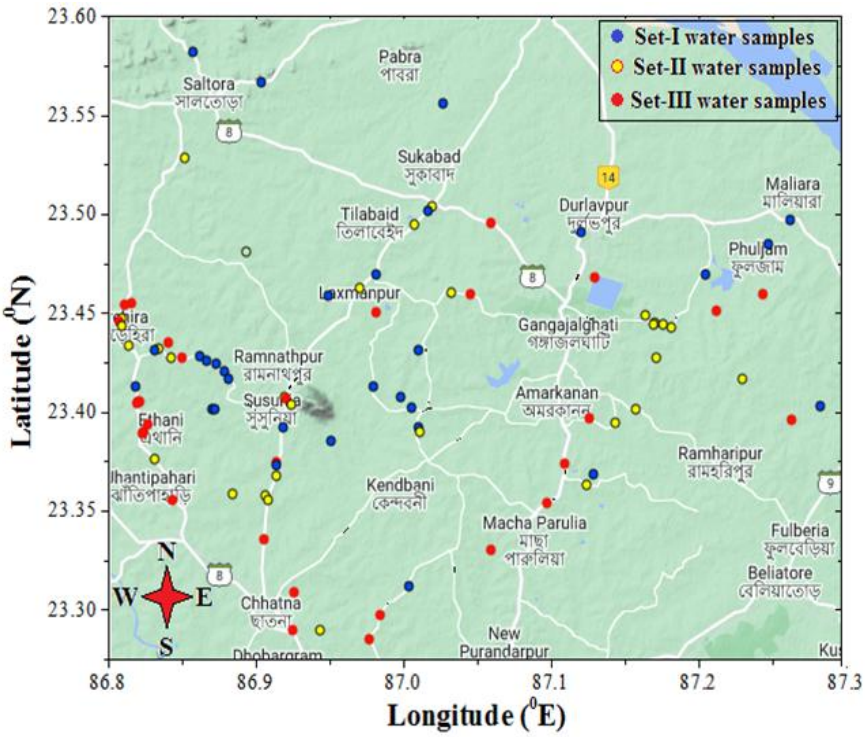

Fig.8.1 Tube-well water sample collection sites

Winter, summer and monsoon are the three prominent seasons in this region. Therefore, we have divided the entire groundwater radon concentration measurement study according to these three seasons. To analyze the seasonal variation of radon concentration in groundwater, all the samples have been collected at least once in every season (winter, summer and monsoon).

A detail discussion about the sample collection technique is given in **Chapter 6 Section 6.3**.

8.4 Measurement and analysis of seasonal variation of water radon

8.4.1 Radon concentration measurement procedure

During the radon concentration measurement process, the temperature of each water sample was recorded at the time of collection using a field thermometer. This was done by placing the samples within a container filled with the same water to ensure accuracy.

The radon concentrations of 90 selected tube-well water samples, spanning from alluvial plains to high hilly terrains in the Bankura district, were measured in winter, summer, and monsoon seasons. The measurements were conducted using the widely employed portable radon monitor, AlphaGUARD. Given that water temperature is a crucial variable that varies across seasons, it was considered during the analysis.

For further details on the measurement procedure, refer to **Chapter 4 Section 4.1.2**. The study focused on the 90 tube wells as discussed earlier, categorized into high, medium, and low radon concentration ranges. Sets I, II, and III represent samples with radon concentrations of <100 Bq/L (low), 100 - 300 Bq/L (medium), and >300 Bq/L (high), respectively.

The seasonal variation of ^{222}Rn concentration of the water samples of Set - I, Set - II and Set - III are presented in the **Table 8.2 (a, b** and **c)** respectively along with temperature.

Table 8.2(a) Seasonal variation of ^{222}Rn concentration in tube-well water sample

SET - I (< 100 Bq/l)						
Sample No	Winter		Summer		Monsoon	
	Temperature (^{0}C)	^{222}Rn concentration (Bq/l)	Temperature (^{0}C)	^{222}Rn concentration (Bq/l)	Temperature (^{0}C)	^{222}Rn concentration (Bq/l)
1	14.3	21.75 ± 0.59	40.2	15.32 ± 0.40	30.2	13.72 ± 0.75
2	8.7	35.23 ± 1.24	38.5	27.63 ± 0.81	27.6	21.12 ± 0.47
3	13.2	60.48 ± 1.89	39.4	48.61 ± 1.31	28.1	32.34 ± 1.12
4	14.7	73.29 ± 2.03	41.6	61.48 ± 2.04	29.3	52.27 ± 1.20
5	15.6	80.62 ± 2.31	37.8	67.50 ± 2.52	27.4	59.18 ± 1.32
6	6.9	26.35 ± 0.82	38.5	19.16 ± 0.68	34.2	15.52 ± 0.31
7	10.2	34.23 ± 1.45	34.6	26.18 ± 0.88	33.5	23.11 ± 0.57
8	11.3	77.45 ± 3.18	39.7	62.66 ± 2.02	33.6	55.21 ± 1.54
9	15.4	52.38 ± 2.41	42.6	41.22 ± 1.12	29.7	34.92 ± 1.23
10	13.6	48.72 ± 2.01	44.5	36.78 ± 0.96	30.7	25.33 ± 0.29

11	14.2	26.67 ± 1.14	37.6	17.07 ± 0.45	29.3	12.22 ± 0.19
12	11.2	40.12 ± 1.85	33.9	29.13 ± 0.56	30.7	19.50 ± 0. 60
13	18.5	65.43 ± 1.21	36.7	51.6 ± 1.68	29.4	46.82 ± 0.87
14	8.3	78.28 ± 2.67	38.4	69.63 ±1.85	30.4	56.53 ± 2.09
15	7.6	85.81 ± 3.61	40.2	68.42 ± 1.63	29.4	63.56 ± 1.92
16	11.6	51.30 ± 2.17	41.6	40.36 ± 1.31	27.6	35.22 ± 0.75
17	9.2	39.23 ± 1.67	37.6	32.81 ± 0.91	29.7	22.67 ± 0.79
18	10.9	82.47 ± 3.91	38.4	38.00 ± 1.23	32.6	59.95 ± 1.42
19	12.8	57.23 ± 2.65	35.9	45.37 ± 1.27	31.4	39.49 ± 1.02
20	14.6	53.75 ± 2.12	39.4	40.70 ± 0.86	34.6	33.50 ± 0.75
21	9.4	36.47 ± 0.86	37.6	23.45 ± 0.45	32.7	19.63 ± 0.42
22	7.9	50.06 ± 1.82	39.8	35.08 ± 0.71	30.6	23.15 ± 0.59
23	17.3	75.46 ± 2.37	37.9	54.63 ± 1.05	29.5	46.36 ± 0.88
24	16.1	88.42 ± 3.72	41.5	72.19 ± 1.45	34.7	56.73 ± 1.78
25	13.6	95.36 ± 2.56	39.1	83.56 ± 1.69	32.2	73.50 ± 2.15
26	12.1	41.30 ± 1.09	38.1	50.91 ± 1.23	27.6	39.55 ± 0.68
27	13.7	49.23 ± 0.95	40.2	34.10 ± .75	33.4	27.40 ± 0.33
28	15.6	92.14 ± 2.96	38.6	78.63 ± 2.54	36.5	69.45 ± 1.85
29	12.5	67.36 ± 1.69	40.9	47.52 ± 0.95	29.8	38.91 ± 0.63
30	13.9	63.98 ± 2.61	38.5	47.57 ± 1.04	30.4	35.31 ± 0.75

Table 8.2(b) Seasonal variation of ^{222}Rn concentration in tube-well water sample

SET – II (100 - 300 Bq/l)						
Sample No	**Winter**		**Summer**		**Monsoon**	
	Temperature (^{0}C)	**^{222}Rn concentration (Bq/l)**	**Temperature (^{0}C)**	**^{222}Rn concentration (Bq/l)**	**Temperature (^{0}C)**	**^{222}Rn concentration (Bq/l)**
31	12.5	127.26 ± 2.60	42.7	95.34 ± 2.84	32.2	72.69 ± 1.68
32	18.7	234.45 ± 5.63	38.5	187.45 ± 3.64	28.5	155.96 ± 3.25
33	10.2	198.47 ± 4.32	35.8	162.07 ± 3.42	27.6	145.50 ± 3.62
34	7.7	223.36 ± 4.96	42.8	189.54 ± 3.69	31.7	165.14 ± 4.28
35	9.6	125.80 ± 3.02	36.4	89.60 ± 1.68	28.6	78.33 ± 1.68
36	6.9	221.91 ± 6.08	40.9	174.52 ± 3.21	33.7	142.67 ± 3.64
37	11.6	225.15 ± 4.95	38.1	189.50 ± 2.69	34.8	157.48 ± 3.94
38	15.2	124.38 ± 3.85	44.6	107.19 ± 1.67	29.4	73.40 ± 1.85
39	14.3	255.10 ± 7.36	35.8	185.26 ± 5.50	31.5	168.40 ± 5.21
40	17.1	156.25 ± 4.95	37.8	126.95 ± 2.69	33.6	114.80 ± 3.64
41	13.5	198.39 ± 5.78	38.4	157.56 ± 3.65	30.5	134.74 ± 3.05
42	10.8	294.18 ± 6.57	34.6	259.40 ± 6.23	33.7	220.36 ± 6.31
43	14.6	268.07 ± 5.65	40.1	221.85± 5.27	28.1	195.00 ± 4.52
44	11.2	293.54 ± 74.62	37.5	261.35 ± 6.28	26.7	230.25 ± 4.98
45	9.2	195.80 ± 5.27	41.6	191.50 ± 6.5	29.4	174.04 ± 4.5
46	14.3	291.14 ± 6.41	40.3	246.23 ± 3.67	28.6	207.00 ± 5.37
47	8.4	295.62 ± 7.87	36.7	211.54 ± 4.62	33.4	152.41 ± 3.64
48	9.7	194.30 ± 5.36	39.1	189.63 ± 6.63	32.5	168.52 ± 3.78
49	11.5	285.01 ± 6.92	37.6	217.52 ± 4.62	32.4	233.34 ± 5.43
50	12.7	226.74 ± 7.56	42.5	158.90 ± 3.24	34.7	109.20 ± 2.67
51	7.2	162.11 ± 6.30	36.8	113.70 ± 2.68	31.2	77.55 ± 1.46
52	15.3	269.22 ± 5.95	41.8	179.94 ± 3.94	37.5	150.46 ± 3.01
53	15.9	233.47 ± 7.04	38.5	184.38 ± 4.26	30.1	160.09 ± 3.67
54	14.7	258.43 ± 5.64	42.8	202.10 ± 5.39	27.8	170.44 ± 2.38
55	12.6	160.80 ± 3.56	40.2	105.61 ± 2.01	34.5	94.70 ± 1.96

56	10.8	256.45 ± 6.34	39.7	206.47 ± 4.07	36.7	177.39 ± 3.75
57	13.4	260.00 ± 7.61	41.6	181.54 ± 3.87	31.4	157.32 ± 5.23
58	16.4	159.30 ± 4.65	41.5	129.27 ± 3.21	34.1	118.64 ± 4.21
59	14.6	290.86 ± 7.51	38.6	237.53 ± 5.34	28.7	203.47 ± 6.38
60	11.7	191.05 ± 3.42	42.3	158.96 ± 3.64	33.2	129.34 ± 2.85

Table 8.2(c) Seasonal variation of ^{222}Rn concentration in tube-well water sample

SET – III (> 300 Bq/l)						
Sample No	**Winter**		**Summer**		**Monsoon**	
	Temperature (^{0}C)	**^{222}Rn concentration (Bq/l)**	**Temperature (^{0}C)**	**^{222}Rn concentration (Bq/l)**	**Temperature (^{0}C)**	**^{222}Rn concentration (Bq/l)**
61	7.2	605.70 ± 17.35	42.7	480.41 ± 7.56	31.8	445.30 ± 8.67
62	12.5	911.50 ± 25.36	37.4	790.66 ± 14.62	32.5	680.06 ± 22.23
63	14.6	3232.73 ± 85.23	40.8	2265.10 ± 50.64	27.5	1851.62 ± 46.97
64	27.8	756.95 ± 24.32	39.6	680.62 ± 17.25	30.2	512.33 ± 13.67
65	8.9	2418.95 ± 52.36	36.4	2131.80 ± 40.57	28.4	1952.86 ± 33.49
66	7.5	1048.54 ± 23.35	35.8	815.04 ± 18.24	32.1	652.16 ± 8.96
67	11.8	2856.53 ± 55.39	44.2	2262.82 ± 36.85	28.5	1851.37 ± 33.64
68	14.5	890.51 ± 24.36	40.3	810.68 ± 17.32	36.2	745.36 ± 21.87
69	16.7	677.48 ± 15.37	38.5	625.45 ± 11.72	33.5	546.71 ± 10.41
70	17.3	596.45 ± 14.62	34.8	524.00 ± 9.67	28.5	482.72 ± 9.54
71	12.6	355.70 ± 8.75	39.2	280.65 ± 5.39	34.1	180.14 ± 3.34
72	14.5	661.18 ± 13.64	42.7	530.18 ± 9.57	31.2	415.64 ± 8.07
73	17.6	382.85 ± 7.71	38.2	305.1 ± 9.19	28.7	345.39 ± 10.23
74	11.4	506.07 ± 14.25	35.6	420.00 ± 7.64	33.5	347.35 ± 7.23
75	15.2	368.91 ± 9.32	39.1	310.30 ± 6.34	32.6	287.28 ± 6.31
76	10.4	498.36 ± 16.48	37.9	455.50 ± 10.11	31.5	387.14 ± 7.92
77	12.5	406.35 ± 10.27	39.2	385.28 ± 6.54	28.6	356.47 ± 8.65
78	8.2	440 .02 ± 8.95	42.3	392.30 ± 7.56	33.4	370.50 ± 7.21
79	9.7	527.52 ± 10.68	36.7	365.18 ± 7.32	32.7	281.83 ± 5.61
80	11.3	346.47 ± 8.24	38.5	264.33 ± 5.98	37.4	217.10 ± 4.53
81	12.7	405.77 ± 9.62	36.4	390.92 ± 8.75	31.9	340.65 ± 6.76
82	15.6	511.87 ± 12.77	41.5	427.80 ± 8.37	33.5	375.14 ± 8.62
83	16.8	332.47 ± 6.54	39.2	275.19 ± 5.67	32.8	305.55 ± 8.43
84	14.9	556.8 ± 15.42	42.9	450.00 ± 10.16	26.4	407.30 ± 9.14
85	11.2	418.92 ± 13.47	36.7	361.68 ± 8.63	30.1	347.43 ± 7.08
86	9.5	348.30 ± 12.37	43.5	305.28 ± 6.47	32.5	277.21 ± 5.52
87	12.4	456.72 ± 9.64	42.6	295.87 ± 6.24	27.4	236.50 ± 7.68
88	7.8	390.18 ± 7.94	36.9	320.07 ± 6.84	33.1	290.45 ± 5.44
89	14.2	477.64 ± 11.35	39.2	345.33 ± 7.25	30.7	311.47 ± 6.83
90	16.4	396.62 ± 8.41	41.8	284.55 ± 5.62	34.2	267.12 ± 5.34

Seasonwise variations of radon concentrations in each water sample of Set - I, Set - II and Set - III have been graphically presented in **Fig. 8.2 (a, b** and **c)** respectively.

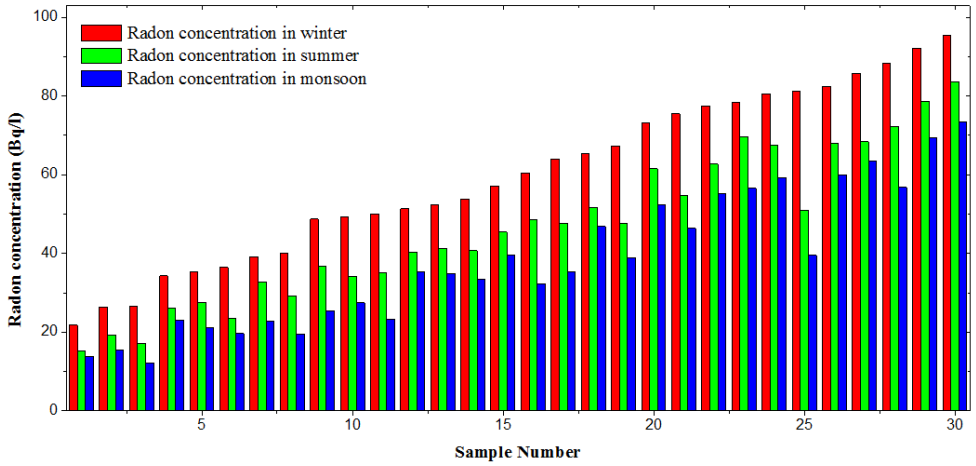

Fig. 8.2(a) Seasonal variation of radon concentration in Set – I water samples

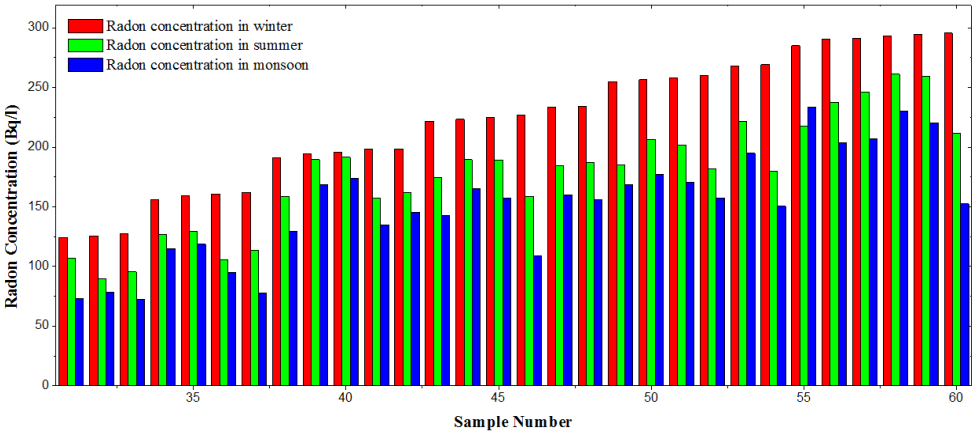

Fig. 8.2(b) Seasonal variation of radon concentration in Set – II water samples

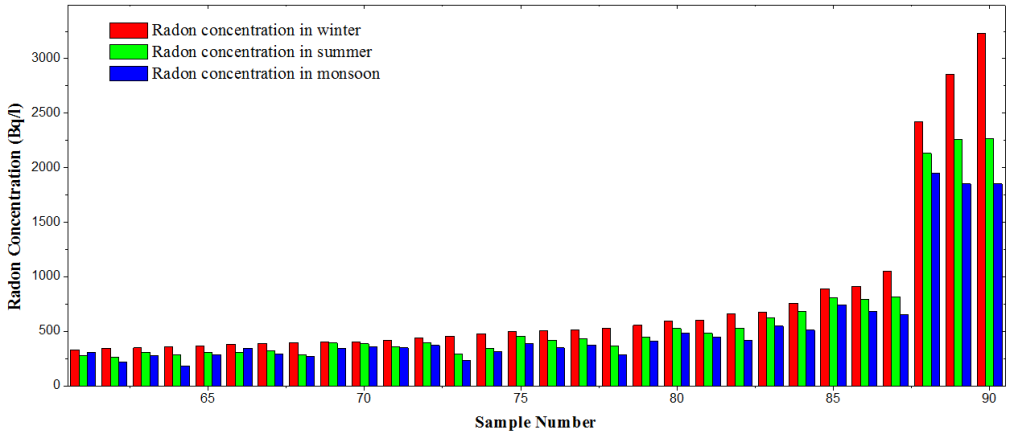

Fig.8.2(c) Seasonal variation of radon concentration in Set - III samples

Fig. 8.2 (**a, b** and **c**) clearly show that each sample of all sets exhibits the highest value in winter and decreases to the lowest in the rainy season.

The summary of seasonal variation in ^{222}Rn concentration of the water samples of Set - I, Set – II and Set - III is presented in **Table 8.3**.

Table 8.3 Summary of seasonal variation of ^{222}Rn concentration in tube-wells water

	Radon concentration in Monsoon (Bq/l)			Radon concentration in Summer (Bq/l)			Radon concentration in Winter (Bq/l)		
	Min.	Max.	Avg.	Min.	Max.	Avg.	Min.	Max.	Avg.
Set -I	12.2 ± 0.2	74 ± 2	38 ± 3	15.3 ± 0.4	84 ± 2	47 ± 3	21.8 ± 0.6	95 ± 3	59 ± 4
Set -I	73 ± 2	233 ± 5	151 ± 8	90 ± 2	261 ± 6	178 ± 9	124 ± 4	296 ± 7	223 ± 10
Set -III	180 ± 3	1953 ± 34	532 ± 28	264 ± 6	2265 ± 51	618 ± 32	333 ± 6	3233 ± 85	760 ± 36

To compare the variation of radon concentration in water samples with season for all the data sets, we have tabulated the average concentrations of Set - I, Set - II and Set - III for monsoon, summer and winter in **Table 8.4**.

Table 8.4 Comparison of season wise average radon concentration

	Monsoon	Summer		Winter	
	Avg. ^{222}Rn conc. (Bq/l)	Avg. ^{222}Rn conc. (Bq/l)	> Monsoon by %	Avg. ^{222}Rn conc. (Bq/l)	> Monsoon by %
Set - I	38 ± 3	47 ± 4	24	59 ± 4	55
Set - II	151 ± 8	178 ± 9	18	223 ± 10	48
Set - III	532 ± 28	618 ± 32	16	760 ± 36	43

Table 8.4 reveals that the average radon concentration values of summer and winter are greater than the monsoon average value by 24% and 55% respectively for Set – I, by 18% and 48% respectively for Set – II and by 16% and 43% respectively for Set - III. It is evident that radon concentration changes drastically in winter w.r.t to monsoon for all three sets.

To know the spatial distribution of radon concentration of all the samples in monsoon, summer and winter, 3D surface plots have been shown in **Fig. 8.3 (a, b** and **c)** respectively.

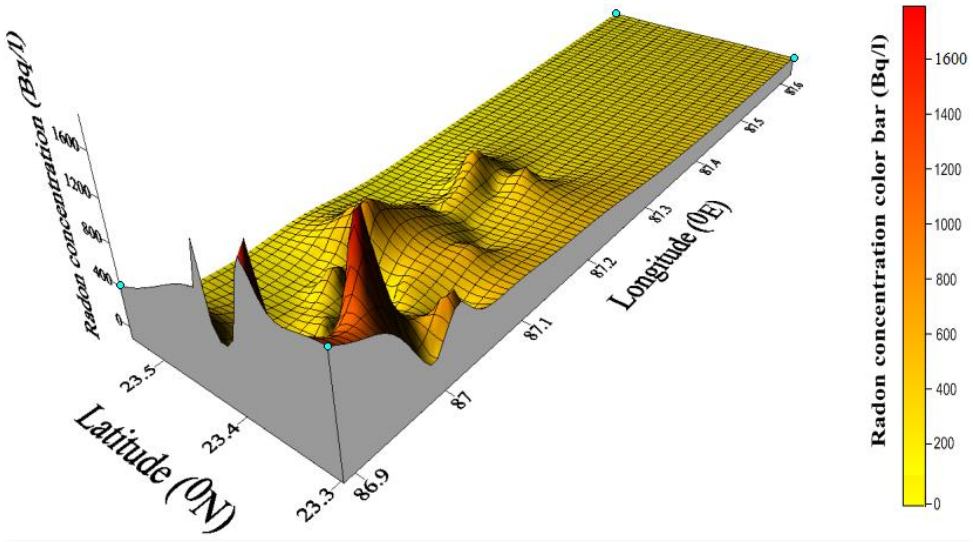

Fig. 8.3(a) 3D surface plot of the samples in monsoon

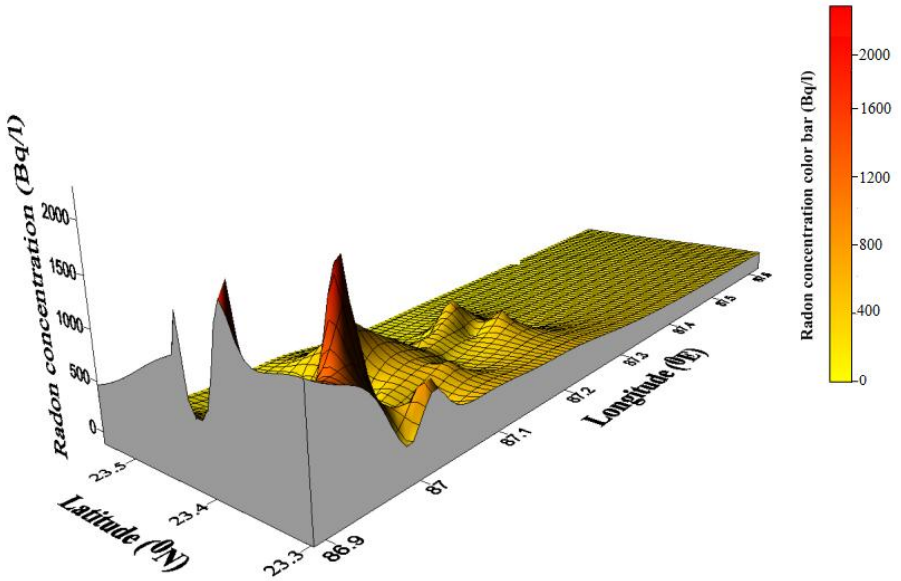

Fig. 8.3(b) 3D surface plot of the samples in summer

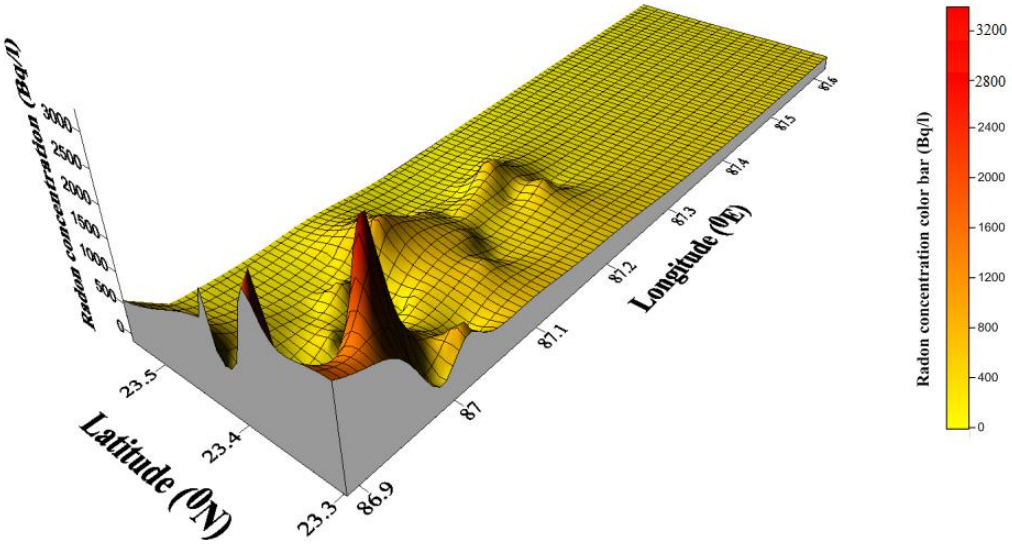

Fig. 8.3(c) 3D surface plot of the samples in winter

Summary of the season-wise variation of daily average temperature in all water samples are tabulated in **Table 8.5**.

Table 8.5 Summary of the temperature of the water samples

	Daily average temperature of the water samples (^{0}C)								
	Winter			Monsoon			Summer		
	Minimum	Maximum	Average	Minimum	Maximum	Average	Maximum	Average	Minimum
Set - I	5.2	14.1	11.4	24.7	33.5	27.4	37.6	45.6	41.5
Set - II	6.4	14.6	10.9	25.4	33.4	27.6	37.8	44.2	41.4
Set - III	5.7	14.5	11.6	24.4	34.5	28.9	36.9	44.5	40.9

From **Table 8.5** we can observe that the daily average temperature differences between the seasons for the samples of three sets are quite prominent.

The elevated concentration of radon in winter can be attributed to two primary factors. Firstly, the substantial decrease in temperature during winter leads to an increase in the water solubility of radon, resulting in higher concentrations in water samples (***Weigel 1978; Schubert et al. 2012***). Additionally, the extended period of no rainfall reduces water levels in tube wells, causing the extraction of drinking water from deeper aquifer layers where radon concentration tends to be relatively high (***Choubey et al. 2003; Prasad et al. 2008; Divya and Prakash 2018; Naskar et al. 2022***).

Conversely, in summer, the higher temperatures reduce the solubility of radon in water, although the lowered water levels in tube wells contribute to increased radon concentrations in water samples (***Schubert et al. 2012; Divya and Prakash 2018***). Furthermore, the elevated degree of rock weathering in summer, facilitated by high temperatures, results in weathered rock pieces with larger surface areas, enhancing radon concentration in water as it passes through these rocks (***Naskar et al. 2022***). Collectively, these factors contribute to higher radon concentrations in water samples during summer compared to the rainy season.

During the monsoon, heavy rainfall raises the water column level in tube wells, particularly in wells near lineaments. The considerable rise in groundwater level during the monsoon allows rainwater to easily mix with groundwater through soil pores and lineaments, significantly reducing radon concentration levels in tube well water (***Nag and Ghosh 2013; Kiliari et al. 2010***).

Our seasonal variation analysis reveals that radon concentration in all water samples is highest in winter, decreases in summer, and reaches its lowest point during the monsoon.

8.5 Evaluation of water radon dose to the locals

As all the samples show seasonal variation, it is imperative to estimate the season-wise monthly radon dose to aware the public. Generally, annual effective doses are calculated to measure the radon related hazards. But in this work, we are focusing on the seasonal variation of radon in water. So, monthly effective radon dose of the water samples has been estimated following the UNSCEAR proposed approaches (***UNSCEAR 2000***).

Monthly Inhalation Dose

Monthly inhalation dose from water-borne air radon has been obtained by the following relation (***UNSCEAR 2000***):

$$D_{Inhalation} = C_{Rn} \times DCF \times T \times F \times I \quad (8.1)$$

Where; $D_{Inhalation}$ = Monthly inhalation dose of indoor radon (μSv/month), C_{Rn} = ^{222}Rn concentration in water sample (kBq/m^3), DCF = The dose coefficient factor for inhalation of water-borne radon (6.7×10^{-6} mSv/h/Bq/m^3, ***ICRP 2017***), T = The transfer factor of radon in indoor air from water (10^{-4}, ***Nazaroff 1985; USNRC 1999; UNSCEAR 2000***), F = The indoor radon equilibrium factor (0.4, ***UNSCEAR 2000***), I = Average monthly indoor occupancy time (hr/month).

The local people mainly depend on agricultural work for their livelihood and every day spend almost 9 hours on the farmland (***Naskar et al. 2022***). According to this consideration, we have taken the average monthly indoor occupancy time of (15 × 365)/12 = 456.25 hours/month for inhalation dose calculation.

Monthly Ingestion Dose

Estimation of monthly ingestion dose from water sample has been carried out by the following relation (***UNSCEAR 2000***):

$$\boldsymbol{D_{Ingestion} = C_{RnW} \times C_W \times EDC} \quad (8.2)$$

Where; $D_{Ingestion}$ = Monthly ingestion dose from water radon (μSv/month), C_{RnW} = ^{222}Rn concentration in water sample (Bq/L), C_W = Average monthly water consumption (litre/month), EDC = The effective dose coefficient for ingestion of water radon (6.9×10^{-7} mSv/Bq, ***ICRP 2017***).

The amount of water that an individual needs for drinking depend on their age, gender, physical activity, physiological condition, illness, etc. (***USNRC 1976***). Also, the daily intake of water by the local people depends on the temperature and humidity of their living environment (***USNRC 1976***). It has been observed that daily water consumption can vary widely from place to place around the world and the people who live in a very hot and humid climate generally intake a higher amount of water (***WHO 2011***). According to these considerations many researchers have set their average daily water intake values (***Tayyeb et al. 1998; Kendall and Smith 2002; Grandjean 2005; Somlai et al. 2007; Ravikumar and Somashekhar 2018; Divya and Prakash 2018; Rani et al. 2021***). In view of these works, we have discussed with the local people of Bankura to know their overall daily water usage and the local people have informed us that the daily direct water intake amount for children and adults is in between the range of 2 - 4 litre/day. Therefore, we have taken an intermediate value for daily water intake of 3 litre/day (***Naskar et al. 2022***) and the calculated average monthly water consumption of the local people is (3×365)/12 = 91.25 litre/month.

Total monthly effective dose

The total monthly effective dose from water radon has been estimated by adding the monthly inhalation dose and the monthly ingestion dose as follows (***UNSCEAR 2000***):

$$D_{Total} = D_{Inhalation} + D_{Ingestion} \quad (8.3)$$

Monthly radon dose values of all the samples have calculated using relation 8.1-8.3. The estimated monthly radon dose values are presented in Table **8.6 (a, b** and **c)**.

Table 8.6a Estimated monthly dose values for the samples having radon activity < 100 Bq/l

Set I											
Winter				Summer				Monsoon			
Activity	Monthly Dose (μSv/month)			Activity	Monthly Dose (μSv/month)			Activity	Monthly Dose (μSv/month)		
	Ingestion	Inhalation	Total		Ingestion	Inhalation	Total		Ingestion	Inhalation	Total
21.75	6.95	3.58	10.53	15.32	4.90	2.52	7.42	13.72	4.39	2.26	6.65
35.23	11.26	5.79	17.05	27.63	8.83	4.54	13.37	21.12	6.75	3.47	10.22
60.48	19.32	9.94	29.26	48.61	15.53	7.98	23.51	32.34	10.33	5.32	15.65
73.29	23.41	12.04	35.45	61.48	19.64	10.10	29.74	52.27	16.7	8.59	25.29
80.62	25.75	13.25	39.00	67.5	21.56	11.09	32.65	59.18	18.91	9.73	28.64
26.35	8.42	4.33	12.75	19.16	6.12	3.15	9.27	15.52	4.96	2.55	7.51
34.23	10.94	5.63	16.57	26.18	8.37	4.30	12.67	23.11	7.39	3.80	11.19
77.45	24.74	12.73	37.47	62.66	20.02	10.29	30.31	55.21	17.64	9.07	26.71
52.38	16.73	8.61	25.34	41.22	13.17	6.77	19.94	34.92	11.16	5.74	16.9
48.72	15.56	8.01	23.57	36.78	11.75	6.04	17.79	25.33	8.09	4.17	12.26
26.67	8.52	4.39	12.91	17.07	5.46	2.80	8.26	12.22	3.91	2.01	5.92
40.12	12.82	6.59	19.41	29.13	9.31	4.78	14.09	19.50	6.23	3.21	9.44
65.43	20.90	10.75	31.65	51.60	16.48	8.48	24.96	46.82	14.96	7.70	22.66
78.28	25.01	12.86	37.87	69.63	22.24	11.44	33.68	56.53	18.06	9.29	27.35
85.81	27.41	14.10	41.51	68.42	21.86	11.24	33.10	63.56	20.30	10.44	30.74
51.3	16.39	8.43	24.82	40.36	12.89	6.63	19.52	35.22	11.25	5.79	17.04
39.23	12.53	6.45	18.98	32.81	10.48	5.39	15.87	22.67	7.25	3.73	10.98
82.47	26.34	13.55	39.89	68.00	21.72	11.17	32.89	59.95	19.15	9.85	29.00
57.23	18.28	9.41	27.69	45.37	14.50	7.45	21.95	39.49	12.62	6.49	19.11
53.75	17.17	8.83	26.00	40.70	13.00	6.68	19.68	33.50	10.70	5.51	16.21
36.47	11.65	6.00	17.65	23.45	7.49	3.85	11.34	19.63	6.27	3.23	9.50
50.06	15.99	8.23	24.22	35.08	11.21	5.76	16.97	23.15	7.40	3.81	11.21
75.46	24.11	12.40	36.51	54.63	17.45	8.97	26.42	46.36	14.81	7.62	22.43
88.42	28.24	14.53	42.77	72.19	23.06	11.86	34.92	56.73	18.12	9.32	27.44
95.36	30.46	15.67	46.13	83.56	26.69	13.72	40.41	73.50	23.48	12.08	35.56
81.3	25.97	13.36	39.33	50.91	16.26	8.36	24.62	39.55	12.64	6.50	19.14
49.23	15.73	8.09	23.82	34.10	10.90	5.60	16.50	27.40	8.76	4.51	13.27

92.14	29.43	15.14	44.57	78.63	25.12	12.91	38.03	69.45	22.19	11.41	33.60
67.36	21.52	11.07	32.59	47.52	15.18	7.81	22.99	38.91	12.43	6.40	18.83
63.98	20.44	10.51	30.95	47.57	15.20	7.81	23.01	35.31	11.28	5.80	17.08

Table 8.6b Estimated monthly dose values for the samples having radon activity > 100-300 Bq/l

Set II											
Winter				**Summer**				**Monsoon**			
Activity	**Monthly Dose (µSv/month)**			**Activity**	**Monthly Dose (µSv/month)**			**Activity**	**Monthly Dose (µSv/month)**		
	Ingestion	**Inhalation**	**Total**		**Ingestion**	**Inhalation**	**Total**		**Ingestion**	**Inhalation**	**Total**
127.26	40.65	20.91	61.56	95.34	30.45	15.66	46.11	72.69	23.22	11.94	35.16
234.45	74.88	38.51	113.39	187.45	59.87	30.79	90.66	155.96	49.81	25.62	75.43
198.47	63.39	32.60	95.99	162.07	51.77	26.62	78.39	145.5	46.47	23.90	70.37
223.36	71.34	36.69	108.03	189.54	60.54	31.13	91.67	165.14	52.75	27.13	79.88
125.80	40.18	20.67	60.85	89.60	28.62	14.72	43.34	78.33	25.02	12.87	37.89
221.91	70.88	36.45	107.33	174.52	55.74	28.66	84.40	142.67	45.57	23.44	69.01
225.15	71.91	36.99	108.9	189.50	60.53	31.13	91.66	157.48	50.30	25.87	76.17
124.38	39.73	20.43	60.16	107.19	34.24	17.61	51.85	73.40	23.45	12.06	35.51
255.10	81.48	41.91	123.39	185.26	59.17	30.43	89.60	168.40	53.79	27.66	81.45
156.25	49.91	25.67	75.58	126.95	40.55	20.85	61.40	114.80	36.67	18.86	55.53
198.39	63.37	32.59	95.96	157.56	50.33	25.88	76.21	134.74	43.04	22.14	65.18
294.18	93.96	48.32	142.28	259.40	82.85	42.61	125.46	220.36	70.38	36.2	106.58
268.07	85.62	44.04	129.66	221.85	70.86	36.44	107.30	195.00	62.28	32.03	94.31
293.54	93.75	48.22	141.97	261.35	83.47	42.93	126.40	230.25	73.54	37.82	111.36
195.80	62.54	32.17	94.71	191.50	61.17	31.45	92.62	174.04	55.59	28.59	84.18
291.14	92.99	47.82	140.81	246.23	78.64	40.44	119.08	207.00	66.12	34.00	100.12
295.62	94.42	48.56	142.98	211.54	67.57	34.75	102.32	152.41	48.68	25.04	73.72
194.30	62.06	31.92	93.98	189.63	60.57	31.15	91.72	168.52	53.83	27.68	81.51
285.01	91.03	46.82	137.85	247.52	79.06	40.66	119.72	233.34	74.53	38.33	112.86
226.74	72.42	37.25	109.67	158.90	50.75	26.10	76.85	109.20	34.88	17.94	52.82
162.11	51.78	26.63	78.41	113.7	36.32	18.68	55.00	77.55	24.77	12.74	37.51
269.22	85.99	44.22	130.21	179.94	57.47	29.56	87.03	150.46	48.06	24.72	72.78
233.47	74.57	38.35	112.92	184.38	58.89	30.28	89.17	160.09	51.13	26.30	77.43
258.43	82.54	42.45	124.99	202.1	64.55	33.19	97.74	170.44	54.44	28.00	82.44
160.80	51.36	26.42	77.78	105.61	33.73	17.35	51.08	94.70	30.25	15.56	45.81
256.45	81.91	42.13	124.04	206.47	65.95	33.91	99.86	177.39	56.66	29.14	85.80
260.00	83.04	42.71	125.75	181.54	57.98	29.82	87.8	157.32	50.25	25.84	76.09
159.3	50.88	26.17	77.05	129.27	41.29	21.23	62.52	118.64	37.90	19.49	57.39
290.86	92.90	47.78	140.68	237.53	75.87	39.01	114.88	203.47	64.99	33.42	98.41
191.05	61.02	31.38	92.40	158.96	50.77	26.11	76.88	129.34	41.31	21.25	62.56

Table 8.6c Estimated monthly dose values for the samples having radon activity > 300 Bq/l

Set III											
Winter				Summer				Monsoon			
Activity	Annual Dose			Activity	Annual Dose			Activity	Annual Dose		
	Ingestion	Inhalation	Total		Ingestion	Inhalation	Total		Ingestion	Inhalation	Total
605.70	193.45	99.49	292.94	480.41	153.44	78.91	232.35	445.30	142.22	73.15	215.37
911.50	291.12	149.72	440.84	790.66	252.52	129.87	382.39	680.06	217.20	111.70	328.90
3232.73	1032.46	530.98	1563.44	2265.10	723.42	372.04	1095.46	1851.62	591.37	304.13	895.50
756.95	241.76	124.33	366.09	680.62	217.38	111.79	329.17	512.33	163.63	84.16	247.79
2418.95	772.56	397.32	1169.88	2131.80	680.85	350.15	1031.00	1952.86	623.70	320.76	944.46
1048.54	334.88	172.23	507.11	815.04	260.31	133.87	394.18	652.16	208.29	107.12	315.41
2856.53	912.31	469.19	1381.50	2262.82	722.69	371.67	1094.36	1851.37	591.29	304.09	895.38
890.51	284.41	146.27	430.68	810.68	258.92	133.15	392.07	745.36	238.05	122.43	360.48
677.48	216.38	111.28	327.66	625.45	199.76	102.73	302.49	546.71	174.61	89.80	264.41
596.45	190.50	97.97	288.47	524.00	167.36	86.07	253.43	482.72	154.17	79.29	233.46
355.70	113.61	58.43	172.04	280.65	89.64	46.10	135.74	180.14	57.54	29.59	87.13
661.18	211.17	108.60	319.77	530.18	169.33	87.08	256.41	415.64	132.75	68.27	201.02
382.85	122.28	62.89	185.17	305.10	97.45	50.11	147.56	285.39	91.15	46.88	138.03
506.07	161.63	83.13	244.76	420.00	134.14	68.99	203.13	347.35	110.94	57.06	168.00
368.91	117.83	60.60	178.43	310.30	99.11	50.97	150.08	287.28	91.76	47.19	138.95
498.36	159.17	81.86	241.03	455.50	145.48	74.82	220.30	387.14	123.65	63.59	187.24
406.35	129.78	66.75	196.53	385.28	123.05	63.28	186.33	356.47	113.85	58.56	172.41
440.00	140.53	72.27	212.80	392.30	125.30	64.44	189.74	370.50	118.33	60.86	179.19
527.52	168.48	86.65	255.13	365.18	116.63	59.98	176.61	281.83	90.01	46.30	136.31
346.47	110.66	56.91	167.57	264.33	84.43	43.42	127.85	217.10	69.34	35.66	105.00
405.77	129.60	66.65	196.25	390.92	124.86	64.21	189.07	340.65	108.80	55.96	164.76
511.87	163.48	84.08	247.56	427.80	136.63	70.27	206.90	375.14	119.82	61.62	181.44
332.47	106.19	54.61	160.80	275.19	87.89	45.20	133.09	255.55	81.62	41.98	123.60
556.80	177.83	91.46	269.29	450.00	143.72	73.91	217.63	407.30	130.09	66.90	196.99
418.92	133.80	68.81	202.61	361.68	115.52	59.41	174.93	347.43	110.97	57.07	168.04
348.30	111.24	57.21	168.45	305.28	97.50	50.14	147.64	277.21	88.54	45.54	134.08
456.72	145.87	75.02	220.89	295.87	94.50	48.60	143.10	236.50	75.54	38.85	114.39
390.18	124.62	64.09	188.71	320.07	102.23	52.57	154.80	290.45	92.77	47.71	140.48
477.64	152.55	78.46	231.01	345.33	110.29	56.72	167.01	311.47	99.48	51.16	150.64
396.62	126.68	65.15	191.83	284.55	90.88	46.74	137.62	267.12	85.32	43.88	129.20

In view of the wide variation of estimated dose that are presented in **Figure 8.6 (a, b** and **c)**, a summary of the estimated dose values is presented in **Table 8.7.**

Table 8.7 Summary of the monthly radon dose

	Monthly effective radon dose (μSv/month)																	
	Monsoon						Summer						Winter					
	Inhalation		Ingestion		Total		Inhalation dose		Ingestion dose		Total effective dose		Inhalation dose		Ingestion dose		Total effective dose	
	Range	Avg.	Range	Avg.	Range	Avg.	Range	Avg.	Range	Avg.	Range	Avg.	Range	Avg.	Range	Avg.	Range	Avg.
Set I	2.01 - 12.08	6.31	3.91 - 23.48	12.27	5.92 - 35.56	18.58	2.52 - 13.73	7.66	4.90 - 26.69	14.88	7.42 - 40.42	22.54	3.58 - 15.67	9.81	6.95 - 30.46	19.07	10.53 - 46.13	28.88
Set II	11.94 - 38.33	24.85	23.22 - 74.53	48.32	35.16 - 112.86	73.17	14.72 - 42.93	29.31	28.62 - 83.47	56.99	43.34 - 126.40	86.29	20.43 - 48.56	36.56	39.73 - 94.42	71.08	60.16 - 142.98	107.64
Set II	29.59 -	87.3	57.54 - 623	169.	87.13 - 944.	257.	43.42 - 372.	101.	84.43 - 723.	197.	127.85 - 1095	299.	54.61 - 530.9	124.75	106.19 - 1032.	242.56	160.80 - 1563.	367.

I	32 0.7 6	8	.70	8 9	46	2 7	05	5 8	42	5 1	.47	0 9	8		46		44	3 1

As expected it is observed from **Table 8.7** that in winter the estimated dose values are higher than that of summer and monsoon for all three sets. For better risk assessment due to water radon, the average monthly total effective dose is converted to the equivalent total annual effective dose for Set - I, Set - II and Set - III water samples and are presented in **Table 8.8**.

Table 8.8 Season-wise average monthly total effective dose with the corresponding equivalent total annual effective dose for the three sets

	Monsoon		**Summer**		**Winter**	
	Average monthly total effective dose (μSv/month)	**Equivalent total annual effective dose (μSv/yr)**	**Average monthly total effective dose (μSv/month)**	**Equivalent total annual effective dose (μSv/yr)**	**Average monthly total effective dose (μSv/month)**	**Equivalent total annual effective dose (μSv/yr)**
Set - I	18.58	222.96	22.54	270.48	28.88	346.56
Set - II	73.17	878.04	86.29	1035.48	107.64	1291.68
Set - III	257.27	3087.24	299.09	3589.08	367.31	4407.72

From **Table 8.8** it may be concluded that the equivalent total annual effective dose of Set - I, Set - II and Set - III for all of the three seasons have exceeded the EU Commission and WHO recommended reference dose limit of 100 μSv/yr (***EU 2001, WHO 2011***).

It is clear from the analyses that local people are at risk from water radon in all seasons. The picture is more alarming for Set-III samples. The use of these tube-wells water for drinking can cause health hazards to the inhabitants of this region. Generally, in winter people keep their windows and doors closed which may enhance the indoor air radon concentration resulting higher inhalation dose and so chance of lung cancer increases. Such high radon concentration in tube-well water calls for regular radon monitoring of water sources. It is better to avoid the tube wells which contain high radon levels in the water, specifically in winter. Otherwise to overcome these conditions minimization of radon levels in drinking water should be done before direct water consumption.

8.6 Conclusions

In this paper results of seasonal variation of radon concentration measurements in water samples collected from 90 selected tube-wells having widely varying water radon concentrations and situated in different parts of the Bankura district, West Bengal has been presented.

It may be conclude that, the seasonal variation as observed by the present study may be attributed to the following reasons: In monsoon radon concentration in tube well water decreases due to the mixing of rainwater with the groundwater aquifer. Radon concentration in summer increases with respect to monsoon because of the lowering of

the groundwater level as well as due to weathering effect. In winter groundwater level also remains low with respect to monsoon but more importantly radon concentration increases drastically due to lower temperature persisting in winter which increases the solubility of radon in water. Hence, the radon concentration in monsoon is the lowest and that in winter is the highest. Maybe the wide variation of temperature and rainfall throughout the measuring period causes this drastic change in radon levels in the groundwater samples.

The estimated equivalent annual total effective doses calculated from the average monthly radon doses exceed the recommended limit of 100 μSv/yr for all seasons. The inhabitants should be made aware of the radon risk from water, especially in winter. The local authorities should be requested for taking some necessary remedial actions to reduce the radon level in tube-well water and ensure people's protection from radon risks. At least the people should be advised to avoid direct drinking from the tube wells and if possible should boil the water or stir well before drinking. Boiling or stirring should be done in an open environment to get rid of air radon.

References

Das, K., & Mondal, N. K. (2016). Dental fluorosis and urinary fluoride concentration as a reflection of fluoride exposure and its impact on IQ level and BMI of children of Laxmisagar, Simlapal Block of Bankura District, WB, India. Environmental monitoring and assessment, 188, 1-14.

Das, S. (2017). Delineation of groundwater potential zone in hard rock terrain in Gangajalghati block, Bankura district, India using remote sensing and GIS techniques. Modeling Earth Systems and Environment, 3(4), 1589-1599.

Divya, P. V., & Prakash, V. (2018). Seasonal variation of radon concentration in water and assessment of whole-body dose to the public along South-west coast of Kerala, India. Radiation Protection and Environment, 41(2), 84-87.

Goswami, T., & Ghosal, S. (2022). Understanding the suitability of two MCDM techniques in mapping the groundwater potential zones of semi-arid Bankura District in eastern India. Groundwater for Sustainable Development, 17, 100727.

Grandjean, A. C. (2005). Water requirements, impinging factors, and recommended intakes. Nutrients in drinking water, 25.

ICRP. (2017). International Commission on Radiological Protection occupational intakes of radionuclides: part 3. ICRP publication 137, Ann. ICRP 46(3-4), 297-320.

Inácio, M., Soares, S., & Almeida, P. (2017). Radon concentration assessment in water sources of public drinking of Covilhã's county, Portugal. Journal of Radiation Research and Applied Sciences, 10(2), 135-139.

Kendall, G. M., & Smith, T. J. (2002). Doses to organs and tissues from radon and its decay products. Journal of Radiological Protection, 22(4), 389.

Kiliari, T., Tsiaili, A., & Pashalidis, I. (2010). Lithological and seasonal variations in radon concentrations in Cypriot groundwaters. Journal of radioanalytical and nuclear chemistry, 284(3), 553-556.

Nag, S. K., & Ghosh, P. (2013). Delineation of groundwater potential zone in Chhatna Block, Bankura District, West Bengal, India using remote sensing and GIS techniques. Environmental earth sciences, 70, 2115-2127.

Naskar, A. K., Gazi, M., Mondal, M., & Deb, A. (2022). Water radon risk in Susunia hill area: an assessment in terms of radiation dose. Environmental Science and Pollution Research, 29(8), 11160-11171.

Nazaroff, W. W., Doyle, S. M., & Nero, A. V. (1985). Potable water as a source of airborne radon in US dwellings: a review and assessment. submitted to Health Physics.

Prasad, Y., Prasad, G., Gusain, G. S., Choubey, V. M., & Ramola, R. C. (2009). Seasonal variation on radon emission from soil and water. Indian Journal of Physics, 83, 1001-1010.

Rangaswamy, D. R., Srinivasa, E., Srilatha, M. C., & Sannappa, J. (2016). Measurement of radon concentration in drinking water of Shimoga district, Karnataka, India. Journal of Radioanalytical and Nuclear Chemistry, 307, 907-916.

Rani, S., Kansal, S., Singla, A. K., & Mehra, R. (2021). Radiological risk assessment to the public due to the presence of radon in water of Barnala district, Punjab, India. Environmental Geochemistry and Health, 43(12), 5011-5024.

Ravikumar, P., & Somashekar, R. K. (2018). Distribution of 222Rn in groundwater and estimation of resulting radiation dose to different age groups: a case study from Bangalore City. Human and Ecological Risk Assessment: An International Journal, 24(1), 174-185.

Schubert, M., Paschke, A., Lieberman, E., & Burnett, W. C. (2012). Air–water partitioning of 222Rn and its dependence on water temperature and salinity. Environmental science & technology, 46(7), 3905-3911.

Smetanová, I., Holý, K., Müllerová, M., & Polášková, A. (2010). The effect of meteorological parameters on radon concentration in borehole air and water. Journal of radioanalytical and nuclear chemistry, 283(1), 101-109.

Somlai, K., Tokonami, S., Ishikawa, T., Vancsura, P., Gáspár, M., Jobbágy, V., ... & Kovács, T. (2007). 222Rn concentrations of water in the Balaton Highland and in the southern part of Hungary, and the assessment of the resulting dose. Radiation measurements, 42(3), 491-495.

Tayyeb, Z. A., Kinsara, A. R., & Farid, S. M. (1998). A study on the radon concentrations in water in Jeddah (Saudi Arabia) and the associated health effects. Journal of environmental radioactivity, 38(1), 97-104.

UNSCEAR. (2000). United Nations Scientific Committee on the effects of atomic radiations. The General Assembly with Scientific Annex, New York.

USNRC (1976). United States Nuclear Regulatory Commission. Calculation of annual doses to man from routine releases of reactor effluents for the purpose of evaluation compliance with 10 CFR part 50, appendix I (No. REG/G--1.109 (3-76)). Nuclear Regulatory Commission.

USNRC, U. (1999). Risk assessment of radon in drinking water. Committee on risk assessment of exposure to radon in drinking water, board on radiation effects research, commission on life sciences, National Research Council.

Weigel, F. (1978). Radon. Chem. Ztg, 102(9), 287-299.

WHO, G. (2011). Guidelines for drinking-water quality. World health organization, 216, 303-304.

Xinwei, L. (2006). Analysis of radon concentration in drinking water in Baoji (China) and the associated health effects. Radiation protection dosimetry, 121(4), 452-455.

Chapter – 9

Elevated Radon Level in Drinking Water of Ajodhya Hill Area of West Bengal, India: Probable Health Impact on Lung and Stomach

9.1 Introduction

Radon gas is undetectable by our senses as it has no color, taste, or odor. The most stable isotope of radon is the natural radionuclide ^{222}Rn, which has a half-life of 3.8 days and it decays by releasing highly energetic alpha (α) particles (5.49 MeV). In the uranium (^{238}U) decay chain ^{222}Rn and its daughters are the decay products, which mainly spread out from different sources like rock, soil, and then mix with groundwater.

The availability and quality of drinking water are crucial factors for maintaining public health. The concentration of radioactive materials in groundwater varies widely depending on the bedrocks of the aquifer (***Naskar et al. 2018, 2022***). Studies have shown that the concentration of radon in groundwater is usually higher than that of surface water sources (***WHO 2009***). Thus, it is essential to consider the radon content in groundwater used for drinking purposes (***USEPA 1991; WHO 2009***). Detail discussion about radon is given in **Chapter 6 Section 6.1**.

9.1.1 Objectives of the present study

The primary purpose of the present study is to measure the radon level in drinking water at some parts of Purulia district of West Bengal, India. As radon in drinking water is big concern for public health, the annual effective doses and the Excess Lifetime Cancer Risks (ELCR) due to water radon have been estimated for all the samples.

This area is located in the Chotanagpur plateau region. The bedrocks of this area are enriched with high mineralization. Also, several fracture zones and faults have been crisscrossed this area. Therefore, the geological settings and the porous sub surface of this area enhances the chance of high radon levels in the tube-wells water.

Moreover, recently this type of research work has been done by Mitra et al. (***Mitra et al. 2021***) and they have reported high radon levels in some tube well water. They have mainly covered the eastern part of the district for water sample collection. Their findings have prompted us to carry out an exhaustive radon level measurement in drinking water over the other parts of the district including Ajodhya hill and its surrounding regions which remain unexplored so far. We have covered an area of almost 3500 km^2 around the western part of the Purulia district for water radon measurement.

We have performed such type of research work in different parts of West Bengal (***Naskar et al. 2018, 2022***) which are located in the Chotanagpur plateau region. In fact we are trying to gradually develop a radon mapping profile in drinking water of the entire Chotanagpur plateau region and to find out the possible reasons behind the elevated radon level in ground water, in this region.

9.2 Study area

Purulia district lies between (22.60 ^{0}N, 85.75 ^{0}E – 23.50 ^{0}N, 86.65 ^{0}E) with 6259 km^2 geographical area. Purulia is the western-most district of West Bengal, India. Due to the tropical location with its geographical shape as well as function like a funnel, Purulia has a national importance. It funnels not only the tropical monsoon current from the Bay of Bengal to the subtropical parts of north-west India, but also acts as a gateway between the developed industrial belts of West Bengal and the remote areas of Jharkhand. The nature of terrain and its features indicate that except hilly areas, the general height ranges between 200 – 300 m above mean sea-level. Two main hills of the district are Ajodhya (677 m) and Panchet (643 m). The map of this study area with respect to West Bengal and India is presented in **Figure 9.1**.

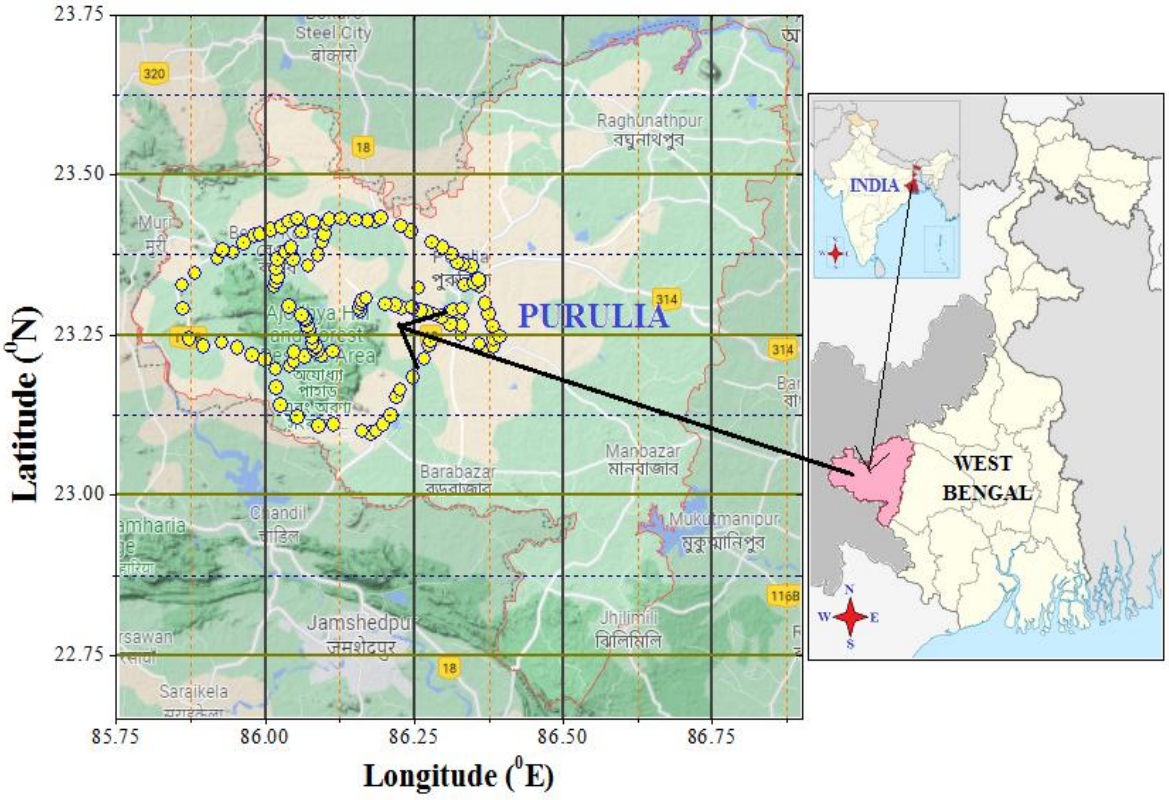

Fig. 9.1 Map of the study area

Ajodhya hill and its surrounding areas are located at the western part of Purulia district. It is the easternmost part of the Chhotanagpur Plateau and extended part of Eastern Ghats range. Seismically this area is characterized under the earthquake prone Zone II (***Bhaya and Chakrabarty 2016***).

This area consists of diverse groups of rocks that are composed in various geological ages ranging from archaean to recent time. Mainly this area is covered with the rocks like granite, granite gneiss, mica schist, sandstone, shale, limestone, quartzite and slate (***Baidya 1992; Gupta 1998***). The Chotonagpur plateau covers most parts of the study area. There are several fault lines, fracture zones present in this area (***Acharya and Nag 2013***).

Two major share zones South Purulia Share Zone (SPSZ) and North Purulia Share Zone (NPSZ) passes through the Purulia district (***Geological Quadrangle Map 73I 1948***).

Surface land of this area is almost covered with the laterite soils which originate from the granite and gneiss bed rocks (***Bhaya and Chakrabarty 2016***). Laterite soils are usually very shallow, well drained and gravelly. As a result the soil is lightly textured with high porosity and poor water holding capacity.

Climate of this region is characterized as tropical because of very hot summer, child winter and humid monsoon with moderate rainfall. Average temperature ranges between 10 - 40 °C throughout the year. Average annual rainfall varies between 1100 - 1500 mm and almost 50% of the water runs off due to the undulating topography (***Acharya and Nag 2013***). Therefore, local people mainly depend on the tube-wells water for drinking, farming and domestic uses.

A very large number of tourists from all over India come to visit Purulia annually to witness the charm of the natural scenery of Ajodhya hill with water falls, beautiful dams, traditional cultural programs and the local tribal habitations of Ajodhya and its surrounding areas.

9.3 Sample Collection

Water sample collection has been conducted within the time interval of December, 2021 - June, 2022. In this survey a total number of 120 tube-well water samples have been collected. The bore-hole depths of the selected tube wells are recorded on the basis of information obtained from local inhabitants and widely vary between 20 - 55 m. Details about water sampling procedure is discussed in **Chapter 6 Section 6.3.**

A global positioning system (GPS) meter is used to obtain the position of the tube-wells by recording the corresponding latitude and longitude. Locations of the sampling sites are presented in **Figure 9.2**. For sample collection our strategies are to i) collect as many water samples as we can at different locations in the study area while maintaining a gap of about 5 kilometers between two water sampling points and ii) while maintaining the gap, water samples are obtained from those tube wells that are used by the local people. Maintaining these two criterions we have gathered a total of 120 tube-well water samples and measured their radon concentration.

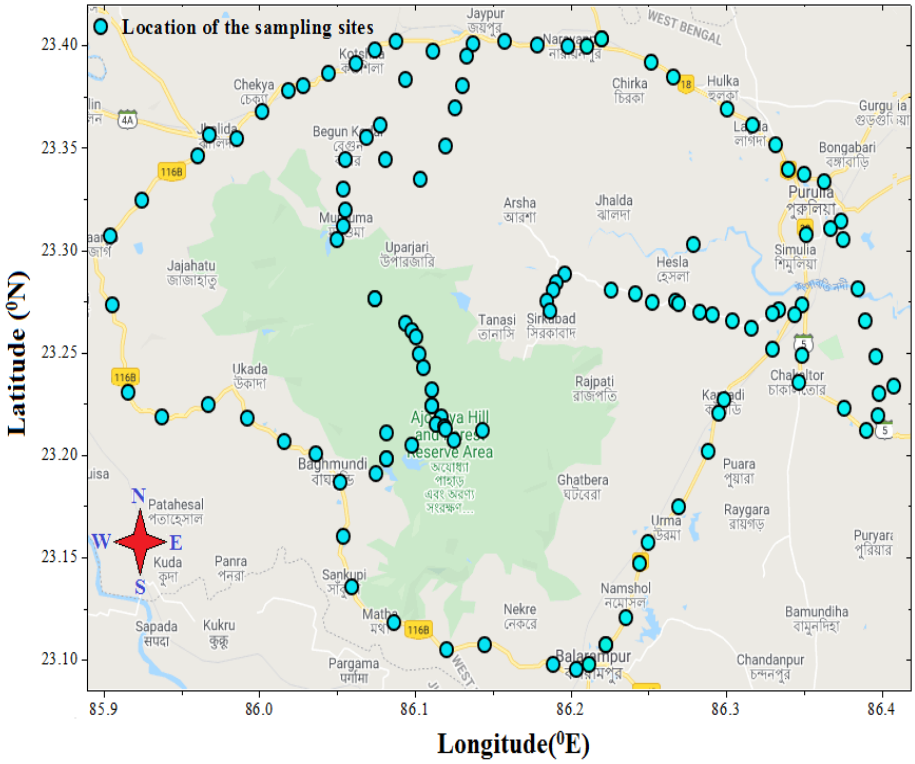

Fig. 9.2 Location of the tube-wells

9.4 Measurement and Analysis

9.4.1 Radon concentration measurement procedure

Radon concentrations of the collected samples are measured by Alpha Guard radon monitor in temporary laboratory located within the study area. Detail about radon concentration measurement procedure has discussed in **Chapter 4 Section 4.3**. Temperature and pH levels of each sample have been measured using a thermometer and a pH meter respectively by holding them within another container filled with the same tube-wells water.

9.4.2 Estimation of radon dose

Taking into account the entrance of radon gas into human body both via ingestion of water and inhalation of water-borne air radon, we have estimated the annual effective radon doses and the excess life time cancer risk values for the water samples. The dose exposures due to water-borne radon have been calculated using by the parameters given in the UNSCEAR reports (***UNSCEAR 2000***) as are discussed in **Chapter 6 Section 6.4.2**.

Annual water intake

As per the UNSCEAR (***2000***) r ecommendation, for ingestion dose estimation the annual water intake should only include direct tap water. It is difficult to obtain this estimate

for any particular population. So, we have estimated the annual effective ingestion dose by taking the UNSCEAR proposed weighted average annual water intake of 60 l/yr direct from tap. This will provide possible lowest dose due to intake of radon contaminated water.

However, many workers of this field (***Ademola and Ojeniran 2017; Mitra et al. 2021; Duggal et al. 2017, 2020***) are considering total annual water intake for estimating ingestion dose using UNSCEAR (***2000***) formula. We have also estimated ingestion dose using the total annual consumption of water of the people of the study area so that we have an idea of the least as well as highest expected radiation exposure to local people due to water borne radon. Local people of this area have informed us that on an average they take 4.5 litre of water per day. This information sounds little bit exaggerated though this area is hot, humid and most of the people are hardworking (farmers). We have no other source of information and so have to rely on the words of the local people. However, such high water intake have been reported by other researchers (***Howard et al. 2003; Ademola and Ojeniran 2017; Mitra et al. 2021***) in condition like ours.

9.4.2.1 Assessment of life time cancer risk

The Excess Life time Cancer Risk (ELCR) has also been calculated using the following relation (***UNSCEAR 2000; ICRP 2010***):

$$\boldsymbol{ELCR = D_{Total} \times L \times F_{Risk}} \tag{9.1}$$

Where; D_{Total} = total annual effective dose (μSv/yr), L = average duration of life (70 yr, ***UNSCEAR 2000; WHO 2009; ICRP 2010***), F_{Risk} = fatal cancer risk (5.5×10^{-2} Sv^{-1}, ***ICRP 2010***).

9.5 Results and discussions

9.5.1 Water radon concentration study

For this study radon concentration of 120 tube-well water samples have been measured. Results of this study are presented in **Table 9.1**.

Table 9.1 Radon concentration values of the water samples

Sample Id	Latitude (°N)	Longitude (°E)	Tube-well Depth (m)	Activity (Bq/l)	pH
TW - 1	23.31394	85.90545	31	31.05	7.0
TW - 2	23.27836	85.90658	32	116.93	6.9
TW - 3	23.23358	85.91740	32	42.39	7.1
TW - 4	23.33188	85.92586	31	166.41	6.8
TW - 5	23.22147	85.93943	33	161.94	8.0
TW - 6	23.35455	85.96270	31	23.69	7.4
TW - 7	23.22739	85.96943	33	264.56	7.2
TW - 8	23.36564	85.97032	31	16.61	7.2
TW - 9	23.36345	85.98776	30	26.72	7.1

TW - 10	23.22047	85.99502	33	138.57	7.7
TW - 11	23.37728	86.00474	30	24.78	6.8
TW - 12	23.20850	86.01859	33	151.10	7.3
TW - 13	23.38841	86.02181	30	24.91	7.5
TW - 14	23.39096	86.03106	29	25.99	7.3
TW - 15	23.20213	86.03931	33	49.62	7.5
TW - 16	23.39681	86.04793	29	43.03	7.2
TW - 17	23.31200	86.05311	27	64.17	6.9
TW - 18	2318742	86.05527	33	10.25	7.1
TW - 19	23.31902	86.05694	27	298.63	7.0
TW - 20	23.16022	86.05711	33	103.12	7.3
TW - 21	23.33815	86.05721	27	21.97	7.3
TW - 22	23.32700	86.05880	27	55.92	7.1
TW - 23	23.35281	86.05898	27	10.54	7.5
TW - 24	23.13397	86.06299	33	30.60	7.2
TW - 25	23.40190	86.06575	29	25.02	6.5
TW - 26	23.36409	86.07237	28	19.02	7.6
TW - 27	23.28157	86.07776	47	90.41	8.0
TW - 28	23.28107	86.07566	50	126.81	7.8
TW - 29	23.40934	86.07780	29	23.68	6.8
TW - 30	23.19228	86.07835	26	97.29	7.1
TW - 31	23.37044	86.08121	28	27.20	7.6
TW - 32	23.35278	86.08449	47	70.51	7.7
TW - 33	23.21318	86.08545	25	19.45	7.5
TW - 34	23.19988	86.08556	26	5.71	8.2
TW - 35	23.19983	86.08556	27	84.59	6.9
TW - 36	23.11564	86.09056	33	32.76	7.0
TW - 37	23.41353	86.09135	28	17.58	7.2
TW - 38	23.39388	86.09750	28	37.29	7.6
TW - 39	23.26879	86.09774	50	166.34	7.2
TW - 40	23.26502	86.10215	27	370.00	7.2
TW - 41	23.20652	86.10222	26	320.68	6.9
TW - 42	23.26194	86.10477	50	124.39	7.0
TW - 43	23.25332	86.10675	27	121.54	7.0
TW - 44	23.34283	86.10762	45	40.97	7.1
TW - 45	23.24618	86.10960	52	88.55	7.3
TW - 46	23.23475	86.11474	27	25.15	6.8
TW - 47	23.22684	86.11504	26	284.83	6.8
TW - 48	23.22681	86.11509	54	491.19	7.2
TW - 49	23.40843	86.11559	28	7.18	7.8
TW - 50	23.21712	86.11747	25	100.00	6.9
TW - 51	23.22133	86.12080	55	174.36	7.1
TW - 52	23.21580	86.12312	25	49.24	7.5
TW - 53	23.21486	86.12389	26	104.89	6.9
TW - 54	23.36020	86.12413	43	10.15	7.8
TW - 55	23.10165	86.12491	33	193.78	6.8
TW - 56	23.20925	86.12935	36	39.33	6.7
TW - 57	23.37968	86.13038	42	26.49	8.1
TW - 58	23.39085	86.13478	42	39.71	7.0

TW - 59	23.40597	86.13768	42	22.83	6.8
TW - 60	23.41247	86.14188	42	12.82	6.8
TW - 61	23.21451	86.14806	25	78.13	6.9
TW - 62	23.10447	86.14897	33	374.12	6.5
TW - 63	23.41372	86.16205	42	22.52	7.3
TW - 64	23.41152	86.18368	41	44.22	7.0
TW - 65	23.28021	86.18981	26	46.40	6.9
TW - 66	23.27543	86.19182	26	18.46	6.9
TW - 67	23.28619	86.19395	36	510.20	7.3
TW - 68	23.09430	86.19415	34	41.18	6.8
TW - 69	23.29023	86.19584	36	163.68	7.7
TW - 70	23.29408	86.20169	25	12.11	7.2
TW - 71	23.41120	86.20357	39	121.72	7.1
TW - 72	23.09164	86.20912	34	120.5	6.7
TW - 73	23.41090	86.21605	39	112.43	6.9
TW - 74	23.09410	86.21694	34	95.51	7
TW - 75	23.41473	86.22523	39	124.35	7.6
TW - 76	23.10409	86.22839	34	52.80	7.0
TW - 77	23.28589	86.23154	36	71.92	6.9
TW - 78	23.11806	86.24130	34	50.43	7.2
TW - 79	23.28413	86.24752	36	103.73	7.1
TW - 80	23.14577	86.25025	34	111.13	6.9
TW - 81	23.15688	86.25572	35	162.25	7.0
TW - 82	23.40282	86.25763	39	148.94	7.2
TW - 83	23.27979	86.25819	36	146.68	7.4
TW - 84	23.39530	86.27246	39	43.90	6.7
TW - 85	23.28068	86.27361	36	255.12	7.5
TW - 86	23.27946	86.27564	23	135.68	7.3
TW - 87	23.17533	86.27565	36	45.83	6.9
TW - 88	23.30969	86.28552	39	72.59	7.2
TW - 89	23.27482	86.28945	36	158.37	6.8
TW - 90	23.20341	86.29456	36	17.02	7.4
TW - 91	23.27365	86.29758	36	103.49	7.6
TW - 92	23.22285	86.30176	36	81.15	7.1
TW - 93	23.22986	86.30500	36	18.29	8.2
TW - 94	23.37890	86.30712	39	22.74	6.9
TW - 95	23.27012	86.31044	23	73.02	7.0
TW - 96	23.26683	86.32279	36	60.83	7.1
TW - 97	23.37070	86.32391	39	170.08	7.5
TW - 98	23.25565	86.33655	36	260.39	7.2
TW - 99	23.27387	86.33678	36	451.92	6.9
TW - 100	23.36048	86.33912	39	109.45	7.5
TW - 101	23.27634	86.34120	36	413.18	6.8
TW - 102	23.34782	86.34703	39	34.18	7.2
TW - 103	23.27349	86.35135	25	250.10	6.8
TW - 104	23.23895	86.35370	37	28.53	6.9
TW - 105	23.25279	86.35568	37	134.29	7.1
TW - 106	23.27874	86.35622	36	42.57	7.3
TW - 107	23.34536	86.35726	39	147.49	7

TW - 108	23.31422	86.35897	20	127.65	7.1
TW - 109	23.34190	86.37057	39	29.98	7.2
TW - 110	23.31739	86.37457	38	186.38	7.0
TW - 111	23.32163	86.38106	38	63.33	6.6
TW - 112	23.31183	86.38296	38	579.47	8.0
TW - 113	23.22535	86.38350	37	89.68	7.4
TW - 114	23.28652	86.39208	38	426.76	7.7
TW - 115	23.27052	86.39744	38	170.50	7.5
TW - 116	23.21434	86.39785	38	33.83	7.5
TW - 117	23.25217	86.40419	38	83.06	7.3
TW - 118	23.22174	86.40555	38	32.59	7.4
TW - 119	23.23293	86.40593	38	54.74	7.3
TW - 120	23.23662	86.41605	38	55.92	7.1

Form **Table 9.1** it is clear that the radon concentration levels of the water samples have widely fluctuated between 5.71 ± 0.29 - 579.47 ± 23.18 Bq/l with an average of 110.00 ± 6.61 Bq/l. To have a pictorial view of radon concentration profile in the tube-wells water a scatter plot of the data set is presented in **Fig. 9.3**.

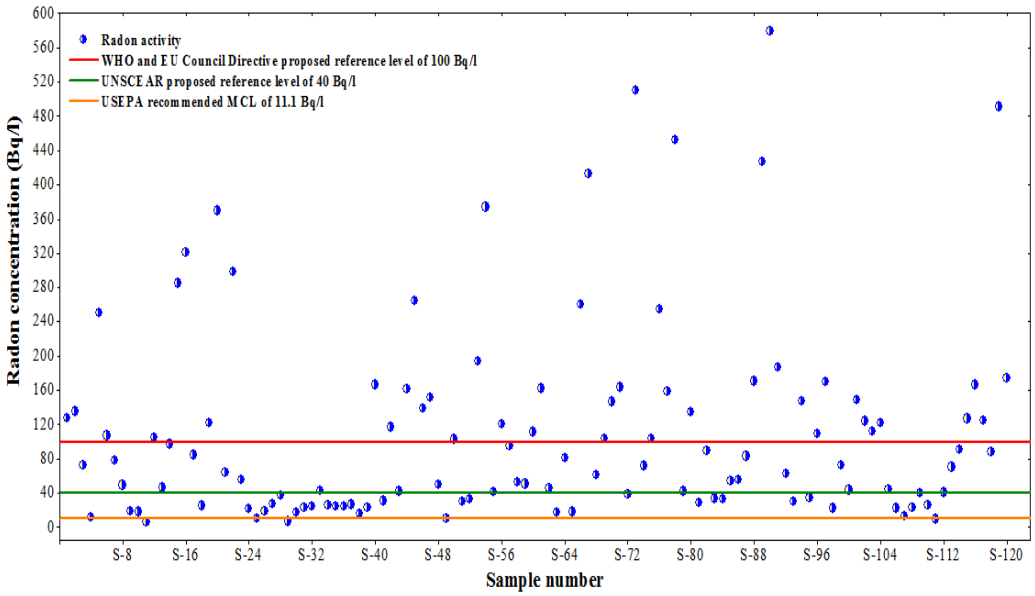

Fig. 9.3 Variation of radon concentration in the tube-well water samples

From **Fig. 9.3** it can be clearly observed that radon levels in 115 samples (almost 96%) have exceeded the USEPA proposed maximum contamination level (MCL) of 11.1 Bq/L. When we compare these results with the UNSCEAR proposed reference range of radon levels for safe drinking water of 4 - 40 Bq/l, 39 samples (almost 33%) have showed radon levels below the limit. However, if we consider the WHO and the EU Commission recommended reference level of 100 Bq/l for radon contaminated drinking water, estimated radon concentration of 49 water samples (almost 41%) have exceeded the reference limit.

To demonstrate the overall variation pattern of radon concentration levels in the tube-well water samples, the frequency distribution plot of radon concentration in 120 water

samples is presented in **Fig. 9.4**.

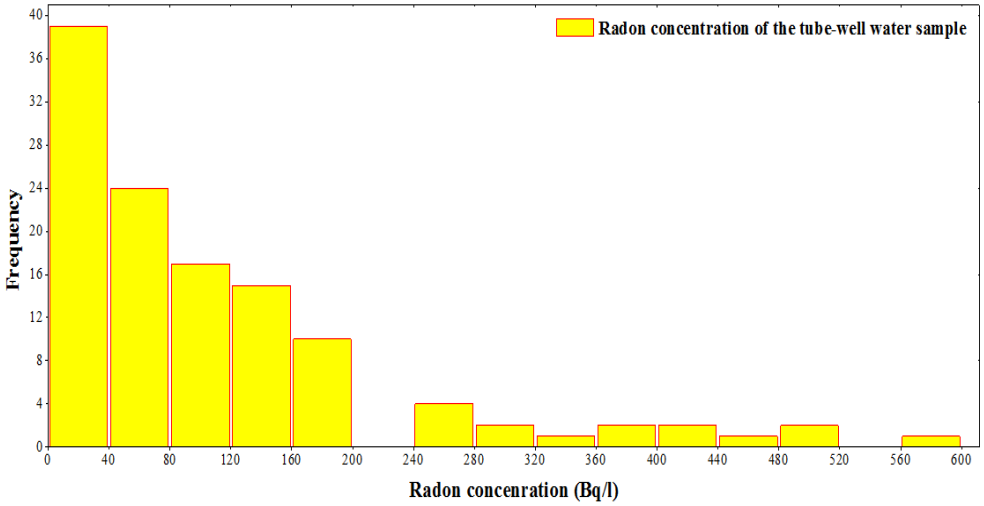

Fig. 9.4 Frequency distribution of radon concentration levels in the tube-well water

Fig. 9.4 indicates that the frequency distribution may well fit in the log-normal form like other radon distributions (***Pinti et al. 2004; Naskar et al. 2018, 2022***).

To understand the statistical properties of the data set, important statistical parameters like skewness and excess kurtosis are determined using the conventional formula by Hopkins and Weeks (***Hopkins and Weeks 1990***). Other statistical parameters are calculated using the well-established formulae by Dixon and Massey (***1951***).The obtained statistical parameters for radon concentration measurement in the 120 tube-well water samples are summarized in **Table 9.2**.

Table 9.2 Statistical description of the tube-well water samples

Statistical Parameters	Value
Sample Size	120
Minimum	5.71 ± 0.29 (Bq/l)
Maximum	579.47 ± 23.18 (Bq/l)
Average	110.00 ± 6.61 (Bq/l)
Variance	13423.50
Standard Deviation	115.86 (Bq/l)
Median	72.26 (Bq/l)
Mode	55.92 (Bq/l)
Skewness	2.01
Excess Kurtosis	4.08

Here the standard deviation value is higher than the average radon concentration, which indicates highly asymmetric nature of the distribution (***Hopkins and Weeks 1990***). The skewness value of 2.01 suggests a positively skewed distribution which is bunched up at the left with a longer tail stretching toward the right. The excess kurtosis value of

4.08 refers that the distribution is leptokurtic in nature (***Fraser et al. 2001***) and it has a sharp peak with fatter tail than a normal distribution. In view of the corresponding skewness and excess kurtosis values of the distribution it can be concluded that the distribution does not follow a normal distribution pattern (***Press et al. 1992***).

To easily identify the radiation prone zones, spatial variation of radon concentration in the tube-well water is shown in **Fig. 9.5**.

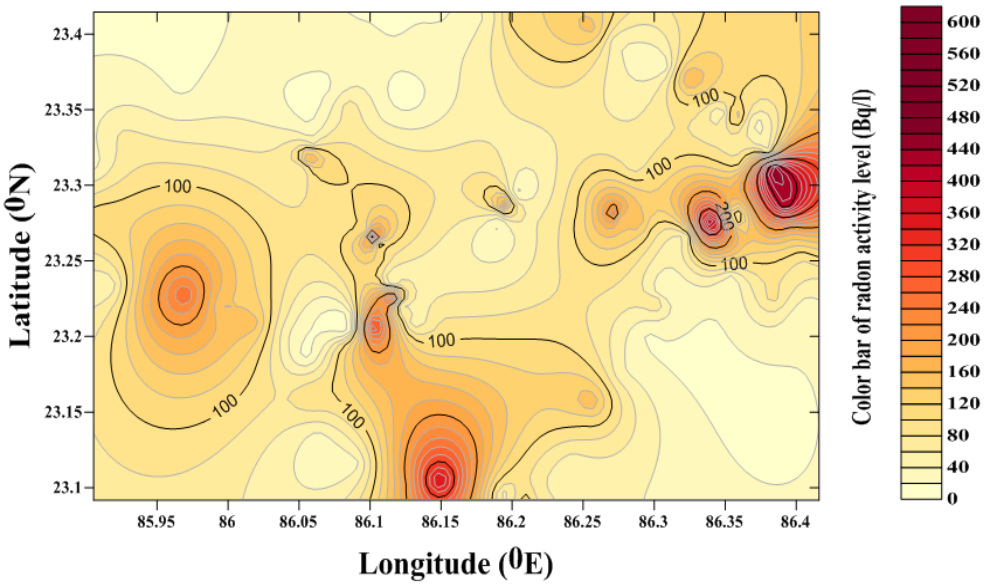

Fig. 9.5 Spatial variation of radon concentration of the tube-well water samples

In **Fig. 9.5** it can be clearly observed that radon levels in the tube-wells water of Palanja (23.31183 ^{0}N, 86.38296 ^{0}E), Sirkabad (23.28619 ^{0}N, 86.19395 ^{0}E), Kalha (23.22681 ^{0}N, 86.11509 ^{0}E) and Barakdi (23.27387 ^{0}N, 86.33678 ^{0}E) areas show very high values.

Actually these values are of 579.47 ± 23.18 Bq/l, 510.2 ± 25.37 Bq/l, 491.19 ± 18.96 Bq/l and 451.92 ± 20.11 Bq/l respectively. Highly mineralized porous sub-surface of this area is mainly composed of schist, granite and quartzite rocks. Generally granitic and quartzite rocks contains elevated levels of ^{238}U sources (***Torgersen et al. 1990; Hall et al. 2020***) and the heterogeneous lithology of the area with presence of numerous faults, shears and fracture zones may increase upward migration of radon gas from the uranium sources (***Wanty et al. 1992***). After that the emanated radon easily mixes in to the groundwater aquifers (***Howard et al. 2013***) which may increase the radon levels of these tube-wells water.

Overall wide variation of radon concentration in tube-well water may be due to the different geological structure of the groundwater aquifer from where these tube-wells water comes from (***Vaupotic et al. 1994; Mitra et al. 2021***). The tube-well depths may also have played a big roll behind this fluctuation of radon levels in the tube-wells water (***Yalim et al. 2007; Naskar et al. 2022***). Moreover, large variation of ^{222}Rn concentrations found in the tube-well water of the same area may be attributed to the fact that the

parent radionuclides of ^{222}Rn are not uniformly distributed in the same rock-types (***Folger et al. 1994***) and also may be due to significant amount of radon emanation along the fracture walls, fault zones and near the surface of the rock (***Choubey and Ramola 1997***).

To know the impact of tube-well depth on radon concentration, variation of radon levels in tube-well water with their corresponding depth is plotted in **Fig. 9.6**.

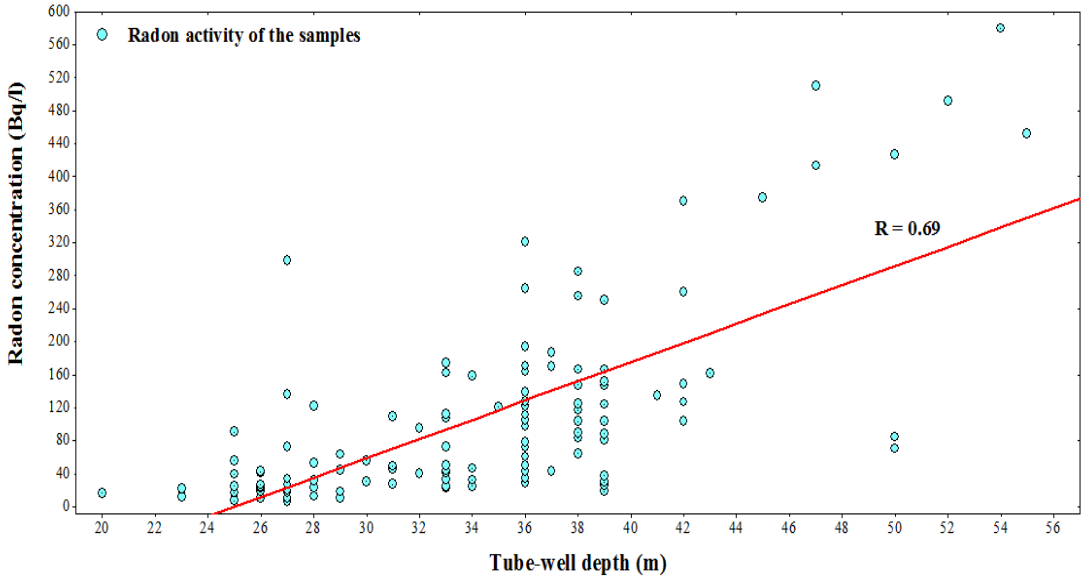

Fig. 9.6 Variation of radon concentration with tube-wells depth in different regions

Fig. 9.6 shows a very prominent relationship between tube-well depth and corresponding radon concentration. To have a quantitative measurement of the relationship between them Pearson Correlation Coefficient has been calculated (***Steele 2004; Benesty et al. 2009***). Measured value of the correlation coefficient factor (R) of 0.69 reveals a very strong positive linear correlation between the tube-well depths with their corresponding radon levels. By pumping the tube-wells, water is extracted from the groundwater aquifers which lower the water table of the aquifers (***LeGrand 1987***). As depth of the tube well increases, water gets a chance to interact with larger thickness of the aquifer and hence may carry more radon (***Choubey et al. 2003; Bourai et al. 2012***).

The fundamental water-quality parameter pH has been measured to know whether these water samples are suitable for drinking or not and also its impact on radon concentration level. Generally the neutral pH of pure water at room temperature is 7.0 and in surface water sources pH value ranges between 6.5 and 8.0 (***WHO 2009***). Presence of coal or shale in groundwater can decreases the pH levels to less than 4.0. On the other hand, in some regions where groundwater flows through sedimentary rocks like limestone can have pH value higher than 8.5 (***Vinson et al. 2009***). Normally the pH levels in groundwater sources vary in between 6.0 - 8.5 depending on the type of bed rocks of the aquifers (***Vinson et al. 2009***). However, if pH values in drinking water sources are not in the range of 6.5 - 8.5 then consumption of water from these sources can produce staining, etching or scaling like dangerous skin diseases (***Dietrich and Burlingame 2015;***

USEPA 2018).

The measured pH values of the tube-well water samples have ranged between 6.5 and 8.2 with a mean of 7.2. Results show that pH values of all samples are in between the USEPA proposed secondary maximum contamination pH range of 6.5 - 8.5 (***BIS 2012; USEPA 2018***). The study manifests that 102 samples (almost 85%) have pH levels in the range of 6.5 - 7.5 which may indicate the presence of sandstones, quartzs and granites in the bedrocks of the water aquifers (***Vinson et al. 2009***).

An attempt has been made to find out the possible correlation between the pH and the radon concentration of the tube-well water samples. We have plotted radon concentration against pH values in **Fig. 9.7**.

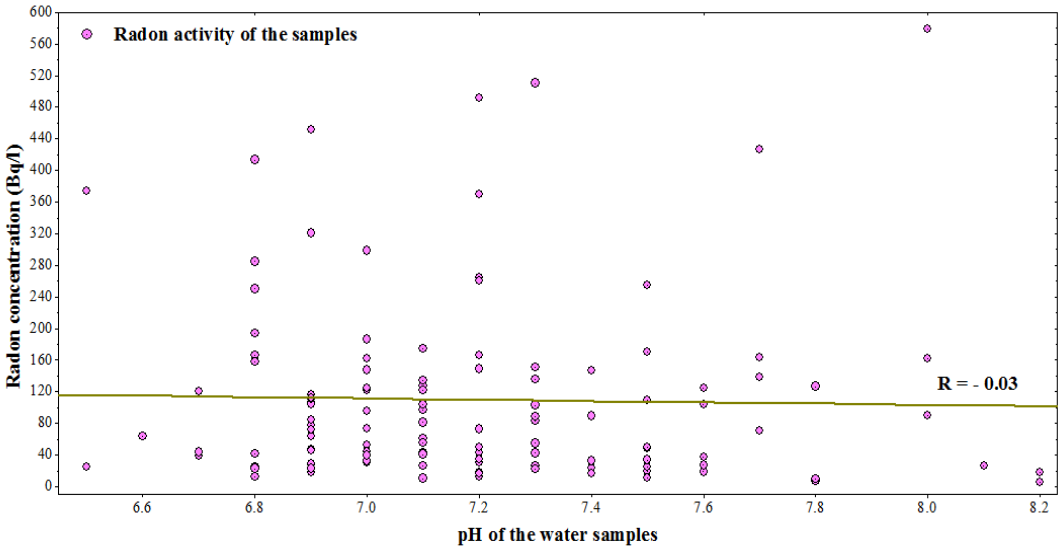

Fig. 9.7 Variation of radon concentration with pH of the water samples

In this plot no significant relationship has been observed between pH and radon concentration. Pearson correlation coefficient has been estimated (***Steele 2004; Benesty et al. 2009***). It gives a correlation coefficient factor (R) of - 0.03 which suggest almost no correlation between pH and radon concentration.

To have a comparative view of our own studies of radon level in drinking water, as well as to compare them with the global scenario we have presented worldwide radon data in **Table 9.3**.

Table 9.3 Measurements of water radon concentration in different parts of the world

Sampling Site	Water Type	Sl. No.	^{222}Rn Conc. (Bq/l)		References
			Range	Avg.	
Susunia hill area, India	Tube-well water	316	1.78 - 3213.50	128. 30	***Naskar et al. 2022***

Purulia, India	Tube-well water	35	1.13 - 457.35	117.48	***Mitra et al. 2021***
Ajodhya hill area, India	Tube-well water	120	5.71 - 579.47	110.00	***This Study***
Bakreswar and Tantloi, India	Tube-well water	173	3.30 - 803.00	106.78	***Naskar et al. 2018***
Aldama, Mexico	Tap water	37	4.30 - 42.00	27.30	***Sujo et al. 2004***
Canada	Well water	198	0.20 - 310.00	25.20	***Pinti et al., 2014***
Mashhad, Iran	Surface, Well and Tap water	51	0.06 - 46.09	16.24	***Binesh et al. 2012***
Karnataka, India	Well, Hand-pump and Tube-well	38	3.10 - 38.50	13.60	***Rangaswamy et al. 2016***
Algeria	Bottled mineral water	7	2.60 - 14.00	7.00	***Amrani 2002***
Zonguldak, Turkey	Tap, Natural spring, Thermal spring and Catchment water	24	0.32 - 88.22	6.70	***Koray et al. 2014***
Sakarya, Turkey	Spring water	24	0.75 - 22.80	5.41	***Tabar and Yakut 2014***
Jeddah, Saudi Arabia	Tap, Flush, Gallon, Mineral and other water	52	0.92 – 14.87	3.96	***Tayyeb et al. 1998***
Poland	Tap and Well water	89	0.42 - 10.52	2.68	***Bem et al. 2014***
Kulachi, Pakistan	Tap, Pond, Tube-well and Hand-pump water	20	0.33 – 1.46	0.92	***Nasir and Shah 2012***
Kerala, India	Well water	17	0.03 - 1.31	0.29	***D'Cunha et al. 2011***

Table 6.3 and **Table 7.3** (previous chapters) provide some worldwide data on radon activity measurements in water, mainly used for drinking purposes. To have a more comprehensive view few more studies which includes water samples from different sources are presented in **Table 9.3**. When the results of this area are compared with other reported values presented in **Table 6.3**, **Table 7.3** and **Table 9.3**, it is clear that among the reported results only one have much higher average radon concentration in drinking water (***Inácio et al. 2017***) and the other three have comparable average radon concentration in water with the present study. Mitra et al. **(*2021*)** reported data which are also in Purulia district and show comparable activity with our studies **(*Naskar et al. 2018, 2022***). Within our studied regions, Susunia hill area has highest activity in water.

So, all the regions where studies have been performed are important so far radon in water is concerned and needs regular radon monitoring.

9.5.2 Annual effective radon dose

The estimated radon dose values for the water samples are calculated using relation **6.1** to **6.3**, considering annual water intake as discussed in **Section 9.4.2** and are presented in **Table 9.4**

Table 9.4 Annual effective dose values of the water samples

Sample Id	Annual effective dose (μSv/yr)				
	Inhalation	Ingestion		Total	
		for 4.5 l/d intake	for 60 l/yr intake	for 4.5 l/d intake	for 60 l/yr intake
TW - 1	78.25	178.50	6.53	256.75	84.77
TW - 2	294.67	672.21	24.56	966.87	319.22
TW - 3	106.83	243.69	8.91	350.52	115.73
TW - 4	419.36	956.65	34.95	1376.01	454.30
TW - 5	408.09	930.96	34.01	1339.05	442.10
TW - 6	59.70	136.19	4.98	195.89	64.68
TW - 7	666.70	1520.89	55.56	2187.59	722.25
TW - 8	41.86	95.49	3.49	137.35	45.35
TW - 9	67.34	153.61	5.62	220.95	72.95
TW - 10	349.20	796.61	29.10	1145.81	378.30
TW - 11	62.45	142.46	5.21	204.90	67.65
TW - 12	380.78	868.64	31.74	1249.41	412.51
TW - 13	62.78	143.21	5.24	205.98	68.01
TW - 14	65.50	149.42	5.46	214.91	70.96
TW - 15	125.05	285.26	10.43	410.30	135.47
TW - 16	108.44	247.37	9.04	355.81	117.48
TW - 17	161.71	368.9	13.48	530.61	175.19
TW - 18	25.83	58.93	2.16	84.76	27.99
TW - 19	752.55	1716.75	62.72	2469.30	815.26
TW - 20	259.87	592.82	21.66	852.68	281.52
TW - 21	55.37	126.31	4.62	181.67	59.98
TW - 22	140.92	321.48	11.75	462.39	152.67
TW - 23	26.57	60.60	2.22	87.16	28.78
TW - 24	77.12	175.92	6.43	253.03	83.54
TW - 25	63.06	143.84	5.26	206.89	68.31
TW - 26	47.94	109.35	4.00	157.28	51.93
TW - 27	227.84	519.75	18.99	747.58	246.82
TW - 28	319.57	729.00	26.64	1048.57	346.2
TW - 29	59.68	136.14	4.98	195.81	64.65
TW - 30	245.18	559.30	20.44	804.47	265.61
TW - 31	68.55	156.37	5.72	224.91	74.26
TW - 32	177.69	405.35	14.81	583.03	192.50
TW - 33	49.02	111.82	4.09	160.83	53.10
TW - 34	14.39	32.83	1.20	47.22	15.59
TW - 35	213.17	486.29	17.77	699.46	230.94

TW - 36	82.56	188.33	6.88	270.89	89.44
TW - 37	44.31	101.07	3.70	145.37	48.00
TW - 38	93.98	214.38	7.84	308.35	101.81
TW - 39	419.18	956.25	34.94	1375.43	454.11
TW - 40	932.40	2127.04	77.70	3059.44	1010.10
TW - 41	808.12	1843.51	67.35	2651.63	875.46
TW - 42	313.47	715.09	26.13	1028.55	339.59
TW - 43	306.29	698.71	25.53	1004.99	331.81
TW - 44	103.25	235.53	8.61	338.78	111.85
TW - 45	223.15	509.06	18.60	732.20	241.75
TW - 46	63.38	144.59	5.29	207.96	68.66
TW - 47	717.78	1637.42	59.82	2355.19	777.59
TW - 48	1237.80	2823.73	103.15	4061.53	1340.95
TW - 49	18.10	41.28	1.51	59.37	19.61
TW - 50	252.00	574.88	21.00	826.88	273.00
TW - 51	439.39	1002.36	36.62	1441.74	476.01
TW - 52	124.09	283.07	10.35	407.16	134.43
TW - 53	264.33	602.99	22.03	867.31	286.35
TW - 54	25.58	58.35	2.14	83.93	27.71
TW - 55	488.33	1114.00	40.70	1602.32	529.02
TW - 56	99.12	226.1	8.26	325.21	107.38
TW - 57	66.76	152.29	5.57	219.04	72.32
TW - 58	100.07	228.29	8.34	328.36	108.41
TW - 59	57.54	131.25	4.80	188.78	62.33
TW - 60	32.31	73.70	2.70	106.01	35.00
TW - 61	196.89	449.15	16.41	646.04	213.30
TW - 62	942.79	2150.73	78.57	3093.51	1021.35
TW - 63	56.76	129.47	4.73	186.22	61.48
TW - 64	111.44	254.21	9.29	365.65	120.73
TW - 65	116.93	266.75	9.75	383.67	126.68
TW - 66	46.52	106.13	3.88	152.65	50.40
TW - 67	1285.71	2933.02	107.15	4218.72	1392.85
TW - 68	103.78	236.74	8.65	340.51	112.43
TW - 69	412.48	940.96	34.38	1353.43	446.85
TW - 70	30.52	69.62	2.55	100.14	33.07
TW - 71	306.74	699.74	25.57	1006.48	332.30
TW - 72	303.66	692.73	25.31	996.39	328.97
TW - 73	283.33	646.34	23.62	929.66	306.94
TW - 74	240.69	549.07	20.06	789.75	260.75
TW - 75	313.37	714.86	26.12	1028.22	339.48
TW - 76	133.06	303.54	11.09	436.59	144.15
TW - 77	181.24	413.46	15.11	594.69	196.35
TW - 78	127.09	289.91	10.60	417.00	137.68
TW - 79	261.40	596.32	21.79	857.72	283.19
TW - 80	280.05	638.86	23.34	918.91	303.39
TW - 81	408.87	932.74	34.08	1341.61	442.95
TW - 82	375.33	856.22	31.28	1231.55	406.61
TW - 83	369.64	843.23	30.81	1212.87	400.44
TW - 84	110.63	252.38	9.22	363.00	119.85

TW - 85	642.91	1466.63	53.58	2109.53	696.48
TW - 86	341.92	780.00	28.50	1121.91	370.41
TW - 87	115.50	263.47	9.63	378.96	125.12
TW - 88	182.93	417.31	15.25	600.23	198.18
TW - 89	399.10	910.43	33.26	1309.53	432.36
TW - 90	42.90	97.85	3.58	140.74	46.47
TW - 91	260.80	594.94	21.74	855.74	282.53
TW - 92	204.50	466.52	17.05	671.01	221.54
TW - 93	46.10	105.15	3.85	151.24	49.94
TW - 94	57.31	130.73	4.78	188.04	62.09
TW - 95	184.02	419.78	15.34	603.79	199.35
TW - 96	153.30	349.70	12.78	502.99	166.07
TW - 97	428.61	977.75	35.72	1406.35	464.32
TW - 98	656.19	1496.92	54.69	2153.10	710.87
TW - 99	1138.84	2597.98	94.91	3736.82	1233.75
TW - 100	275.82	629.21	22.99	905.02	298.80
TW - 101	1041.22	2375.27	86.77	3416.49	1127.99
TW - 102	86.14	196.50	7.18	282.63	93.32
TW - 103	630.26	1437.77	52.53	2068.02	682.78
TW - 104	71.90	164.02	6.00	235.91	77.89
TW - 105	338.42	772.00	28.21	1110.42	366.62
TW - 106	107.28	244.73	8.94	352.01	116.22
TW - 107	371.68	847.89	30.98	1219.56	402.65
TW - 108	321.68	733.83	26.81	1055.51	348.49
TW - 109	75.55	172.35	6.30	247.90	81.85
TW - 110	469.68	1071.46	39.14	1541.13	508.82
TW - 111	159.60	364.07	13.30	523.66	172.90
TW - 112	1460.27	3331.23	121.69	4791.50	1581.96
TW - 113	226.00	515.55	18.84	741.55	244.83
TW - 114	1075.44	2453.34	89.62	3528.78	1165.06
TW - 115	429.66	980.17	35.81	1409.83	465.47
TW - 116	85.26	194.49	7.11	279.74	92.36
TW - 117	209.32	477.50	17.45	686.81	226.76
TW - 118	82.13	187.36	6.85	269.48	88.98
TW - 119	137.95	314.69	11.50	452.64	149.45
TW - 120	140.92	321.48	11.75	462.39	152.67

The estimated annual doses from the tube-well water samples due to inhalation of water-borne radon have ranged from 14.39 - 1460.26 μSv/yr with an average of 277.19 μSv/yr.

In this study the estimated annual doses due to ingestion of radon containing water for 60 l/yr water consumption have ranged from 1.19 – 121.69 μSv/yr with an average of 23.09 μSv/yr and considering the annual water intake of 4.5 × 365 = 1642.5 l/yr the estimated annual ingestion doses vary between 32.83 - 3331.23 μSv/yr with an average of 632.35 μSv/yr which may be somewhat over estimated value.

The total annual effective doses from the water radon of the samples for 60 l/yr water

consumption vary between 15.59 – 1581.95 μSv/yr with an average of 300.14 μSv/yr and for 1642.50 l/yr water water consumption 47.21 - 4791.49 μSv/yr with an average of 909.54 μSv/yr.

In view of the risks associated with water radon the EU Commission and the WHO have recommended a reference level of 100 μSv/yr (***EU 2001; WHO 2009***) for the annual effective dose received from water dissolved radon. If the estimated annual effective dose in drinking water exceed the limit of 100 μSv/yr remedial measures are necessary to reduce the radon levels.

With respect to WHO and EU Commission recommendation it has been found that for 60 l/yr water intake 84 samples (almost 70%) and for 1642.50 l/yr water intake 115 samples (almost 96%) have higher total annual effective dose values. The estimated Excess Lifetime Cancer Risk (ELCR) associated with the radon contaminated water samples for 60 l/yr water intake vary between 0.06 - 6.09 × 10^{-3} with an average of 1.16 × 10^{-3} and for 1642.50 l/yr water intake widely fluctuate between 0.18 - 18.45 × 10^{-3} with an average of 3.5 × 10^{-3}. For 60 l/yr water consumption the ELCR values of 51 (about 43 %) samples and for 1642.50 l/yr water consumption 118 (about 98%) samples are high compared to the UNSCEAR recommended world average safe limit of 0.29 × 10^{-3} (***USCEAR 2000***).

Therefore, very high annual effective dose values and the high ELCR values indicate significant chances of occurrence of cancer.

9.6 Conclusions

This **Chapter** reports the measurement of radon concentration level in 120 tube-well water samples collected from Ajodhya hill and its surrounding areas at Purulia district of West Bengal, India.

Radon concentrations of almost 96% of the water samples show greater values than the USEPA proposed MCL of 11.1 Bq/l. However, almost 68% samples have higher concentration levels than the UNSCEAR proposed reference level of 40 Bq/l, whereas almost 41% samples exceed the WHO and the EU Council Directive recommended reference level of 100 Bq/l.

In the study area high mineralised bedrocks of the groundwater aquifers and the critical geological formation with multiple faults, fracture zones may be the main reasons behind the high radon concentration in tube-well water samples of some sites.

No significant ccorrelation has been found between pH level of the water samples with their radon concentration. However, radon concentration is found to be significantly correlated with the depth of the tube-wells as was observed in the previous study (**Chapter 7**).

Results of water radon dose estimation show that total annual effective doses to the users of almost 70 % tube-wells for 60 l/yr water intake and for 1642.50 l/yr water intake of almost 96% of these tube wells exceed the WHO and EU Commission proposed permissible limit of 100 μSv/yr. Also ranges of ELCR values of the samples indicate serious threats regarding the risks of developing cancer to the local people.

Local people should be made aware of the radiological risks from water and should be advised to adopt local measures for reduction of radon in water before using it.

In this study area as well as other areas studied, we have largely concentrated on the anticipation of the health risks of the local population as a result of exposure to water-born radon. The actual health impacts due to radon from drinking water on the local population have not been investigated. However, as this is important, we want to assess that aspect in near future.

References

Acharya, T., & Nag, S. K. (2013). Study of groundwater prospects of the crystalline rocks in Purulia District, West Bengal, India using remote sensing data. Earth Resources, 1(2): 54-59.

Ademola, J. A., & Ojeniran, O. R. (2017). Radon-222 from different sources of water and the assessment of health hazard. Journal of Water and Health, 15(1), 97-102.

Amrani, D. (2002). Natural radioactivity in Algerian bottled mineral waters. Journal of Radioanalytical and nuclear chemistry, 252(3), 597-600.

Baidya, T. K. (1992). Apatite-magnetite deposit in the Chhotanagpur gneissic complex, Panrkidh area, Purulia district, West Bengal. Indian J. Geol., 64, 84-95.

Bem, H., Plota, U., Staniszewska, M., Bem, E. M., & Mazurek, D. (2014). Radon (^{222}Rn) in underground drinking water supplies of the Southern Greater Poland Region. Journal of Radioanalytical and Nuclear Chemistry, 299(3), 1307-1312.

Benesty, J., Chen, J., Huang, Y., & Cohen, I. (2009). Pearson correlation coefficient. In Noise reduction in speech processing. Springer, Berlin, Heidelberg, 2, 1-4.

Bhaya, S., & Chakrabarty, A. (2016). Application of geoinformatics in pattern analysis of seditious activity in Purulia district of West Bengal in relation to it's geographic and socio-economic background. Int J Sci Res Publ, 6(9).

Binesh, A., Mowlavi, A. A., & Mohammadi, S. (2012). Estimation of the effective dose from radon ingestion and inhalation in drinking water sources of Mashhad, Iran. Iran. J. Radiat. Res., 10(1), 37-41.

BIS (2012). Indian Standard Drinking Water — Specification (Second Revision) IS 10500; 2012. ICS 13.060.20. May 20125. © BIS 2012.

Bourai, A. A., Gusain, G. S., Rautela, B. S., Joshi, V., Prasad, G., & Ramola, R. C. (2012). Variations in radon concentration in groundwater of Kumaon Himalaya, India. Radiation protection dosimetry, 152(1-3), 55-57.

Choubey, V. M., & Ramola, R. C. (1997). Correlation between geology and radon levels in groundwater, soil and indoor air in Bhilangana Valley, Garhwal Himalaya, India. Environmental Geology, 32(4), 258-262.

Choubey, V. M., Bartarya, S. K., & Ramola, R. C. (2003). Radon in groundwater of eastern Doon valley, Outer Himalaya. Radiation measurements, 36(1-6), 401-405.

Council Directive 2013/51/EURATOM, (2013). Laying down requirements for the protection of the health of the general public with regard to radioactive substances

in water intended for human consumption. Official Journal of the European Union L (296):12-21.

D'Cunha, P., Narayana, Y., Karunakara, N., Yashodhara, I., & Kumara, S. (2011). Concentration of 222 Rn in drinking water along coastal Kerala and evaluation of ingestion doses. Radiation Protection and Environment, 34(3), 197.

Dietrich, A. M., & Burlingame, G. A. (2015). Critical review and rethinking of USEPA secondary standards for maintaining organoleptic quality of drinking water. Environmental science & technology, 49(2), 708-720. DOI: 10.1021/es504403t

Dixon, W. J., & Massey Jr, F. J. (1951). Introduction to statistical analysis. McGraw-Hill.

Duggal, V., Sharma, S., & Mehra, R. (2017). Radon levels in drinking water of Fatehabad district of Haryana, India. Applied Radiation and Isotopes, 123, 36-40.

Duggal, V., Sharma, S., & Mehra, R. (2020). Risk assessment of radon in drinking water in Khetri Copper Belt of Rajasthan, India. Chemosphere, 239, 124782.

EU. (2001). Recommendation on the protection of the public against exposure to radon in drinking water supplies. Office Journal of the European Community, 85-88.

Folger, P. F., Nyberg, P., Wanty, R. B., & Poeter, E. (1994). Relationships between ^{222}Rn dissolved in ground water supplies and indoor 222Rn concentrations in some Colorado front range houses. Health Physics, 67(3), 245-253.

Fraser, D. F., Gilliam, J. F., Daley, M. J., Le, A. N., & Skalski, G. T. (2001). Explaining leptokurtic movement distributions: intrapopulation variation in boldness and exploration. The American Naturalist, 158(2), 124-135.

Geological Quadrangle Map 73I, 1948. Geological Survey of India, Calcutta.

Hall, F. R., Boudette, E. L., & Olszewski, W. J. (2020). Geologic controls and radon occurrence in New England. In Radon, radium, and other radioactivity in ground water (pp. 15-30). CRC Press.

Hopkins, K. D., & Weeks, D. L. (1990). Tests for normality and measures of skewness and kurtosis: Their place in research reporting. Educational and psychological measurement, 50(4), 717-729.

Howard, G., Bartram, J., Water, S., & World Health Organization. (2003). Domestic water quantity, service level and health (No. WHO/SDE/WSH/03.02). World Health Organization.

Howard, B. J., Beresford, N. A., Copplestone, D., Telleria, D., Proehl, G., Fesenko, S., ... & Wells, C. (2013). The IAEA handbook on radionuclide transfer to wildlife. Journal of Environmental radioactivity, 121, 55-74.

ICRP. (2010). Conversion Coefficients for Radiological Protection Quantities for External Radiation Exposures. ICRP Publication 116, Ann. ICRP 40: 2-5.

Inácio, M., Soares, S., & Almeida, P. (2017). Radon concentration assessment in water sources of public drinking of Covilhã's county, Portugal. Journal of Radiation Research and Applied Sciences, 10(2), 135-139.

Koray, A., Akkaya, G., Kahraman, A., & Kaynak, G. (2014). Measurements of radon concentrations in waters and soil gas of Zonguldak, Turkey. Radiation protection dosimetry, 162(3), 375-381.

LeGrand, H. E. (1987). Radon and radium emanations from fractured crystalline rocks–a conceptual hydrogeological model. Groundwater, 25(1), 59-69.

Mitra, S., Chowdhury, S., Mukherjee, J., Sutradhar, S., Mondal, S., Barman, C., & Deb, A. (2021). Assessment of radon (^{222}Rn) activity in groundwater and soil-gas in Purulia district, West Bengal, India. Journal of Radioanalytical and Nuclear Chemistry, 330(3), 1331-1338.

Nasir, T., & Shah, M. (2012). Measurement of annual effective doses of radon from drinking water and dwellings by CR-39 track detectors in Kulachi City of Pakistan. Journal of Basic & Applied Sciences, 8, 528-536.

Naskar, A. K., Gazi, M., Barman, C., Chowdhury, S., Mondal, M., Ghosh, D., ... & Deb, A. (2018). Estimation of underground water radon danger in Bakreswar and Tantloi Geothermal Region, India. Journal of Radioanalytical and Nuclear Chemistry, 315(2), 273-283.

Naskar, A. K., Gazi, M., Mondal, M., & Deb, A. (2022). Water radon risk in Susunia hill area: an assessment in terms of radiation dose. Environmental Science and Pollution Research, 29(8), 11160-11171.

Pinti, D. L., Retailleau, S., Barnetche, D., Moreira, F., Moritz, A. M., Larocque, M., ... & Valadez, A. (2014). 222Rn activity in groundwater of the St. Lawrence Lowlands, Quebec, eastern Canada: relation with local geology and health hazard. Journal of environmental radioactivity, 136, 206-217.

Press, W. H., Teukolsky, S. A., Vetterling, W. T., & Flannery, B. P. (1992). Numerical recipes in C. The Art of Scientific Computing Second Edition. CAMBRIDGE UNIVERSITY PRESS.

Rangaswamy, D. R., Srinivasa, E., Srilatha, M. C., & Sannappa, J. (2016). Measurement of radon concentration in drinking water of Shimoga district, Karnataka, India. Journal of Radioanalytical and Nuclear Chemistry, 307(2), 907-916.

Steele, J. Michael. The Cauchy-Schwarz master class: an introduction to the art of mathematical inequalities. Cambridge University Press, 2004.

Tabar, E., & Yakut, H. (2014). Radon measurements in water samples from the thermal springs of Yalova basin, Turkey. Journal of Radioanalytical and Nuclear Chemistry, 299(1), 311-319.

Tayyeb, Z. A., Kinsara, A. R., & Farid, S. M. (1998). A study on the radon concentrations in water in Jeddah (Saudi Arabia) and the associated health effects. Journal of environmental radioactivity, 38(1), 97-104.

Torgersen, T., Benoit, J., & Mackie, D. (1990). Controls on groundwater Rn-222 concentrations in fractured rock. Geophysical Research Letters, 17(6), 845-848.

UNSCEAR. (2000). Effects of Ionizing Radiation. United Nations, New York, 453-487.

USEPA. (1991). Federal Register 40 Parts 141 and 142: national primary drinking water regulations; radionuclides: proposed rule.

USEPA, W. (2018). Edition of the Drinking Water Standards and Health Advisories Tables: United States Environmental Protection Agency. Off Water.

Vaupotic, J., Krizman, M., Planinić, J., Pezdic, J., Adamic, K., Stegnar, P., & Kobal, I. (1994). Systematic indoor radon and gamma measurements in kindergartens and play schools in Slovenia. Health physics, 66(5), 550-556.

Vinson, D. S., Vengosh, A., Hirschfeld, D., & Dwyer, G. S. (2009). Relationships between radium and radon occurrence and hydrochemistry in fresh groundwater from fractured crystalline rocks, North Carolina (USA). Chemical Geology, 260(3-4), 159-171.

Wanty, R. B., Lawrence, E. P., & Gundersen, L. (1992). A theoretical model for the flux of radon from rock to ground water. Geological Society of America Special Paper, 271, 73-78.

World Health Organization. (2009). WHO handbook on indoor radon: a public health perspective. World Health Organization.

Yalim, H. A., Akkurt, I., Ozdemir, F. B., Unal, R., Sandikcioglu, A., & Akkurt, A. (2007). The measurement of radon and radium concentrations in well water in the Afyonkarahisar area of Turkey. Indoor and Built Environment, 16(1), 77-81.

Chapter –10

Impact of Meteorological Parameters on Soil Radon: Investigation using Machine Learning Techniques

10.1 Introduction

Uranium radionuclides are distributed in varying concentrations throughout the Earth's crust. These radionuclides undergo a series of decay processes until they reach a stable lead isotope (^{206}Pb). Within the ^{238}U decay series, the resulting products are primarily solid elements, with the exception of radon, which exists in a gaseous state. Following its generation from the parent radium (^{226}Ra), radon gas is conveyed through soil pores via diffusion and advection processes (***Sextro 1987; Søgaard-Hansen and Damkjaer 1987***). In soils with high permeability, the transport of radon gas can extend across significant distances (***Mogro-Campero and Fleischer 1977***).

The levels of radon gas activity in the soil and its release into the air are significantly influenced by variations in environmental conditions, including changes on an hourly, diurnal, and seasonal basis. Factors such as atmospheric pressure, soil pressure, soil temperature, air temperature, soil moisture, humidity, rainfall, and wind speed exert a strong impact on both the presence of radon in the soil and its exhalation into the atmosphere (***Schery et al. 1984; Asher Bolinder et al. 1990; Washington and Rose 1990; Schumann and Gundersen 1996; Kojima 1998; Schubert and Schulz 2002; Sundal et al. 2008; Mazur and Kozak 2014; Yang et al. 2019***).

Radon activity also changes due to natural phenomenon like earthquake, volcanic eruption etc. The detection of changes in radon (^{222}Rn) activity in soil gas and groundwater as potential earthquake precursors has been a subject of extensive research worldwide for many years, with numerous studies investigating this phenomenon (***Ulomov and Mavashev 1971; Bichard 1976; Külahcı et al. 2009; Woith 2015; Deb et al. 2016, 2018***). Researchers, including Ghosh et al. (***2009***), have highlighted the significance of not only seismic activities but also meteorological parameters such as soil moisture, rainfall, ambient temperature, and barometric pressure in influencing radon emanation from the soil. Consequently, distinguishing between radon anomalies caused by seismic events and those resulting from non-seismic changes poses a considerable challenge. To address this challenge in earthquake prediction studies utilizing soil radon fluctuations, the application of theoretical and empirical algorithms to eliminate meteorological and other by non-seismic effects is deemed necessary (***Torkar et al. 2010***). Fujiyoshi et al. (***2006***) have emphasized the importance of such research in understanding the true causes of radon activity changes in soil, contributing to more accurate earthquake predictions.

Additionally, the presence of radon in soil gas is identified as a primary source of indoor air radon (***Nazaroff 1992; Chen and Ford 2017***), a known health hazard linked to lung cancer. Therefore, understanding the impact of meteorological parameters on soil radon emission becomes crucial for implementing effective measures to mitigate indoor air radon exposure (***Sesana et al. 2003***).

This study explores the interaction between atmospheric parameters (soil temperature, soil pressure, humidity, air temperature, and rainfall) and soil radon activity in Kolkata, West Bengal, India, over the course of a year. The investigation involves a correlation study, employing Pearson's correlation coefficient (R) to analyze the influence of individual meteorological parameters on soil radon emanation. Recognizing the limitations of Pearson's correlation for studying the combined effect of these parameters, the study employs common and robust Machine Learning (ML) techniques, including Principle Component Regression (PCR), Support Vector Regression (SVR), Random Forest (RF), and Gradient Boosting Machine (GBM). The use of ML techniques in various research fields, including radon-related studies, has demonstrated success (***Külahcı et al. 2009; Mustafa et al. 2012; Ballabio et al. 2016; Bui et al. 2016; Ly et al. 2019; Vamathevan et al. 2019; Van Dao et al. 2020; Rivera and Bonilla 2020; Hosseini et al. 2020; Mustafa et al. 2022***). However, for predicting the impact of meteorological parameters on soil radon, only a few researchers have utilized these techniques (***Torkar et al. 2010; Hosoda et al. 2020***). Thus, this study aims to contribute to the understanding of the role of meteorological parameters in soil radon using ML methods.

10.2 Monitoring site

Soil radon monitoring for this study has been performed at Jadavpur university campus at Kolkata in West Bengal, India. Jadavpur (22.4990° N, 88.3716° E) is a southern neighborhood of Kolkata metropolis, resting on the east bank of river Hooghly, on the lower Ganges Delta of eastern India. Due to the location of the basin at the junction point of three lithospheric active plate viz. the Indian Plate, the Burma Plate and the Tibetan (Eurasian) Plate posing high seismic susceptibility in the region (***Bengtsson et al. 2012***). The Bengal Basin is one of the largest sediment reservoirs in the world (***Alam et al. 2003***). At the mouth of the Ganga-Brahmaputra - Meghna River systems Bengal Basin creates the lower floodplain and delta plain deposits of India and Bangladesh (***Roy and Roser 2012***). Krishna et al. (***2016***) have reported that the sedimentary pathways are an emergence of Himalayan source material in the Bengal Basin in greater detail. This area is positioned at the top of the western part of the central hinge zone of Bengal Basin. The 25 km long hinge zone is located at a depth of about 45 km below the surface. Several faults are present in this region among them some faults are active till now (***Shiuly and Narayan 2012; Deb et al. 2018***). Sub-surface of this region is mostly covered by silt, clay and various types of sand and gravel. According to the occurrence of earthquakes, the Bureau of Indian Standards has declared this area to be inside the seismic zone III (***Bhatia et al. 1999***). Geological map of Kolkata is depicted in **Figure 10.1**.

Soil radon monitoring has been conducted for this study at the Jadavpur University campus in Kolkata, West Bengal, India. Jadavpur (22.4990° N, 88.3716° E) is situated in the southern part of the Kolkata metropolis, along the eastern bank of the River Hooghly, within the lower Ganges Delta of eastern India. This location is noteworthy due to its positioning at the convergence of three tectonically active plates: the Indian

Plate, the Burma Plate, and the Tibetan (Eurasian) Plate, rendering the region highly susceptible to seismic activity (***Bengtsson et al. 2012***). The Bengal Basin, where Jadavpur is situated, is recognized as one of the largest sediment reservoirs globally (***Alam et al. 2003***). Acting as the lower floodplain and delta plain deposits of India and Bangladesh, the Bengal Basin is formed at the mouth of the Ganga-Brahmaputra-Meghna River systems (***Roy and Roser. 2012***). Krishna et al. (***2016***) have extensively detailed the sedimentary pathways, highlighting the emergence of Himalayan source material in the Bengal Basin.

Jadavpur is positioned at the top of the western part of the central hinge zone of the Bengal Basin, a 25 km long zone located approximately 45 km below the surface. This region exhibits several faults, with some remaining active (***Shiuly and Narayan 2012; Deb et al. 2018***). The sub-surface composition in this area primarily consists of silt, clay, and various types of sand and gravel. Given the seismic activity, the Bureau of Indian Standards designates this area as seismic zone III (***Bhatia et al. 1999***). For a visual representation, the geological map of Kolkata is provided in **Figure 10.1**.

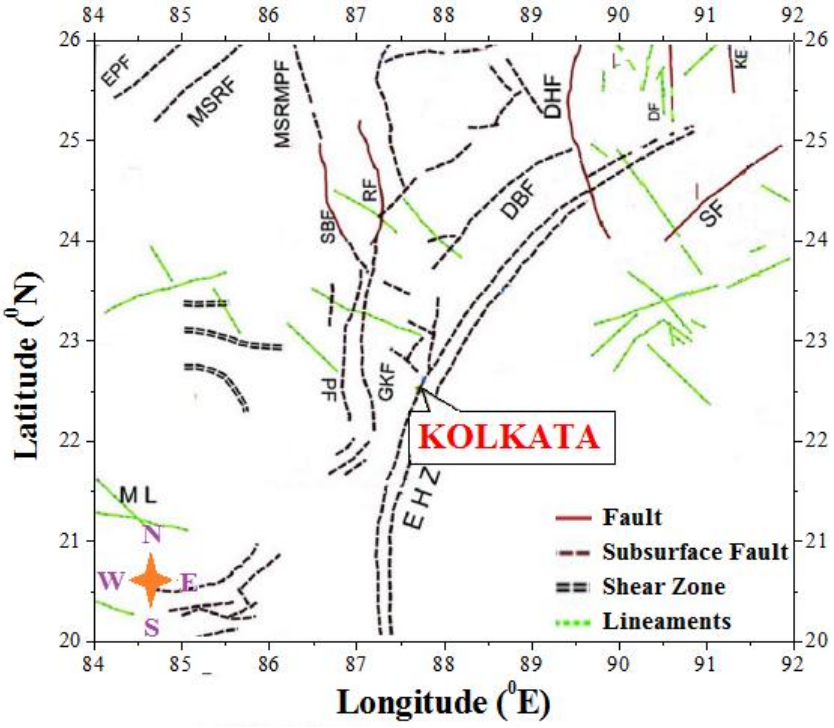

Fig. 10.1 Tectonic map of Kolkata and its adjacent areas (modified after ***Shiuly and Narayan 2012; Deb et al. 2018***)

According to the Köppen Climate Classification (***Peel et al. 2007***), Jadavpur exhibits characteristics of a tropical wet and dry climate, featuring a daily average temperature of 27 °C (***IMD 2015***). The region experiences a daily average high and low temperatures of approximately 31 °C and 22 °C, respectively (***IMD 2015***). The summer season, extending from March to May, is generally hot and humid, with temperatures ranging from 30 °C to 40 °C (***IMD 2015***). During dry periods of summer, maximum temperatures

frequently exceed 40 °C (***IMD 2015***). The winter season spans from December to February, with average low temperatures ranging from 9 °C to 23 °C (***IMD 2015***).

Early summer witnesses 'Kalbaishakhi' thunderstorms and heavy rains, providing some relief from the intense heat and humidity (***Banerji 1938***). From June to September, the Bay of Bengal branch of the South-West monsoon brings moderately high rainfall to the city, contributing significantly to its annual precipitation of about 1600 mm (***IMD 2015***). The measurement site's location is illustrated in **Figure 10.2**.

Fig. 10.2 Location of the soil radon monitoring site in Jadavpur, Kolkata

10.3 Measurement procedure and analysis methods

10.3.1 Experimental set-up

For continuous monitoring of radon gas in soil, a widely used radon monitor BARASOL BMC2 manufactured by Algade (France) has been installed at Jadavpur University Campus of Kolkata in West Bengal, India. Installed at a depth of 1 meter below the ground surface, this semiconductor detector instrument operates within the range of 0 - 1 GBq/m^3, effectively measuring soil radon activity.

For continuous monitoring of radon gas in soil, a widely used radon monitor BARASOL BMC2 manufactured by Algade (France) has been installed at Jadavpur University Campus of Kolkata in West Bengal, India. The time interval of measurement for the present work is 1 day. The time series data are recorded by the software RnView2. Detail about the detector is discussed in **Chapter 4 Section 4.2**. Meteorological data, including air temperature, humidity, and rainfall, are sourced from the Indian Meteorological Department (IMD), Kolkata. The investigation, conducted from June

2016 to May 2017, explores the influence of meteorological parameters and other factors on soil radon dynamics.

10.3.2 Machine learning techniques

The utilization of Machine Learning (ML) techniques in the field of environmental sciences has experienced a significant surge in recent years, as evidenced by various studies (***Kanevski 2009; Li et al. 2011; Micheletti et al. 2014; Lary et al. 2016; Heung et al. 2016; Hengl et al. 2017; Nussbaum et al. 2018***). ML techniques offer distinct advantages over traditional statistical models, particularly in their ability to effectively manage the intricacies of multidimensional non-linear relationships and the inherent distribution of diverse datasets (***Fouedjio and Klump 2019***). Consequently, the popularity of ML techniques is rapidly growing for predictive tasks in highly complex systems, eclipsing classical statistical models in certain scenarios (***Henderson et al. 2005; Nussbaum et al. 2018; Li et al. 2019***).

This current study employs four ML techniques - Principle Component Regression (PCR), Support Vector Regression (SVR), Random Forest (RF), and Gradient Boosting Machine (GBM). These techniques have demonstrated promising results in addressing similar multiparameter problems in previous research (***Kleine et al. 2017; Taherei et al. 2018; Hengl et al. 2018; Mostajabi et al. 2019***). Notably, in the realm of radon-related studies, the application of ML techniques has been relatively limited, with only a handful of researchers exploring their potential (***Zmazek et al. 2003, 2010; Torkar et al. 2010; Kropat et al. 2015; Timkova et al. 2017; Janik et al. 2018; Petermann et al. 2021***).

Principle Component Regression

In Principle Component Regression (PCR), the initial step involves subjecting the predictor set to principal component analysis. Following this, a subset of principal components (PCs) that collectively account for a specific percentage of variance in the predictor set, such as 95%, is selected. Importantly, the chosen PCs are orthogonal, ensuring the absence of inter-correlation among them. Subsequently, a multiple regression equation is employed to establish a connection between the selected principal components and the target variable.

Support Vector Regression

Vladimir Vapnik introduced Support Vector Regression (SVR) within the context of classification and regression analysis (***Cortes and Vapnik 1995; Chapelle et al. 2002***). This method, rooted in statistical learning frameworks, stands out as a highly robust prediction technique. In the realm of regression analysis, SVR aims to mitigate the impact of outliers on regression equations. To achieve this, SVR employs an objective function, as outlined by Kuhn and Johnson in 2013, with the specific purpose of minimizing the influence of outliers. The objective function is meticulously defined by a subset of training samples known as support vectors. In instances involving higher-

dimensional nonlinear problems where identifying a hyperplane becomes challenging, SVR strategically employs the "kernel trick." This technique resolves the hyperplane identification challenge without substantially increasing computational costs, as highlighted by Petermann et al. in 2021.

Random Forest

Breiman (***2001***) introduced the Random Forest (RF), an algorithm utilizing both classification and regression techniques. Not reliant on distributional assumptions, RF excels in addressing nonlinear problems by aggregating sets of classification/regression trees (***Loh 2011***). The inclusion of more trees in the forest effectively diminishes variance or Root Mean Square Error (RMSE). Individual trees in RF are characterized by low bias and high variance, fitting well with training data but prone to over fitting with minor changes in the dataset. To mitigate this, RF employs bootstrap aggregation or bagging ensemble algorithm, enhancing predictive accuracy by reducing variance in predictions. Both classification and regression algorithms within RF, derive the final prediction by averaging predictions across all trees whether classifying or predicting numeric values (***Petermann et al. 2021***). RF offers notable advantages, including high accuracy, efficient processing of large datasets, and the ability to highlight the importance of predictors in classification. This technique finds widespread application across various fields, such as medical science (***Ishwaran et al. 2008; Tsuji et al. 2012; Shah et al. 2014***), environmental science (***Kropat et al. 2015; Rodriguez-Galiano et al. 2015; Hengl et al. 2018; Mosavi et al. 2020***), among others.

Gradient Boosting Machine

The Gradient Boosting Machine (GBM) employs a highly effective boosting ensemble technique to capture the intricacies of nonlinear function dependencies (***Janik et al. 2018; Hosoda et al. 2020***). Unlike traditional ensemble methods that rely on simple averaging of models, boosting methods, as a family, adopt a constructive approach to ensemble formation aimed at correcting prediction errors. The fundamental concept of boosting involves sequentially introducing new models to the ensemble. Each subsequent model seeks to rectify the predictions of the preceding one, leading to a collaborative improvement in overall accuracy. This sequential addition of models often utilizes straightforward decision trees, commonly known as weak learners, which make limited decisions. During each iteration, predictions or contributions of these weak learners are amalgamated through methods like simple voting or averaging. This amalgamation is designed to minimize a loss function or cost function (***Janik et al. 2018***). Consequently, through the collaborative efforts of many weak learners, a robust learner, referred to as a strong learner, is developed. In the realm of radon research, only a limited number of researchers have employed the GBM technique. However, their findings consistently indicate that the GBM model outperforms other models in studies related to radon (***Janik et al. 2018; Rafique et al. 2020; Li et al. 2021***).

10.4 Results and discussions

10.4.1 Temporal evolution of radon activity and meteorological parameters

Daily time series of radon activity as well as various meteorological parameters like maximum air temperature (maxT), minimum air temperature (minT), maximum humidity (maxH), minimum humidity (minH), rainfall, soil temperature (soilT) and soil pressure (soilP) during June 2016 to May 2017 have been plotted in **Figure 10.3**.

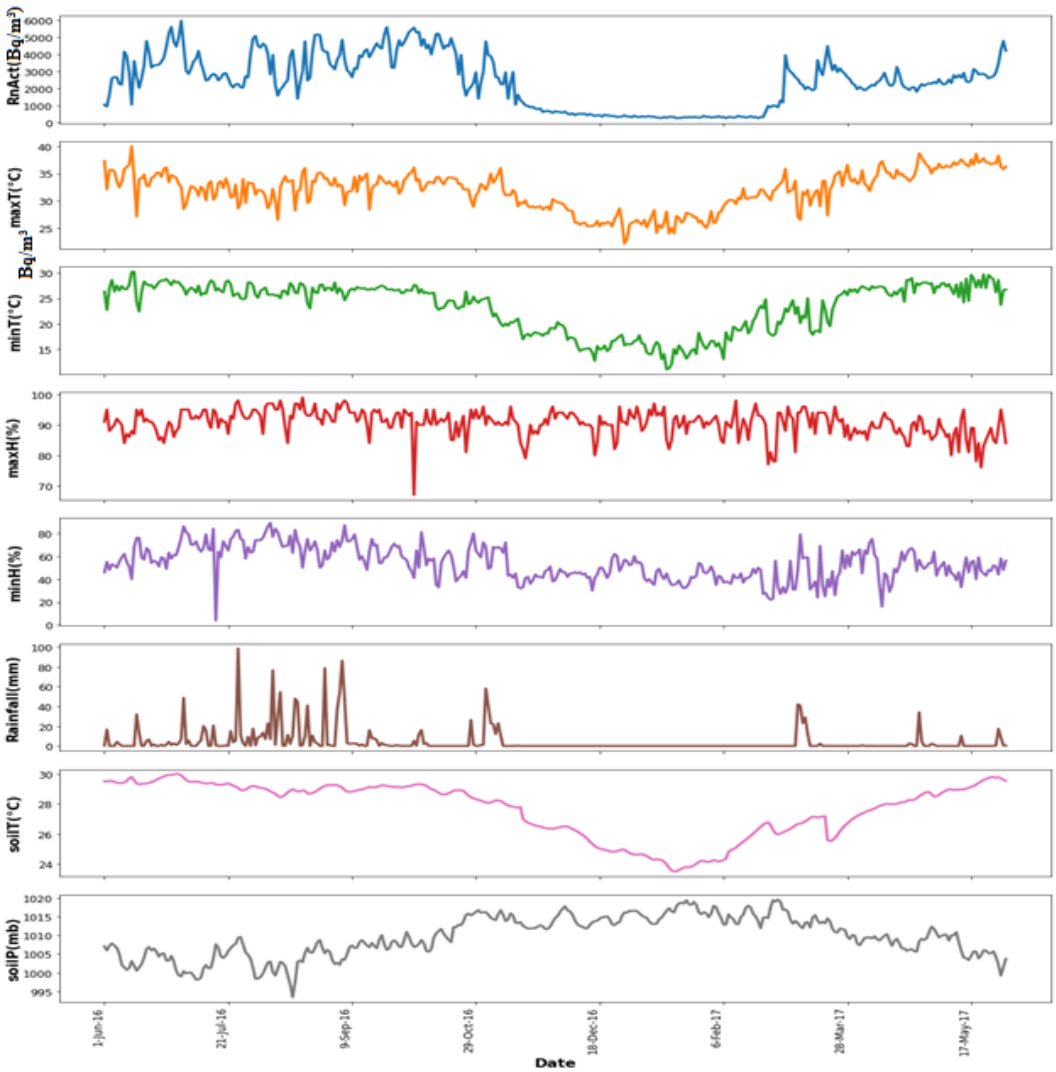

Fig. 10.3 Daily variation of radon activity and different meteorological parameters (Max. and Min. Temperature, Humidity and Rainfall) during 01/06/2016 to 31/05/2017

Upon visual examination, it is evident that atmospheric temperature, soil temperature, and rainfall exhibit a positive correlation with radon activity. Conversely, soil pressure demonstrates a negative association with soil radon levels. While no distinct relationship with maximum humidity has been identified, a decrease in radon activity is observed with a decrease in minimum humidity. Radon activity tends to be higher on

warmer days compared to colder winter days. During the summer, rising soil temperatures, attributed to a decrease in soil pressure, result in increased radon gas transportation in the soil (***Mazur and Kozak 2014***). Additionally, the soil undergoes warming throughout the summer, causing the expansion of soil cracks and consequently augmenting radon gas transportation (***Asher-Bolinder et al. 1990***). The lowest radon activity is noted during December, January, and February when soil temperature is at its minimum and soil pressure is at its maximum. It is also observed that radon activity is lower during dry months (months with less rainfall) compared to wet months. In months with precipitation, soil radon gas readily mixes with rainwater in the subsurface of the measuring site, leading to an increased transportation of the gas.

Season wise values of radon activity and other meteorological parameters have been listed in **Table 10.1**. Four seasons have been used here- Monsoon extending from June to September (JJAS), Post-monsoon during October and November (ON), winter from December to February (DJF), Summer from March to May (MAM).

Table 10.1 Values of average daily ^{222}Rn activity and other meteorological parameters during different seasons

Season	**Avg. daily ^{222}Rn activity (Bq)**	**Avg. daily maxT (°C)**	**Avg. daily minT (°C)**	**Avg. daily maxH (%)**	**Avg. daily minH (%)**	**Avg. daily Rainfall (mm)**	**Avg. daily SoilT (°C)**	**Avg. daily SoilP (mb)**
JJAS	3462.9	32.9	26.8	92.3	65.8	291.1	29.2	1004.1
ON	2899.3	32.0	22.4	90.1	52.1	129.3	28.1	1012.3
DJF	407.2	27.6	16.6	90.3	43.2	0.0	25.0	1015.4
MAM	2592.5	34.7	25.7	88.8	49.0	78.2	27.9	1009.3

From **Table 10.1** it is clear that the average daily maxT has been highest and lowest during summer and winter respectively, whereas, average daily minT, average daily minH and average daily soilT have been highest and lowest during monsoon and winter respectively. On the other hand, average daily soilP has shown opposite picture with highest value in winter and lowest in monsoon. The average daily maxH has been highest and lowest during monsoon and summer respectively. Highest amount of average daily rainfall has occurred during monsoon whereas no rainfall has been observed during winter. From **Table 10.1**, it is evident that average daily radon activity has been minimum during dry and cold winter (DJF) whereas it has been maximum during warm and wet monsoon (JJAS).

10.4.2 Effect of heavy rainfall

Careful examinations of time series have shown that radon activity has decreased drastically after heavy rainfall events and increased thereafter. According to IMD more

than 64.5 mm rainfall in a day is considered as heavy rainfall. Four number of heavy rainfall events have been found during the study period. The heavy rainfall has occurred on 25th July (98.6 mm), 8th August (76.5 mm), 29th August (78.6 mm) and 5th September (86.2 mm). Changes in radon activity after heavy rainfall have been shown in **Figure 10.4**.

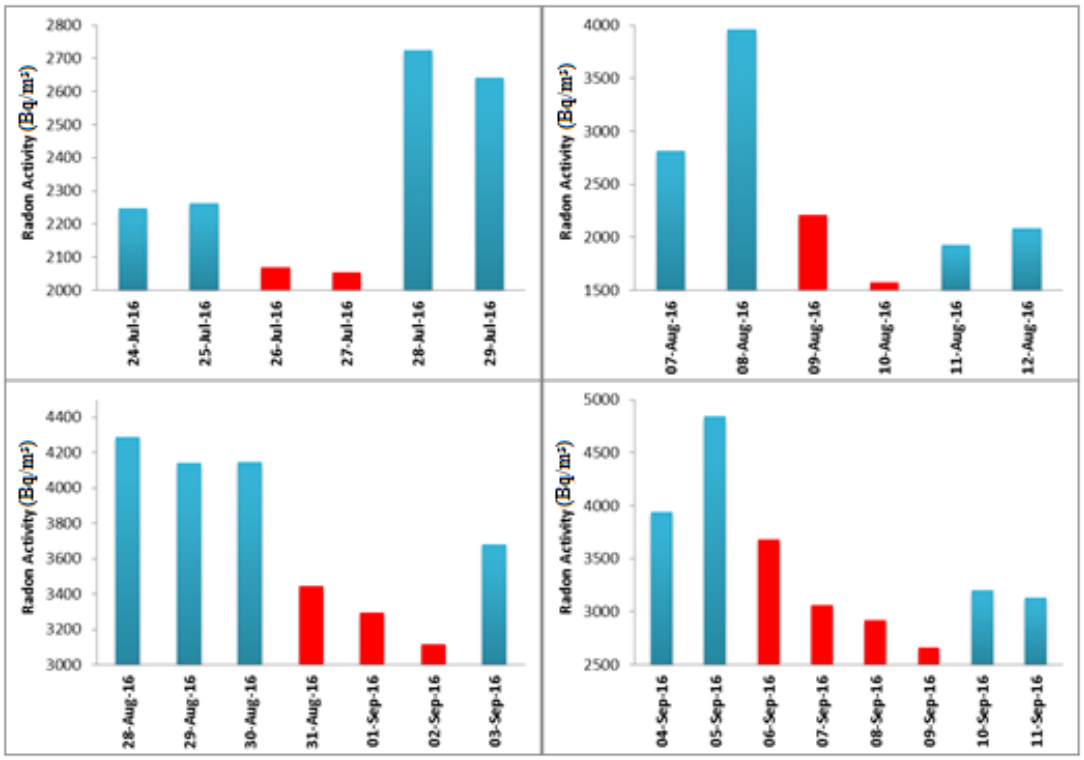

Fig. 10.4 Change in radon activity after heavy rain events during the study period

For the initial occurrence, there was a notable decrease in radon activity for the following two days after July 25th, followed by a subsequent significant increase. A parallel pattern was observed in the second event on August 8th, where the rise thereafter was gradual. The third event on August 29th showed no immediate change in activity, but a noteworthy reduction was noted over the following three days. In the case of the last event on September 5th, radon activity experienced a continuous four-day decline, followed by a subsequent increase. This observed pattern could potentially be attributed to elevated soil moisture levels, leading to the dissolution of diffusing radon. Additionally, the deep percolation of rainwater might contribute to the dilution of radon activity (***Singh et al. 1988***). Notably, similar findings of an inverse relationship between heavy rainfall and radon activity have been reported by Gableman (***1972***) and Ghosh and Balla (***1981***).

10.4.3 Relation between radon activity and meteorological parameters

To investigate the correlation between meteorological parameters and radon activity across various time frames, Pearson's correlation coefficient (R) was computed at daily, weekly (7-day), biweekly (15-day), and monthly intervals. The data for daily radon and

meteorological variables were first averaged over 1-day, 7-day, 15-day, and 1-month periods before conducting the correlation analysis. The results are summarized in **Table 10.2**.

Table 10.2 Correlation coefficient for meteorological variable with radon activity at different time scale

Time interval	maxT	minT	maxH	minH	Rainfall	SoilT	SoilP
daily	0.61***	0.74***	0.09*	0.43***	0.21***	0.78***	-0.62***
7days	0.70***	0.80***	0.11	0.58***	0.33**	0.84***	-0.67***
15days	0.72***	0.83***	0.17	0.66***	0.47**	0.86**	-0.71***
monthly	0.73***	0.87***	0.27	0.75***	0.60**	0.90***	-0.77***

'***', '**' and '*' implies significant at 1%, 5% and 10% level respectively.

The data presented in **Table 10.2** highlights that, with the exception of soil pressure (soilP), all other factors exhibit a positive correlation with radon activity. The analysis reveals that the correlation (R) values increase with longer time scales. Notably, the lowest R values are associated with the daily time scale, while the highest R values are observed at the monthly time scale. Across all four time scales, maxT, minT, minH, soilT, and soilP exhibit highly significant correlations with radon activity at the 1% level. Rainfall demonstrates significant R values at the 1% level on a daily scale and at the 5% level on other time scales. Maximum humidity displays a significant correlation (at the 10% level) solely on the daily scale, with no significant R values identified on other scales. Among the five parameters, soil temperature emerges as the most significantly correlated variable, while maximum humidity proves to be the least significant in terms of correlation.

10.4.4 Combined effect of meteorological parameters

In preceding sections, we explored the impact of individual meteorological parameters on radon activity. In reality, radon concentration may exhibit a complex simultaneous dependence on multiple parameters. Consequently, the collective influence of these parameters on radon activity was evaluated using machine learning techniques such as principal component regression (PCR), support vector regression (SVR), random forest regression (RF), and gradient boosting machine (GBM). The machine learning models were trained with 80% randomly selected data, while the remaining data was reserved for testing purposes. The relative importance of meteorological parameters during model training is shown in **Figure 10.5**.

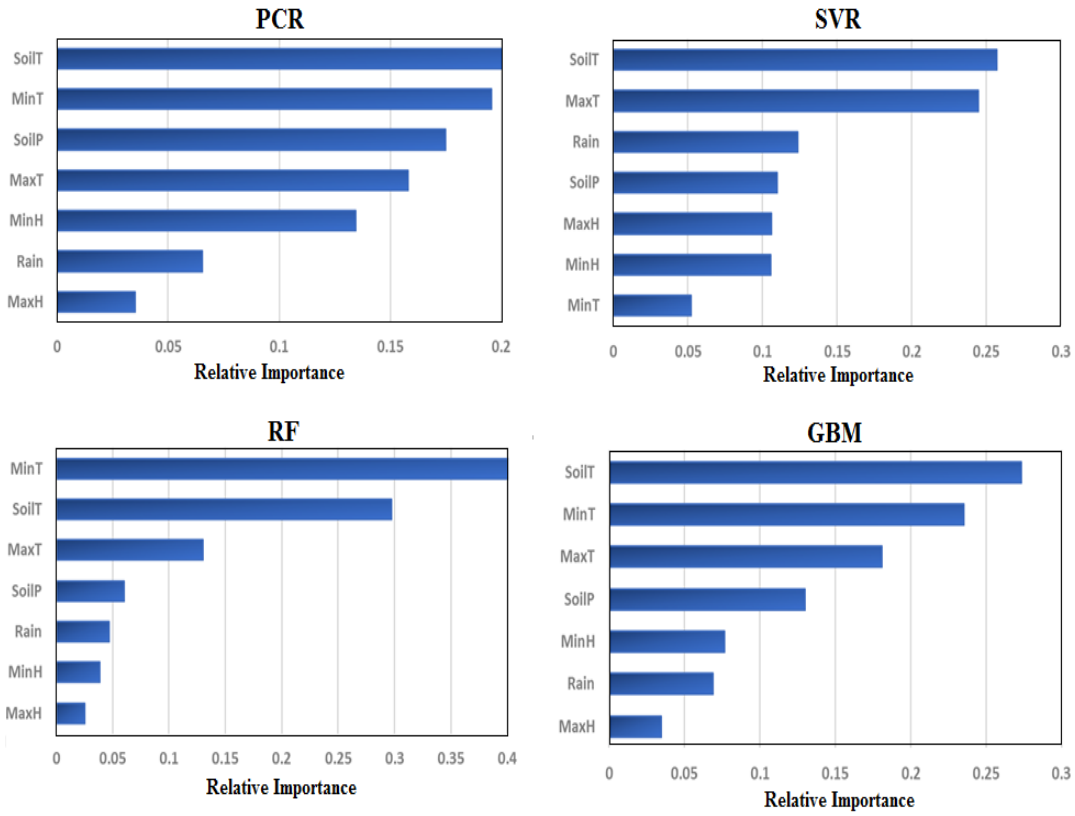

Fig. 10.5 Relative importance of the different predictors during the model training for PCR, SVR, RF and GBM

The performances of ML models have been depicted by **Fig. 10.6**.

(a)

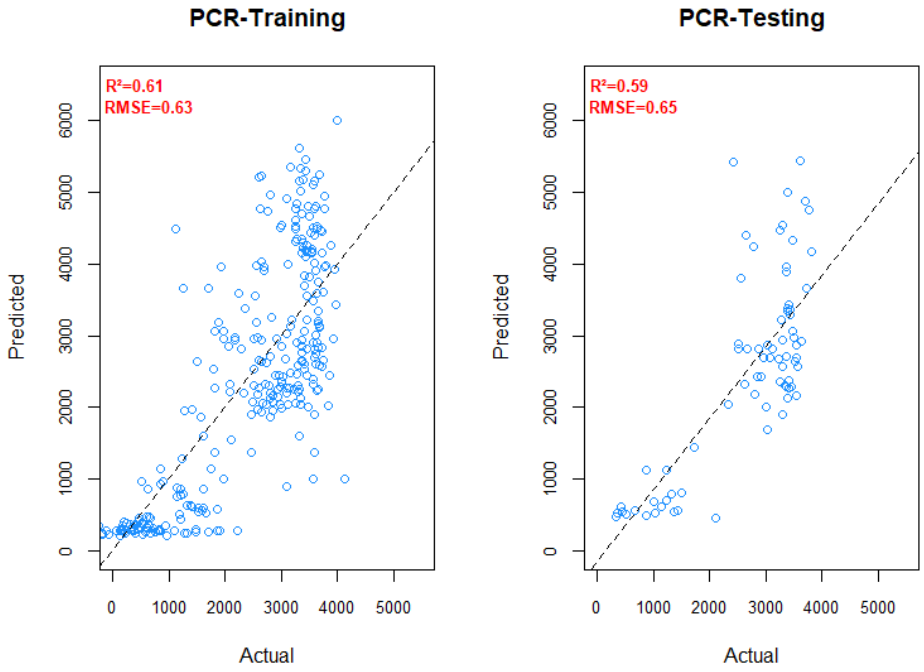

(b)

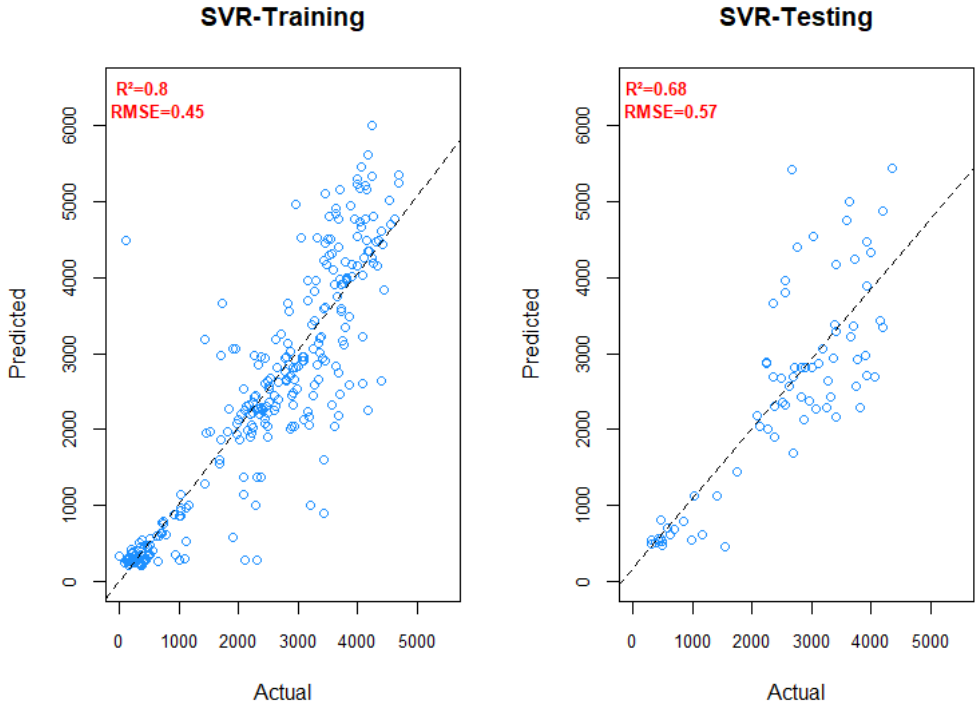
SVR-Training
R²=0.8
RMSE=0.45
Predicted
Actual
0
1000
2000
3000
4000
5000
6000
SVR-Testing
R²=0.68
RMSE=0.57
Predicted
Actual

(c)


RF-Training
R²=0.96
RMSE=0.22
Predicted
Actual
0
1000
2000
3000
4000
5000
6000
RF-Testing
R²=0.79
RMSE=0.46
Predicted
Actual

(d)

Fig. 10.6 Scatter plot between Predicted and Actual ^{222}Rn Concentration during training and testing period for (a) PCR (b) SVR (c) RF and (d) GBM. R^2 and RMSE values have been mentioned in the top of the plot in red.

Performance of four ML models in terms of R^2 and RMSE values are presented in **Table 10.3**.

Table 10.3 Performance of four ML models in terms of R^2 and RMSE during training and testing period

ML techniques	R^2		RMSE	
	Training	Testing	Training	Testing
PCR	0.61	0.59	0.63	0.65
SVR	0.8	0.68	0.45	0.57
RF	0.96	0.79	0.22	0.46
GBM	0.92	0.77	0.29	0.48

In case of PCR, soil temperature and minimum air temperature have been the most influential predictors whereas rainfall and maximum humidity has been the least important parameters (**Figure 10.5**). PCR model has obtained R-squared value of 0.61 (0.59) and RMSE value of 0.63 and 0.65 during training (testing), respectively (**Figure 10.6a**).

Radial basis function has been chosen as kernel in SVR model. For hyper-parameter tuning has been performed by considering all parameter combinations and finding the

best combination through 10-fold cross-validation. The estimated best parameter combination has been cost = 2 and epsilon = 0.1 for the present study. Soil temperature and maximum air temperature have been selected as the most important features by SVR whereas minimum temperature has been the least important parameters (**Figure 10.5**). SVR models have explained 80% (68%) of ^{222}Rn variance during training (testing). RMSE values of 0.45 and 0.57 have been obtained during training and testing, respectively (**Figure 10.6b**).

Two hyper-parameter number of trees (ntree) and the number of parameters randomly sampled as candidates at each split (mtry) have been optimized in RF model. The best result has been found for ntree=250 and mtry=4. Minimum air temperature has been by far the most important variable in RF model (**Figure 10.5**). Soil temperature also has considerable impact on ^{222}Rn concentration. Humidity parameters have been the least important predictors. RF model performance has been much better than PCR and SVR. It has obtained R-squared value of 0.96 (0.79) and RMSE value of 0.22 and 0.46 during training (testing), respectively (**Figure 10.6c**).

In case of GBM, best result has been obtained for 1000 trees having maximum depth of 5. The shrinkage parameter or learning rate has been kept as 0.01 while minimum 10 number of observations have been utilized in the terminal nodes of the trees. Soil temperature and minimum air temperature have been selected as the most important features by GBM whereas maximum humidity been the least important parameters (**Figure 10.5)**. GBM models have explained 92% (77%) of ^{222}Rn variance during training (testing). RMSE values of 0.29 and 0.48 have been obtained during training and testing, respectively (**Figure 10.6d**). So, GBM models have performed slightly less than RF in terms skill metrics. However, the difference between results of training and testing period for GBM model is much smaller compared to RF models. Hence, this model may produce more robust and reliable results without over-fitting.

However, some studies have revealed that for time series datasets, random data splitting for cross-validation reduces significance (***Roberts et al. 2017, Bergmeir et al. 2018***). Therefore, "Rolling Forecasting Origin" split has been carried out between in-sample (training) and test data (***Bergmeir et al. 2018***). Training dataset starts from the first 90 days and test data is always the data for 'next' 30 days. Every plot shows the 5-day moving average of the respective measure i.e., MAPE (Mean Absolute Percentage Error) and SMAPE (Scaled Mean Absolute Percentage Error). The plot has been generated by rolling the origin on to the end (i.e., the last training data-point is on the 335th day) and shown in **Figure 10.7**. Throughout the range in which the analysis was done, the measures (MAPE and SMAPE) have been more or less similar, independent of the machine learning method, and close to 30-35%.

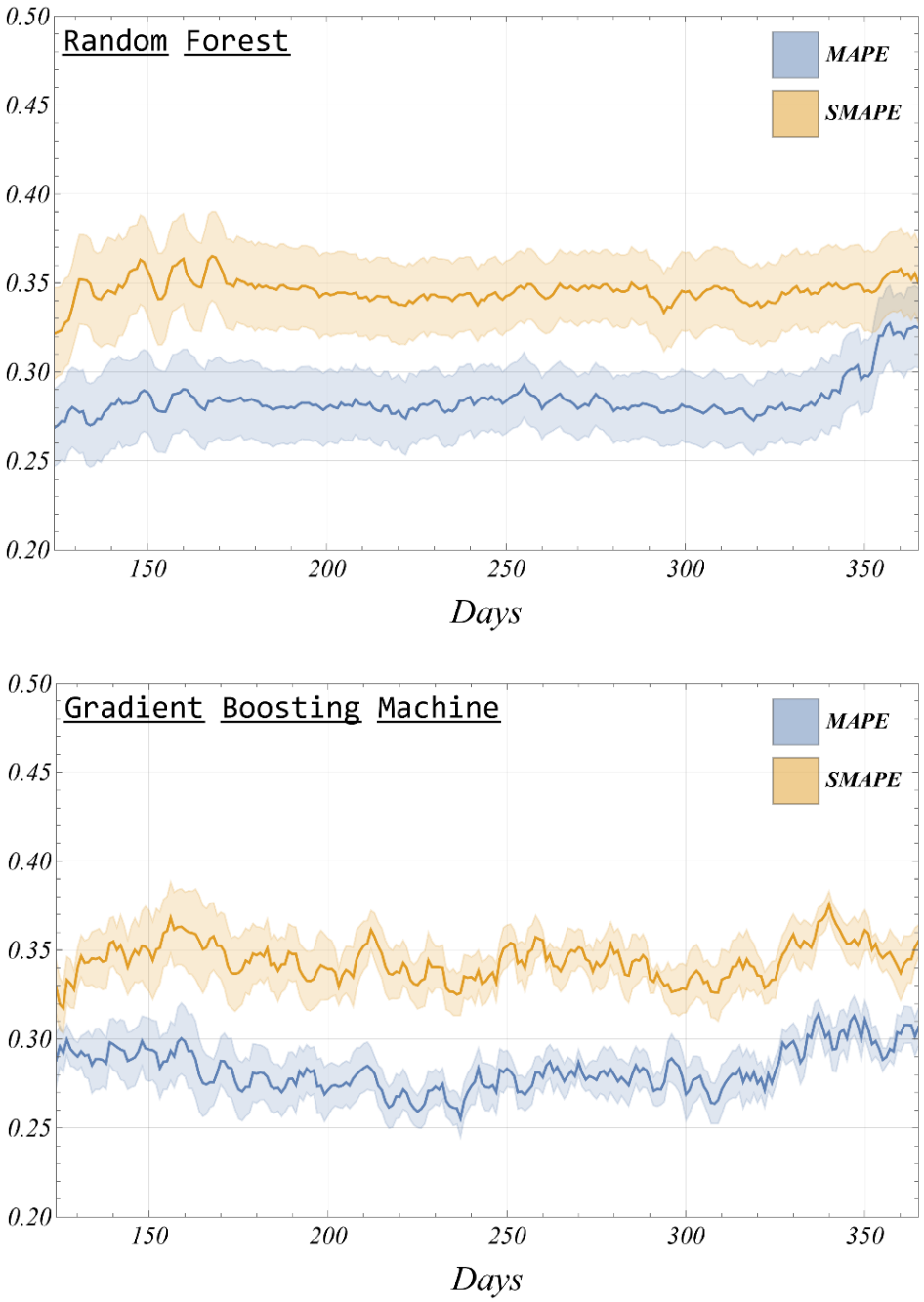

Fig. 10.7 5-day moving average of MAPE (Mean Absolute Percentage Error) and SMAPE (Scaled Mean Absolute Percentage Error) obtained through "Rolling Forecasting Origin" split

10.5 Conclusions

This investigation involves the analysis of data collected through a year-long continuous monitoring period (from June 2016 to May 2017) focused on soil radon activity and relevant meteorological parameters at the measurement site within the Jadavpur University Campus area. The study explores the seasonal fluctuations of radon activity and associated parameters, examining their impact on radon activity using correlation analysis and a machine learning approach.

During winter (December to January), characterized by low soil temperature, high soil pressure, and reduced rainfall, the study found the minimum radon activity. Conversely, the warm and wet rainy season (June to July), marked by higher soil temperature and lower pressure, exhibited maximum radon activity.

At a monthly scale, meteorological parameters demonstrated a greater influence on radon activity compared to the daily scale, as evidenced by correlation values. With the exception of soil pressure, all other parameters exhibited positive correlations with radon activity. Among these, soil temperature emerged as the most significant parameter in terms of correlation, while maximum humidity showed the least significance, lacking a significant R value except at the daily scale.

Although rainfall generally displayed a low positive correlation with radon activity, heavy rainfall events had a negative impact, resulting in a considerable reduction in activity observed after four such events during the study period.

Machine learning models highlighted soil temperature as the most influential parameter for radon emission, followed by minimum and maximum air temperature, while humidity parameters had a negligible effect. Among the models, Random Forest (RF) and Gradient Boosting Machine (GBM) outperformed Support Vector Regression (SVR) and Principal Component Regression (PCR). GBM exhibited more robust and consistent results during both training and testing periods, suggesting its reliability for future studies.

This study identified key meteorological parameters influencing radon activity, emphasizing the need to account for these non-seismic effects as noise in earthquake prediction models to extract the genuine earthquake signal.

References

Alam, M., Alam, M. M., Curray, J. R., Chowdhury, M. L. R., & Gani, M. R. (2003). An overview of the sedimentary geology of the Bengal Basin in relation to the regional tectonic framework and basin-fill history. Sedimentary geology, 155(3-4), 179-208.

Asher-Bolinder, S., Owen, D. E., & Schumann, R. R. (1990). Pedologic and climatic controls on RN-222 concentrations in soil gas, Denver, Colorado. Geophysical Research Letters, 17(6), 825-828.

Ballabio, C., Panagos, P., Lugato, E., Huang, J. H., Orgiazzi, A., Jones, A., ... & Montanarella, L. (2018). Copper distribution in European topsoils: An assessment based on LUCAS soil survey. Science of the Total Environment, 636, 282-298.

Banerji, B.N. (1938). Nature of 'Nor'westers' of Bengal and their similarity with others. Beitr. Physik fr. Atmos 24, 231-233.

Bengtsson, L., Herschy, R. W., & Fairbridge, R. W. (2012). Encyclopedia of lakes and reservoirs. Monographiae Biologicae, 53, 10-26.

Bergmeir, C., Hyndman, R. J., & Koo, B. (2018). A note on the validity of cross-validation for evaluating autoregressive time series prediction. Computational Statistics & Data Analysis, 120, 70-83.

Bhatia, S. C., Kumar, M. R., & Gupta, H. K. (1999). A probabilistic seismic hazard map of India and adjoining regions.

Bichard, G. F. (1976). An inexpensive radon earthquake prediction concept. EOS, Trans. Am. Geophys. Union, 57, 957.

Breiman, L. (2001). Random forests. Machine learning, 45, 5-32.

Bui, D. T., Khosravi, K., Tiefenbacher, J., Nguyen, H., & Kazakis, N. (2020). Improving prediction of water quality indices using novel hybrid machine-learning algorithms. Science of the Total Environment, 721, 137612.

Chapelle, O., Vapnik, V., Bousquet, O., & Mukherjee, S. (2002). Choosing multiple parameters for support vector machines. Machine learning, 46, 131-159.

Chen, J., & Ford, K. L. (2017). A study on the correlation between soil radon potential and average indoor radon potential in Canadian cities. Journal of environmental radioactivity, 166, 152-156.

Cortes, C., & Vapnik, V. (1995). Support-vector networks. Machine learning, 20, 273-297.

Deb, A., Gazi, M., & Barman, C. (2016). Anomalous soil radon fluctuations–signal of earthquakes in Nepal and eastern India regions. Journal of Earth System Science, 125, 1657-1665.

Deb, A., Gazi, M., Ghosh, J., Chowdhury, S., & Barman, C. (2018). Monitoring of soil radon by SSNTD in Eastern India in search of possible earthquake precursor. Journal of Environmental Radioactivity, 184, 63-70.

Fouedjio, F., & Klump, J. (2019). Exploring prediction uncertainty of spatial data in geostatistical and machine learning approaches. Environmental Earth Sciences, 78(1), 38.

Fujiyoshi, R., Sakamoto, K., Imanishi, T., Sumiyoshi, T., Sawamura, S., Vaupotic, J., & Kobal, I. (2006). Meteorological parameters contributing to variability in 222Rn activity concentrations in soil gas at a site in Sapporo, Japan. Science of the total environment, 370(1), 224-234.

Gableman, J. W. (1972). Radon emanometry of Starks salt dome. Calcasieu Parish, Lousiana, USAEC Report RME-4114, US Atomic Energy Commission, GPO.

Ghosh, D., Deb, A., & Sengupta, R. (2009). Anomalous radon emission as precursor of earthquake. Journal of Applied Geophysics, 69(2), 67-81.

Ghosh, P. C., & Bhalla, N. S. (1981). On the behaviour and measurement of thoron (220 Rn) in soil. Indian Journal of Earth Sciences, 8(1), 1-9.

Henderson, S. R., Guiliano, D., Presneau, N., McLean, S., Frow, R., Vujovic, S., ... & Boshoff, C. (2005). A molecular map of mesenchymal tumors. Genome biology, 6, 1-11.

Hengl, T., Mendes de Jesus, J., Heuvelink, G. B., Ruiperez Gonzalez, M., Kilibarda, M., Blagotić, A., ... & Kempen, B. (2017). SoilGrids250m: Global gridded soil information based on machine learning. PLoS one, 12(2), e0169748.

Hengl, T., Nussbaum, M., Wright, M. N., Heuvelink, G. B., & Gräler, B. (2018). Random forest as a generic framework for predictive modeling of spatial and spatio-temporal variables. PeerJ, 6, e5518.

Heung, B., Ho, H. C., Zhang, J., Knudby, A., Bulmer, C. E., & Schmidt, M. G. (2016). An overview and comparison of machine-learning techniques for classification purposes in digital soil mapping. Geoderma, 265, 62-77.

Hosoda, M., Tokonami, S., Suzuki, T., & Janik, M. (2020). Machine learning as a tool for analysing the impact of environmental parameters on the radon exhalation rate from soil. Radiation Measurements, 138, 106402.

Hosseini, F. S., Choubin, B., Mosavi, A., Nabipour, N., Shamshirband, S., Darabi, H., & Haghighi, A. T. (2020). Flash-flood hazard assessment using ensembles and Bayesian-based machine learning models: Application of the simulated annealing feature selection method. Science of the total environment, 711, 135161.

IMD (2015). India Meteorological Department. Climatological Normals: 1981 – 2010.

Ishwaran, H., Kogalur, U. B., Blackstone, E. H., & Lauer, M. S. (2008). Random survival forests.

Kanevski, M., Timonin, V., & Pozdnukhov, A. (2009). Machine learning for spatial environmental data: theory, applications, and software. EPFL press.

Kanevski, M., Timonin, V., & Pozdnukhov, A. (2009). Machine learning for spatial environmental data: theory, applications, and software. EPFL press.

Kleine Deters, J., Zalakeviciute, R., Gonzalez, M., & Rybarczyk, Y. (2017). Modeling PM 2.5 urban pollution using machine learning and selected meteorological parameters. Journal of Electrical and Computer Engineering, 2017.

Kojima, H. (1998). The exhalation rate of radon in the atmosphere and the influencing factors.

Krishna, K. S., Ismaiel, M., Srinivas, K., Rao, D. G., Mishra, J., & Saha, D. (2016). Sediment pathways and emergence of Himalayan source material in the Bay of Bengal. Current Science, 363-372.

Kropat, G., Bochud, F., Jaboyedoff, M., Laedermann, J. P., Murith, C., Palacios, M., & Baechler, S. (2015). Predictive analysis and mapping of indoor radon concentrations in a complex environment using kernel estimation: an application to Switzerland. Science of the Total Environment, 505, 137-148.

Kuhn, M., & Johnson, K. (2013). Applied predictive modeling (Vol. 26, p. 13). New York: Springer.

Külahcı, F., İnceöz, M., Doğru, M., Aksoy, E., & Baykara, O. (2009). Artificial neural network model for earthquake prediction with radon monitoring. Applied Radiation and Isotopes, 67(1), 212-219.

Lary, D. J., Alavi, A. H., Gandomi, A. H., & Walker, A. L. (2016). Machine learning in geosciences and remote sensing. Geoscience Frontiers, 7(1), 3-10.

Li, J., Heap, A. D., Potter, A., & Daniell, J. J. (2011). Application of machine learning methods to spatial interpolation of environmental variables. Environmental Modelling & Software, 26(12), 1647-1659.

Li, L., Blomberg, A. J., Stern, R. A., Kang, C. M., Papatheodorou, S., Wei, Y., ... & Koutrakis, P. (2021). Predicting monthly community-level domestic radon concentrations in the greater boston area with an ensemble learning model. Environmental Science & Technology, 55(10), 7157-7166.

Li, L., Ruan, H., Liu, C., Li, Y., Shuang, Y., Alù, A., ... & Cui, T. J. (2019). Machine-learning reprogrammable metasurface imager. Nature communications, 10(1), 1082.

Loh, W. Y. (2011). Classification and regression trees. Wiley interdisciplinary reviews: data mining and knowledge discovery, 1(1), 14-23.

Ly, H. B., Pham, B. T., Dao, D. V., Le, V. M., Le, L. M., & Le, T. T. (2019). Improvement of ANFIS model for prediction of compressive strength of manufactured sand concrete. Applied Sciences, 9(18), 3841.

Mazur, J., & Kozak, K. (2014). Complementary system for long term measurements of radon exhalation rate from soil. Review of Scientific Instruments, 85(2).

Micheletti, N., Foresti, L., Robert, S., Leuenberger, M., Pedrazzini, A., Jaboyedoff, M., & Kanevski, M. (2014). Machine learning feature selection methods for landslide susceptibility mapping. Mathematical geosciences, 46, 33-57.

Mogro-Campero, A., & Fleischer, R. L. (1977). Subterrestrial fluid convection: a hypothesis for long-distance migration of radon within the earth. Earth and Planetary Science Letters, 34(2), 321-325.

Mosavi, A., Sajedi-Hosseini, F., Choubin, B., Taromideh, F., Rahi, G., & Dineva, A. A. (2020). Susceptibility mapping of soil water erosion using machine learning models. Water, 12(7), 1995.

Mostajabi, A., Finney, D. L., Rubinstein, M., & Rachidi, F. (2019). Nowcasting lightning occurrence from commonly available meteorological parameters using machine learning techniques. Npj Climate and Atmospheric Science, 2(1), 41.

Mustafa, A., Tariq, Z., Mahmoud, M., Radwan, A. E., Abdulraheem, A., & Abouelresh, M. O. (2022). Data-driven machine learning approach to predict mineralogy of organic-rich shales: An example from Qusaiba Shale, Rub'al Khali Basin, Saudi Arabia. Marine and Petroleum Geology, 137, 105495.

Mustafa, M. R., Rezaur, R. B., Saiedi, S., & Isa, M. H. (2012). River suspended sediment prediction using various multilayer perceptron neural network training algorithms—a case study in Malaysia. Water resources management, 26, 1879-1897.

Nazaroff, W. W. (1992). Radon transport from soil to air. Reviews of geophysics, 30(2), 137-160.

Nussbaum, M., Spiess, K., Baltensweiler, A., Grob, U., Keller, A., Greiner, L., ... & Papritz, A. (2018). Evaluation of digital soil mapping approaches with large sets of environmental covariates. Soil, 4(1), 1-22.

Peel, M. C., Finlayson, B. L., & McMahon, T. A. (2007). Updated world map of the Köppen-Geiger climate classification. Hydrology and earth system sciences, 11(5), 1633-1644.

Petermann, E., Meyer, H., Nussbaum, M., & Bossew, P. (2021). Mapping the geogenic radon potential for Germany by machine learning. Science of the Total Environment, 754, 142291.

Rafique, M., Tareen, A. D. K., Mir, A. A., Nadeem, M. S. A., Asim, K. M., & Kearfott, K. J. (2020). Delegated regressor, a robust approach for automated anomaly detection in the soil radon time series data. Scientific reports, 10(1), 3004.

Rivera, J. I., & Bonilla, C. A. (2020). Predicting soil aggregate stability using readily available soil properties and machine learning techniques. Catena, 187, 104408.

Roberts, D. R., Bahn, V., Ciuti, S., Boyce, M. S., Elith, J., Guillera-Arroita, G., ... & Dormann, C. F. (2017). Cross-validation strategies for data with temporal, spatial, hierarchical, or phylogenetic structure. Ecography, 40(8), 913-929.

Rodriguez-Galiano, V., Sanchez-Castillo, M., Chica-Olmo, M., & Chica-Rivas, M. J. O. G. R. (2015). Machine learning predictive models for mineral prospectivity: An evaluation of neural networks, random forest, regression trees and support vector machines. Ore Geology Reviews, 71, 804-818.

Roy, D. K., & Roser, B. P. (2012). Geochemistry of Tertiary sequence in Shahbajpur-1 well, Hatia trough, Bengal basin, Bangladesh: provenance, source weathering and province affinity. Journal of Life and Earth Science, 7, 1-13.

Schery, S. D., Gaeddert, D. H., & Wilkening, M. H. (1984). Factors affecting exhalation of radon from a gravelly sandy loam. Journal of Geophysical Research: Atmospheres, 89(D5), 7299-7309.

Schubert, M., & Schulz, H. (2002). Diurnal radon variations in the upper soil layers and at the soil-air interface related to meteorological parameters. Health Physics, 83(1), 91-96.

Schumann, R. R., & Gundersen, L. C. (1996). Geologic and climatic controls on the radon emanation coefficient. Environment International, 22, 439-446.

Sesana, L., Caprioli, E., & Marcazzan, G. M. (2003). Long period study of outdoor radon concentration in Milan and correlation between its temporal variations and dispersion properties of atmosphere. Journal of Environmental Radioactivity, 65(2), 147-160.

Sextro, R. G. (1987). Understanding the origin of radon indoors—Building a predictive capability. Atmospheric Environment (1967), 21(2), 431-438.

Shah, A. D., Bartlett, J. W., Carpenter, J., Nicholas, O., & Hemingway, H. (2014). Comparison of random forest and parametric imputation models for imputing missing data using MICE: a CALIBER study. American journal of epidemiology, 179(6), 764-774.

Shiuly, A., & Narayan, J. P. (2012). Deterministic seismic microzonation of Kolkata city. Natural Hazards, 60, 223-240.

Singh, M. A. N. W. I. N. D. E. R., Ramola, R. C., Singh, S. U. R. I. N. D. E. R., & Virk, H. S. (1988). The influence of meteorological parameters on soil gas radon. Journal of Association of Exploration Geophysicists, 9(2), 85-90.

Sogaard-Hansen, J., & Damkjaer, A. (1987). Determining 222Rn diffusion lengths in soils and sediments. Health Physics, 53(5), 455-459.

Sundal, A. V., Valen, V., Soldal, O., & Strand, T. (2008). The influence of meteorological parameters on soil radon levels in permeable glacial sediments. Science of the total environment, 389(2-3), 418-428.

Taherei Ghazvinei, P., Hassanpour Darvishi, H., Mosavi, A., Yusof, K. B. W., Alizamir, M., Shamshirband, S., & Chau, K. W. (2018). Sugarcane growth prediction based on meteorological parameters using extreme learning machine and artificial neural network. Engineering Applications of Computational Fluid Mechanics, 12(1), 738-749.

Timkova, J., Fojtikova, I., & Pacherova, P. (2017). Bagged neural network model for prediction of the mean indoor radon concentration in the municipalities in Czech Republic. Journal of Environmental Radioactivity, 166, 398-402.

Torkar, D., Zmazek, B., Vaupotič, J., & Kobal, I. (2010). Application of artificial neural networks in simulating radon levels in soil gas. Chemical Geology, 270(1-4), 1-8.

Tsuji, S., Midorikawa, Y., Takahashi, T., Yagi, K., Takayama, T., Yoshida, K., ... & Aburatani, H. (2012). Potential responders to FOLFOX therapy for colorectal cancer by Random Forests analysis. British journal of cancer, 106(1), 126-132.

Ulomov, V. I. (1971). The Tashkent earthquake of 26 April 1966. Acad. Nauk Uzbek SSR FAN, 188-192.

Vamathevan J, Clark D, Czodrowski P, Dunham I, Ferran E, Lee G, ..., Zhao S (2019) Applications of machine learning in drug discovery and development. Nature reviews Drug discovery 18(6): 463-477.

Van Dao D, Jaafari A, Bayat M, Mafi-Gholami D, Qi C, Moayedi H, ..., Pham BT (2020) A spatially explicit deep learning neural network model for the prediction of landslide susceptibility. Catena 188: 104451.

Washington JW, Rose AW (1990) Regional and temporal relations of radon in soil gas to soil temperature and moisture. Geophysical Research Letters 17(6): 829-832.

Woith, H. (2015). Radon earthquake precursor: A short review. The European Physical Journal Special Topics, 224(4), 611-627.

Yang J, Busen H, Scherb H, Hürkamp K, Guo Q, Tschiersch J (2019) Modeling of radon exhalation from soil influenced by environmental parameters. Science of the Total Environment, 656: 1304-1311.

Zmazek B, Džeroski S, Torkar D, Vaupotič J, Kobal I (2010) Identification of radon anomalies in soil gas using decision trees and neural networks. Nukleonika 55(4): 501-505.

Zmazek B, Todorovski L, Džeroski S, Vaupotič J, Kobal I (2003) Application of decision trees to the analysis of soil radon data for earthquake prediction. Applied radiation and isotopes 58(6): 697-706.

Chapter 11

Concluding Remarks and Future Directions

11.1 Conclusions and future scope of the thesis work

- Air radon study in underground spaces of Kolkata municipal area (KMC) and its adjacent areas reveal that in basements and subways radon concentrations are considerably low. In some cases it is even lower than that of the corresponding background radon concentrations, suggesting that the constructions are well built having very low amount of cracks or seepage paths. Though high radon concentration is very unlikely, still underground metro stations which are heavily used are yet to be checked for radon concentration.

  Hence in a highly populated city like Kolkata, multilevel basement should be advised for skyscrapers and these basements should be encouraged to be used as much as possible.

- An exhaustive water radon measurement has been performed in three different regions, namely, Bakreswar & Tantloi geothermal area, Susunia hill and Ajodhya hill areas belonging to Chotanagpur plateau region. The entire region experienced a series of fissure eruptions over decades during the Rajmahal volcanic activity and is rich in mineralization. The study reveals elevated level of water radon concentration in most of the places having average values around or above the reference level suggested by WHO and EU. In some places radon levels are high even in the context of global scenario. Analyses show a strong positive correlation of radon concentration with tube well depth in most of the regions. Seasonal variation of radon concentration has been studied in one of the considered areas. It is observed that radon activity is lowest in monsoon and increases almost 50 % in winter when it becomes highest.

  The situation demands proper attention by the local authorities and conduction of public awareness programmes. Proper radon mitigation procedure should be adopted wherever necessary, specially in the winter when radon concentration reaches its maximum. It is better to use USEPA suggested Granular Activated Carbon (GAC) method or aeration technique for reducing water radon. At least the local people should be advised not to consume water directly from tap, if possible boil or stir the water well before drinking. Boiling should be done in open space so that indoor air radon concentration does not increase. Moreover, deep tube wells should be avoided as much as possible.

  We have only estimated health risk due to water borne radon. Health surveys should be conducted in the radon prone areas to know whether there is any correlation between radon concentrations and ailment pattern of the local people.

  As radon is found to be high in most of the studied areas a radon map of the total Chotanagpur plateau and adjacent regions should be developed as soon as possible. Radon monitoring should be done regularly and its seasonal variation has to be examined more exhaustively in different regions as the variations have

been found to be significantly high. Moreover, other radionuclides present in the water as well as different ions like Na^{+}, K^{+}, Ca^{+}, Mg^{++}, Al^{+++}, Cl^{-}, F^{-} should be estimated along with radon and correlations between the radionuclides and the chemical ions need to be investigated to get some hint regarding the possible source of radioactivity in water.

- Study of correlation between meteorological parameters like maxT, minT, minH, soilT, soilP and rainfall with soil radon has been done at Jadavpur University Campus, West Bengal, India. Monthly meteorological data demonstrates a greater influence on radon than daily variations. Among the five parameters, soil temperature emerges as the most significantly correlated variable, while maximum humidity proves to be the least significant in terms of correlation. Heavy rainfall negatively impacts radon activity. Machine learning models highlight soil temperature's dominance, with Gradient Boosting Machine showing most consistent reliability. The identification of true earthquake signals are expected to be more precise due to removal of these non-seismic influences.

  In future similar studies using ML techniques will be performed using larger time series data so that training and testing may be done more effectively. Moreover, soil radon time series data obtained from monitoring station situated within the earthquake probe zones will be analysed using more robust ML techniques for reliable prediction of earthquakes.